University of Glasgow

Seren, Daniel B. (1982) *Monohulls and multihulls in transit: aspects of physical and theoretical modelling in restricted water*.PhD thesis.

http://theses.gla.ac.uk/6337/

Copyright and moral rights for this thesis are retained by the author

A copy can be downloaded for personal non-commercial research or study, without prior permission or charge

This thesis cannot be reproduced or quoted extensively from without first obtaining permission in writing from the Author

The content must not be changed in any way or sold commercially in any format or medium without the formal permission of the Author

When referring to this work, full bibliographic details including the author, title, awarding institution and date of the thesis must be given

Glasgow Theses Service
http://theses.gla.ac.uk/
theses@gla.ac.uk

MONOHULLS AND MULTIHULLS IN TRANSIT: ASPECTS OF PHYSICAL AND THEORETICAL MODELLING IN RESTRICTED WATER

By;

Daniel B. Seren, B.Sc.

Thesis submitted for the Degree of Ph.D.

at

The Dept. of Naval Architecture and Ocean Engineering

The University of Glasgow

- September 1982 -

Declaration

Except where reference is made to the work of others, this thesis is believed to be original.

CONTENTS

Figures

Tables

NOMENCLATURE

A - Channel cross-sectional area = Wh

a - distance between centre of underwater resistance and point of application of the towing force

$B, B(x)$ - (local) ship breadth

$B^*(r)$ - Fourier transform of $B(x)$ curve

c - control surface chord

C_B - block coefficient

C_D - drag coefficient

C_{FL} - Blasius skin-friction coefficient = $\frac{1.328}{\sqrt{R_N}}$

C_{FT} - ITTC turbulent skin-friction coefficient = $\frac{0.075}{(\log R_N - 2)^2}$

C_{pl} - longitudinal prismatic coefficient

C_S - mean sinkage coefficient = $\frac{s_M \times 100}{L}$

C_{SQ} - non-dimensional squat coefficient

C_T - trim coefficient = $\tau \times 100$

C_{TOT} - total resistance coefficient = $\frac{R_T}{\frac{1}{2}\rho U^2 S}$

C_W - wire self-drag coefficient = $\left(\frac{v}{U}\right)^2 \left(\frac{Sp}{S}\right) C_D$

C_{wp} - waterplane area coefficient

$C(\theta)$ - amplitude function of cosine wave

D_L - resistance decrement due to laminar flow upstream from trip-wire

d - distance of centre of underwater resistance below waterline

e - a parameter = $\frac{1}{\left(1 + \left(\frac{W_c - 2B}{B}\right)\right)}$

F - total vertical force

F_h - Froude depth number = $\frac{U}{\sqrt{gh}}$

F_h^L - lower critical speed

F_h^U - upper critical speed

F_L - Froude length number = $\frac{U}{\sqrt{gL}}$

$F_{(x)}^{(1)}$ - first-order (inner region) arbitrary function

$F_{(x)}^{(2)}$ - second-order (inner region) arbitrary function

$F_*^{(2)}$ - second-order (inner region) arbitrary function

g - acceleration due to gravity

$G(x,y)$ - Green's function (unit source)

h - water depth

Δh - drop in water-level in channel

i - dimensionless distance from the surface referred to b.l. thickness

J - a constant

K_o - wave number = g/U^2

k - a constant

L - ship/model length between perpendiculars

L_H - length of hull

L_S - length of strut

ℓ - wave length

LCB - longitudinal centre of buoyancy

LCF - longitudinal centre of flotation

M_H - trimming moment due to horizontal forces

$m, m(x)$ - (local) blockage = $\frac{S(x)}{A}$

P, p - fluid pressure

p_H - hydrostatic pressure

q - trip-wire diameter

R_F - frictional resistance component

R_L - longitudinal radius of gyration

R_N - Reynold's Number

R_R - residuary resistance

R_T - total resistance

R_{Vc} - viscous catamaran resistance

R_{Vd} - viscous demi-hull resistance

R_{Vf} - viscous form resistance

R_W - wave resistance

R_{Wd} - demi-hull wave resistance

R_{Wi} - wave interference resistance

R_x - x - Reynold's Number = $\frac{Ux}{\nu}$

r - geosim length ratio

r_w - trip-wire self-drag

S - total wetted surface

$S(x)$ - (local) model/ship cross-sectional area

$S^*(r)$ - Fourier transform of $S(x)$ curve

S_p - surface area of protrusion

S_{LH} - surface area of hull

S_{LS} - surface area of strut

$S(\theta)$ - amplitude function of sine wave

s_{FP} - sinkage at F.P.

s_{AP} - sinkage at A.P.

s_M - mean sinkage $= \frac{s_{FP} + s_{AP}}{2}$

T - maximum ship draught

T_T - total trim

T_H - trim due to horizontal forces

T_V - trim due to vertical forces

U - (undisturbed) steady ship/model velocity

$U_1(x)$ - mean (local) flow velocity $= U + u(x)$

$u(x)$ - (local) longitudinal perturbation velocity $= \phi_x$

UKC - underkeel clearance

v - velocity in the b.l. at the trip-wire location

v_h - speed of translation wave in shallow water

v_∞ - speed of translation wave in deep water

W - channel width

W_e - catamaran overall width

w - a ratio $= \frac{U_1(x)}{U}$

$y=f(x,z)$ - hull surface equation

$y=\eta(x,y)$ - free surface equation

y - hull spacing

z - distance between waterplane and towing point

Φ, ϕ - velocity potential

ϕ_N - rate of change normal to the cross-section

ε - a small positive parameter

δ - $\sqrt{1 - F_h^2}$

δ^* - boundary layer displacement thickness

δ_T - boundary layer thickness

$\psi(r,y)$ - Fourier transform of velocity potential ϕ

μ - source strength

ρ - fluid density

ν - kinematic viscosity

α, β - numerical values for parabolic velocity distribution

α_S, β_S, α_B, β_B - Constants in $S(x)$ and $B(x)$ curves

α_a - true angle-of-attack of control surface

γ - laminar b.l. pressure gradient parameter

λ_S - (Tuck) sinkage coefficient

λ_T - (Tuck) trim coefficient

θ - an angle

∇ - displacement volume (also denotes Laplacian operator)

Δ - displacement = $\rho\nabla$

τ - trim angle

Acknowledgement

This thesis is based on research carried out during the period 1979 - 1982 in the Dept. of Naval Architecture and Ocean Engineering at the University of Glasgow. The work was sponsored by the Science and Engineering Research Council Marine Technology Directorate.

I am deeply grateful to Prof. D. Faulkner, to the Acting Head of Dept., Mr. N.S. Miller, and to my supervisor, Dr. A.M. Ferguson, for the help, encouragement and advice on many aspects of the work. I am also indebted to Dr. R.C. McGregor for his advice throughout the research, and to the staff and technicians of the Hydrodynamics Laboratory for their invaluable assistance with the model tests and the use of the computing facilities.

I am very grateful to Miss. I. Campbell, Mrs. L. Robinson and Miss P. McKay for the patient assistance with the typing of the final manuscript.

Finally, I am particularly indebted to my wife and family for their unflagging support and encouragement throughout this work.

Summary

This study addresses the problems of the theoretical and experimental modelling of mono-hull and multi-hull ship-to-bottom interaction in restricted water, with a particular emphasis on the phenomenon of "squat". It falls within a category of problems re-introduced by the advent of large-sized ships and platforms, for which the considerations of the physical constraints assume pronounced importance.

The work set out to characterise the nature of the forces acting under various practical conditions and consider their influence on the vessel's trajectory with the objective of producing a prediction method which employs minimum early-design-stage input. The complex relationship existing between the ship or offshore platform and the shallow-water environment is examined in light of the available hydrodynamic and hydraulic mathematical models and the inherent theoretical assumptions are studied in detail. Although the theoretical models provide a valuable insight, a universally applicable theory, which allows a routine solution with arbitrary Froude depth number and lateral restrictions, does not exist at present.

The experimental work demonstrates limitations and illustrates features not apparent from theoretical studies by examining, qualitatively and quantitatively, relevant aspects of mono-hull and multi-hull behaviour in restricted and unrestricted shallow-water. The representative models used were of a modern full-form ship, a SWATH and a number of offshore platform designs currently in operation.

The first part of the work presents an extensive study of a wide range of parameters affecting the mono-hull vertical-plane forces in restricted water. Effects of underkeel clearance, speed, self-propulsion, lateral restrictions, bulbous-bow shape, initial trim, draught, a sudden variation in depth, transverse location in channel and the effect of proximity of a stationary ship/quay are presented and discussed. The considerable amount of experimental data accumulated at Glasgow University and elsewhere, permit a very reasonable degree of confidence in the conclusions. The appropriate theoretical basis, which allows extrapolation into the intermediate finite-width channel (as distinct from narrow), is found to be a combination of the hydraulic and hydrodynamic approaches. Owing to the wide range of contributing factors and because the available theoretical concepts are based on inherent simplifications, empiricism is shown to play an important role in connecting theory and experiment. A computer program was written based on the theory and it demonstrates the utility and power of the systematic experimental approach to the formulation of a semi-empirical prediction

method, giving a rapid means of producing reasonably accurate data to those concerned with its application to ships in restricted waterways.

The second part of the work examines some theoretical and experimental/operational aspects of mobile platforms in the transit draught condition. The major test variables included water depth, speed, lateral restrictions, transverse hull spacing, turbulence stimulation, effect of towing point height, type of ballast, shape of hull-endings and the effect of a vertical-plane control surface. Attention is given to factors which form a part of the experiments and whose assesment is of primary importance to the scaling problems experienced by multi-hulls in existing towing tanks. Their effects on the measured shallow-water resistance and squat are analysed. The experiments indicate that the prediction of the vertical-plane force and moment may be accomplished by the same approach as employed for mono-hulls. However, the wide range of factors influencing the behaviour, combined with the limited empirical data avilable do not permit the extension of the mono-hull program at present.

The work provides a useful compendium of information on a wide range of aspects of mono-hull and multi-hull behaviour in a confined environment with broader experimental and practical applications. Some theoretical methods are examined and proposed.

CHAPTER 1

Introduction

(1.1) Background

A characteristic feature of current advances in offshore technology is the increasing number, size and speed of mono-hulls and the growth of multi-hulls for various applications. Their appearance has resulted in some operational difficulties and, consequently, increased interest in hydrodynamic problems associated with water restricted in depth and/or lateral extent. The transport of dangerous cargoes and their possible impact on the environment, has introduced a note of urgency into the subject and increased the benefits of resolving the areas of uncertainty.

Casualty statistics regarding the causes and frequency of damage, cost of repair and time lost to repair, illustrate the relative importance of grounding/stranding in relation to other categories. A recent survey, based upon the experience of 1,104 vessels of different flags and trades during 1978, shows grounding/stranding to rate as the 3rd most frequent cause of damage, Table 1, [10]. An examination of the total expenditure of money and time

required to repair the resulting damage, shows the grounding/stranding category to rank highly in both. For example, the total repair costs expended as a result of this cause rank top and account for more than 1/5th of the total. If combined with other categories of striking and contact, the repair costs amount to approximately 1/2 the total. A similar situation prevails when considering the portion of the total repair time expended. Since the shipowner bears a large portion of the cost of lost revenue, grounding represents a significant cost to both underwriters and shipowners. The continous increase in size and draught of vessels in relation to the water depths, ensures that this trend will continue and indicates that the various interaction problems are beneficial areas of research to pursue.

Cause	No. of Reports	Avg. Repair Cost Index	Avg. Repair Time (Days)
Contact with Structure	161	24.1	6.9
Collision with Vessel	139	33.5	9.4
Grounding/Stranding	112	84.9	12.1
Cause Unknown	107	47.3	2.5
Heavy Weather	105	25.8	11.2
Crew Negligence	96	33.6	14.2
Struck Submerged Object	49	45.2	7.8
Shipbuilder's or Shiprepairer's Negligence	32	65.2	14.1
Surging at Dock or Pier	19	43.7	10.0
Stevedore Damage	19	5.0	5.0
Fire	17	49.7	28.1
Design Fault	16	213.6	49.9
Encounter with Ice	16	40.1	9.9
Propeller Damage	14	22.8	6.7
Electrical Failure	10	19.2	13.0
Latent Defect	9	42.0	9.7
Explosion	8	69.3	45.0
Contamination of Machinery	8	52.6	17.1
Struck Floating Object	6	39.2	7.3
Freezing Damage	3	19.5	13.0
Automation Control Failure	2	16.1	7.0
Overpressurization of Tanks	1	63.2	17.0
All Others	120	28.5	11.6
Total	1,069	41.9	10.6

Table 1; Causes of Damage

Owing to the understandable reluctance of shipboard personnel to hazard their vessels by conducting experiments under close-to-grounding conditions, the only significant advances may be obtained by theory and/or model tests. Past research has demonstrated that hydrodynamic effects induced by depth and/or lateral restrictions are significant, with effects which are at times contrary to intuition, and may cause unpredictable ship behaviour and the erosion of safety factors. The problem is somewhat complicated by the terminology, since the terms "shallow" and "finite" depth, "finite" and "narrow" width, are not absolute but relative to the vessel's dimensions. Hence, in addition to the hazardous situation typically encountered in existing confined harbours and waterways, the modern vessel frequently encounters shallow-water conditions far offshore and in water previously considered deep for smaller vessels, see Fig.1. Shallow-water remains, however, no less a hazard for small ships in minor waterways and ports.

One of the primary risks when operating in a confined physical environment is the danger of grounding. It is extremely important to be able to predict which of the vessel's extremities will experience the greatest sinkage and ground. Where the underkeel clearance is low, reasonable accuracy is demanded in order to ensure safety and to avoid unduly reducing the earning capacity of the vessel by overcaution. This requires a sound knowledge of the vessel's tendency to "squat".

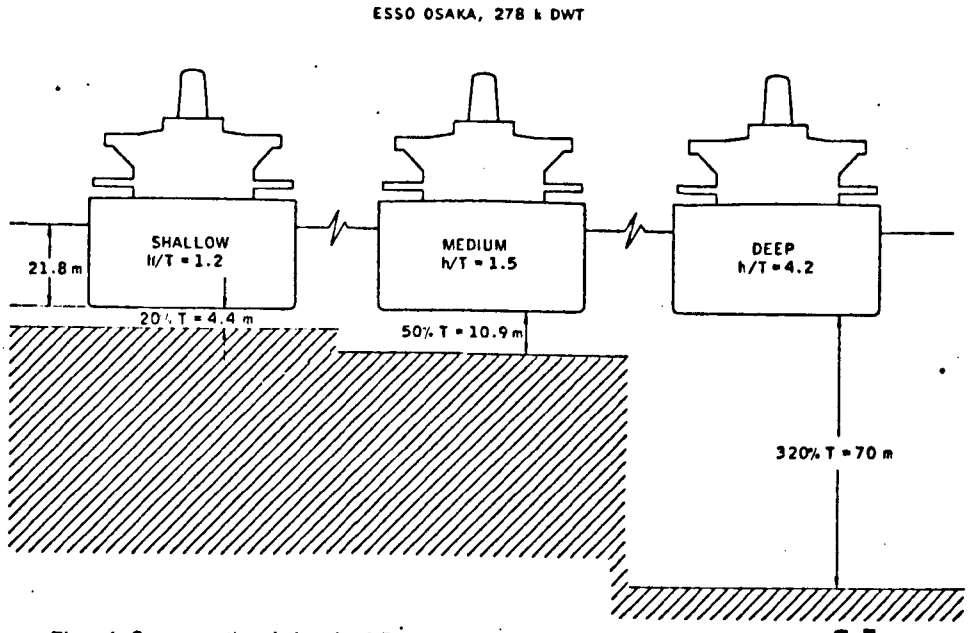

Fig. 1 Cross-sectional sketch of *Esso Osaka* relative to the three water depths [14]

In 1975, the National Ports Council of the United Kingdom published a 2-volume report of an investigation entitled "Port Approach Design - A Survey of Ship Behaviour" [53]. This was essentially a comprehensive literature survey of shallow-water research followed by a state-of-the-art statement. The investigation, involving mono-hull aspects only, concluded that "....due to the diversity of research methodology and conflicting results, few definitive answers could be given with a high degree of accuracy", The study identified certain aspects of ship behaviour requiring further research which were concentrated under 5 subject headings, one of which is "The squat of ships underway in shallow and confined waters". A contract was placed with NMI for the work to be undertaken over a period of several years and the first 2 reports were published during 1980. The NPC work is complementary and details aspects not covered in this thesis.

From early studies at Glasgow it became apparent that sinkage and trim underway have obvious practical applications and, owing to the practice of measuring changes in sinkage and trim in conjuction with resistance tests, a considerable amount of data under controlled conditions had been collected and analysed. Full-scale experiments had been conducted on a number of full-form ships in both deep and shallow-water. The subsequent objective was an extensive study of a wide range of squat related effects using a representative model of a modern, full-form ship, in order to examine the existing theories and provide a reasonably accurate prediction method. In 1979, a programme of deep and shallow-water mono-hull experiments was devised and carried out with a model of the M.V. "Wellpark", a modern (1977) bulk-carrier whose grounding incident in the La-Plata estuary was investigated by Glasgow University, see Ferguson, Seren and McGregor [28]. The experimental programme was subsequently extended to examine and incorporate the effects of lateral restrictions.

In common with mono-hulls, structures for offshore engineering, whether fixed or floating, go through a floating phase before reaching their final destination. In this condition, whether towed or self-propelled, the rig floats at a light draught with normally only the hulls immersed, the remaining structure being clear of the water. Transit between sites, or from semi-sheltered waters to location, often involves passage through considerable

stretches of relatively shallow-water. Experiments show that the (deep-water) resistance of full-scale and model-scale multi-hull offshore configurations can be predicted by using the appropriate sub-critical and super-critical R_N , respectively, see Grekoussis and Miller [33]. The problem is, however, that no analogous data exists for their sinkage and trim and, therefore, it is essential to attempt to reproduce the full-scale flow pattern on model-scale. Since no information on the shallow-water water behaviour of offshore platforms appears to have been published to date, a study of the parameters affecting multi-hull squat and resistance in shallow-water was included under the sponsorship of the SERC Marine Technology Programme.

During 1981, the High Speed Marine Vehicle Panel of the 16th ITTC prepared a hydrodynamic technology status report related to the SWATH concept, see Wilson [85]. The study concluded with various recommendations which also indicate that little published information exists for SWATHs in shallow-water. Amongst the work recommended are a study of the methods of turbulence stimulation, the review of available methods for determining wall and shallow-water effects on sinkage, trim and total resistance and the documentation of the effects of appendages and control surfaces on the rise of the centre of gravity and trim of the SWATH, particularly as related to the adopted test technique. As a result, a SWATH model was also incorporated into the experimental programme.

It is against the above general background that this study is placed.

(1.2) Basic Concepts

Since the terminology and methods of formal representation used by researchers vary, a justification of those selected is necessary. In the process a degree of quantitativeness is attached to the somewhat abstract terms used.

(1.2.a) The Squat Phenomena

All ships and offshore platforms, when underway, are subject to hydrodynamic pressure changes and friction induced trimming moments which alter their draught and trim in comparison with that when stationary. The term "squat" includes both the change in draught and the contribution due to trim underway, at any hull extremity of interest. The usual approach to squat is to treat it a steady-state problem, presenting curves for mean sinkage and trim at varying depths and speeds. The at-rest position defines the static draught and the resultant draught at forward speed, when corrected by the steady state mean sinkage and trim, is sometimes refered to as the "dynamic draught". This is somewhat of a misnomer because it is dynamic in the sense that it results from the hydrodynamic effects at forward speed and sea-bed proximity, but it is static in the sense that it is an equlibrium position under the

influence of a steady externally applied force. Hence, the term "dynamic" is avoided throughout the present work.

With a few notable exceptions, the majority of the methods used to obtain the squat component of underkeel clearance ignore the contribution due to trim. In fact, since (as will be shown) trim effects may dominate at low underkeel clearances, to be reliable any approach must consider both sinkage and trim, preferably seperately.

Besides the immediate practical application, investigations by Conn and Ferguson [12], Ferguson [27], Dand [21] and others, indicate that the sinkage and trim underway are important in the studies of the physics of ship (viscous form) resistance and other 'draught dependent' phenomena.

(1.2.b) The Analogy with Certain Gas Flows

The fact that shallow-water flows are equivalent to certain flows of a compressible gas has long been appreciated, see Stoker [71]. In particular, there is a close analogy between long-wave theory and linear aerodynamics which manifests itself in the equivalence between the Froude number based on water depth and the Mach number, see Tuck and Taylor [76]. This is confirmed by both theory and experiment, indicating that the ratio of the vehicle speed and the fundamental wave speed in the medium is of primary importance. The Froude depth number,

$F_h = U/\sqrt{gh}$, is employed as the speed parameter in shallow-water throughout this thesis.

Most practical interest lies in the subcritical range of Froude depth numbers, and greatest usefulness is attained in the limit as $F_h \dashrightarrow 0$, in which case the free-surface becomes a "rigid" plane of symmetry.

(1.2.c) Preliminary Definitions

This study is concerned primarily with (laterally) "unrestricted shallow-water", which is restricted in depth only, and with "restricted shallow-water", where restrictions are imposed in both depth and width. The shallow-water regime classifies a range of depths throughout where bottom proximity has a dominant effect on the vessel behaviour. This requires the water-depth to be comparable with the ship draught and indicates that the water-depth to ship-draught ratio is of considerable significance. The depth-draught ratio, h/T, where T is the maximum ship draught, is employed throughout this thesis. The present study assumes that, in terms of the depth-draught ratio, the shallow-water regime is confined to $1.0 < h/T < 2.0$. The distinction between "shallow water" and water of "finite depth" is important, particularly from the theoretical point of view. The "finite-depth" regime classifies a range of depths throughout where the sea/tank bottom has a significant, but not dominant, effect on ship hydrodynamics. Experiments

indicate that the "finite-depth" regime is confined to $2.0 \leq h/T \leq 5.0$. $h/T > 5.0$ may be considered "deep water" for all practical purposes.

The term (laterally) "restricted" may be further divided into "finite" and "narrow" regimes. The "finite-width" regime is normally assumed to extend between $1 < W/L < 3$. For widths greater than approximately 3 ship lengths, theory indicates that conditions become equivalent to laterally unrestricted shallow-water. (Experimental data suggests, however, that W/L ratios greater than 1.5 are approximately equivalent to (laterally) unrestricted shallow-water conditions). Widths less than 1 ship length, or comparable with the ship breadth, are considered "narrow" requiring a 1-D approach.

(1.2.d) Contributing Factors and Formal Representation

In order to reduce the problem to that of solving only one boundary-value problem and enable an evaluation of the more important parameters of interest, both vessel speed and water-depth were assumed to be sufficiently slowly varying functions of time to neglect unsteadiness. However, since inevitably bottom and side-wall geometry will affect the behaviour, unsteadiness is investigated separately, see section (4.3.d).

Even within this simplified framework, the underkeel clearance underway depends on a wide range of factors. It

is affected by local environmental conditions (such as water depth, lateral restrictions, current, thermoclines, sea-state, variations in bottom topography, channel/fairway geometry, position in channel, wind, density, etc.) and by hull features (such as, number of hulls, geometry, trim, draught, number and type of propulsion, hull fittings, appendages, etc.) From these only a number could be selected and examined.

In the plotting of the results, certain non-dimensional parameters have been used,

(a) The non-dimensional sinkage coefficient,

$$C_S = \frac{100(s_{FP} + s_{AP})}{2L} = \frac{100 \times s_M}{L} \qquad \ldots\ldots (1.2.1.a)$$

(b) The non-dimensional trim coefficient,

$$C_T = \frac{100(s_{FP} - s_{AP})}{L} = \tau \times 100 \qquad \ldots\ldots (1.2.1.b)$$

where s_{FP} and s_{AP} are the sinkages measured at the forward and aft perpendicular, respectively, and τ is the trim angle in radians. The above have been non-dimensionalized, and are presented as a percent of the ship length. This is because the length remains fairly constant throughout changes in speed and operating condition and C_T is then usefully a direct measure of the trim angle, see Dand [16]. Sinkage is assumed negative in the downward z-direction, while trim is defined negative when by-the-bow.

CHAPTER 2

Theoretical Approaches

(2.1) General

Practical problems in ship hydrodynamics have generally resisted theoretical modelling, not because the basic physical principles governing the problem at hand were unknown but because their 3-D mathematical representation has been relatively intractable. It is, therefore, normally necessary to make restrictive assumptions, about the nature of the fluid, its motion and its generation, which yield more tractable mathematical formulations without significantly diverging from reality. Fortunately, a number of problems, in which the consideration of shallow water effects as well as the complexities of the physical environment are important, can be described reasonably well by the resulting approximate approaches.

It is generally accepted that the desired theory can be attained by neglecting surface-tension effects and considering the fluid to be ideal (ie. incompressible, irrotational, inviscid and homogenous). Within this framework there have been several different approaches which can be distinguished according to the simplifying

assumptions made. The main theoretical simplification suggests itself on the basis of the physical circumstances and results from the hypothesis that the depth of the water is small in comparison to some other significant length (say, the characteristic length of the surface waves). The only assumption made in deriving the general theory (in addition to those customary in hydrodynamics) is that the hydrodynamic pressure is independent of the depth. (It is, however, also possible to derive this hydrostatic pressure relation as the lowest order approximation in a formal perturbation scheme, see Friedrichs [30]). The resulting 2-D "shallow-water theory" is valid for waves whose amplitude is not necessarily small (provided the hydrostatic pressure relation is not invalidated) and leads to a system of non-linear partial differential equations and to formidable mathematical difficulties. A mathematical analogy with certain cases of motion of compressible gases, to which special exact solutions exist, leads to some valuable solutions.

The difficulties have led to the extensive use of linear approximations in hydrodynamics. Linearization is obtained by rejecting all the non-linear terms in the equations of motion and the boundary conditions, on the additional assumptions that that the departure of the free-surface from a plane and the fluid velocity from a uniform stream is small. The resulting "linearized shallow water theory" is applicable, with good approximation, to many practical problems although its solutions are subject

to severe limitations. It is consistent with this type of approximation to satisfy the free-surface boundary conditions at the undisturbed position z=0, rather than at the appropriate vertical elevation of the free-surface at $z= \eta (x,y)$. This "rigid" free-surface condition can only be justified on the ground that the Froude depth number is low, as when the characteristic wave-length is vanishingly small and the dominant hydrodynamic forces are those associated with the fluid inertia. Since the speed of ships in restricted water is generally reduced for reasons of navigational safety and, to a lesser extent, increased resistance, the neglect of free-surface effects (or equivalently the zero-Froude number approximation) seems more plausible in restricted water than is the case for unrestricted deep water. However, a difficulty with the linearized version is that it clearly breaks down whenever the slope of any boundary surface (ship, water surface, side or bottom) is not small. In order to make further progress it is necessary to restrict the form of the immersed body, so that its motion through the water does not violate the basic assumptions of linearization. As shown later, this allows the construction of an approximate solution by solving a sequence of 2-D sub-problems, see (2.2.a).

J.H. Michell's [51] analytical treatment of the steady fluid flow past a ship-like body was the first to be based upon hull geometry assumptions, requiring the ship to be "thin" (ie, its beam to length ratio of $O(\varepsilon)$, where

ε is a small positive parameter, and its draught to length ratio of O(1), or of the order of the ship length). In spite of many recent developments, Michell's approximate method has dominated the subsequent experimental and theoretical work, particularly in the field of wave resistance. It has since been imbedded in a systematic perturbation procedure by Peters and Stoker [56], who were the first to note that the calculation of sinkage and trim is as much a part of the first-order theory as is the wave resistance. Most subsequent treatments, however, disregard the fact that the method yields explicit formulae for the (deep water) sinkage and trim of the ship. This appears to have been exploited only by Havelock [84], Dand [21] and, more recently, by Yeung [88] on the basis of formulae derived by Wehausen [82]. Another less appreciated feature of Michell's original paper, is his solution for the laterally unrestricted shallow water problem for a wall-sided "thin" ship with no bottom clearance. (The result was later rediscovered by Joukowski [39] and used extensively in aerodynamics). Although Michell's investigation serves as a basis for subsequent shallow-water theories of squat, it cannot provide for the vertical force and moment which are necessarily zero for "thin" wall-sided struts with no underkeel clearance.

Since practical ships are not "thin" (their breadth to draught ratio is normally greater than 1), other approximation schemes were sought. The "flat" ship theory, introduced by Hogner [35] to overcome the limitations of

the "thin" ship, is limited to hulls with negligible draught (such as planing craft) and suffers from similar drawbacks although "reversed", since now the draught to length ratio is assumed of $O(\varepsilon)$ while the breadth to length ratio is of $O(1)$. Another approximation scheme, a "slender" ship approximation, based on the assumption that both beam and draught are small in comparison to the ship length (ie. of $O(\varepsilon)$), would intuitively seem better suited to conventional ship forms. The method has its origins in aerodynamics and was introduced to hydrodynamics, more or less simultaneously, by Maruo [45], Vossers [81] and Tuck [73], the last being the more systematic approach. A major feature distinguishing slender-body hydrodynamics from those of aerodynamics is the appearance of a free-surface and, therefore, gravity (or Froude number) as an extra parameter. This parameter requires a reasonable assumption about its order of magnitude with respect to ε. The usual procedure in analysing ship wave resistance is to assume that $g=O(1)$ as $\varepsilon \longrightarrow 0$, ie. $1/F_L^2 = O(1)$. This means that gravity dominates the free-surface near the body but ordinary gravity waves occur at a large distance from it. (Conversely, if $g=O(\varepsilon)$ then gravity waves occur near the body but vanish at large distances away, where the free-surface becomes a "rigid" plane.) This distinction between the "inner" field and "outer" field behaviour suggests a method of solution which makes these differences clear.

The classical work in applying the "slender" ship

theory to the prediction of shallow water effects on ship hydrodynamics is due to Tuck [74], who verified that Michell's conclusions with regard to (zero) wave resistance still hold for arbitrary ship geometry, provided the ship is slender. By removing the geometrical limitations of the "thin" ship, Tuck obtained the steady-state sinkage and trim of a slender ship moving with steady speed in laterally unrestricted shallow water of uniform depth. By assuming that $F_h=O(1)$, Tuck's analysis contains the leading order effects of the free-surface and uses the method of matched asymptotic expansions to construct an approximate solution for the subcritical and supercritical regimes in terms of the Froude depth number.

The theory was shown by Tuck to be in fair quantitative but good qualitative agreement with model experiments of Graff, Kracht and Weinblum [32], when evaluated at a water-depth to ship-length ratio of 1/8. The tendency of the theory to underestimate the subcritical sinkage and trim was confirmed, for a towed full-form model, by Dand [19], and is consistent with the 3-D finite (as distinct from shallow) depth theory of Tuck and Taylor [76]. The shallow water limit of the finite-depth theory, attained by allowing the depth to tend to zero relative to the characteristic wavelength, indicates that for a mathematically shaped ship the 2-D "shallow water theory" provides acceptable results up to a water-depth to ship-length ratio of 1/10. (Considering a ship length-beam ratio of 6 and beam-draught ratio of 3, this is equivalent

to a water-depth to ship-draught ratio of 1.8.) The approach is invalid in the transcritical regime where the linear approximation does not apply and predicts infinite squat at the critical (F_h=1) speed.

Various other generalizations have been made of Tuck's original treatment. Some success in developing an appropriate non-linear theory has been achieved by Lea and Feldman [44] and generalized by Mei [49]. By modifying Tuck's perturbation analysis for the neighbourhood of the critical speed, the transonic equation in aerodynamics was obtained. In better agreement with reality, this theory predicts finite and continous squat values throughout the transcritical regime and points out the importance of non-linear effects. More recently, Maruo and Tachibana [46] analysed ship sinkage in the subcritical and transcritical regimes using a method which enables the solution to preserve the non-linear characteristics of the governing equation. The calculations based on this approach illustrate the dependence on water depth and suggest that Tuck's linear approach does not represent an assymptote of the non-linear results. A rough comparison with experimental data was obtained. Although valuable theoretically, the transcritical regime is of negligible practical value in laterally unrestricted shallow water, since full-form displacement ships seldom attain the speed necessary to induce transcritical (or supercritical) phenomena under such conditions. These regimes may, however, assume greater practical significance under

laterally restricted conditions, particularly in narrow, shallow channels. Lateral restrictions (or the increased blockage resulting therefrom) have a significant effect on the critical speed. Tuck [75] extended the approach to treat the case of subcritical motion along the centreline of a rectangular channel, although the validity of the formulae is restricted to channels of finite (as distinct from narrow) breadth. Beck, Newman and Tuck [6] extended the analysis to include the case of a ship travelling along the centreline of a dredged channel surrounded on both sides by shallow-water. Using the same approach, Beck [5] examined the problem of a ship operating off the centreline of a rectangular channel.

The possibility of estimating the sinkage and trim by subdividing the hull surface into a number of panels and so calculating the pressure distribution over the hull was examined by Dand [19]. Utilizing the Gadd [31] method, the approach was shown to require a very detailed description of the hull geometry, made heavy demands on computer time and, therefore, precludes rapid estimation using minimum input design data. The theoretical assumptions are similar in nature to those made by the hydrodynamic approach of Tuck, and the results of the two methods were shown to be in close agreement.

Taken to its lowest approximation, the "shallow water" theory yields the basic 1-D theory used in hydraulics to study the flow in open channels (although the latter is

derived by somewhat different arguments). This is the simplest and most common method of analysis, yielding entirely adequate solutions to many problems requiring the determination of the total forces, rather than pressure distributions, or average velocities rather than velocity distributions. In a 1-D analysis, velocities and pressures are assumed to vary only with the general direction of flow and the mean values of the velocity on planes normal to this flow direction are adopted for the purposes of calculation. The approach is only useful in channels of a width comparable to the ship breadth, where the 1-D character of the flow combined with the hydrostatic assumption implies that the ship simply rides up and down with the (local) water level. Under such conditions the ship may be replaced by a fixed obstacle and a "hydraulic analogy" approach used. This results in formulae which are commonly used to connect the midship mean sinkage with the geometric particulars of various channel cross-sections, in both the subcritical and supercritical regimes in terms of the Froude depth number. In narrow, shallow channels the transcritical and supercritical regimes assume greater practical significance. Within the hydraulic context it has been shown that there exists a wide range of transcritical speeds (including the critical), throughout which steady-speed is theoretically impossible and, in practice, a "bore" forms ahead of the ship if any attempt is made to exceed it. Commencing with a clever application by Kreitner [44], later expanded by Kinoshita [41], Constantine [13] and, more recently, Dand and Ferguson

[23], the approach has had important applications in restricted waterway operation. It also has led to a number of blockage formulas used in model testing.

Theory provides an essential insight into the nature of the problem and is a necessary foundation to its scientific understanding and solution. Some knowledge of the nature of the physical approximations inherent in the (2-D) hydrodynamic and (1-D) "hydraulic analogy" approaches is also necessary in assessing their limitations and applicability to the problem examined. The detailed derivation and discussion of the mathematical formulations follows. An analysis of the effects of each of the assumptions made is contained in later chapters.

(2.2) The Hydrodynamic Approach, Unrestricted Shallow Water

In this section the "slender" ship solution of the problem is developed by formulating the boundary-value problem for the appropriate velocity potential and following a solution technique based on the method of matched asymptotic expansions. Only the linear, or lowest order, problem will be solved and the theory then used to predict the hydrodynamic vertical (sinkage) force and (trim) moment for the laterally unrestricted shallow-water condition. The physical interpretation of the approximations is discussed.

(2.2.a) Problem Formulation

The problem to be solved is that of the steady motion of a (rigid) slender ship translating with a speed U on the free surface of an ideal fluid in shallow-water.

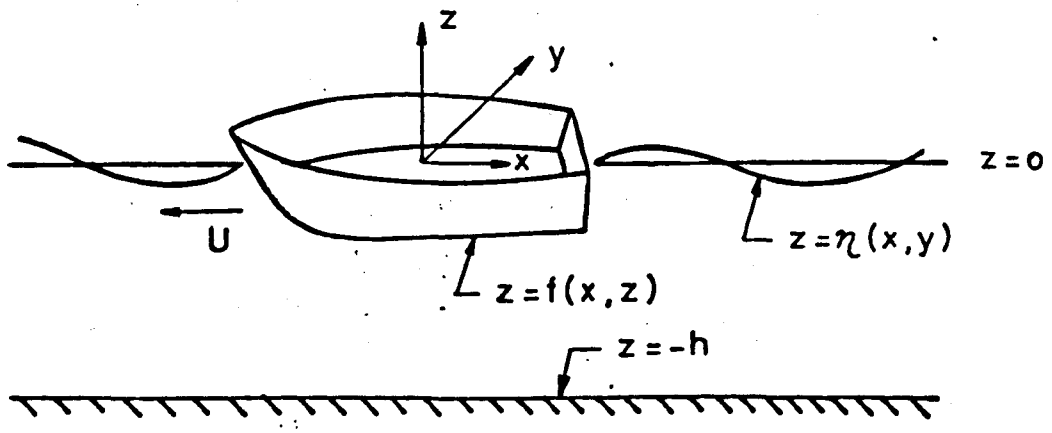

Fig.2; Coordinate System

Following Tuck [74], a Cartesian (x,y,z) coordinate system is employed with the origin located amidships, the z axis positive upwards and the x-axis coincident with the ship longitudinal centerline, positive towards the stern. The z=0 plane is coincident with the free-surface and the fluid assumed to occupy the domain $-h<z<0$, except for the interior the body. The ship is assumed fixed and the fluid flow velocity, U, steady in the positive x-direction, see Fig.2.

The slenderness assumption is formulated by letting the ship beam and draught be small, of $O(\varepsilon)$, with respect to its length. The shallowness assumption is introduced by assuming the water depth to be of $O(\varepsilon)$, or of the ship draught. To ensure significant wavemaking, the Froude depth number, $F = U/\sqrt{g\varepsilon h}$, is assumed of O(1). This implies that the conventional Froude number based on length, F_L, is small and of $O(\varepsilon^{\frac{1}{2}})$. However, since it may be shown that the results which follow are equally valid in the limit as the free-surface becomes a "rigid" wall, the linearised free-surface condition is imposed. The slenderness and shallowness assumptions are not unrealistic and will later permit a decomposition of the full 3-D problem formulated here into two sub-problems, the so-called "inner" and "outer" problems, according to whether the distance from the longitudinal axis is of $O(\varepsilon)$ or O(1), respectively.

The mathematical formulation of the problem in terms of the hydrodynamic theory is then as follows. There

exists a velocity potential ϕ (x,y,z), the positive gradient of which represents the fluid perturbation velocities induced by the ship, which will satisfy Laplace's equation throughout the fluid domain (except possibly in the vicinity of the wake region)

$$\nabla^2\phi = \phi_{xx} + \phi_{yy} + \phi_{zz} = 0 \qquad \ldots\ldots (2.2.1)$$

(where the letters in parenthesis show the dependence on the space coordinates and subscripts without parenthesis always mean differentiation), subject to suitable boundary conditions on the bounding surfaces and the imaginary surface at infinity.

These are the kinematic condition on the bottom, assumed a plane surface z=-h,

$$\phi_z = 0 \qquad \ldots\ldots (2.2.2)$$

the kinematic boundary condition on the ship's hull, described by y= f(x,z),

$$(U + \phi_x)f_x + \phi_z f_z - \phi_y = 0 \qquad \ldots\ldots (2.2.3)$$

Imposing the linearized free-surface boundary condition on the undisturbed plane z=0,

$$U^2\phi_{xx} + g\phi_z = 0 \qquad \ldots\ldots (2.2.4)$$

The boundary-value problem is completed by requiring that the potential vanish in all directions at large distances from the body,

$$\phi \to 0 \quad \text{as} \quad \sqrt{x^2 + y^2 + z^2} \to \infty \qquad \ldots\ldots (2.2.5)$$

The problem is now represented by an approximate mathematical model. Within the limitations of the initial assumptions, the flow is specified by the solution of Laplace's equation subject to the foregoing (mixed) boundary conditions.

In accordance with the method of matched asymptotic expansions, Van Dyke [79], the above boundary-value problem is first recast into an "outer" problem, valid far from the ship, and an "inner" problem, valid very near the ship. The "inner" and "outer" solutions are simpler compared to the solution valid everywhere throughout the fluid and are treated as complementary approximations. The method involves loss of boundary conditions, since the "inner" expansion cannot be expected to satisfy conditions in the "outer" region and vice-versa. Therefore, neither is a complete solution. The two solutions are then assumed to be simultaneously valid provided they can be matched in a so-called "intermediate" region, far from the body in the "inner" domain but very near the body in the "outer" domain. The matching requirement effectively replaces the missing boundary condition at infinity in the "inner" domain and on the body in the "outer" domain and yields a

complete solution.

(2.2.b) The "Inner" Problem

The "inner" region, near the ship, is that region where owing to the slenderness assumption both y and z are small compared to the ship length. Mathematically, the coordinates assume the following orders of magnitude, $x=O(1)$ while $y,z=O(\varepsilon)$. Since the coordinates are not treated in a similiar manner it is useful to introduce "inner" variables Y,Z "stretched" according to $Y=y/\varepsilon$ and $Z=z/\varepsilon$. The capitalized quantities are then by assumption O(1) in the "inner" domain. It is assumed that the unknown velocity potential ϕ can be expanded in an asymptotic series in ε of the form,

$$\phi(x,Y,Z) = \varepsilon\phi^{(1)}(x,Y,Z) + \varepsilon^2\phi^{(2)}(x,Y,Z) + \ldots + \varepsilon^n\phi^{(n)}(x,Y,Z) \quad \ldots\ldots (2.2.6)$$

where the supercripts in parenthesis denote the order (of the highest derivative) of the equation.
The "inner" solution is governed by (2.2.1 - 2.2.4) but not the condition at infinity. When the above expansion is substituted in the Laplace equation (2.2.1) and the terms of common power grouped to $O(\varepsilon^2)$, it is found that,

$$\nabla^2(Y,Z)\phi^{(1)} = 0 \quad \ldots\ldots (2.2.7.a)$$

$$\nabla^2(Y,Z)\phi^{(2)} = 0 \quad \ldots\ldots (2.2.7.b)$$

That is, each of the individual terms in the asymptotic expansion is an independent solution of the Laplace equation in the Y,Z plane , normal to the x-axis. Each must also satisfy the bottom boundary condition (2.2.2), ie. $\phi^{(n)}=0$ on Z=-h and therefore,

$$\phi^{(1)}_Z = 0 \qquad \text{..... (2.2.8.a)}$$

$$\phi^{(2)}_Z = 0 \qquad \text{..... (2.2.8.b)}$$

The boundary condition on the hull surface and free-surface are the same as for a "slender" ship in water of infinite depth. The detailed development is given by Newman and Tuck [55]. The boundary condition on the hull, Y= f(x,z), may be written in the form,

$$\phi^{(1)}_N = 0 \qquad \text{..... (2.2.9.a)}$$

$$\phi^{(2)}_N = Uf_x(1 + f_Z{}^2)^{-\frac{1}{2}} \qquad \text{..... (2.2.9.b)}$$

where N is the outward normal to the ship cross-section (or Y,Z plane, expressed in "inner" variables) at station x. ϕ_N denotes the rate of change of ϕ normal to the cross-section. It is an approximation to the kinematic boundary condition on the actual hull surface and represents an apparent normal flow velocity across a cyllinder with a shape identical to the body cross-section at any given station along its length. The "inner" region free-surface condition (2.2.4) reduces for the first two

terms of the expansion to,

$$\phi_Z^{(1)} = 0 \qquad \text{..... (2.2.10.a)}$$

$$\phi_Z^{(2)} = 0 \qquad \text{..... (2.2.10.b)}$$

That is, the free-surface appears "rigid" in the "inner" region. The boundary condition at infinity (2.2.5) will subsequently be replaced by the matching requirement.

The "inner" problem, therefore, consists of a series of 2-D (Neumann) problems, to be solved seperately for each ship (vertical) cross-section. The $\phi^{(1)}$ and $\phi^{(2)}$ problems are illustrated in Fig.3 and 4, respectively. The solution for the first two terms of the expansion was obtained by Tuck [77] and is assisted by the fact that the main interest lies in an "intermediate" region ($Y \to \infty$) which is large compared to the ship beam but small compared to its length. It is,

$$\phi^{(1)} = F^{(1)}(x) \qquad \text{..... (2.2.11.a)}$$

$$\phi^{(2)} = F^{(1)}(x) + F_*^{(2)} \qquad \text{..... (2.2.11.b)}$$

Equation (2.2.11.a) states that the first order potential is a function of x only, where $F^{(1)}(x)$ is an arbitrary function to be found by matching. This is to be expected by (2.2.9.a), where $\phi^{(1)}$ is seen to be constant with respect to both y and z.

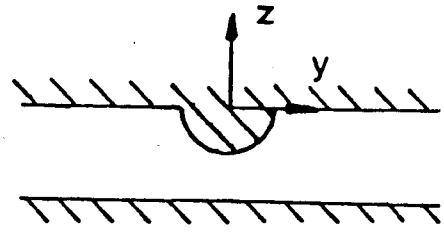

Fig.3; First-Order, "Inner" Region

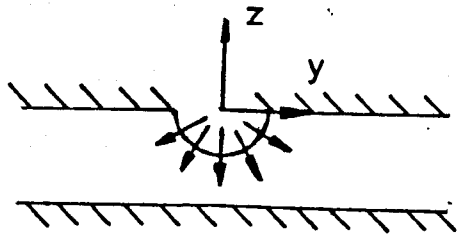

Fig.4; Second-Order, "Inner" Region

The solution to the second-order potential (2.2.11.b) contains two terms. $F^{(2)}(x)$ is associated with the streaming flow past the ship cross-section and its magnitude is unknown. $F_*^{(2)}$ is associated with the flow pushed symmetrically aside by the ship and may be solved by examining the net flux emitted from the body boundary in the intermediate region. Using conservation of mass, the solution may be obtained in terms of the change in ship cross-sectional area,

$$F_*^{(2)} = \frac{US'(x)}{2h} + O(1) \qquad \ldots\ldots (2.2.11.c)$$

where $S(x)$ is the immersed ship cross-sectional area below $z=0$ and the prime denotes differentiation with respect to x. The $O(1)$ term implies that $F^{(2)}(x)$ tends to zero as $Y \to \infty$.

Physically, the second order solution may be anticipated from the fact that the longitudinal motion of the ship displaces the surrounding fluid with an outward flux equal to (minus) the change in the ship cross-sectional area. In shallow-water this flux is constrained by the "rigid" free-surface Z=0 and the bottom Z=-h. Considering a control volume, far from the hull (assumed symmetric about the plane Y=0) but in the "inner" region, the flux must be a horizontal streaming flow divided symmetrically in two directions. The velocity in the y direction at which this pushing aside takes place can be written as,

$$\phi_y = \frac{US'(x)}{2h} \qquad \ldots\ldots (2.2.12)$$

See Tuck [77,78] for a more detailed discussion of the solution to the $\phi^{(1)}$ and $\phi^{(2)}$problem.

(2.2.c) The "Outer" Problem

In the "outer" region, far from the ship, the ship appears to collapse into a line of negligible thickness on the x-axis. Mathematically, the ship, being "slender", is represented in the limit as its beam to length ratio tends to zero, by a line segment $y=0_{\pm}$, $|x|<L/2$ on the x-axis in the horizontal (x,y) plane. For the "outer" problem, x and y are both of O(1) while z is $O(\varepsilon)$ because of the shallowness assumption. The corresponding "outer" problem solution could be obtained by retaining the $Z=z/\varepsilon$ "inner"

variable and carrying out the expansion as in the previous section. Alternatively, utilizing the linearized free-surface condition, the leading order terms will be obtained by assuming that $\phi(x,y,z)$ posesses a Taylor expansion of the form,

$$\phi(x,y,z) = \Phi(x,y) + (z + h)\Phi_z(x,y) + \tfrac{1}{2}(z + h)^2\Phi_{zz}(x,y) + \ldots \quad \ldots\ldots (2.2.13)$$

with respect to z and about the bottom z=-h, valid throughout the "outer" region.

The "outer" solution is governed by (2.2.1 - 2.2.5), except the body boundary condition (2.2.3). The body boundary condition (2.2.3) is not applicable to the "outer" problem, since to an observer of the order of the ship length away, the ship appears to have collapsed into a line. Instead it has to satisfy additional conditions obtained by matching the "inner" and "outer" solutions.

Imposing the bottom boundary condition (2.2.2), the second term in the Taylor expansion vanishes. If Laplace's equation (2.2.1) is rewritten in the form,

$$-\phi_{zz} = \phi_{xx} + \phi_{yy} = \nabla^2(x,y) = 0 \quad \ldots\ldots (2.2.14)$$

then (2.2.13) becomes,

$$\phi(x,y,z) = \Phi(x,y) - \tfrac{1}{2}(z + h)^2\Phi(x,y) + \ldots \quad \ldots\ldots (2.2.15)$$

and

$$\Phi_z = -(z + h)\nabla^2(x,y)\Phi(x,y) \qquad \ldots\ldots (2.2.16.a)$$

$$\Phi_z = -h\nabla^2(x,y)\Phi(x,y) \qquad \ldots\ldots (2.2.16.b)$$

on z=0.

Substituting into the linearized free-surface condition (2.2.4), yields,

$$-gh\nabla^2(x,y)\Phi(x,y) + U^2\Phi_{xx}(x,y) = 0 \qquad \ldots\ldots (2.2.17.a)$$

or alternatively,

$$\delta^2\Phi_{xx} + \Phi_{yy} = 0 \qquad \ldots\ldots (2.2.17.b)$$

where

$$\delta^2 = 1 - F_h^2 \qquad \ldots\ldots (2.2.17.c)$$

That is, the leading term of the "outer" asymptotic expansion of the potential satisfies a 2-D equation in the horizontal (x,y) plane and is independent of the vertical (z) coordinate. The physical interpretation of this approximation is the neglect of the vertical velocity components in comparison to the horizontal components (except very near the ship, ie. the "inner" region). Equation (2.2.17) is identical to that derived and solved by Michell [51] as part of an investigation of the wave resistance of ships. The "outer flow problem is shown in Fig.5.

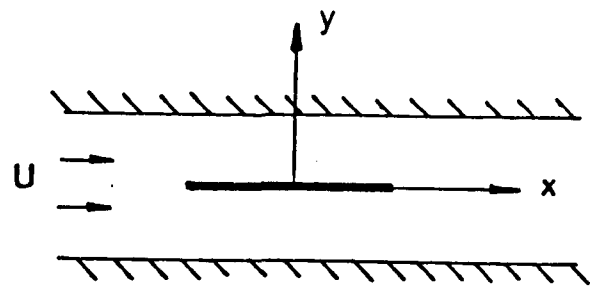

Figure 5: "Outer" Flow Region

The character of the above equation is clearly different depending upon whether $F_h<1$ (subcritical) or $F_h>1$ (supercritical). In any event, since the flow is expected to change significantly as it passes through the critical ($F_h=1$) region, separate solutions must be developed for each case. In fact, equation (2.2.17) is mathematically identical to that governing the linearized, steady-state, 2-D flow in aerodynamics, to which solutions are known. In accordance with section (2.1) only the subcritical regime is considered, within which equation (2.2.17) may be solved formally using Green's function source distributions to yield;

$$\phi^{(1)} = \int_{-\infty}^{\infty} G(x - k, y)\mu(k)\,dk \qquad \ldots\ldots (2.2.18.a)$$

with $G(x,y)=(2\pi\delta)^{-1}\log(x^2 + \delta^2 y^2)^{\frac{1}{2}}$ $\ldots\ldots$ (2.2.18.b)

as the Green's function (or unit source potential) for $F_h<1$. The constant δ is introduced to "stretch" the y-coordinate so that equation (2.2.17) is satisfied instead

of the usual 2-D Laplace equation. k is the source point coordinate and μ is the still unknown source strength to be determined by matching.

(2.2.d) Matching

The two 2-D "inner" and "outer" solutions are consistent provided they can be matched in an "intermediate" region, ($\varepsilon << y << 1$), far from the ship in the "inner" domain but very close to the body in the "outer" domain, where both expressions are valid. The appropriate "outer" solution (2.2.18) is a distribution of 2-D sources along the body axis, which satisfy (2.2.5) at infinity and must be matched with the "inner" solution (2.2.11) near the hull. The matching requirement, which follows, determines the source strength, μ , and ultimately determines the magnitude of the arbitrary constant, $\phi^{(1)}$, of the "inner" solution.

The "inner" and "outer" expansions are matched using a matching principle from Van-Dyke [79,p.90],

"The m-term inner expansion of the n-term "outer" expansion = the n-term outer expansion of the m-term "inner" expansion, for any pair of integers m,n"

The process requires the outer limit of the "inner" solution ($y >> \varepsilon$) and the inner limit of the "outer" solution ($y << 1$). The `2-term` inner expansion of the `1-term`

"outer" solution (2.2.17), near y=0 , is,

$$\phi^{(1)}(x,0) + \mu(x,0)|y| \qquad \ldots\ldots (2.2.19.a)$$

where

$$\phi^{(1)} = \frac{1}{\pi\delta}\int_{-\infty}^{\infty} \mu(k)\log|x-k|\,dk \qquad \ldots\ldots (2.2.19.b)$$

is obtained by setting y=0 in the argument of the logarithm. The `1-term` outer expansion of the `2-term` "inner" solution (2.2.11) is,

$$\phi^{(1)}(x) + \frac{US^1(x)|y|}{2h} \qquad \ldots\ldots (2.2.20)$$

Equating (2.2.19) and (2.2.20) yields,

$$\phi^{(1)}(x) + \frac{US^1(x)|y|}{2h} \qquad \ldots\ldots (2.2.21.a)$$

$$\mu(x) = \frac{US^1(x)}{2h} \qquad \ldots\ldots (2.2.21.b)$$

The matching process is now complete and results in an expression for the source strength in terms of the change in ship (immersed) cross-sectional area. Equations (2.2.19) and (2.2.21) determine the lowest order velocity potential in the "inner" region to be,,

$$\phi^{(1)} = \frac{U}{2\pi h\delta}\int_{-\infty}^{\infty} S^1(k)\log|x-k|\,dk \qquad \ldots\ldots (2.2.22)$$

(2.2.e) The Hydrodynamic Force and Moment

The forces and moments acting on the vessel can be determined by integrating the hydrodynamic pressure over the body surface. The lowest order forces are found in terms of the now known source strength by substituting the "inner" expansion (2.2.11) into the Bernoulli equation,

$$-\frac{p}{\frac{1}{2}\rho U^2} = 2\phi_x + \phi_x^2 + \phi_y^2 + \phi_z^2 \qquad \ldots\ldots (2.2.23)$$

Retaining only terms to the second order, the following expression for the fluid pressure p(x,Y,Z) is obtained,

$$p(x,Y,Z) = \varepsilon p_1(x) + \varepsilon^2\left[p_2(x) + P(x,Y,Z)\right] + O(\varepsilon^3) \qquad \ldots\ldots (2.2.24)$$

where

$$p_1(x) = -\rho U F^{(1)}{}'(x)$$

$$p_2(x) = -\rho U F^{(2)}{}'(x)$$

$$P_2(x,Y,Z) = -\rho U\left[F^{(2)}_{*X} + \tfrac{1}{2}(F^2_{*Y})^2 + \tfrac{1}{2}(F^2_{*Z})^2\right]$$

It is important to note that the pressure acting on the immersed hull has two components, one (p) depending on the longitudinal (x) location only and the other (P) varying around the (vertical) cross-section (or Y,Z plane in "inner" variables) only.

To a first order, in the "inner" region, the hydrodynamic pressure acting on the immersed part of the hull is dominated by the term,

$$p_1(x) = -\rho U F^{(1)'}(x) + O(\varepsilon^2) \qquad \ldots\ldots (2.2.25.a)$$

or, using (2.2.11),

$$p_1(x) = -\rho U \phi^{(1)'} \qquad \ldots\ldots (2.2.25.b)$$

and appears predominantly constant everywhere in the fluid at a given station, irrespective of its cross-sectional shape. This is to be expected since the z-dependence was neglected as part of the shallowness assumption and the y-dependence as part of the slenderness approximation.

From (2.2.22) the longitudinal perturbation velocity, $\phi_x^{(1)}$, is,

$$\phi_x^{(1)} = \frac{U}{2\pi h\delta} \int_{-\infty}^{\infty} \frac{S^1(k)}{x-k}\, dk \qquad \ldots\ldots (2.2.26)$$

The lowest order hydrodynamic force may be found by making use of a relation developed by Newman and Tuck [55],

$$-\iint ds p_1(x) \underset{\sim}{n} = \underset{\sim}{i} \int dx p_1(x) S^1(x) + \underset{\sim}{k} \int dx p_1(x) B(x)$$

The first term on the right hand side is the horizontal-plane (wave resistance) component and is zero in shallow water. The second term is the vertical-plane component. Therefore, to a leading order, the vertical hydrodynamic force is $p_1(x)B(x)$ per unit length and the longitudinal perturbation velocity (2.2.26) may be used to obtain the vertical-plane force (positive upwards) and

moment (positive bow-up) acting on the ship from pressure integration in the forms,

$$F = -\rho U \int_{-L/2}^{L/2} B(x)\,\phi_x^{(1)}\,dx \qquad \ldots\ldots (2.2.27.a)$$

$$M = \rho U \int_{-L/2}^{L/2} (xB(x))\,\phi_x^{(1)}\,dx \qquad \ldots\ldots (2.2.27.b)$$

where B(x) denotes the local waterplane offset (or beam).

In the subcritical case, integrating (2.2.27) by parts before substituting (2.2.26) and (2.2.17.c), the hydrodynamic force and moment may be written as,

$$F = \frac{\rho U^2}{2\pi h\sqrt{1-F_h^2}} \int_{-L/2}^{L/2} dx \int_{-L/2}^{L/2} B^1(x)\,S^1(k)\log|x-k|\,dk \qquad \ldots\ldots (2.2.28.a)$$

$$M = -\frac{\rho U^2}{2\pi h\sqrt{1-F_h^2}} \int_{-L/2}^{L/2} dx \int_{-L/2}^{L/2} (xB^1(x))\,S^1(k)\log|x-k|\,dk \qquad \ldots\ldots (2.2.28.b)$$

(2.2.f) Sinkage and Trim

The sinkage and trim may now be estimated by equating the derived force and moment with the hydrostatic restoring force and moment. If sinkage and trim are assumed small, the following expressions for the restoring force and moment may be applied,

$$F = \rho g s_M \int_{-L/2}^{L/2} B(x)\,dx \qquad \ldots\ldots (2.2.29.a)$$

$$M = \rho g \tau \int_{-L/2}^{L/2} x^2 B(x)\,dx \qquad \ldots\ldots (2.2.29.b)$$

where s_M is the mean sinkage, τ the trim angle in radians and it is assumed that $GM_L = BM_L$. Equating (2.2.28) and (2.2.29) and introducing the non-dimensional sinkage and trim coefficients (1.2.1), it follows that,

$$C_s = 100 \frac{\nabla F_h^{\,2}}{L^3\sqrt{1-F_h^{\,2}}}\ \lambda_s \qquad \ldots\ldots (2.2.30.a)$$

with λ_s

$$= -\frac{L^2 \int_{-L/2}^{L/2} dx \int_{-L/2}^{L/2} B^1(x) S^1(k) \log|x-k|\,dk}{2\pi \int_{-L/2}^{L/2} B(x)\,dx \int_{-L/2}^{L/2} S(x)\,dx} \qquad \ldots\ldots (2.2.30.b)$$

and $$C_T = 100 \frac{\nabla F_h^{\,2}}{L^3\sqrt{1-F_h^{\,2}}}\ \lambda_T \qquad \ldots\ldots (2.2.31.a)$$

with λ_T;

$$= \frac{L^3 \int_{-L/2}^{L/2} dx \int_{-L/2}^{L/2} (xB^1(x)) S^1(k) \log|x-k|\,dx}{2\pi \int_{-L/2}^{L/2} x^2 (B(x)\,dx \int_{-L/2}^{L/2} S(x)\,dx} \qquad \ldots\ldots (2.2.31.b)$$

where $\nabla = \int_{-L/2}^{L/2} S(x)dx$ is the volume of displacement.

(2.2.g) Qualitative Features

An interesting feature of the first-order theory is that the sinkage and trim coefficients depend only on the hull geometry and do not depend explicitly on the water depth. Hence, plotting against the Froude depth number

will result in a unique curve. The approach implies that there is no dependence of the hydrodynamic pressure on depth, which suggests that underneath sections with low underkeel clearance the flow passes aside to maintain constant pressure, rather than increase its velocity. The theory also indicates that in the subcritical regime in terms of the Froude depth number a (downward) sinkage force is to be expected.

As the first-order hydrodynamic theory yields zero wave resistance in shallow-water, it inherently neglects any contribution from the horizontal non-viscous component multiplied by some fraction of the draught. In addition, not all ship forms can be generated by singularities, distributed over the longitudinal centreplane, the waterplane or the hull surface. In particular, it is impossible to expect the blunt bow or stern sections to be adequately represented by the slender or thin-ship theories since the slenderness or thinness assumptions are violated locally there.

In order to deduce additional qualitative features capable of generalization and to establish parameters which are a function of the hull shape, it is useful to represent the ship form analytically. A simple expression which is well suited to the problem in hand and which reasonably approximates the full-form ship surface, was suggested by Vermeer [80]. If the hull-from is appropriately non-dimensionalized with respect to the ship length,

maximum breadth and cross-sectional area and the LCF and LCB assumed positive when measured aft of midships, then,

$$(a) \quad B(x)=1-x^2+\alpha_B x^2(1-x)+\beta_B x^3(1-x^2)$$

$$(b) \quad S(x)=1-x^2+\alpha_S x^2(1-x^2)+\beta_S x^3(1-x^2)$$

The hull geometry parameters are defined by,

$$C_{wp} = \frac{1}{2}\int_{-1}^{1} B(x)\,dx = \frac{2}{3}\left(1+\frac{\alpha_B}{5}\right)$$

$$C_{pl} = \frac{1}{2}\int_{-1}^{1} S(x)\,dx = \frac{2}{3}\left(1+\frac{\alpha_S}{5}\right)$$

$$LCF = \frac{1}{4C_{wp}}\int_{-1}^{1} xB(x)\,dx = \frac{\beta_B}{35C_{wp}}$$

$$LCB = \frac{1}{4C_{pl}}\int_{-1}^{1} xS(x)\,dx = \frac{\beta_S}{35C_{pl}}$$

$$R_L^2 = \frac{1}{8C_{wp}}\int_{-1}^{1} x^2B(x)\,dx = \frac{1}{14C_{wp}}\left(\frac{2}{3}C_{wp}-\frac{8}{15}\right)$$

where C_{wp} and C_{pl} are the waterplane-area and longitudinal prismatic coefficients, LCB and LCF the longitudinal centres of buoyancy and floatation, respectively, and R_L is the radius of gyration.

The expressions (2.2.30.b) and (2.2.31.b) may be expressed in terms of Fourier integrals, see section (2.3.b). Following a calculation procedure outlined by Vermeer, expressions for λ_S and λ_T in terms of the hull geometry parameters are obtained,

$$\lambda_S = -\frac{1}{6\ C_{wp}C_{pl}}\left[32 - 40(C_{wp} + C_{pl}) + 75(C_{pl})(C_{wp}) - 980(C_{wp})(C_{pl})(LCF)(LCB)\right] \quad \ldots\ldots (2.2.32.a)$$

$$\lambda_T = \frac{7}{18\pi C_{wp}C_{pl}R^2}\left[20(LCB)(C_{pl}) + 24\ (LCF)(C_{wp}) - 45(LCB)(C_{wp})(C_{pl}) - 39(LCF)(C_{wp})^2\right] \quad \ldots\ldots (2.2.32.b)$$

It is apparent that for LCB=LCF=0, λ_T =0 and no trim can be expected for ships with fore-and-aft symmetry (this can also be deduced from the original expression (2.2.31.b)). Since the last term in (2.2.32.a) is small and may be discarded, it is clear that asymmetry has a neglible effect on the ship sinkage but a dominant effect on the ship trim. Assymetry could be induced by initial (static) trim, the ship motion itself or viscous effects, even if the ship possesses fore-and-aft symmetry in the level-keel condition. Consequently, matters become considerably more complicated when attempting to deduce additional qualitative observations with regard to trim. (However, neglecting such "external" effects, it is possible to speculate that because the LCB of full-form ships normally lies forward of midships, while the LCF lies aft midships, a trim-by-bow is to be expected in the level-keel condition.)

In the level-keel condition assymetry is controlled by the ship form itself. Expressions (2.2.32) suggest that

when the fullness distribution is sufficiently limited through, say, a high block-coefficient, the λ_S and, particularly, the λ_T values, may be expected to vary only through a very limited range. This would be the case when limiting the block-coefficient to between, say, 0.8 and 0.9 but would not apply to fine form ships with block coefficients of, say 0.5 to 0.6, for which relatively large variations in the position of LCF and LCB are possible. Based on theoretical observations, Tuck [76] noted that λ_S varied between 1.4 and 1.53 over a wide range of B(x) and S(x) curve shapes, including mathematically defined curves and actual ship shapes. Using a mean value of 1.46, good agreement with full-form models was confirmed by Dand [19], while Hooft [38] reported agreement with experiments using a λ_T value of 1. The above λ_S and λ_T values indicate that sinkage is the dominant phenomenon in the subcritical range of Froude depth numbers. However, this may not be the case at very low underkeel clearances, throughout where viscous effects dominate.

A general expression for the non-dimensional squat, C_{SQ} , may be written as,

$$C_{SQ} = C_S \pm 1/2\ C_T$$

$$= 100\ (\pm\lambda_S \pm \tfrac{1}{2}\lambda_T)\ \frac{\nabla F_h^{\,2}}{L^3\sqrt{1-F_h^{\,2}}}$$

or for small F_h ,

$$C_{SQ} = J \frac{BTC_B U^2}{L^2 h}$$

where J is a constant to be determined.

From this expression it may be further noted that both sinkage and trim are directly proportional to the block coefficient and the square of the ship's speed and inversely proportional to the depth-draught and length-breadth ratios.

(2.3) The Hydrodynamic Approach, Finite-width Shallow Water

Proceeding in a similar fashion the analysis may be generalised to include the effects of finite-width lateral restrictions on the steady-state, subcritical motion along the centreline of a shallow channel of rectangular cross-section, Fig. 6.

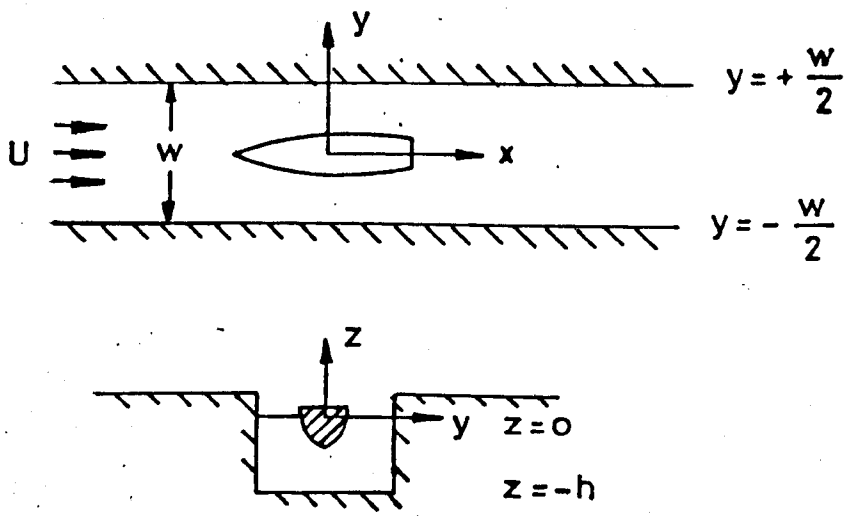

Fig. 6: Coordinate System

(2.3.a) Problem Formulation and Solution Outline

The problem formulation and the solution procedure are similar to that of section (2.2), see for example Beck et al [6] and Tuck [75], and thus only changes induced by the lateral restrictions are presented and discussed.

In addition to the slenderness and shallowness assumptions introduced in section (2.2.a), the channel width is assumed of O(1) or comparable to the ship length.

This implies that the effect of the lateral restrictions appears in the "outer" problem only. The "inner" problem is identical to that for the laterally unrestricted shallow-water in section (2.2.b) and involves solving a sequence of 2-D (Neumann) problems in the vertical (y,z) plane.

From section (2.2.c), the problem in the "outer" region reduces to a 2-D problem in the horizontal (x,y) plane, where ϕ (x,y) satisfies equations (2.2.17),

$$\delta^2 \phi_{xx} + \phi_{yy} = 0$$

where

$$\delta^2 = 1 - F_h^2$$

in the half-space (x,y): $-\infty < x < \infty$, $|y| < 1/2W$, for $F_h < 1$, where W is the channel width.

In the "outer" region the ship collapses into a line, $y=0\pm, |x| < L/2$, on the x-axis. The nature of the limiting boundary condition on the resulting "equivalent hull" was established by the "inner" expansion of section (2.2.b) and is expressed by (2.2.12),

$$\phi_y = \pm \frac{US^1(x)}{2h} \qquad \text{on} \quad y = 0\pm, \ |x| \leq L/2$$

and $\phi_y = 0$ on $|x| > L/2$

The boundary condition at infinity (2.2.5) is replaced by that on the channel walls,

$$\phi_y(x, \tfrac{1}{2}W) = 0 \qquad \text{on} \quad -\infty < x < \infty \qquad \ldots\ldots (2.3.1)$$

and, finally,

$$\phi_x(x,y) = 0 \qquad \ldots\ldots (2.3.2.a)$$

$$\phi_y(x,y) = 0 \qquad \ldots\ldots (2.3.2.b)$$

as $x \to \pm \infty$, $|y| \leq \tfrac{1}{2}W$

The "outer" boundary-value problem solution is derived by applying Fourier synthesis in x and is detailed in Appendix A.

In the subcritical ($F_h < 1$) range, the appropriate solution is,

$$\phi(x,y) = \frac{iU}{4\pi h\delta} \int_{-\infty}^{\infty} \exp(-irx) S^*(r) \cosh[r\delta(|y| - \tfrac{1}{2}W)] \operatorname{cosech}(\tfrac{1}{2}Wr\delta)\, dr \qquad \ldots\ldots (2.3.3)$$

As in section (2.2.e), in order to determine the leading-order hydrodynamic forces the value of the derivative of the potential acting along the hull, y=0 , is required. Writing,

$$\phi(x,y) = \lim_{y \to 0} \phi(x,y) \qquad \ldots\ldots (2.3.4.a)$$

yields,

$$\phi^{(1)} = \frac{iU}{4\pi h\delta} \int_{-\infty}^{\infty} \exp(-irx) S^*(r) \coth(\tfrac{1}{2}Wr\delta) dr \qquad \ldots\ldots (2.3.4.b)$$

From which the longitudinal perturbation velocity $\phi_x(x,0)$ is derived by differentiation,

$$u(x) = \phi_x^{(1)}$$
$$= \frac{U}{4\pi h\delta} \int_{-\infty}^{\infty} \exp(irx)\, rS^*(r) \coth(\tfrac{1}{2}Wr\delta)\, dr \qquad \ldots\ldots (2.3.5)$$

Inserting (2.3.5) into expressions (2.2.26), the vertical (sinkage) force,

$$F = -\frac{\rho U^2}{4\pi h\delta} \int_{-\infty}^{\infty} rS^*(r)\overline{B^*(r)} \coth(\tfrac{1}{2}Wr\delta)\, dr \qquad \ldots\ldots (2.3.6.a)$$

and moment,

$$M = \frac{\rho U^2}{4\pi h\delta} \int_{-\infty}^{\infty} rS^*(r)\overline{(xB^*(r))} \coth(\tfrac{1}{2}Wr\delta)\, dr \qquad \ldots\ldots (2.3.6.b)$$

are obtained, where,

$$\overline{B^*(r)} = \int_{-L/2}^{L/2} B(x)\exp(-irx)\, dx \qquad \ldots\ldots (2.3.7.a)$$

$$\overline{xB^*(r)} = \int_{-L/2}^{L/2} (xB(x))\exp(-irx)\, dx \qquad \ldots\ldots (2.3.7.b)$$

are complex conjugates of the transforms.

Following the procedure of section (2.2.f) and substituting for δ from (2.17.c), the subcritical, non-dimensional sinkage and trim coefficients are obtained in the form,

$$C_s = 100 \frac{F_h^2}{\sqrt{1 - F_h^2}} \lambda_s \qquad \ldots\ldots (2.3.8.a)$$

with

$$\lambda = \frac{1}{4\pi L} \frac{\int_{-\infty}^{\infty} rS^*(r)\overline{B^*(r)}\coth(\tfrac{1}{2}Wr\delta)\,dr}{\int_{-L/2}^{L/2} B(x)\,dx} \qquad \ldots\ldots (2.3.8.b)$$

and

$$C_T = 100 \frac{F_h^2}{\sqrt{1 - F_h^2}} \lambda_T \qquad \ldots\ldots (2.3.9.a)$$

with

$$\lambda_T = \frac{1}{4\pi} \frac{\int_{-\infty}^{\infty} rS^*(r)\,(\overline{xB^*(r)})\coth(\tfrac{1}{2}Wr\delta)\,dr}{\int_{-L/2}^{L/2} x^2 B(x)\,dx} \qquad \ldots\ldots (2.3.9.b)$$

(2.3.b) The Limiting Case as W ---► ∞

Assuming $F_h << 1$, as W ----► ∞ the hyperbolic cotangent tends to unity and equations (2.3.9) , say, become,

$$F = -\frac{\rho U^2}{4\pi h\delta} \int_{-\infty}^{\infty} rS^*(r)\overline{B^*(r)}\,dr \qquad \ldots\ldots (2.3.10.a)$$

$$M = \frac{\rho U^2}{4\pi h\delta} \int_{-\infty}^{\infty} rS^*(r)\,(\overline{xB^*(r)})\,dr \qquad \ldots\ldots (2.3.10.b)$$

and it may be shown, Beck et al [6], that the above reduce to the corresponding expressions (2.2.27) derived by solving the laterally unrestricted boundary-value problem

using a Green's function source distribution.

The hydrodynamic approach appears, therefore, uniformly valid throughout the infinite and finite-width subcritical F_h range.

(2.3.c) The Limiting Case as W ---► 0

To determine the validity of the hydrodynamic approach in narrow (as distinct from finite-width) channels, it is simplest to examine the longitudinal perturbation velocity term (2.3.5).

As $F_h << 1$ and W ---► 0 , it may be shown that,

$$\lim_{W \to 0} (\coth(\tfrac{1}{2}Wr\delta)) = \frac{1}{\tfrac{1}{2}Wr\delta} \qquad \ldots\ldots (2.3.11)$$

and it follows that the longitudinal perturbation velocity along the hull reduces to,

$$u(x) = \phi_x = \frac{U}{2\pi hW\delta} \int_{-\infty}^{\infty} \exp(-irx) S^*(r)\, dr \qquad \ldots\ldots (2.3.12)$$

Transforming this expression using equation (A.2) in Appendix A and substituting for δ, yields,

$$u(x) = \frac{Um(x)}{1 - F_h^2} \qquad \ldots\ldots (2.3.13)$$

where m(x)=S(x)/Wh is the local blockage factor.

This approximation will be later compared with the corresponding limiting expression derived by the "hydraulic analogy" method.

The sinkage force and trim moment (2.3.6) are reduced to,

$$F = -\frac{\rho U^2}{2\pi h\delta^2 W}\int_{-\infty}^{\infty} S^*(r)\overline{B^*(r)}\,dr \qquad \ldots\ldots (2.3.14.a)$$

$$M = \frac{\rho U^2}{2\pi h\delta^2 W}\int_{-\infty}^{\infty} S^*(r)\left(\overline{xB^*(r)}\right)dr \qquad \ldots\ldots (2.3.14.b)$$

Using the convolution (or Faltung) definition to obtain a generalized form of Parseval's Theorem (Sneddon [69]), the intergrand of (2.3.14.a), say, may be written in the form,

$$\frac{1}{2\pi}\int_{-\infty}^{\infty} S^*(r)\overline{B^*(r)}\,dr = \int_{-L/2}^{L/2} S(x)B(x)\,dx$$

and similarly for the integrand of (2.3.14.b). Consequently, as $W \dashrightarrow 0$, the hydrodynamic sinkage force and trim moment (2.3.14) may be written as,

$$F = -\frac{\rho U^2}{A(1 - F_h^{\,2})}\int_{-L/2}^{L/2} S(x)B(x)\,dx \qquad \ldots\ldots (2.3.15.a)$$

$$M = \frac{\rho U^2}{A(1 - F_h^{\,2})}\int_{-L/2}^{L/2} S(x)\left(xB(x)\right)dx \qquad \ldots\ldots (2.3.15.b)$$

Equating the hydrodynamic force and moment with the hydrostatic restoring force and moment and expressing the result in terms of the non-dimensional sinkage and trim coefficients,

$$C_s = \frac{100F_h^2}{WL(1 - F_h^2)} \frac{\int_{-L/2}^{L/2} S(x)B(x)\,dx}{\int_{-L/2}^{L/2} B(x)\,dx} \qquad \ldots\ldots (2.3.16.a)$$

$$C_T = \frac{100F_h^2}{W(1 - F_h^2)} \frac{\int_{-L/2}^{L/2} S(x)\,(xB(x))\,dx}{\int_{-L/2}^{L/2} x^2B(x)\,dx} \qquad \ldots\ldots (2.3.16.b)$$

(2.3.d) Qualitative Features

The main qualitative features have been discussed in the laterally unrestricted condition, section (2.2.g). To fascilitate the mathematical treatment, the finite-width theory is based on a reference width comparable with the ship length. Although not dependent on the water depth, the non-dimensional sinkage and trim coefficients now depend explicitly on the Froude depth number and channel width, which appear in combination in the argument of the hyperbolic cotangent. Consequently, irrespective of how slow the vessel moves, the flow conditions become critical when the depth and/or width of available water become sufficiently small. If F_h is close to the critical, any channel becomes effectively a narrow channel and invalidates the linearisation of the theory.

A mathematical feature, noted by Tuck [75], is that in

the limiting case as W tends to 0, the singularity in the sinkage and trim expressions becomes stronger, changing from an inverse square root (for example, equations (2.3.8)) to an inverse first power (for example, equations (2.3.30)). However, the critical speed is not necessarily coincident with the limiting speed. This problem will be discussed fully in section (2.4.d)..

(2.4) The "Hydraulic Analogy" Approach, Narrow Channels

The (linearized) shallow-water theory of the previous sections, is an approximate theory which results from the assumption that the hydrodynamic part of the pressure distribution (except in the immediate vicinity of the hull) is independent of the vertical (z) coordinate. Equivalently, the pressure variation, p, along the vertical is as given by hydrostatics,

$$p = \rho g(\eta - z)$$

It may be observed that,

$$p_x = \rho g \eta_x$$

and it follows that the x-component of acceleration, and hence the velocity, are independent of z and uniform along the vertical.

One dimensional considerations lead to a simpler form of the continuity equation which, for the steady-state conditions, relates the mean flow velocity in a given direction to the flow cross-sectional area normal to that direction, on the assumption that the free-surface is "rigid".

The resulting simplified equations do not differ from those derived for analysing the flow in open pipes in hydraulics. As initially applied by Kreitner [42] and emulated by others, the "hydraulic analogy" method offers a

sensible means of evaluating the ship sinkage and investigating the complex hydraulic phenomena in narrow channels. Later suggestions by Tuck and Taylor [76], Dand and Ferguson [23] and Yamaguchi et al [86] permit the evaluation of trim for hulls with no longitudinal symmetry and the extension of the 1-D method to laterally unrestricted shallow-water.

(2.4.a) Problem Formulation and Solution

The following derivation is a simple extension of the original Kreitner approach. The technique requires the flow to be conceptually altered to a steady one by viewing the vessel as being at-rest and the water in the channel, at some distance from the ship, as moving with a uniform velocity equal and opposite to that of the ship. An inherent assumption is that the ship sinkage is equal to the change in water level, i.e. the normal sinkage and trim owing to the motion in laterally unrestricted shallow-water is neglected. For convenience and later comparisons with the hydrodynamic theory, the ship is assumed stationary on the centreline of a narrow channel of uniform rectangular cross-section, see Fig.7. The channel is assumed to extend to infinity in both directions and the undisturbed flow velocity far ahead and astern of the ship is U. The ship cross-sectional area is S(x), its beam is B(x) and the mean local flow velocity has only an x-component, $U_1(x)$ at station x.

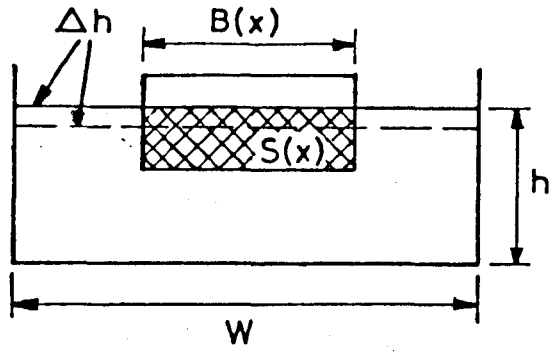

Fig. 7: Restricted Channel Symbols

Continuity requires,

$$AU = (A - S(x) - (W - B(x)\Delta h)U_1(x) \qquad \ldots\ldots (2.4.2.a)$$

where

$$U_1(x) = U + u(x) \qquad \ldots\ldots (2.4.2.b)$$

u(x) is the longitudinal perturbation velocity (or "back-flow") due to the ship presence at station x and $\Delta h(x)$ is the local water surface draw-down. From Bernoulli,

$$p_H = \frac{\Delta h}{h} = \frac{U_1^2(x)}{2g} - \frac{U^2}{2g} \qquad \ldots\ldots (2.4.2.a)$$

$$= F_h^2 \frac{u(x)}{U}[1 + \frac{1}{2}\frac{u(x)}{U}] \qquad \ldots\ldots (2.4.2.b)$$

Inserting (2.4.2) in (2.4.1), after some manipulation, yields the governing equation,

$$(\frac{U_1(x)}{U})^3 \frac{F_h^2}{2}(1 - \frac{B(x)}{W}) - [1 - m(x) + \frac{F_h^2}{2}(1 - \frac{B(x)}{W})](\frac{U_1(x)}{U} + 1) = 0 \qquad \ldots\ldots (2.4.3)$$

where $m(x)=S(x)/Wh$ is the local blockage ratio and $F_h = U/\sqrt{gh}$

is the Froude depth number. For any fixed value of F_h and $B(x)/W$, equation (2.4.3) may be solved for $U_1(x)/U$ at any x-coordinate when the local blockage is known. The drop in water level varies along the hull, commencing with zero at the bow up to a maximum at the maximum ship cross-section and back to zero at the stern. Substituting back into the non-dimensionalized Bernoulli equation (2.4.2) and integrating along the hull length, the total (hydrostatic) pressure force and moment are obtained,

$$F = \rho g h \int_{-L/2}^{L/2} p_h(x)\ B(x)\,dx \qquad \ldots\ldots (2.4.4.a)$$

$$M = \rho g h \int_{-L/2}^{L/2} p_H(x)\,(xB(x))\,dx \qquad \ldots\ldots (2.4.4.b)$$

Equating the above expressions with the restoring force and moment, equations (2.2.31), the non-dimensional sinkage and trim coefficients are,

$$C_S = -100\left(\frac{h}{L}\right)\frac{\int_{-L/2}^{L/2} p_H(x)B(x)\,dx}{\int_{-L/2}^{L/2} B(x)\,dx} \qquad \ldots\ldots (2.4.5.a)$$

$$C_T = 100(h)\frac{\int_{-L/2}^{L/2} p_H(x)\,(xB(x))\,dx}{\int_{-L/2}^{L/2} x^2B(x)\,dx} \qquad \ldots\ldots (2.4.5.b)$$

It may easily be shown that,

$$s_{AP} = \frac{L}{200}\,(2C_S - C_T) \qquad \ldots\ldots (2.4.6.a)$$

$$s_{FP} = \frac{L}{200}\,(2C_S + C_T) \qquad \ldots\ldots (2.4.6.b)$$

allowing the evaluation of the sinkages at both perpendiculars.

(2.4.b) The Case of Finite Width

Considering a channel of finite, but large, width the ship breadth may be assumed small in comparison to the tank width and equation (2.4.3) reduces to,

$$\left[\frac{U_1(x)}{U}\right]^2 \frac{F_h^2}{2} - [1 - m(x) + \frac{F_h^2}{2}](\frac{U_1(x)}{U}) + 1 = 0 \quad \ldots\ldots (2.4.7)$$

The above is an exact mathematical expression of the problem. In order to compare with the finite-width result (2.3.13) of the hydrodynamic approach in section (2.3.c), an approximate solution is required. This is derived in Appendix B, where by discarding terms of second order in smallness it is found that the approximate solution for the longitudinal perturbation velocity is,

$$U(x) = \frac{Um(x)}{1 - m(x) - F_h^2} \quad \ldots\ldots (2.4.8)$$

A comparison with equation (2.3.13) illustrates that the hydrodynamic theory will underestimate the longitudinal perturbation (or "back-flow") velocity and, therefore, the vertical-plane force and moment in finite-width (and narrow) channels. In order to arrive at the approximate solution obtained by the hydrodynamic approach, an additional term must be neglected. This implies that the

validty of the finite-width, hydrodynamic aproach is limited to the low blockage and Froude depth number range. The result is compatible with intuitive reasoning since the finite-width theory is based on a reference width of the order of the ship length while the "hydraulic analogy" approach is strictly valid in widths comparable with the ship breadth.

(2.4.c) The Limiting Case as W ----► ∞

As the cross-section of the channel becomes very large compared with that of the ship, m(x) ---► 0 and intuitive reasoning indicates clearly that the flow will not be uniformly distributed over the flow cross-section. This invalidates a basic premise of the 1-D approach and hence u(x) ----► 0, as may be deduced from the approximate solution (2.4.8).

A similar result may be obtained be rearranging equation (2.4.3) using (2.4.4.b). This yields a cubic equation in u(x)/U which may be written in the form,

$$F_h^2\left[\left(\frac{u(x)}{U}\right)^3 + 3\left(\frac{u(x)}{U}\right)^2 + 2\left(\frac{u(x)}{U}\right)\right] + 2m(x)\left[\frac{u(x)}{U} + 1\right] - 2\left(\frac{u(x)}{U}\right) = 0 \quad \ldots\ldots (2.4.9)$$

and the solutions follow immediately,

(a) $m(x)=0$ $\qquad F_h^2 = \dfrac{2}{\left(\frac{u(x)}{U} + 1\right)\left(\frac{u(x)}{U} + 2\right)}$

(b) $F_h^2 = 0$ $\qquad m(x) = \dfrac{\frac{u(x)}{U}}{(\frac{u(x)}{U} + 1)}$

Considering only subcritical ($0<F_h<1$) flow, the most reasonable of the possible solutions is that $u(x)/U=0$.

This result is consistent with the inherent neglect of the sinkage and trim in laterally unrestricted shallow-water.

(2.4.d) The Limiting Speed

Ship speeds are described as steady when all the fluid passes, as is necessitated by continuity, around the hull and astern. The maximum quantity of water that can pass the ship is equivalent to determining the turning value of equation (2.4.3). The procedure results in the following mathematical expression for the critical speed range,

$$m(x) = 1 - \frac{3}{2} F_h^{3/2} + \frac{1}{2} F_h^2 \qquad \ldots\ldots (2.4.10)$$

This is plotted in Fig.8.

It is apprent from Fig.8 that three distinct regimes occur in laterally restricted shallow-water. Equation (2.4.3) permits only a restricted range of Froude depth numbers for any given blockage m(x), namely,

$$0 < F_h < F_h^L \quad \text{and} \quad F_h^U < F_h < \infty \qquad \ldots\ldots (2.4.11)$$

where the subscripts L and U denote the "lower" and "upper" critical speeds speeds respectively.

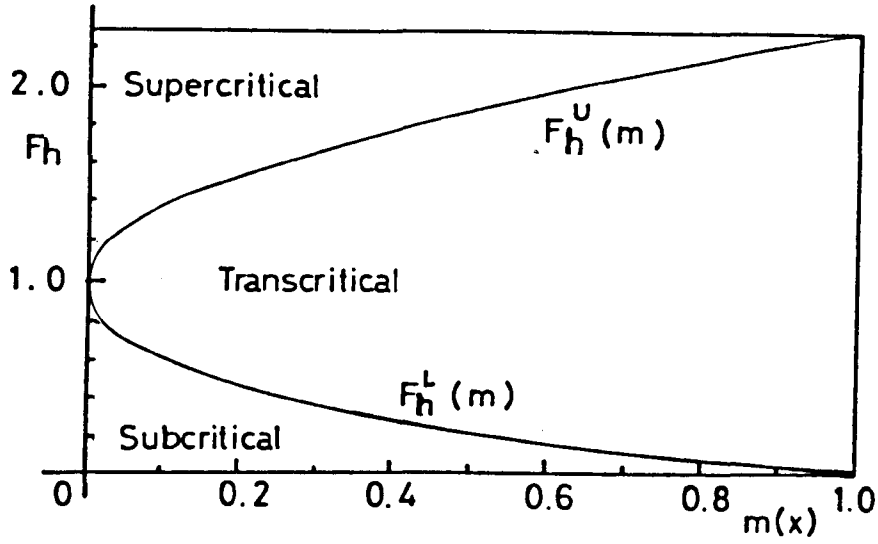

Fig. 8: The Critical Speed Range in a Channel

The limiting speed does not necessarily coincide with the critical speed. With increasing blockage, the transcritical speed range narrows until eventually, in the limiting case of laterally unrestricted shallow water, it is reduced to only one critical speed $F_h^L = F_L^U$.

Kreitner [42], Constantine [13], Hooft [37] discuss the phenomena by analogy to the "hydraulic jump" and present readily surveyable summaries. The sub-and supercritical regimes are steady and in a sense "reversed". In the transcritical regime the Bernoulli and continuity equations cannot be satisfied and the conditions are unsteady. The velocity $U_1(x)$ is such that only a portion

of the water can pass astern, the remainder being damned up in front of the ship in the form of a transverse wave of translation, or "bore". Approaching the critical speed, the solitary wave progressively increases in size and observations show that just below the limiting speed the sinkage (and resistance) increase very rapidly. Correspondingly there is a fall in water level astern of the ship. As the ship begins to "ride" the translation wave, the phenomena combine to increase the trim aft. Consequently, trim becomes the dominant phenomenon in the transcritical regime. At the critical speed the bow wave becomes transverse and since it keeps up with the ship its speed must equal the speed of the "back-flow" relative to the ship. At speeds exceeding the critical, or with depth or lateral restrictions, the solitary wave is unable to keep pace with the ship because it can not exceed the critical speed. The transverse wave disappears and only the divergent (or diagonal) waves remain whose angle with the ship longitudinal axis decreases steadily with increasing speed. In the supercritical region the ship rises bodily and there is a corresponding decrease in resistance.

(2.4.e) Qualitative Features

In addition to the qualitative features discussed in sections (2.2.g) and (2.3.d), since the pressure distribution is now hydrostatic, the ship displacement remains constant and both sinkage and trim depend

explicitly on the water depth (and the blockage ratio). However, the approach inherently neglects trim effects, as the latter are associated with the redistribution of hydrodynamic pressure underway and connected with the appearance of a hull wave-system. In the subcritical range of the Froude depth number a downward sinkage force is to be expected. Notably, as in the case of the hydrodynamic approach, no trim can be expected for ships with fore-and-aft symmetry.

A principal assumption is that the channel is sufficiently narrow (of the order of the ship breadth) so that variations in the water level across the channel breadth can be neglected. A consequence of this assumption is that the theory may be expected to fail when the ship is in the immediate proximity of the bottom and the flow becomes clearly 2-D in nature, non-linear and hydrodynamic forces assume importance.

(2.5) Conclusions

In conclusion it appears that a completely satisfactory theory of universal applicability, which allows a routine solution with arbitrary Froude number and lateral restrictions, does not exist at present. The simplifying assumptions permit a valuable insight into the problem and allow theoretical modelling of the vertical-plane force and moment within the constraints of each case.

The first-order hydrodynamic theory assumes a constant dynamic pressure around and in the immediate vicinity of each ship cross-section. There is no dependence of the hydrodynamic pressure on depth, even underneath cross-sections with low underkeel clearance. Considering water-depths of the same order as the ship draught and with the ship draught and beam assumed small in comparison to the ship length, the dynamic pressure force and, hence, the sinkage and trim underway are obtained. The hydraulic approach is based on a reference width comparable with the ship breadth and on the assumption that the pressure around each ship cross-section is hydrostatic and is connected with the change in water-level in the immediate vicinity of the hull. The hydrostatic pressure and, therefore, the resulting squat, do depend on the water depth. In fact, it would seem more probable that the sinkage and trim should have both a hydrostatic and a hydrodynamic component. At low speeds, such as imposed by environmental restrictions, the former should dominate. As speed is increased, the hydrodynamic component may be expected to become dominant.

An efficient and comprehensive method, valid in any expanse of shallow-water, also requires reference to systematic experimental data and physical observations to overcome any limitations. The qualitative features and limitations outlined by the theoretical considerations will now be examined against quantitative experimental data and the transition from hydrodynamic assumptions to actual hull behaviour discussed.

CHAPTER 3

Initial Numerical Computations and Experimental Results

(3.1) General

In parallel with qualitative theoretical modelling, a comprehensive and systematic series of tests were carried out with a representative 0.8 block-coefficient mono-hull (a modern (1977) bulk-carrier). The immediate purpose of the model tests was a quantitative comparison with the initial numerical computations. The experimental program was then extended with an emphasis on identifying possible physical phenomena of practical value to the problem.

The full details of the model, water-depths, ship operating conditions, the experimental set-up, procedures and methods of analysis used throughout the work, appear in Appendix C. Naked-hull and self-propelled model tests were carried out in calm, deep and shallow water, in both the laterally restricted and unrestricted conditions. Preliminary tests, conducted upon commencing the experimental program, led to a very detailed investigation of the tank bottom and measures were taken to improve the bed and enable experiments to continue at very low depth-draught ratios. The relevant information may be

found in Bradley et al [9].

(3.1.a) Selection of the Experimental Channel Width

Preliminary considerations necessary for the evaluation of the finite-width and narrow channel theoretical approaches included the selection of an appropriate experimental channel width. The selected width had to be within the range of validity of both the 1-D hydraulic and 2-D hydrodynamic theories and represent a realistic channel for later physical observations.

The theoretical considerations of the previous Chapter indicate that the terms "finite-width" and "narrow" are relative to ship length and breadth, respectively. The "interface width", therefore, lies in a region greater than the ship breadth but smaller than the ship length. Considering the representative model used (see Appendix C) this limited the experimental channel width to between 0.5 and 3.0 m.

An additional consideration required the chosen channel width to represent a clearly detectable change from the "infinite" width experiments conducted in a tank-width to ship-breadth ratio of approximately 9.

A model-scale channel width of 2 meters was chosen and resulted in the following,

1. channel-width to ship-length ratio of 0.656

2. channel-width to ship-breadth ratio of 3.86

(3.1.b) The Artifice of Effective Width

In the limiting case of laterally unrestricted shallow-water the problems associated with the 1-D hydraulic approach (discussed in section (2.4.c)) may be overcome by the device of an assumed effective width. This permits the extension of the method by regarding the sinkage and trim in unrestricted shallow-water as resulting from an "effective width" of a fictitious channel, see Yamagouchi [86].

The introduction of this artifice induces a limiting speed "barrier" which does not exist in the corresponding laterally unrestricted problem (that is, owing to imaginary roots there is no solution to equation (2.4.3) in the fictitious channel)). This limitation may be overcome by extrapolating the previously calculated data, as suggested by Dand and Ferguson [23].

(3.2) Theory / Experiment Comparisons

A Fortran IV computer program was written to compute the C_S and C_T coefficients based on the hydrodynamic and hydraulic approaches of (2). After formulating an algorithm, the program was developed for a PDP 11/40

computer as a series of subroutines covering the various aspects of the problem. These were task-built into a separate main program which comprised of input/output statements and other common features. The resulting program served as the basis for the final version and was very flexible, in that its structure facilitated the program check-out and allowed progressive modifications as the information was gathered.

The initial studies assisted in determining the most suitable theoretical basis by examining the theories in light of aspects relevant to the problem. The main conclusions are summarised in the following sections.

(3.2.a) Laterally Restricted Shallow-water

Fig.9 presents towed, naked-hull C_S and C_T experimental data obtained with the model in the load draught, level-keel condition over the range $1.1/ \leq h/T \leq 2.0$, in the channel. For the channel particulars, see Appendix C.

Although for all practical purposes the data appears to lie on unique curves, a closer inspection of the C_S values reveals a slight dependence on the depth-draught ratio. A curve is presented in Fig.9 to indicate how close the data fitted about a mean. The change in trimming behaviour, illustrated by the C_T curves diverging from the mean, appears at the incipience of the transcritical

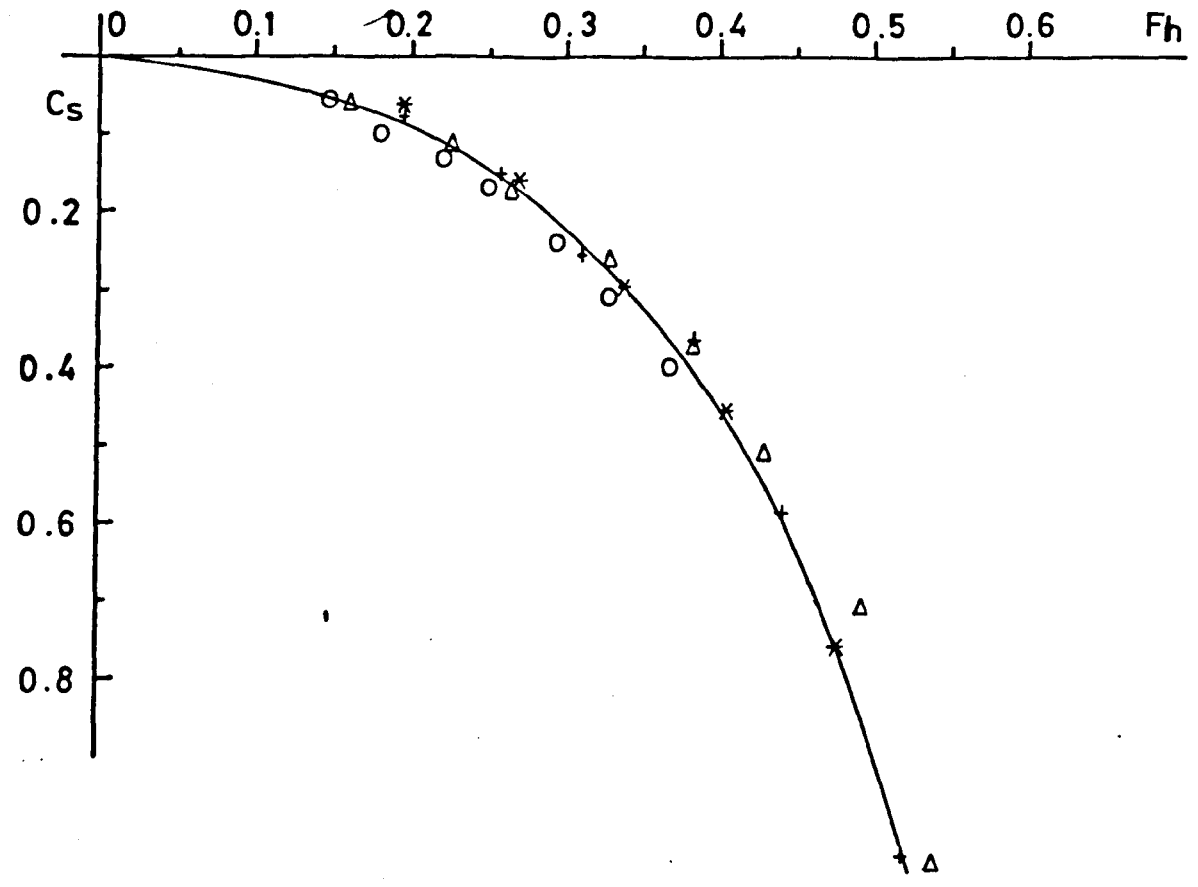

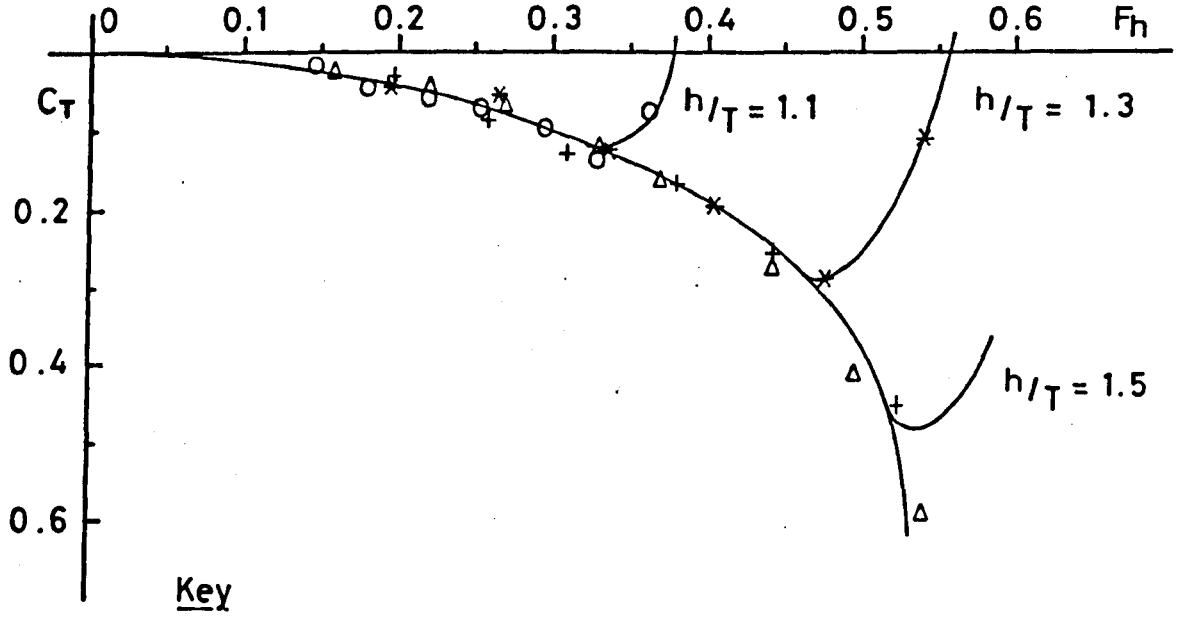

Key

o : $h/_T = 1.1$

* : $h/_T = 1.3$

\+ : $h/_T = 1.5$

Δ : $h/_T = 2.0$

Cs And C_T Against Fh

Type : Bulk Carrier Model

Condition : Naked-Hull, Restricted Water.

Draught : 0.174 m Level Keel

C_B : 0.8

Fig. 9

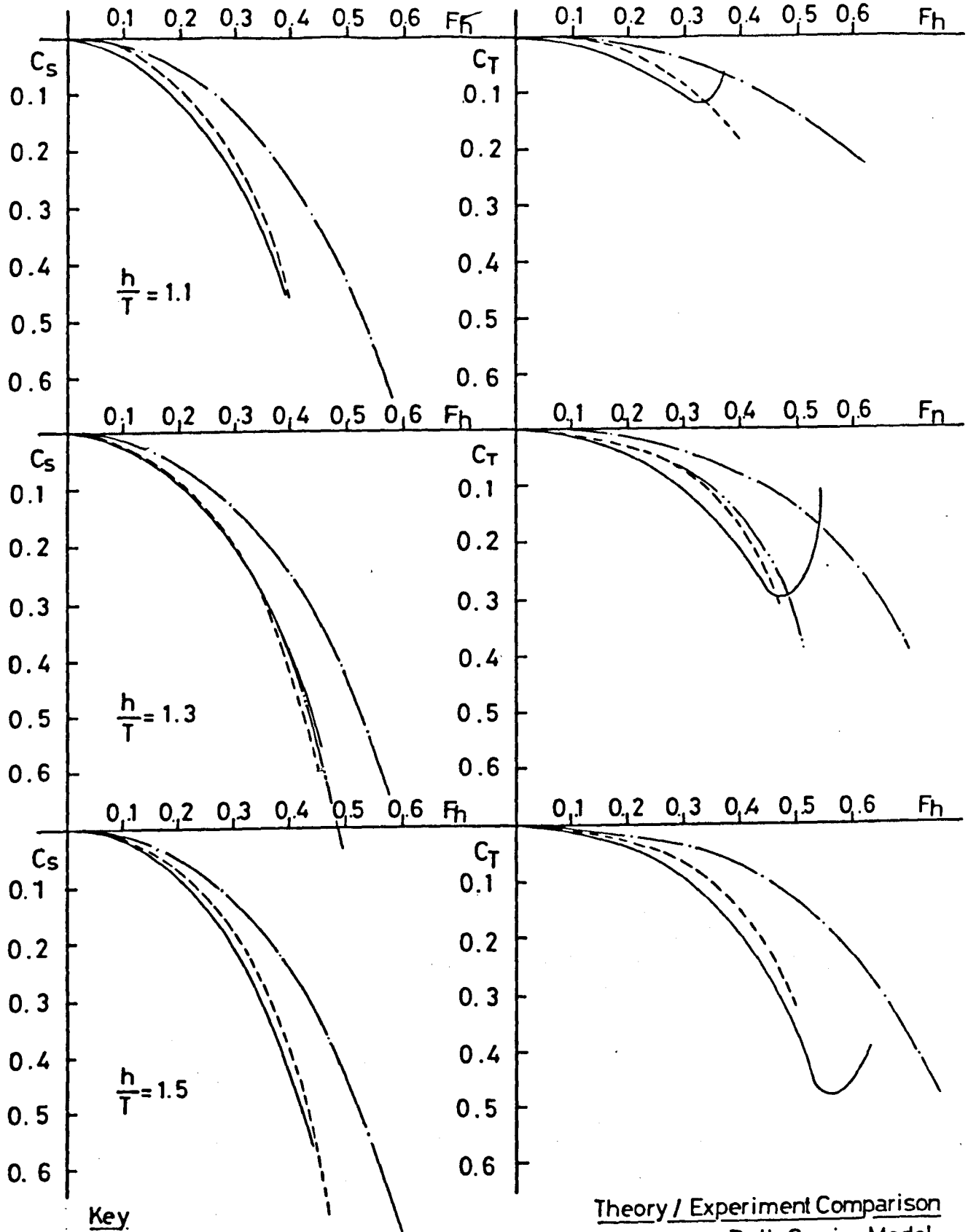

Key

——— : Experiment

– – – – : Hydraulic Theory (Finite Width) (Section 2.4.b)

—·—·— : Hydraulic Theory (Exact) (Section 2.4.a)

—·—·— : Hydrodynamic Theory (Finite Width) (Section 2.3.c)

Theory / Experiment Comparison

Type	:	Bulk Carrier Model
Condition	:	Naked Hull, Restricted Water
Draught	:	0.174m, Level Keel
C_B	:	0.8.
W/L	:	0.656.
W/B	:	3.86.

Fig. 10

SQUAT PREDICTION USING (EXACT) HYDRAULIC THEORY

SCALE ; DATA GENERATED FOR INPUT SCALE.

CONDITION ; NAKED TOWED HULL

AT-REST (MAXIMUM) DRAFT ..... = 0.174 M

AT-REST WATER DEPTH ..... = 0.226 M

WIDTH OF CHANNEL ..... = 2.000 M

BLOCKAGE (BASED ON MIDSHIP SECTION) ..... = 0.198

WIDTH OF CHANNEL/BREADTH OF SHIP ..... = 3.874

MEAN SINKAGE (CS) AND TRIM (CT) COEFFICIENTS;

NOTE; A "*" (STAR) DENOTES LIMITING SPEED.

DEPTH-DRAFT RATIO ..... = 1.30

FROUDE DEPTH NUMBER	CS	CT
0.10	-0.018	-0.006
0.12	-0.026	-0.009
0.14	-0.035	-0.012
0.16	-0.047	-0.016
0.18	-0.060	-0.020
0.20	-0.075	-0.025
0.22	-0.092	-0.031
0.24	-0.111	-0.038
0.26	-0.133	-0.045
0.28	-0.157	-0.054
0.30	-0.185	-0.064
0.32	-0.216	-0.075
0.34	-0.251	-0.087
0.36	-0.291	-0.101
0.38	-0.336	-0.118
0.40	-0.388	-0.137
0.42	-0.449	-0.160
0.44	-0.521	-0.188
0.46	-0.610	-0.223
0.48	-0.723	-0.270
0.50	-0.883	-0.341
0.52	*	*
0.54	*	*
0.56	*	*
0.58	*	*
0.60	*	*

TABLE 3

SQUAT PREDICTION USING FINITE-WIDTH HYDRODYNAMIC THEORY

SCALE ; DATA GENERATED FOR INPUT SCALE.

CONDITION ; SELF-PROPELLED HULL

AT-REST (MAXIMUM) DRAFT ..... = 0.174 M

AT-REST WATER DEPTH ..... = 0.226 M

WIDTH OF CHANNEL ..... = 2.000 M

BLOCKAGE (BASED ON MIDSHIP SECTION) ..... = 0.198

WIDTH OF CHANNEL/LENGTH OF SHIP ..... = 0.656

MEAN SINKAGE (CS) AND TRIM (CT) COEFFICIENTS;

DEPTH-DRAUGHT RATIO ..... = 1.30

FROUDE DEPTH NUMBER	CS	CT
0.10	-0.014	-0.004
0.12	-0.021	-0.005
0.14	-0.028	-0.007
0.16	-0.037	-0.010
0.18	-0.047	-0.012
0.20	-0.059	-0.015
0.22	-0.072	-0.018
0.24	-0.086	-0.022
0.26	-0.102	-0.025
0.28	-0.120	-0.029
0.30	-0.139	-0.034
0.32	-0.161	-0.039
0.34	-0.184	-0.044
0.36	-0.210	-0.050
0.38	-0.237	-0.056
0.40	-0.268	-0.062
0.42	-0.301	-0.069
0.44	-0.338	-0.077
0.46	-0.378	-0.085
0.48	-0.421	-0.094
0.50	-0.469	-0.104
0.52	-0.522	-0.114
0.54	-0.579	-0.126
0.56	-0.643	-0.139
0.58	-0.713	-0.152
0.60	-0.792	-0.168
0.62	-0.799	-0.245
0.64	-0.897	-0.273
0.66	-0.987	-0.303
0.68	-1.100	-0.338
0.70	-1.229	-0.378

TABLE 2

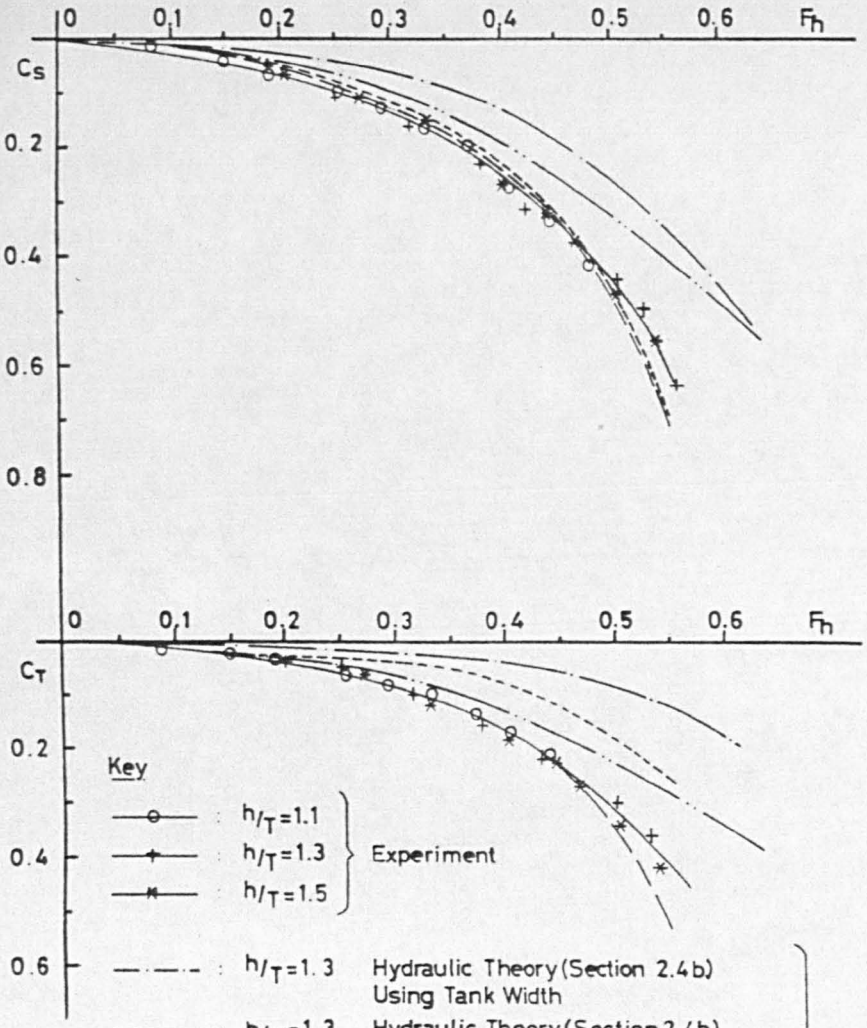

Key

- $h/T = 1.1$, $h/T = 1.3$, $h/T = 1.5$ } Experiment
- $h/T = 1.3$ Hydraulic Theory (Section 2.4b) Using Tank Width
- $h/T = 1.3$ Hydraulic Theory (Section 2.4b) Using Effective Width Of 1. Ship Length
- $h/T = 1.3$ Hydraulic Theory Using Tuck Parameter
- Hydrodynamic Theory (Section 2.2g)

} Theory

Theory / Experiment Comparison

Type	:	Bulk Carrier Model
Condition	:	Naked-Hull, Unrestricted Water
Draught	:	0.174m, Level Keel
C_B	:	0.8

Fig. 11

SQUAT PREDICTION USING HYDRAULIC THEORY

SCALE ; DATA GENERATED FOR INPUT SCALE.

CONDITION ; NAKED TOWED HULL

AT-REST (MAXIMUM) DRAFT ..... = 0.174 M

AT-REST WATER DEPTH ..... = 0.226 M

WIDTH OF CHANNEL ..... = 2.000 M

BLOCKAGE (BASED ON MIDSHIP SECTION) ..... = 0.198

WIDTH OF CHANNEL/BREADTH OF SHIP ..... = 3.874

MEAN SINKAGE (CS) AND TRIM (CT) COEFFICIENTS;

NOTE; A "*" (STAR) DENOTES LIMITING SPEED.

DEPTH-DRAFT RATIO ..... = 1.30

FROUDE DEPTH NUMBER	CS	CT
0.10	-0.018	-0.006
0.12	-0.026	-0.009
0.14	-0.036	-0.012
0.16	-0.047	-0.016
0.18	-0.060	-0.021
0.20	-0.076	-0.026
0.22	-0.093	-0.032
0.24	-0.113	-0.039
0.26	-0.136	-0.047
0.28	-0.162	-0.056
0.30	-0.191	-0.066
0.32	-0.224	-0.079
0.34	-0.263	-0.093
0.36	-0.307	-0.109
0.38	-0.360	-0.129
0.40	-0.422	-0.153
0.42	-0.498	-0.184
0.44	-0.597	-0.226
0.46	-0.739	-0.290
0.48	*	*
0.50	*	*
0.52	*	*
0.54	*	*
0.56	*	*
0.58	*	*
0.60	*	*

TABLE 4

regime. For a given Froude depth number this "barrier" depends on the blockage, see Fig.8, and therefore on the depth-draught ratio. Observations conducted throughout the experiments support the theoretical deductions by means of the hydraulic theory, i.e. the limiting speed "barrier" is always accompanied by the formation of a transverse wave aft of mid-length and a rather sudden grounding by the stern. Exceptions occured at the lowest depth-draught ratio of 1.1, whereby the model bow was observed to bounce off the bottom repeatedly before the formation of the transverse wave and subsequent grounding aft. Hence, although running at a transcritical speed cannot be considered a normal operating condition, it is of considerable importance to be able to predict the approach of the limiting speed theoretically.

Fig.10 presents qualitative and quantitative comparisons with the finite-width hydrodynamic (2.3) and hydraulic (2.4) theories at 3 depth-draught ratios. Tables 2-4 and Fig.10 present typical output data for a depth-draught ratio of 1.3 using early versions of the computer program. The agreement of the hydraulic theory with experiment is good and the difference between its 2 versions insignificant. Tables 2-4 illustrate the good prediction of the limiting speed by the hydraulic approach and the pronounced importance of lateral restrictions. In agreement with theoretical deductions, the finite-width hydrodynamic theory yields a fair qualitative but poor quantitative prediction and is unable to account for the

effects of limiting speed. Both approaches fail to predict the sudden reversal in trim upon grounding.

(3.2.b) Unrestricted Shallow-water

Fig.11 presents a comparison of theory and experiment in laterally unrestricted shallow-water. No dependence on the depth-draught ratio was observed except at close-to-grounding conditions. This is confirmed by earlier findings of Sjostrom [67] and Dand [16,18], the latter reporting a small dependence on the depth-draught ratio on some models. The hydrodynamic approach provides a fair quantitative prediction. In general agreement with the observations of Tuck [76] and Hooft [38], the calculation procedure of section (2.2.g) yields λ_S =1.34 and λ_T =0.91. Subsequent calculations indicated that in order to bring the hydrodynamic theory in line with the experimental data, λ_S =1.43 and λ_T =1.35 would be required. If the latter values are used, a rapid and reasonably accurate estimate of the sinkage and trim in shallow-water is possible using equations (2.2.30) and (2.2.31). The theory will then diverge from experiment only for close-to-grounding conditions.

When based on the actual tank width, the hydraulic approach considerably underestimates both sinkage and trim. Using an effective width of 1 ship length (see section(3.1.b)), good agreement with sinkage is obtained. Upon attaining the limiting speed in the fictitious

channel, the previously calculated values were extrapolated to obtain the C_S and C_T data in laterally unrestricted shallow-water. The trim remains, however, significantly underestimated and requires an additional empirical correction to what may be termed a "3-D" state.

In this process use was made of the procedure suggested by Dand [19], employing Tuck's effective width parameter, $W/L\sqrt{1-F_h^2}$, to correct both sinkage and trim to the naked-hull "3-D" state. Good agreement between theory and experiment was obtained by using this procedure, see Fig.11.

(3.2.c) The Effect of Lateral Restrictions

Fig.12 presents the effects of lateral restrictions on the C_S and C_T coefficients. These show that the introduction of side-walls induces a significant increase in the vessel mean sinkage and a very small increase in trim underway.

The above experimental observations are supported by the theoretical calculations of Tuck [75]. Using hydrodynamic theory Tuck illustrated that, when plotted against an effective width parameter $W/L\sqrt{1-F_h^2}$, the ratio of the infinite to finite-width sinkage and trim lies on a nearly unique curve over a wide range of practical ship shapes, Fig.13 insert. Plotting the ratio of the naked-hull results presented in the two previous sections

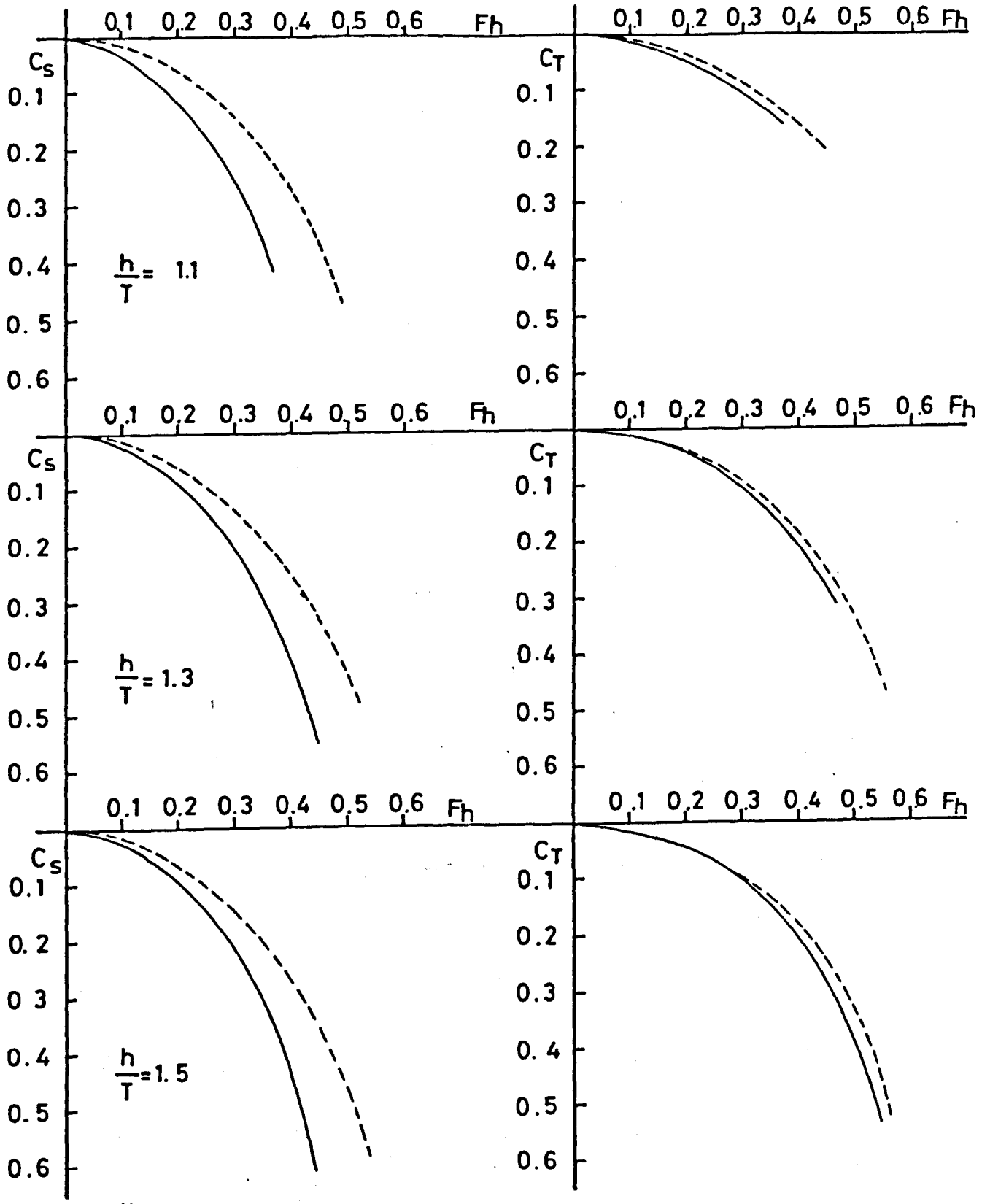

Key

– – – – : Laterally Unrestricted

——— : Restricted Channel

Effect Of Lateral Restrictions On C_S And C_T

Type	:	Bulk Carrier Model
Condition	:	Naked Hull
Draught	:	0.174 m, Level Keel
C_B	:	0.8
W/L	:	0.656
W/B	:	3.86

Fig 12

against the above parameter, Fig.13, confirms the good agreement with the theoretically derived curves. Although the experimental data is outwith the finite-width values considered by the theory, a good and useful agreement in tendencies and magnitude of both sinkage and trim is retained at widths of approximately 2/3 ship length. (This in spite of the fact that the infinite width data used was obtained in a tank of finite, not infinite, width.)

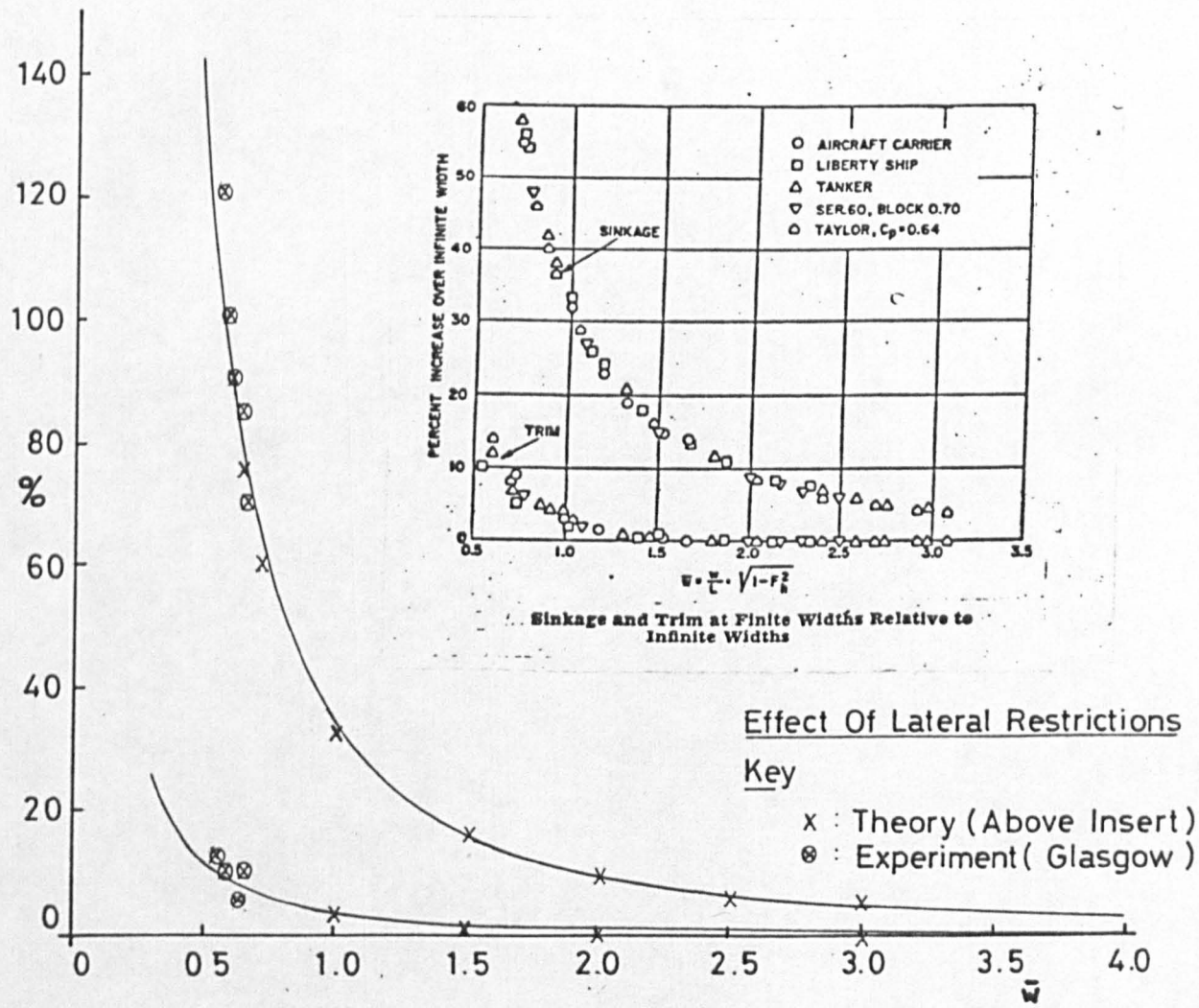

Fig. 13: The Effect of Lateral Restrictions Theory/Experiment

This agreement appears not to be affected by the depth-draught ratio, Table 5.

		h/T=1.1		h/T=1.3		h/T=1.5	
F_h	$\frac{W}{L\sqrt{1-F_h^2}}$	$\frac{C_{SR}}{C_{S\infty}}$	$\frac{C_{TR}}{C_{T\infty}}$	$\frac{C_{SR}}{C_{S\infty}}$	$\frac{C_{TR}}{C_{T\infty}}$	$\frac{C_{SR}}{C_{S\infty}}$	$\frac{C_{TR}}{C_{T\infty}}$
0.1	0.653	1.75	/	1.70		1.75	/
0.2	0.642	1.86	1.15	1.75	1.05	1.80	1.05
0.3	0.626	1.90	1.11	1.85	1.10	1.83	1.10
0.4	0.601	1.95	/	1.90	1.10	1.86	1.12
0.5	0.568	/	/	2.00	1.10	2.00	1.10
0.55	0.547	/	/	2.20	1.12	2.50	1.12

Table 5: Effect of Lateral Restrictions, Influence of h/T

On this evidence, if the gap in experimental data is considered closed by the theory, the above curves may be used to extapolate the laterally unrestricted shallow-water sinkage and trim to the intermediate finite-widths not covered by the present experimental program. This is of considerable importance since many practical channel configurations lie in an intermediate region between the infinite and finite-width regimes.

(3.2.d) Effect of Underkeel Clearance

The experimental data showed clearly that for the given ship features the two main factors affecting the

sinkage and trim are increasing speed and decreasing underkeel clearance. At higher underkeel clearances, the mean sinkage and trim follow the usual Bernoulli behaviour and appear proportional to the velocity squared. However, the data also indicates that the assymetric forces on the vessel increase more rapidly than the speed squared at the small underkeel clearances which may be also be created while underway. In contrast with the theory, section (2.2.g), the importance of trim equals and may exceed the contribution due to sinkage at close-to-grounding conditions. As behaviour changes continuously at such clearances, any value based on the extrapolation of data derived at higher underkeel clearances will err considerably and underestimate, see Seren et al [61].

(3.2.e) The Effect of Hull Geometry

Fig. 14 presents a comparison of sinkage and trim data obtained on 3 models at the load draught, level-keel condition in unrestricted shallow-water. The models represent modern, full-form ships of varying hull parameters and displacement, but with the block coefficient limited to between 0.8 and 0.9. The curves represent the mean of the data collected. Although no measurable effect on the mean sinkage may be observed, trim increases with increasing C_B and decreasing B/T ratio. These changes are confirmed by the comprehensive analysis of over 120 models by Ferguson [27], which showed that within the ranges B/T and C_B examined negligible changes in sinkage but marked

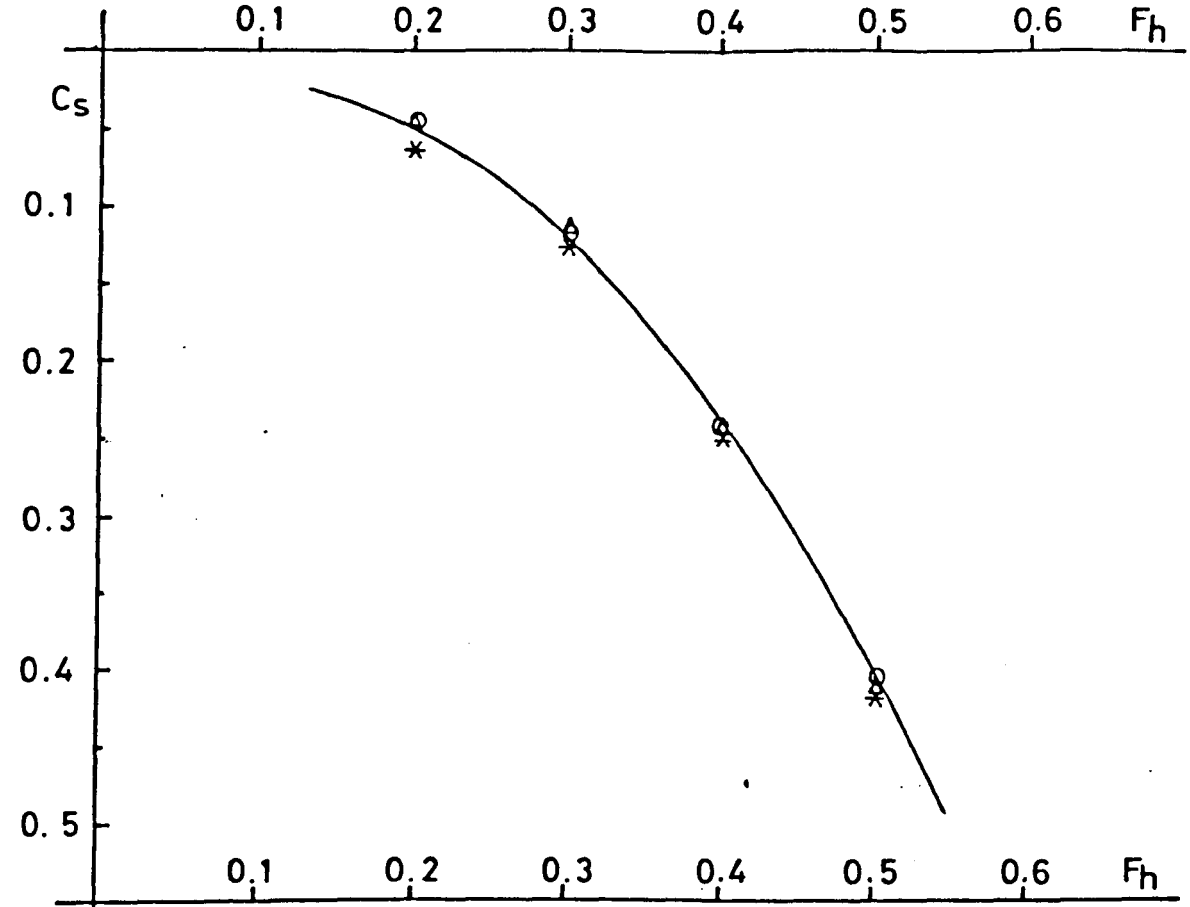

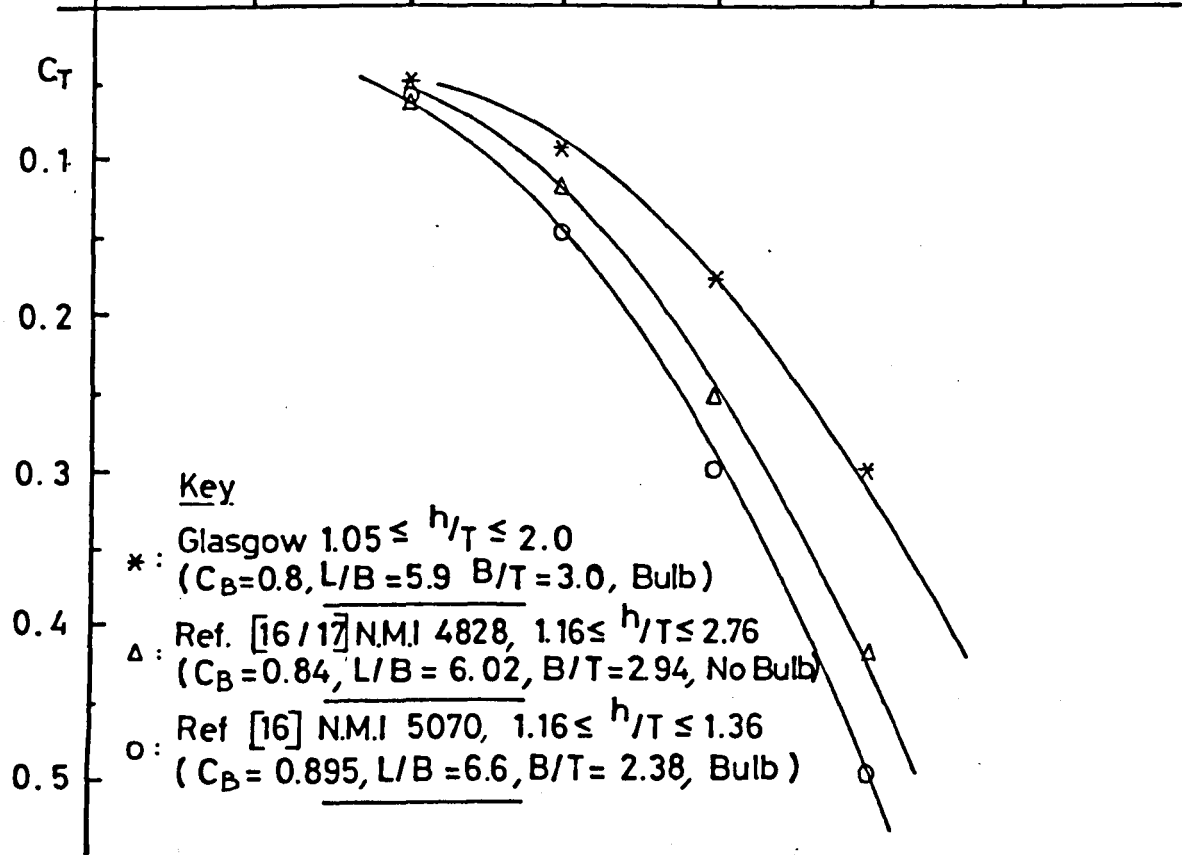

Key

* : Glasgow $1.05 \leq {}^{h}/_{T} \leq 2.0$
(C_B=0.8, L/B =5.9 B/T = 3.0, Bulb)

Δ : Ref. [16 / 17] N.M.I 4828, $1.16 \leq {}^{h}/_{T} \leq 2.76$
(C_B = 0.84, L/B = 6.02, B/T = 2.94, No Bulb)

o : Ref [16] N.M.I 5070, $1.16 \leq {}^{h}/_{T} \leq 1.36$
(C_B = 0.895, L/B = 6.6, B/T = 2.38, Bulb)

Effect Of Hull Form

Condition : Naked Hull Unrestricted Water

Draught : Load Draught

Fig 14

changes in trim are to be expected. Although in general agreement with the qualitative features of section (2.2.g), the results contrast with the theory with regard to the influence of the L/B ratio. Theory indicates that squat is inversely proportional to the L/B ratio while the above data suggests the opposite.

The comparison shows that the hull geometry must be incorporated into any prediction method and it is not satisfactory to use simpler measures of ship shape such as C_B or B/T ratio. Consequently, a purely empirical method based on a parent form, such as suggested for example by Sogreah [24], should be be used with caution unless the effects of variations in the hull form are accounted for.

The observations support the view that sinkage results from the pressure changes due to the increased horizontal flow velocity around the hull. In the load draught, level keel condition, the flow velocity is dominated by the long parallel middle-body and negligibly affected by minor hull geometry changes aft and forward. The effect on trim is more complicated. Trim is the result of a "vertical" moment due to the vertical normal force resultant acting about a transverse axis through the center of rotation and a "horizontal" moment about the same axis owing to the horizontal (resistance) forces acting on the hull. The arm of the "horizontal" component is, at times, expressed as a fraction of the ship draught. The longitudinal position of the normal component is more sensitive to changes in hull

form parameters and the resulting separated flow, depending on factors such as the bulbous-bow and type of propulsion. These are considered in the following sections.

(3.2.f) The Effect of the Bulbous-bow Shape

The effect of fitting a radically different bulbous-bow design on the vessel's sinkage and trim was also examined, see Ferguson, Seren and McGregor [28]. This was to determine whether a larger bulb, which would considerably modify the flow, would induce significant changes in the squatting behaviour. The alternative bulbous-bow was of a Glasgow University design similar to that used on a number of VLCC's, fitted over the original bow and faired into the hull. Fig.15 illustrates the modification by means of a superimposed print showing both the original and redesigned bow. A number of the original experiments were repeated and the changes noted. A comparison of the two sets of results, Fig.16 being typical, showed that the modification leads to minor changes in the force distribution, but not its overall magnitude. The resulting changes in close-to-grounding behaviour did not affect the grounding speed or qualitative behaviour. Consequently, in the load-draught condition the bulbous-bow shape may be considered to have a very small effect and could be omitted from the input hull geometry at this stage (second order influence).

However, it should be borne in mind that effects of

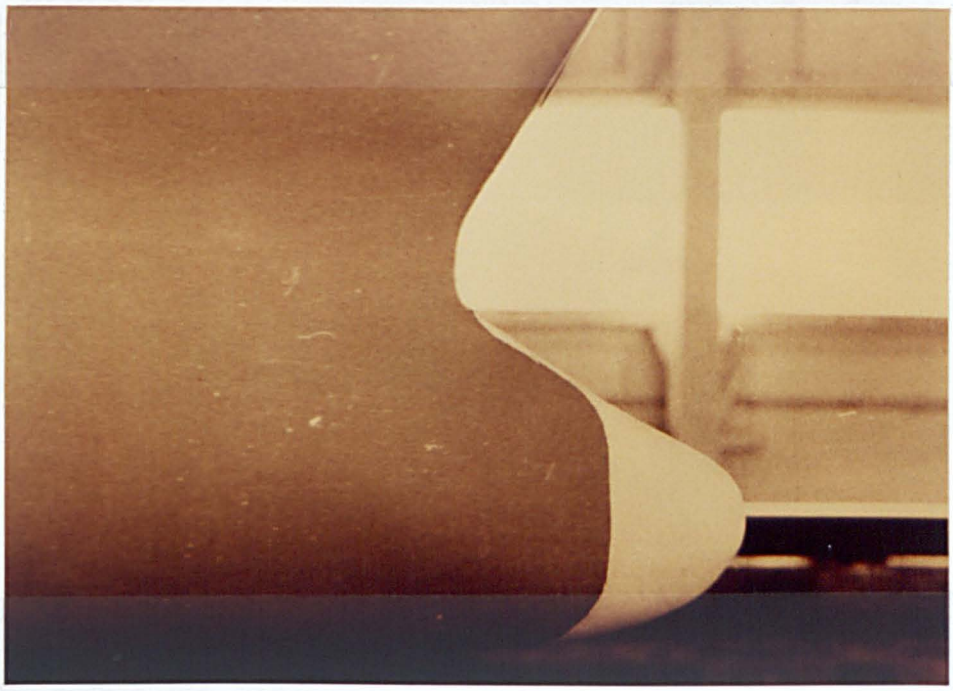

Fig. 15

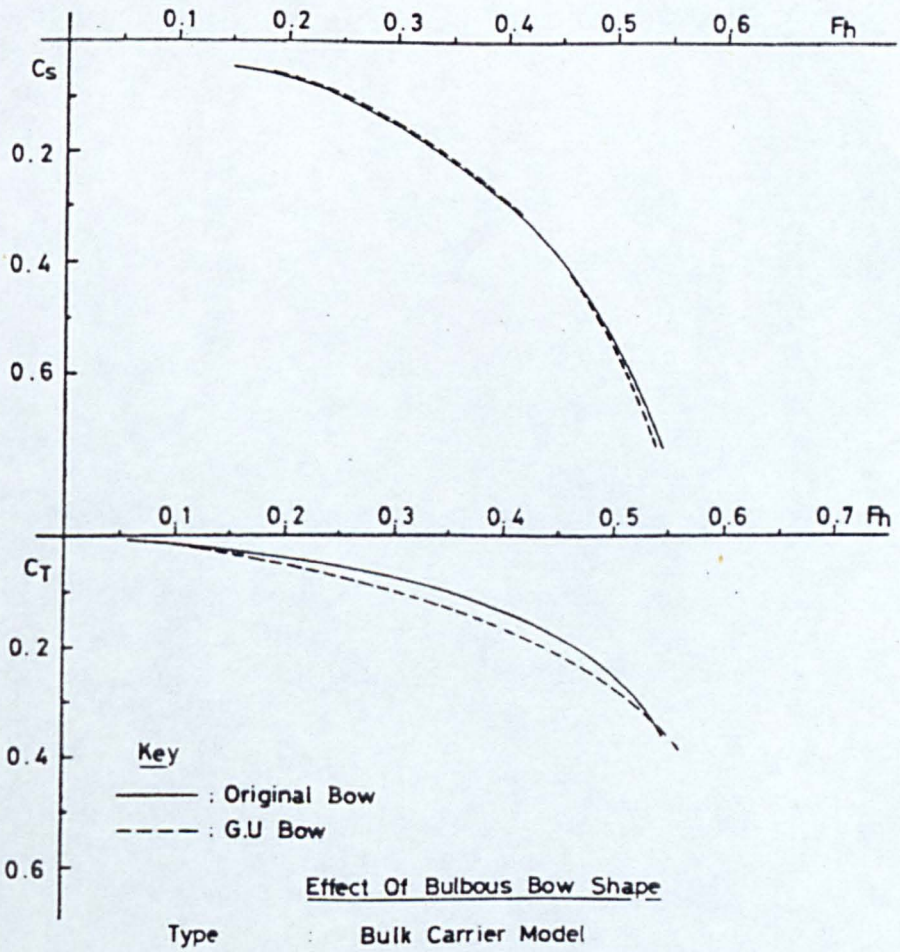

Effect Of Bulbous Bow Shape

Type	:	Bulk Carrier Model
Condition	:	Self-Propelled, Unrestricted Water
Draught	:	0.174 m, Level Keel
		$h/T = 1.2$

Fig. 16

adding a bulb to an otherwise bulb-less hull will influence the boundary-layer development and the wave system along the hull. It is then to be expected that sinkage and, particularly, trim will be affected to a larger extent than by the above changes in shape. No additional experiments into this topic were carried out.

(3.3) The Transition from an "Ideal" to a Real Fluid

The main reasons for the divergence of the theory from the naked-hull experiments of the previous sections, merit discussion. In order to eliminate some of the mathematical difficulties, the classical theories diverge from reality in two major aspects,

1. they are "ideal fluid" theories and inherently unable to handle viscous flow situations and

2. both are "linearized" theories, hence restricted to ships of very small beam to length ratio (either "thin" or "slender"), whose surface slopes are everywhere small, advancing at steady speed, creating waves of infinitesimal height.

At low speeds non-linearities may be expected to be negligible and viscous effects dominate. As speed is increased non-linearities assume a progressively greater importance.

(3.3.a) Viscous Effects

Physical reasoning indicates that full-form ships advancing at relatively low speeds through shallow-water operate in viscosity dominated regions. The normal (deep water) flow pattern is appreciably distorted by the interaction between the boundary layers along the hull and sea bottom and is further aggravated by lateral restrictions. The problem is complicated by the early separation and consequent high viscous form drag experienced by bluff forms, and the difficulty in predicting the effect of shallow-water on separation. The complex viscous nature of the flow is also demonstrated by observations (for example, Moody [52]) which indicate that at low depth-draught ratios the flow becomes largely retarded and is periodically relieved by the shedding of vortices. The experiments of Bazilevsky [4] clearly illustrate the occurence of separation for a towed naked-hull model. It is highly probable, therefore, that viscous effects are responsible for the divergence of theory from experiment at low underkeel clearances, as observed in section (3.2.d).

From the viewpoint of hydrodynamics, problems involving viscous effects are in principle complex analytically (involving the solution of the Navier-Stokes equations) and only approximate approaches have been attempted, notably by Havelock [84] and Eng and Breslin [25]. Although these were intended to assist the wave

resistance problem, clearly, the same phenomena are responsible for the changes in the vertical-plane forces. Investigations indicate that both mean sinkage and trim are related to viscous (form resistance) effects. Mean sinkage is related to frictional form resistance as demonstrated by Horn [36] and Havelock [84], while Guilloton [34], Dand [21] suggest some functional relationship between trim and the viscous pressure resistance. Both trim and viscous pressure effects are dependent on boundary layer growth which in turn is affected by the normal pressure distribution over the hull and by surface waves; i.e., they are influenced by the unbalance between the normal pressure along the body length. The process is pictured phenomenologically in terms of a friction belt whose effect is to reduce the ship slope towards the stern, creating a new "effective" body and inducing changes in the pressure distribution. (This may viewed as modifying the hull form coefficients in section (2.2.g) owing to the virtual lengthening of the hull). Since for bluff forms the viscous pressure effects predominate, viscous phenomena may be expected to have a considerable effect on trim but a negligible effect on the mean sinkage, see (7.5). The suggestion by Tothill [72] that boundary layer growth can be simulated using the 1-D approach (i.e. adding the boundary layer displacement thickness to the ship cross-sectional area along the hull length) disagrees with model observations. The simulation produces a decreasing trim forward with decrease in water depth while naked-hull model experiments yield an increasing trim forward (i.e.

define unique curves when plotted in non-dimensional form, Fig.11). Finally, since the skin-friction component accounts for a significant proportion of the total resistance on conventional ships, the inherent neglect of the contribution from the horizontal viscous force resultant (multiplied by some fraction of the ship draught) to the trimming moment must assume significance.

(3.3.b) Hull Wave-system Effects

Normally, a moving ship generates a set of waves at both its bow and stern. Although the "rigid" free-surface assumption appears plausible at low speeds, it may be expected that agreement with reality will progressively deteriorate with increasing ship speed. The theories entirely neglect the appearance of a hull wave-system and the "screening" effect of the forebody on the afterbody (in fact, the interference of any section on another). Kelvin developed a theory to decribe the pattern of waves generated by a point pressure disturbance moving at steady-speed in deep water. The wave system contour in restricted water is described in detail by Saunders [58] and Sorensen [70]. It is characterised by a pronounced trough at the forward shoulder combined with a trough at the aft shoulder. The greater boundary layer thickness at the stern, combined with the presence of separation damps the wave system aft, while forward little is altered because of the relative boundary layer thinness. In the higher speed range, this wave system may be expected to

give a greater trim-by-bow than predicted on the assumption of non-viscous fluid and a "rigid" free-surface.

The theoretical modelling of the above free-surface effects (i.e. the fullfilment of the free-surface conditions) poses major problems at present.

(3.3.c) Froude Depth Number Effect on Wave Phenomena

Restrictions in available water may interfere with the vertical orbital wave motion. Linear wave theory indicates that in water of finite-depth the translational speed of the wave profile is,

$$v_h = \sqrt{\frac{g\ell}{2\pi}\tanh\left(\frac{2\pi h}{\ell}\right)} \qquad \ldots\ldots (3.3.1.a)$$

$$= v_\infty \sqrt{\tanh\left(\frac{2\pi h}{\ell}\right)} \qquad \ldots\ldots (3.3.1.b)$$

with,

v_h=speed of translation wave in shallow-water

v_∞=speed of translation wave in deep water

ℓ =wave length

and the particles describe elliptical paths instead of the deep water circular orbits.

As the water depth tends to zero, $\tanh(2\pi h/l) \simeq (2\pi h/l)$ and (3.3.1) reduces the limiting value,

$$v_h = \sqrt{gh} \qquad \ldots\ldots (3.3.2)$$

This means that in water of finite-depth the speed of progressive waves is independent of the wavelength and can not exceed the speed of the solitary wave (3.3.2).

According to Schuster [60] and Weinblum [83], the influence of depth restrictions on the wave-making resistance (and, therefore, on the sinkage and trim) becomes noticable only when the ratio of the main axes of the elliptical paths attains a value of approximately 0.95. That is, only when,

$$\tanh(2\pi h/l) < 0.95$$

and $$(2\pi h/l) \simeq (gh/V^2) < 1.83$$

or $$F_h > 0.7 \qquad \ldots\ldots (3.3.3)$$

Therefore, for Froude depth numbers smaller than approximately 0.7, deep water conditions exist and the wave pattern is not affected by lateral or depth restrictions (except for the influence of viscosity, discussed previously).

(3.4) Self-propulsion Effects

The shift from the assumptions and hypotheses of hydrodynamics to the actual ship behaviour involves more than the transition from an "ideal" to a real fluid. The most obvious required extension is the consideration of self-propulsion effects.

(3.4.a) Unrestricted Shallow-water

It was shown in section (3.2.a) that in the naked-hull condition the model exhibits an insignificant dependence on the depth-draught ratio. In contrast, when self-propelled the same model exhibits a clear dependence of these coefficients on the depth-draught ratio, Fig.17. This is further examined in Fig.18,19. The increase in mean sinkage is constant in value throughout the depth-draught ratio range (approximately 15%). The effect of self-propulsion on trim is more complicated and led to a comprehensive analysis of the available shallow-water data at the tank. The results for a depth-draught ratio of $1.0 < h/T \leq 2.0$, are presented in Fig.20 where the curves were faired into zero trim at the (grounding) depth-draught ratio of 1. Good agreement was noted with the correctors of Dand and Ferguson [23]. Figs.20,21 illustrate that while the naked hull model trims increasingly by the head with the decrease in depth-draught ratio, the self-propelled model decreases its trim by bow under the same circumstances.

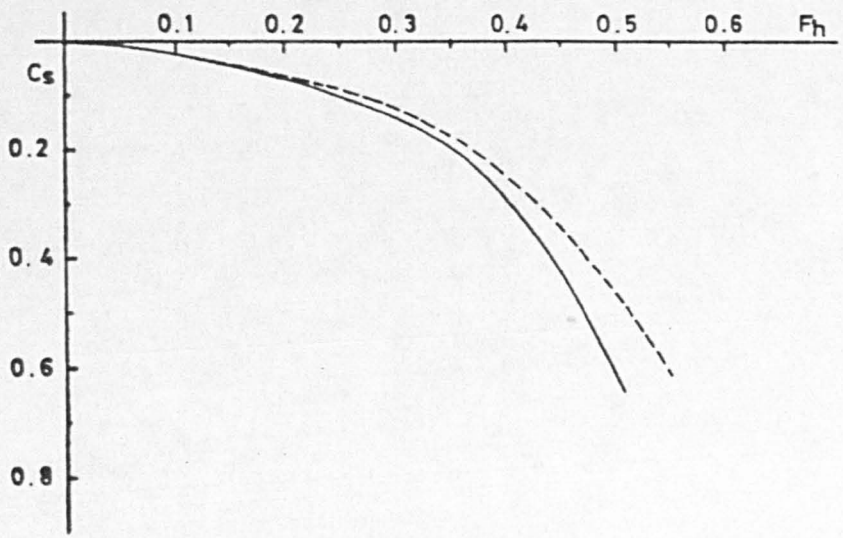

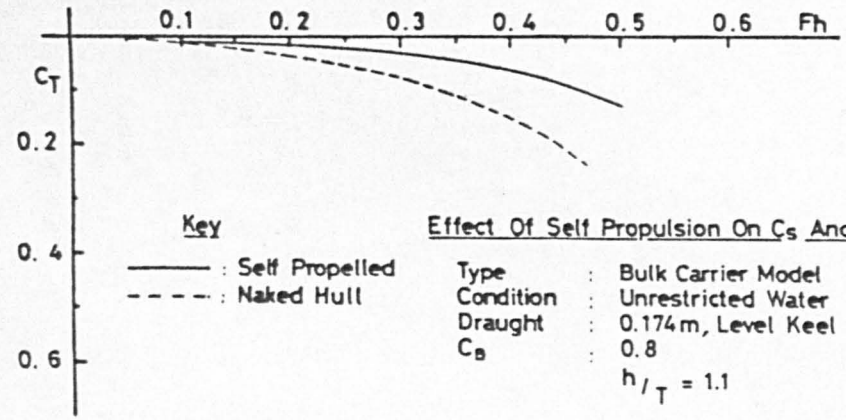

Key

——— : Self Propelled

- - - - : Naked Hull

Effect Of Self Propulsion On C_S And C_T

Type	:	Bulk Carrier Model
Condition	:	Unrestricted Water
Draught	:	0.174m, Level Keel
C_B	:	0.8
		$h/T = 1.1$

Fig 18

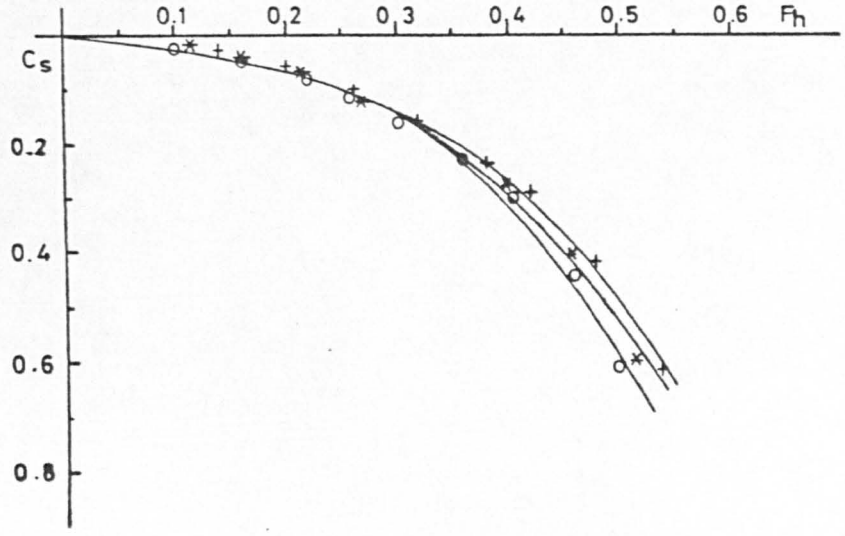

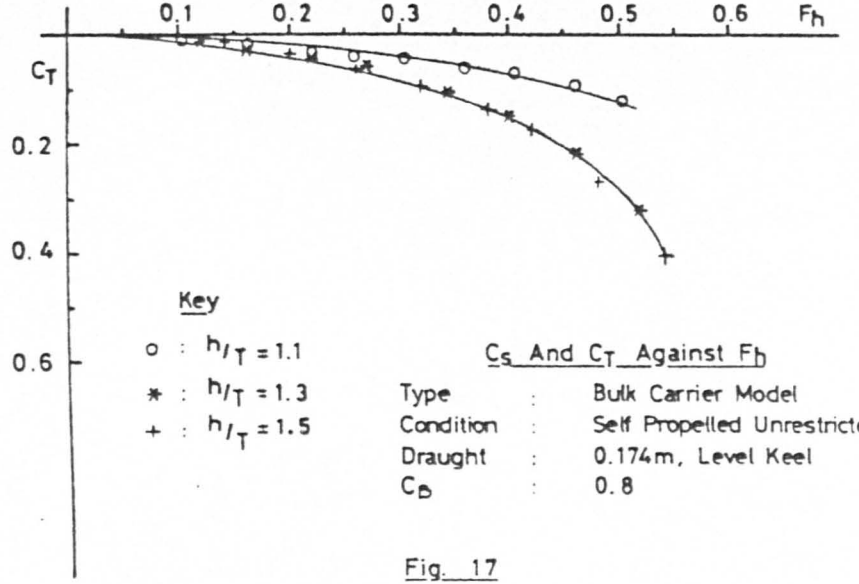

Key

o : $h/T = 1.1$

* : $h/T = 1.3$

\+ : $h/T = 1.5$

C_S And C_T Against F_h

Type	:	Bulk Carrier Model
Condition	:	Self Propelled Unrestricted Water
Draught	:	0.174m, Level Keel
C_B	:	0.8

Fig. 17

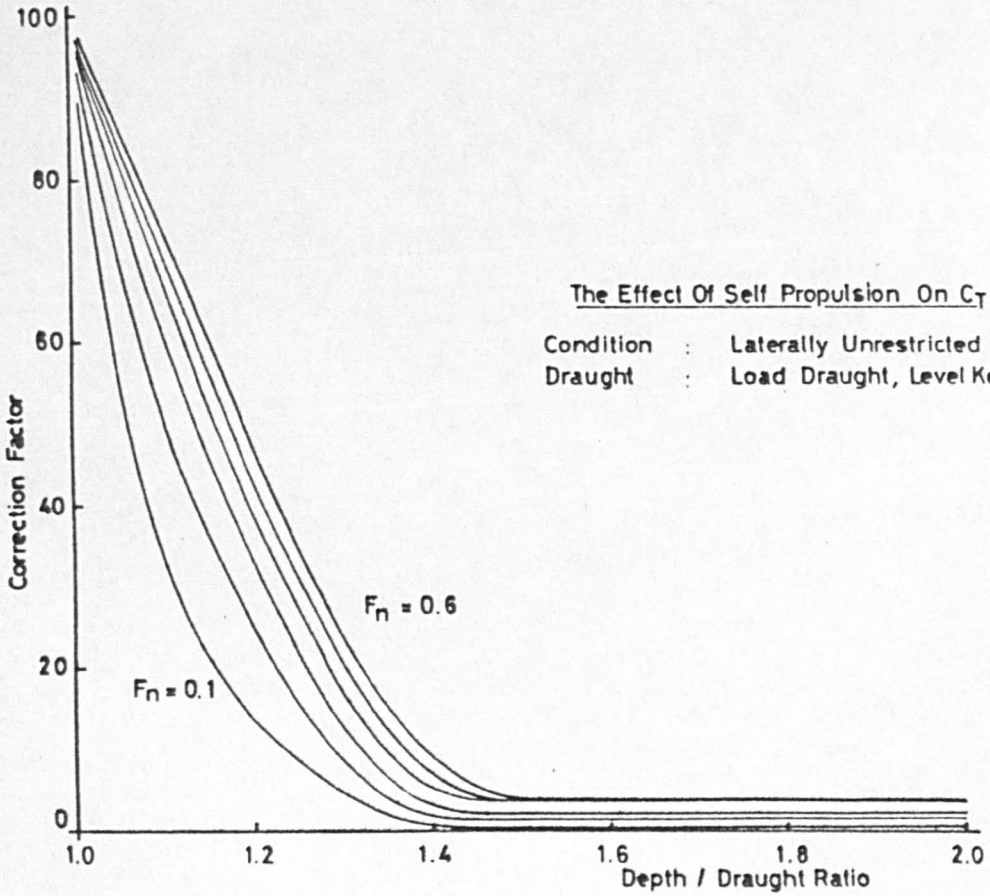

The Effect Of Self Propulsion On C_T

Condition : Laterally Unrestricted Water.
Draught : Load Draught, Level Keel.

Fig. 20

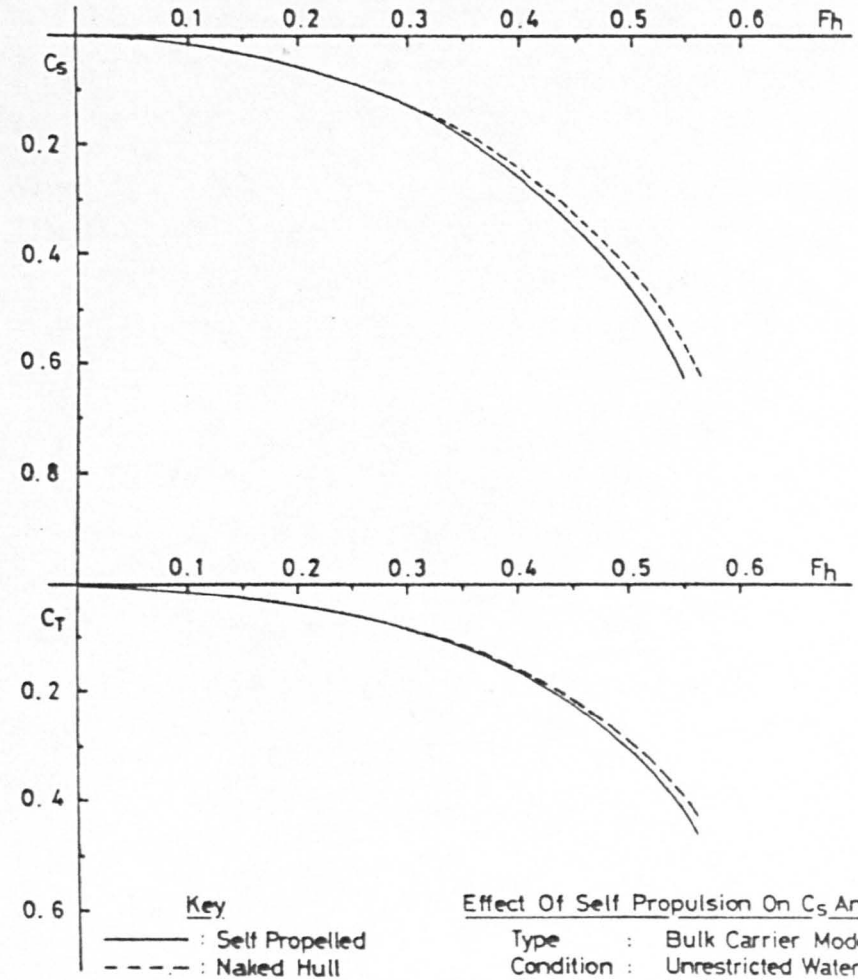

Effect Of Self Propulsion On C_S And C_T

Type : Bulk Carrier Model
Condition : Unrestricted Water
Draught : 0.174m, Level Keel
C_B : 0.8
$h/T = 1.5$

Fig. 19

The results are in agreement with the observations of Bazilevsky [4] and Hooft [38], which show that the screw propeller creates a considerable decrease in pressure over the aft region when compared with the naked hull condition. This decrease in pressure leads to a decrease in stern underkeel clearance and further flow constrictions leading to the increase in mean sinkage.

(3.4.b) The Effect of Lateral Restrictions

Figs.21,22,23 illustrate that the effects of self-propulsion in the restricted channel remain qualitatively similar to those observed in unrestricted shallow water. A quantitative analysis of the data indicated that the correction factors of Fig.20 are, for all practical purposes, equally valid in laterally restricted water.

This is fortunate and permits the use of the universal ratios of section (3.3.c) to extrapolate into finite-widths in the self-propelled mode, or vice-versa. The extrapolation was, in fact, carried out for the representative model and good agreement with the self-propelled experimental results was obtained.

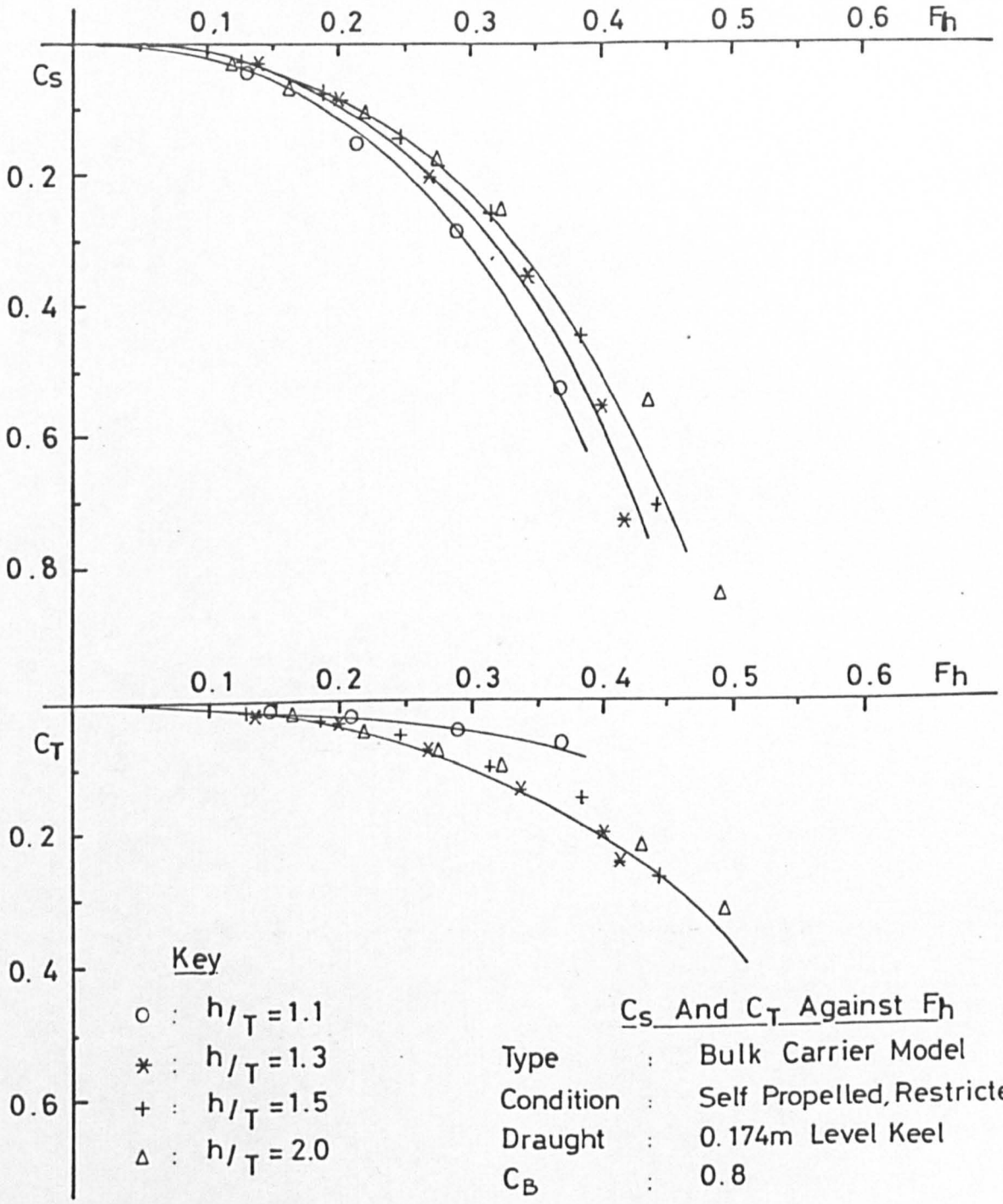

Cs And CT Against Fh

Type	:	Bulk Carrier Model
Condition	:	Self Propelled, Restricted Water
Draught	:	0.174m Level Keel
C_B	:	0.8

Fig 21

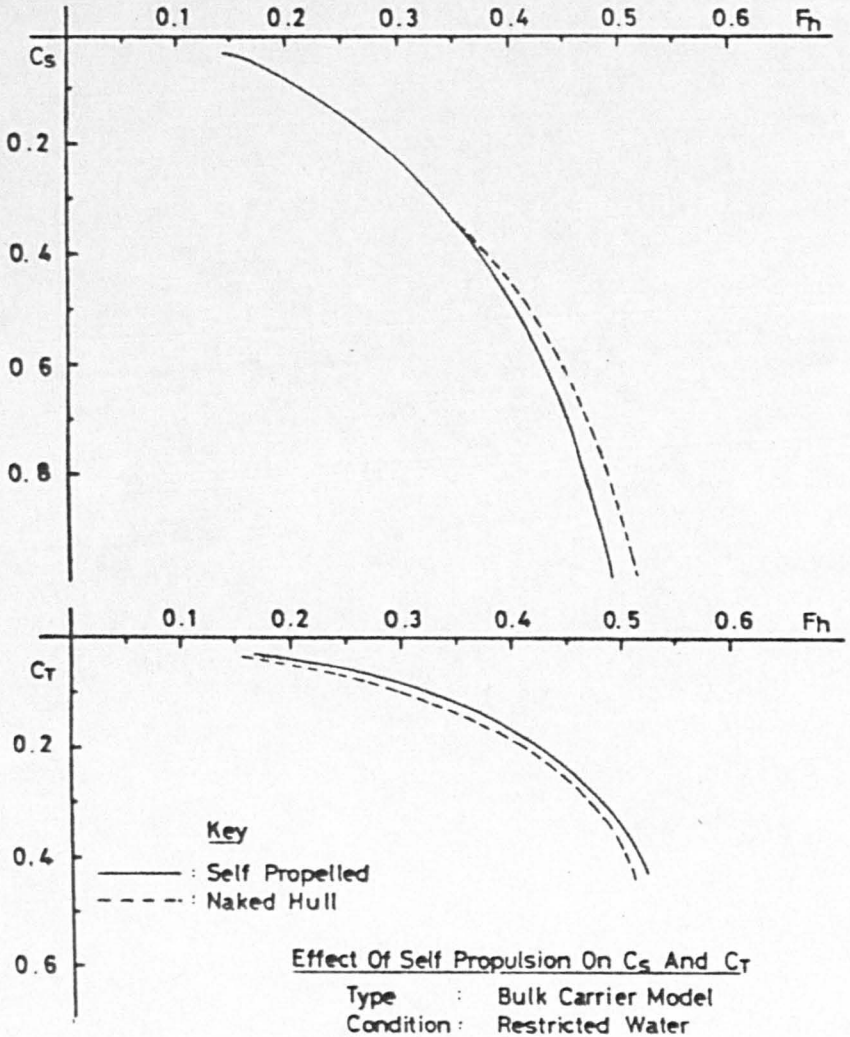

Effect Of Self Propulsion On C_S And C_T

Type	:	Bulk Carrier Model
Condition	:	Restricted Water
Draught	:	0.174m Level Keel
C_B	:	0.8
	:	$h/T = 1.5$

Fig 23

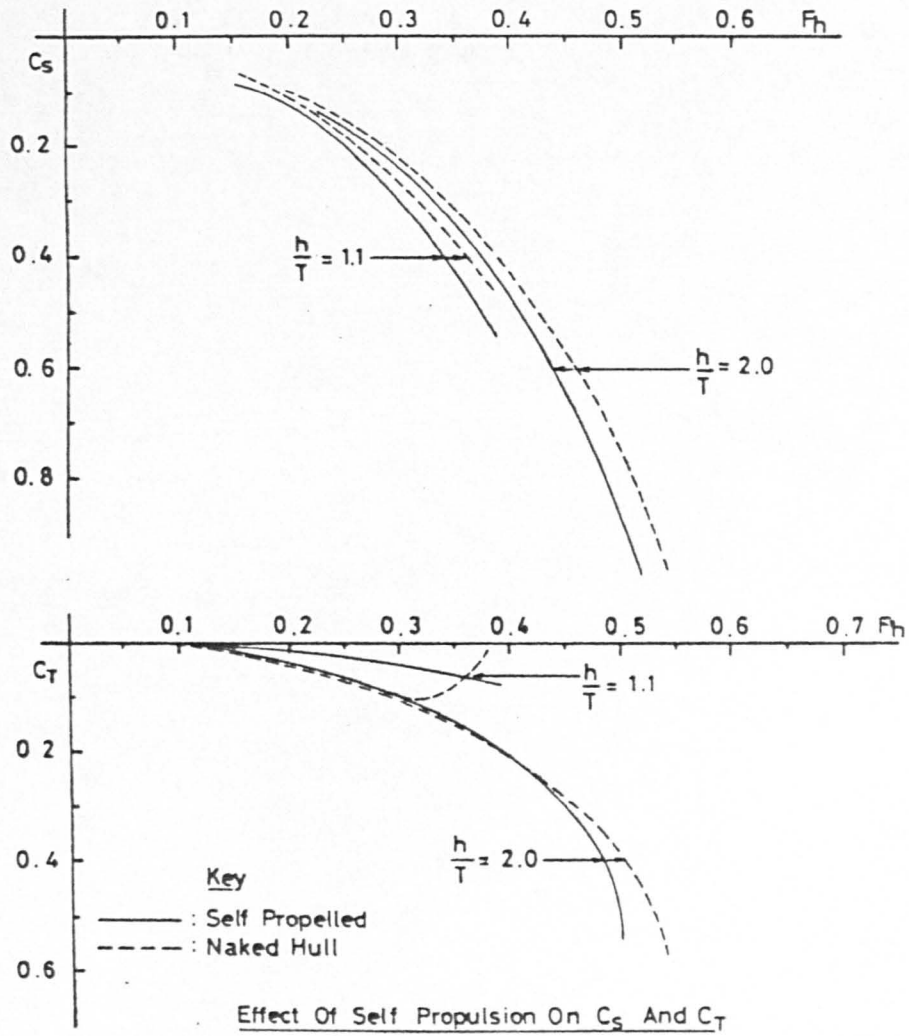

Effect Of Self Propulsion On C_S And C_T

Type	:	Bulk Carrier Model
Condition	:	Restricted Water
Draught	:	0.174m, Level Keel
C_B	:	0.8
	:	$h/T = 1.1, 2.0$

Fig 22

(3.5) The Semi-Empirical Approach

The theory/experiment comparisons indicate that the difficulties in attempting a purely theoretical or purely empirical treatment of the problem are many. The 2-D hydrodynamic approach is a significant and comprehensive qualitative contribution but produces only a rough quantitative guide to ship performance. Both it and the 1-D hydraulic approach must be supplemented and modified through reference to systematic experimental data to cater for the effects of viscosity, hull wave-system and self-propulsion if the prediction method is to cater efficiently for a broad range of vehicles.

In what follows, the hydraulic analogy approach was prefered owing to its conceptual clarity and its ability to cater for the restricted channel case more adequately. The unrestricted shallow-water results may be extrapolated into intermediate finite-widths most efficiently by using hydrodynamic theory. The intermediate, finite-width limiting speed may then be obtained by re-employing the hydraulic theory. This procedure serves as the basis for the computer program and can also be adapted to cater for the effects of self-propulsion.

CHAPTER 4

The Mono-hull Computer Programs

The final version of the mono-hull computer program predicts the sinkage and trim of full-form models in shallow-water ($1.0 < h/T < 2.0$) of any width. Following Dand [19], its' theoretical base is modified by reference to model tests, providing rapid results using early-design-stage input for either the "towed" or "self-propelled" mode. Its range of validity is determined primarily by the available empirical data.

(4.1) The SQUAT Program - Flow Chart

Fig.24 presents the program flow-chart for visual assistance.

(4.1.a) Typical Input

Fig.25 illustrates a typical input routine which is assisted by a series of program prompts. The program accepts model/ship moulded data in the form of at-rest draught waterplane half-breadths at 21 stations and the full sectional areas up to the same waterplane at the same stations. The input unit is the meter. The input allows a choice of F_h, h/T and output scale within its range of

```
>
>RUN SQUAT
IS SHIP DATA ALREADY ON FILE (Y OR N) ? N
ENTER WATERLINE LENGTH OF SHIP/MODEL IN METERS : 200.0
ENTER SHIP/MODEL DRAFT AT FWD PERPENDICULAR : 10.325
ENTER SHIP/MODEL DRAFT AT AFT PERPENDICULAR : 10.325
ENTER 21 WATERLINE OFFSETS FOR THE FOLLOWING STATIONS;
0,.25,.5,.75,1,1.5,2,2.5,3,4,5,6,7,7.5,8,8.5,9,9.25,9.5,9.75,10
1.61
4.41
7.06
9.25
10.87
12.96
13.91
14.1
14.1
14.1
14.1
14.1
14.1
14.1
14.1
13.68
12.0
10.13
7.28
3.835
0.027
ENTER 21 XSEC AREAS TO DRAFT W.P. AT THE SAME STATIONS;(M.SQ.)
1.892
17.363
69.36
117.388
161.05
226.47
261.664
274.092
278.35
279.14
279.14
279.14
279.14
279.14
277.297
262.833
217.83
175.79
117.226
51.13
0.0179
IS DATA TO BE STORED (Y OR N) ? N
ENTER MIN./MAX. VALUES OF FROUDE DEPTH NUMBER: 0.1,0.6
ENTER MIN./MAX. VALUES OF DEPTH-DRAFT RATIO : 1.05,1.3
HOW MANY INCREMENTS OF DEPTH-DRAFT RATIO DESIRED IN THIS RANGE ? 3
DO YOU WISH OUTPUT LISTING (Y OR N) ? Y
DO YOU WISH RESULTS STORED FOR PLOTTING (Y OR N) ? N
PREDICTION REQUIRED IN;(1) RESTRICTED OR (2)
UNRESTRICTED SHALLOW WATER ( 1 OR 2 ) ? 2
PREDICTION REQUIRED FOR (1) TOWED (NAKED-HULL) OR (2)
SELF-PROPELLED MODE ( 1 OR 2 ) ? 1
PREDICTION REQUIRED FOR (1) INPUT OR (2)
OTHER SCALE ( 1 OR 2 ) ? 2
WHAT IS NEW SCALE SHIP L.B.P ? 160.0
```

Fig 25

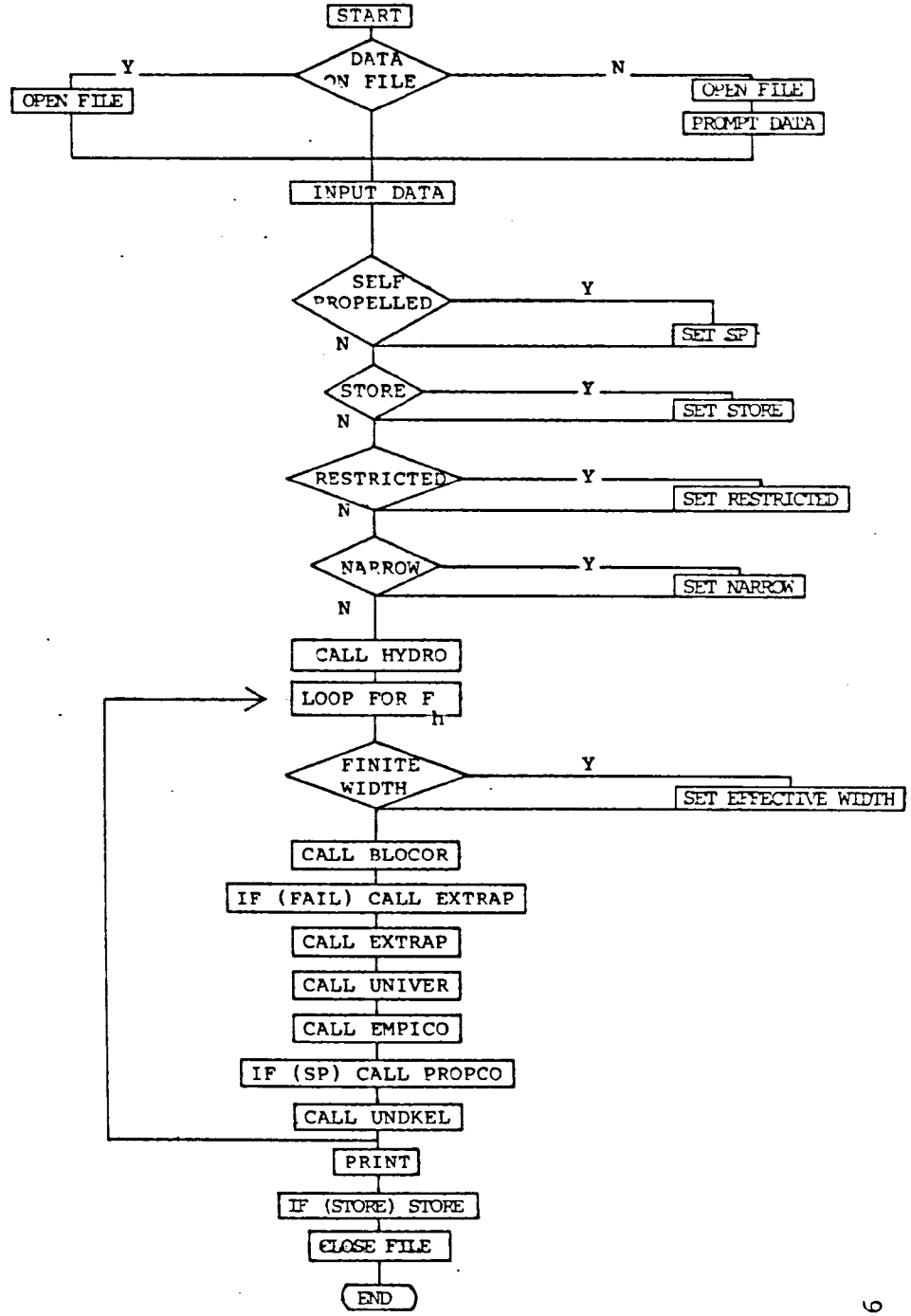

FIG. 24 SQUAT PROGRAM - FLOW CHART

validity, for either laterally restricted or unrestricted shallow-water. If the required output scale is different from the input scale, the program prompts for the new scale ship length. The non-dimensional C_S and C_T results may be stored for subsequent plotting.

(4.1.b) Numerical Methods and Procedures

Upon data input, subroutine HYDRO evaluates the required hydrostatics, calculating all moments about the LCF. The pressure force and moment acting about the at-rest draught waterplane LCF, are calculated by subroutine BLOCOR, solving equation (2.4.3) at each model/ship cross-section by the Newton-Raphson iteration method. This is performed in a fictitious channel of an "effective" width equal to one ship length. The total (hydrostatic) force and moment are obtained by integrating the pressure force and moment derived for each ship/model cross-section along the hull length. Simpson's rule is used throughout for integration. The resulting sinkage and trim are obtained by equating the hydrostatic restoring force and moment with the derived pressure force and moment.

The laterally restricted option is divided internally into "finite" and "narrow" width regimes, depending on the w/L ratio. In the former, defined by $3 \leq w/L \leq 1$, the basic calculation is performed for the laterally unrestricted condition and the results then extrapolated

using the universal ratios of section (3.2.c). The latter were stored in the form,

$$y = Jx^k$$

in subroutine UNIVER. If w/L < 1, the hydraulic analogy approach is employed to yield the usual "narrow" channel "towed" or "self-propelled" modes. A laterally unrestricted shallow-water condition is assumed for w/L > 3.

If owing to imaginary roots there is no solution to equation (2.4.3), the program skips to the next case. The previously calculated C_S and C_T values are then extrapolated using Adams' extrapolation formula, see Abramowitz and Stegun [1],

$$f(n+1) = f(n) + \frac{\Delta x}{24}[55f'(n) - 59f'(n-1) + 37f'(n-2) - 9f'(n-3)]$$

If the derivatives are obtained using the basic formula,

$$f'(x) = \frac{f(x+1) - f(x-1)}{2\Delta x}$$

where Δx is the common interval, a variant of the above extrapolator is obtained in the form,

$$f(n+1) = [11f(n) + 18f(n-1) - 50f(n-2) + 37f(n-3) - 9f(n-4)]$$

This expression proved very satisfactory in practice, see Fig.30. In the unrestricted and finite-width regimes, extrapolated data appears with a star (*) beside it to

differentiate from normally calculated data. In the "narrow" case, the star (*) always denotes the incipience of the transcritical regime or the limiting speed. The limiting (or lower critical speed) for the "finite" and "narrow" modes is obtained using the expression, see Appendix D,

$$F_h^L = \{6\cos(\frac{\theta + 180^o}{3}) - 2(1-m(x)\}^{\frac{1}{2}}$$

In the unrestricted mode, the 3-D "towed" condition is obtained by using empirically derived multipliers which were stored as functions of Tuck's effective width parameter in subroutine EMPICO, see Dand and Ferguson [23]. The effect of self-propulsion on the mean sinkage and trim was approximated by the empirically derived correctors of Fig.13, stored as 5th order polynomials in subroutine PROPCO. Linear interpolation is used to obtain intermediate F_h values for a given h/T. This crude procedure approximates the curve between two adjacent tabulated F_h values by a chord and is adequate for the task, as shown plotted in Fig.26, using subroutine PROPLT.

(4.1.c) Typical Output

Figs.27,28 demonstrate the reasonable agreement (within 10%) between the prediction method and experiment in both the towed and self-propelled modes. A typical computer output, Tables 6-9, is presented for the self-propelled comparison of Fig.28. The output commences

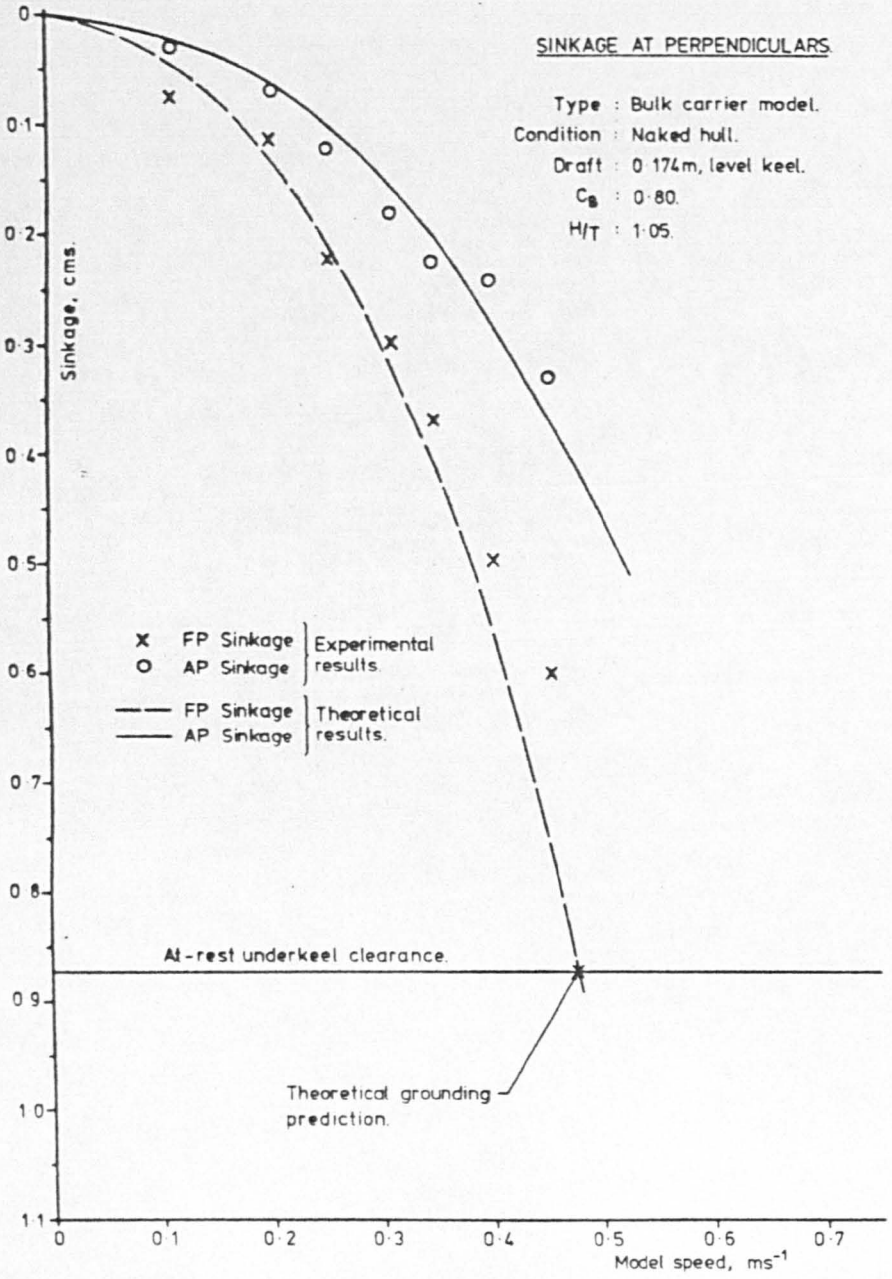

Figure 27

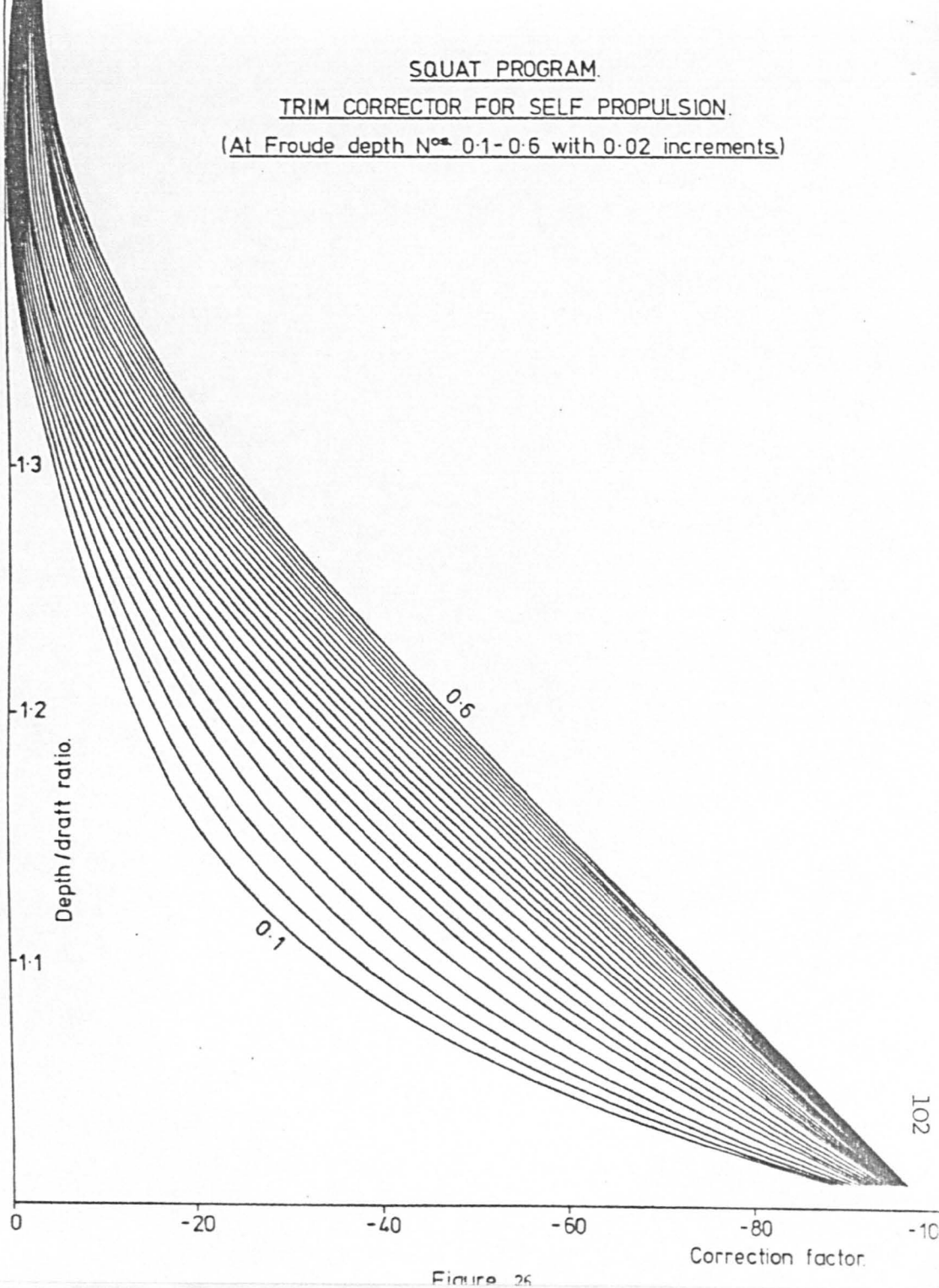

Figure 26

SQUAT PREDICTION FOR UNRESTRICTED SHALLOW-WATER :

SCALE ; AS INPUT.

CONDITION ; SELF-PROPELLED

AT-REST (MAXIMUM) DRAFT ..... = 0.174 M

AT-REST WATER DEPTH ..... = 0.209 M

MEAN SINKAGE (CS) AND TRIM (CT) COEFFICIENTS;

NOTE; A "*" (STAR) DENOTES EXTRAPOLATED VALUE.

DEPTH-DRAFT RATIO ..... = 1.20

FROUDE DEPTH NUMBER	CS	CT
0.10	-0.015	-0.009
0.12	-0.022	-0.012
0.14	-0.030	-0.016
0.16	-0.039	-0.020
0.18	-0.050	-0.025
0.20	-0.062	-0.030
0.22	-0.075	-0.036
0.24	-0.090	-0.043
0.26	-0.107	-0.049
0.28	-0.125	-0.056
0.30	-0.145	-0.064
0.32	-0.168	-0.073
0.34	-0.192	-0.082
0.36	-0.219	-0.092
0.38	-0.250	-0.103
0.40	-0.283	-0.115
0.42	-0.321	-0.130
0.44	-0.365	-0.146
0.46	-0.415	-0.165
0.48	-0.474	-0.188
0.50	-0.548	-0.218
0.52	-0.645	-0.260
0.54	-0.758*	-0.309*
0.56	-0.910*	-0.382*
0.58	-1.057*	-0.445*
0.60	-1.294*	-0.569*

TABLE 7

SHALLOW-WATER SQUAT PREDICTION:

CHECK ON INPUT DATA :

STATION	OFFSET (HALF-BREADTHS) (M)	XSEC AREAS (M**2)
0.00	0.036000	0.000687
0.25	0.090900	0.005631
0.50	0.138000	0.015231
0.75	0.175200	0.024810
1.00	0.191800	0.038622
1.50	0.239800	0.059275
2.00	0.255800	0.075000
2.50	0.258100	0.084091
3.00	0.258100	0.088119
4.00	0.258100	0.089501
5.00	0.258100	0.089501
6.00	0.258100	0.089501
7.00	0.258100	0.089501
7.50	0.258100	0.089060
8.00	0.252000	0.086015
8.50	0.233000	0.077932
9.00	0.191000	0.062324
9.25	0.160000	0.051391
9.50	0.120000	0.038583
9.75	0.072000	0.024388
10.00	0.010900	0.095190

LENGTH BETWEEN PERPENDICULARS ..... = 3.048 M

DRAFT FWD ..... = 0.174 M

DRAFT AFT ..... = 0.174 M

AT-REST TRIM ..... LEVEL-KEEL

WATER-PLANE AREA ..... = 1.375 M**2

LCF AFT OF ST.5 ..... = 0.013 M

LONG. MOM. OF INERTIA ABOUT LCF .... = 0.849 M**4

TABLE 6

UNDERKEEL CLEARANCE AGAINST SPEED ;

NOTE: A "*" (STAR) DENOTES EXTRAPOLATED VALUE.

DEPTH-DRAFT RATIO ..... = 1.20

AT-REST UNDERKEEL CLEARANCE ..... = 0.035 M

SPEED (M/S)	U/K CLEARANCE A.P. (M)	U/K CLEARANCE F.P. (M)
0.14	0.0345	0.0342
0.17	0.0343	0.0340
0.20	0.0342	0.0337
0.23	0.0339	0.0333
0.26	0.0337	0.0329
0.29	0.0334	0.0325
0.31	0.0331	0.0320
0.34	0.0327	0.0314
0.37	0.0323	0.0308
0.40	0.0319	0.0302
0.43	0.0314	0.0294
0.46	0.0308	0.0286
0.49	0.0302	0.0277
0.52	0.0295	0.0267
0.54	0.0288	0.0256
0.57	0.0279	0.0244
0.60	0.0270	0.0231
0.63	0.0259	0.0215
0.66	0.0247	0.0197
0.69	0.0232	0.0175
0.72	0.0214	0.0148
0.74	0.0191	0.0112
0.77	0.0164*	0.0070*
0.80	0.0129*	0.0013*
0.83	0.0094*	-0.0042*
0.86	0.0041*	-0.0133*

TABLE 9

SINKAGE AT A.P. AND F.P. AGAINST SPEED ;

NOTE; A "*" (STAR) DENOTES EXTRAPOLATED VALUE.

DEPTH-DRAFT RATIO ..... = 1.20

AT-REST UNDERKEEL CLEARANCE ..... = 0.035 M

SPEED (M/S)	SINKAGE AT A.P. (M)	SINKAGE AT F.P. (M)
0.14	-0.0003	-0.0006
0.17	-0.0005	-0.0008
0.20	-0.0007	-0.0011
0.23	-0.0009	-0.0015
0.26	-0.0011	-0.0019
0.29	-0.0014	-0.0023
0.31	-0.0017	-0.0028
0.34	-0.0021	-0.0034
0.37	-0.0025	-0.0040
0.40	-0.0030	-0.0047
0.43	-0.0035	-0.0054
0.46	-0.0040	-0.0062
0.49	-0.0046	-0.0071
0.52	-0.0053	-0.0081
0.54	-0.0060	-0.0092
0.57	-0.0069	-0.0104
0.60	-0.0078	-0.0118
0.63	-0.0089	-0.0133
0.66	-0.0101	-0.0152
0.69	-0.0116	-0.0173
0.72	-0.0134	-0.0200
0.74	-0.0157	-0.0236
0.77	-0.0184*	-0.0278*
0.80	-0.0219*	-0.0335*
0.83	-0.0254*	-0.0390*
0.86	-0.0308*	-0.0481*

TABLE 8

with a check print-out of the input data and the hydrostatics calculated, Table 6, and is followed by,

1. C_S and C_T coefficients against the Froude Depth Number, see Table 7

2. Sinkage at FP/AP against speed, see Table 8

3. Underkeel clearance against speed, see Table 9

Fig.29 presents results directly scaled to full-scale. It demonstrates a GO/NO-GO form, recommended for use on board ships. Table 10 presents a typical output in the restricted shallow-water mode.

(4.2) The SQTPLT Program

If plotting is required, the data stored for plotting in the SQUAT program is used by the SQTPLT program to plot C_S and C_T against F_h . Fig.30 presents a typical output plot of the data in Table 7 and, simultaneously, demonstrates the adequacy of the extrapolation procedure of section (4.1.b).

(4.3) Examination of Applicabilty

In this section, the applicability of the method to a number of possible practical situations is examined.

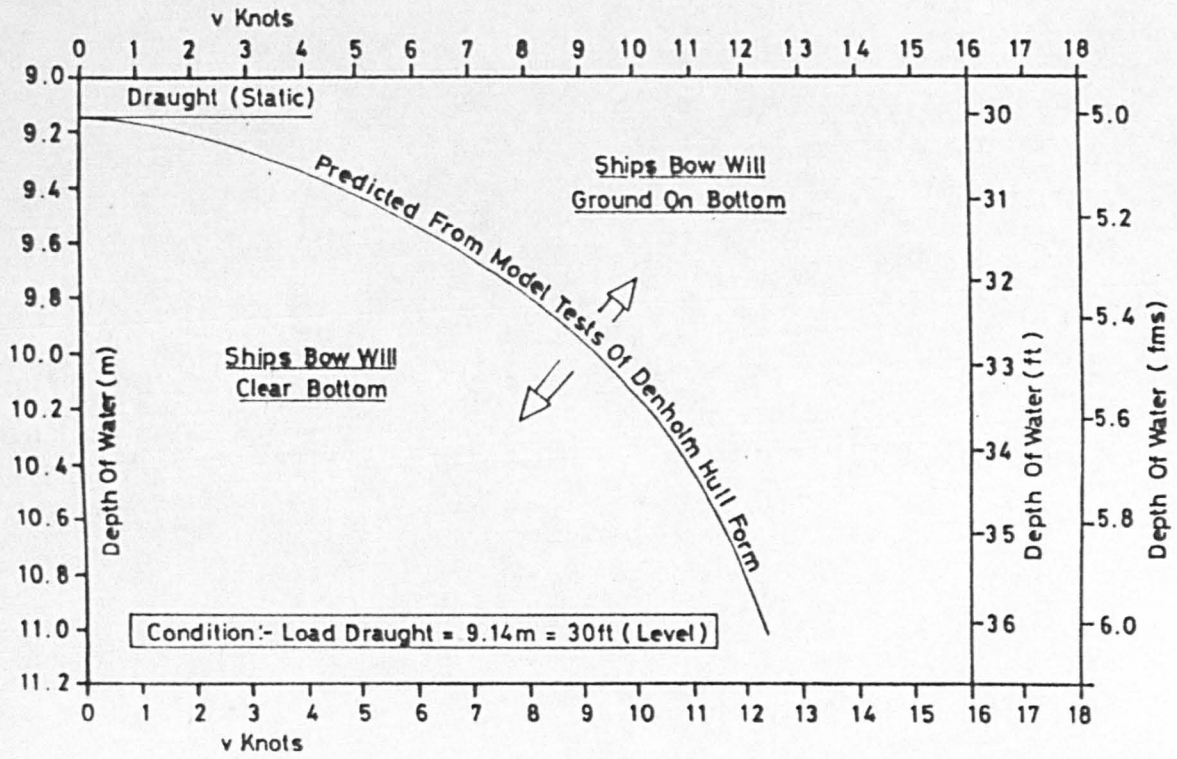

Fig. 29. Go / No Go Chart

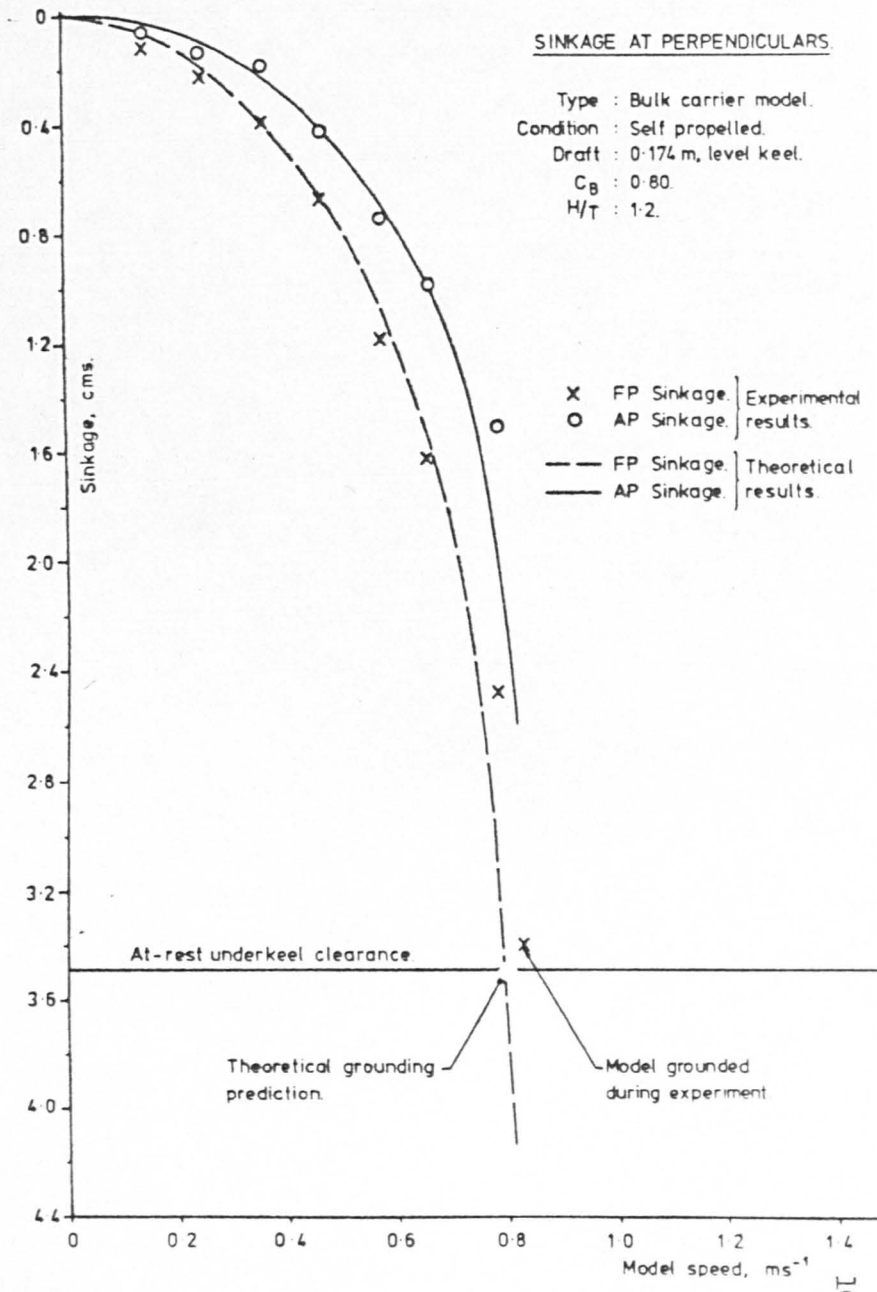

Figure 28

Sinkage At A P/F P As A Function Of Ship Speed
Comparison Of Load Draught And Ballast Draught Conditions

Vessel Type 0.8 C Bulk Carrier
Water Depth 10.97 m

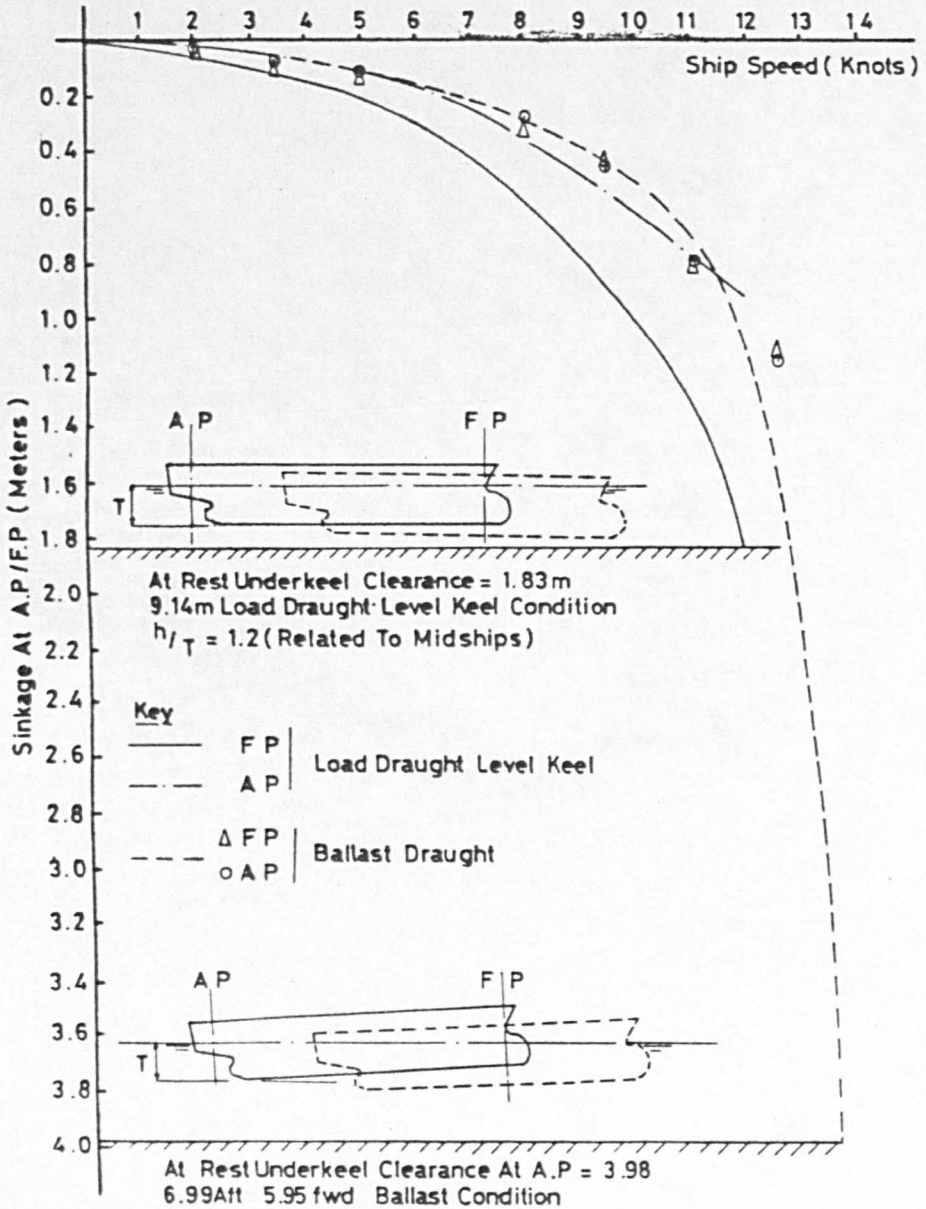

Fig. 31

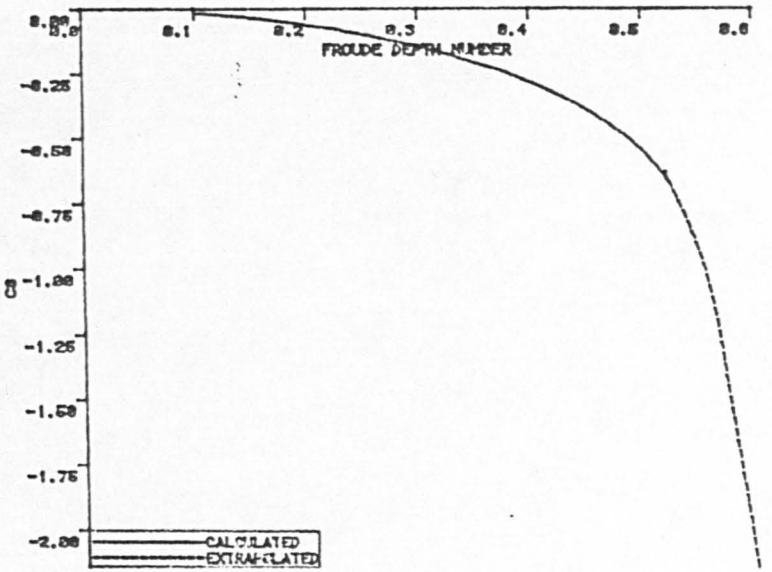

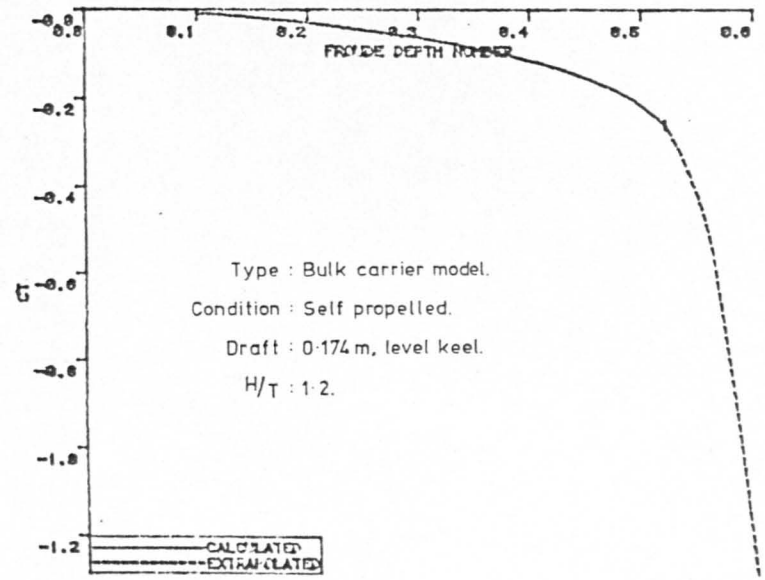

SQUAT PROGRAM
COMPUTER PLOT OF C_S AND C_T AS A FUNCTION OF FROUDE DEPTH NUMBER

Figure 30

(4.3.a) The Effects of Initial Trim and Draught

In agreement with findings reported by Dand [20], the self-propelled model experiments show that the initial (at-rest) trim and draught are an important factor in the subsequent sinkage and trim experienced.

Fig.31 demonstrates the change in behaviour induced by a change in the at-rest draught and trim for a set water depth in laterally unrestricted shallow water. The effect of initial trim is, at times , contrary to intuition and great care should be taken when using the conventional approaches, see Seren et al [61]. For example, in the self-propelled trim-by-stern condition, it is highly probable that any change forward underway will not be great enough to offset the initial (static) trim-by-stern. Owing to the decreased underkeel clearance at the stern and the "venturi" effect, the vessel may ground aft at roughly the same speed it would have grounded forward had it been in the initial (static) level-keel condition. Under such conditions the inherent tendency to change trim underway may be neutralized and the vessel experiences a change in the mean sinkage only. (Incidentally, the same vessel in the ballast, trim-by-stern condition in deep water, experiences a trim-by-bow underway.) An initial trim-by-bow will, on the other hand, initate an earlier grounding by the bow when compared to the level-keel condition. No parallel experiments were conducted in the naked-hull condition.

Fig.32 shows the effect of altering the at-rest trim at a set at-rest draught condition in the restricted channel. Maintaining a constant at-rest diplacement, the initial (at-rest) trim affects only the subsequent trim underway. Changing both the at-rest draught and at-rest trim to a ballast condition, Fig.32, alters the subsequent mean sinkage and trim underway and indicates that there exists an intermediate loading condition at which the model/ship will experience a change in the mean sinkage only, without change of trim. The behaviour in the ballast draught, trim-by-stern condition of a full-form ship is markedly similar to that of finer form ships in the level-keel condition. The general similarity between the immersed form of both suggests that, for a set speed, the trim-by-bow will decrease with increasing fullness aft and fineness forward. Depending on the exact immersed geometry and speed the ship will, at some point, commence to trim by stern.

Fig.32 also demonstrates the applicability of SQUAT program in the self-propelled, ballast draught, trim-by-stern condition in the restricted channel. The comparison shows that the self-propulsion correctors, derived in the level-keel condition, are equally valid in a ballast draught or trimmed condition. When trimmed, the depth-draught ratio changes along the ship length. As input the program accepts moulded data corresponding to the trimmed condition and evaluates the ship sinkage and trim based on the maximum draught (or minimum depth-draught

SQUAT PREDICTION FOR RESTRICTED SHALLOW-WATER
****

SCALE ; AS INPUT.

CONDITION ; SELF-PROPELLED

AT-REST (MAXIMUM) DRAFT ..... = 0.133 M

AT-REST WATER DEPTH ..... = 0.261 M

WIDTH OF CHANNEL ..... = 2.000 M

BLOCKAGE (BASED ON MIDSHIP SECTION) ..... = 0.121

LOWER CRITICAL FROUDE DEPTH NUMBER ..... = 0.587

WIDTH OF CHANNEL/LENGTH OF SHIP ..... = 0.656

MEAN SINKAGE (CS) AND TRIM (CT) COEFFICIENTS;

NOTE; A "*" (STAR) DENOTES EXTRAPOLATED VALUE.

DEPTH-DRAFT RATIO ..... = 1.96

FROUDE DEPTH NUMBER **********	CS ****	CT ****
0.10	-0.012	0.000
0.12	-0.018	0.001
0.14	-0.025	0.001
0.16	-0.033	0.001
0.18	-0.042	0.001
0.20	-0.052	0.002
0.22	-0.064	0.002
0.24	-0.077	0.003
0.26	-0.092	0.003
0.28	-0.109	0.004
0.30	-0.128	0.004
0.32	-0.149	0.005
0.34	-0.172	0.006
0.36	-0.198	0.007
0.38	-0.227	0.009
0.40	-0.260	0.010
0.42	-0.297	0.012
0.44	-0.340	0.015
0.46	-0.388	0.018
0.48	-0.445	0.022
0.50	-0.513	0.028
0.52	-0.595	0.037
0.54	-0.699	0.053
0.56	-0.841	0.086
0.58	-1.008*	0.125*
0.60	-1.241*	0.200*

TABLE 10

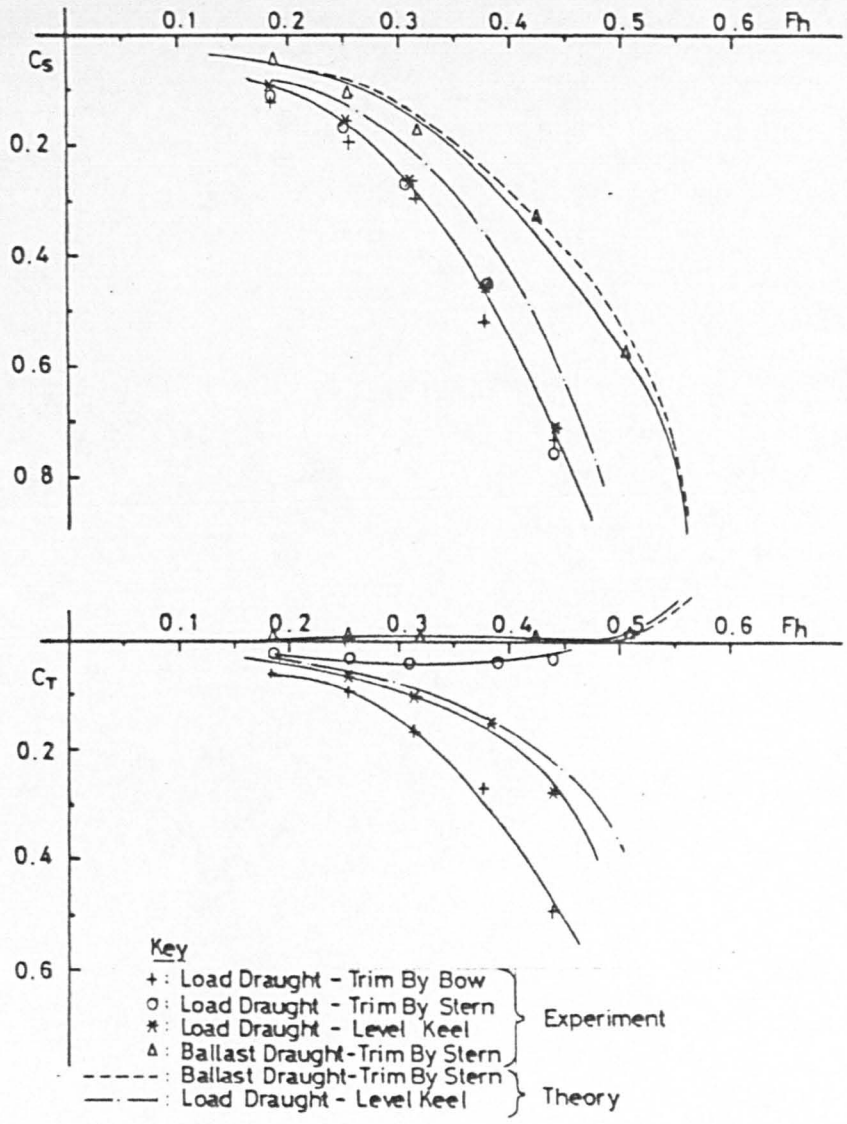

Effect Of Initial Trim And Draught On C_S And C_T

Type	:	Bulk Carrier Model
Condition	:	Self Propelled Restricted Water
C_B	:	0.8
Water Depth	:	0.261 m

Fig. 32

ratio). As shown in the corresponding computer output, Table 10, The method correctly identifies the extremity of interest and determines the grounding speed. Fig.33 exhibits a comparison between the theoretical prediction and experiment in the laterally unrestricted, self-propelled, ballast draught condition.

(4.3.b) Vessel Proximity/Transverse Channel Location

The effect of the transverse location in a channel is presented in Fig.34 for a depth-draught ratio of 1.3. Both sinkage and trim increase with decrease in separation between ship and side wall and are further aggravated by reducing the water depth. The assymetrical configuration is, at present, not allowed for in the method. The theoretical problem is complicated, see Beck [5], but an empirical procedure is available to evaluate the changes induced by sailing in the proximity of a channel bank, see NPC [54].

Similarly, sinkage and trim increases were obtained during tests conducted in the presence of a stationary vessel or wedge-form quay. It was found that a very reasonable approximation for the restriction effects could be obtained by deducting their maximum cross-sectional area from that of the channel (i.e. altering the blockage).

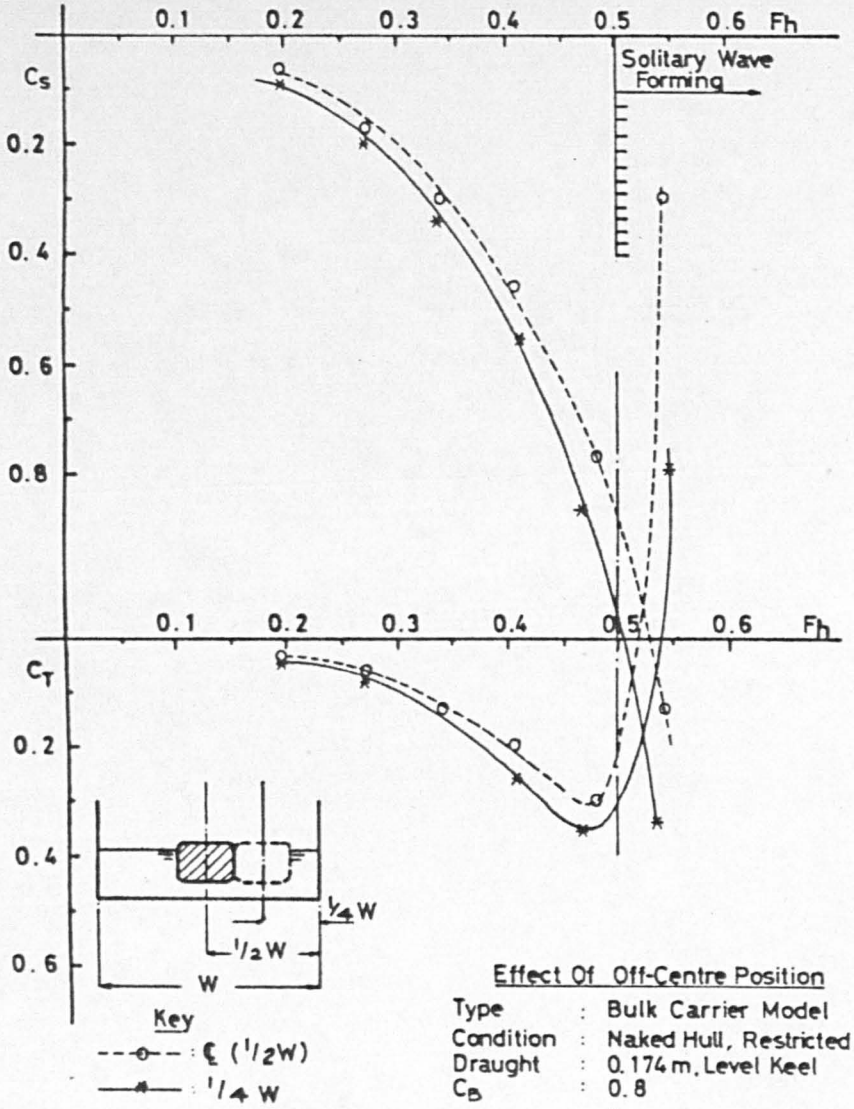

Effect Of Off-Centre Position

Type	:	Bulk Carrier Model
Condition	:	Naked Hull, Restricted Water
Draught	:	0.174 m, Level Keel
C_B	:	0.8
		$h/_T = 1.3$

Fig. 34

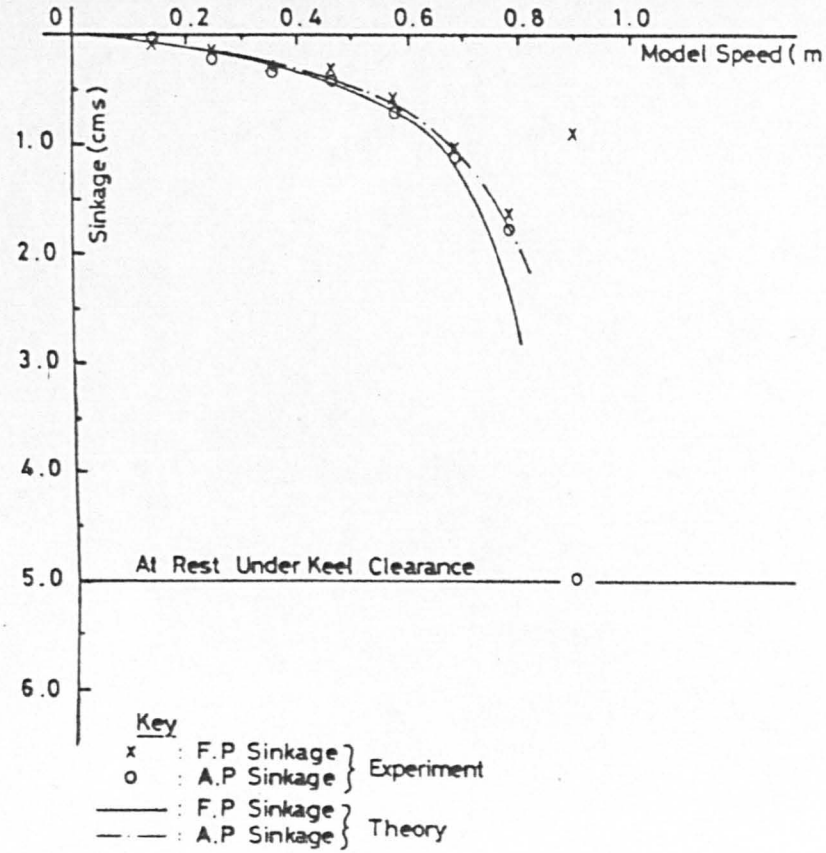

Sinkage At Perpendiculars

Type	:	Bulk Carrier Model
Condition	:	Self Propelled
Draught	:	0.113 m Fwd
		0.123 m Aft
		Ballast Draught
C_B	:	0.8
		$h/_T = 1.37$ (Related To A.P)

Fig. 33

(4.3.c) Extension to Other Channel Shapes

Since the empirical data used were obtained in a tank of rectangular cross-section, the present program version is adapted for a rectangular configuration. No substantial discrepancies are to be expected with other configurations as long as the blockage is approximately the same at similar depth-draught ratios. This is because the hydraulic analogy approach indicates, see section (2.4), that the forces depend on the blockage and not the actual channel shape. However, only a minor program modification is required to allow for other geometrical configurations. Artificial channels are usually trapezoidal, while natural fairways are often approximately parabolic. For the appropriate families of curves, see McNown [48]. No experiments into this topic were carried out.

(4.4) The Effect of a Sudden Depth Variation

There is no doubt that, particularly in shallower waters, bottom topography will affect the sinkage and trim behaviour. This may be deduced on intuitive grounds, since forces and moments vary with distance from the sea-bed. It may also be concluded based on the hydrodynamic analogy between the squat problem and the case of a ship moving parallel to a vertical obstacle. In particular there is a class of shallow water problems, such as approaching trenches and ridges across the fairway, where the vessel moves relatively suddenly from deep to shallow water. In

such a case the transient behaviour will be of interest because the maximum instantaneous draught will be greater than the steady-state draught underway.

Relevant data over a simulated shoaling sandbank were obtained while investigating a full-scale grounding incident, using the mono-hull model employed throughout this thesis, see Ferguson, Seren and McGregor [28]. Tests included two bulbous bows and both a load and ballast draught condition.

(4.4.a) The Influence of the At-Rest Load Condition

Brief experimental evidence is provided in Figs.35,36 in the load and ballast draught conditions, respectively. The results show that, in the load draught, level-keel condition, the vessel's bow has a dangerous tendency to sink towards the sandbank upon approach. The stern exhibits a similar attraction force as the bow leaves the level-run portion of the sandbank. The results show that the bow "senses" the sandbank and, upon approach, responds with a relatively sudden increase in mean sinkage and trim-by-bow, followed by a sudden reversal in trim. According to full-scale evidence on the same ship, this appears to be distinguishable on the full-scale and is of considerable practical significance since it appears to be present in shallow-water regardless of speed. It may, at times, serve as an "alarm", warning of invisible bottom irregularities.

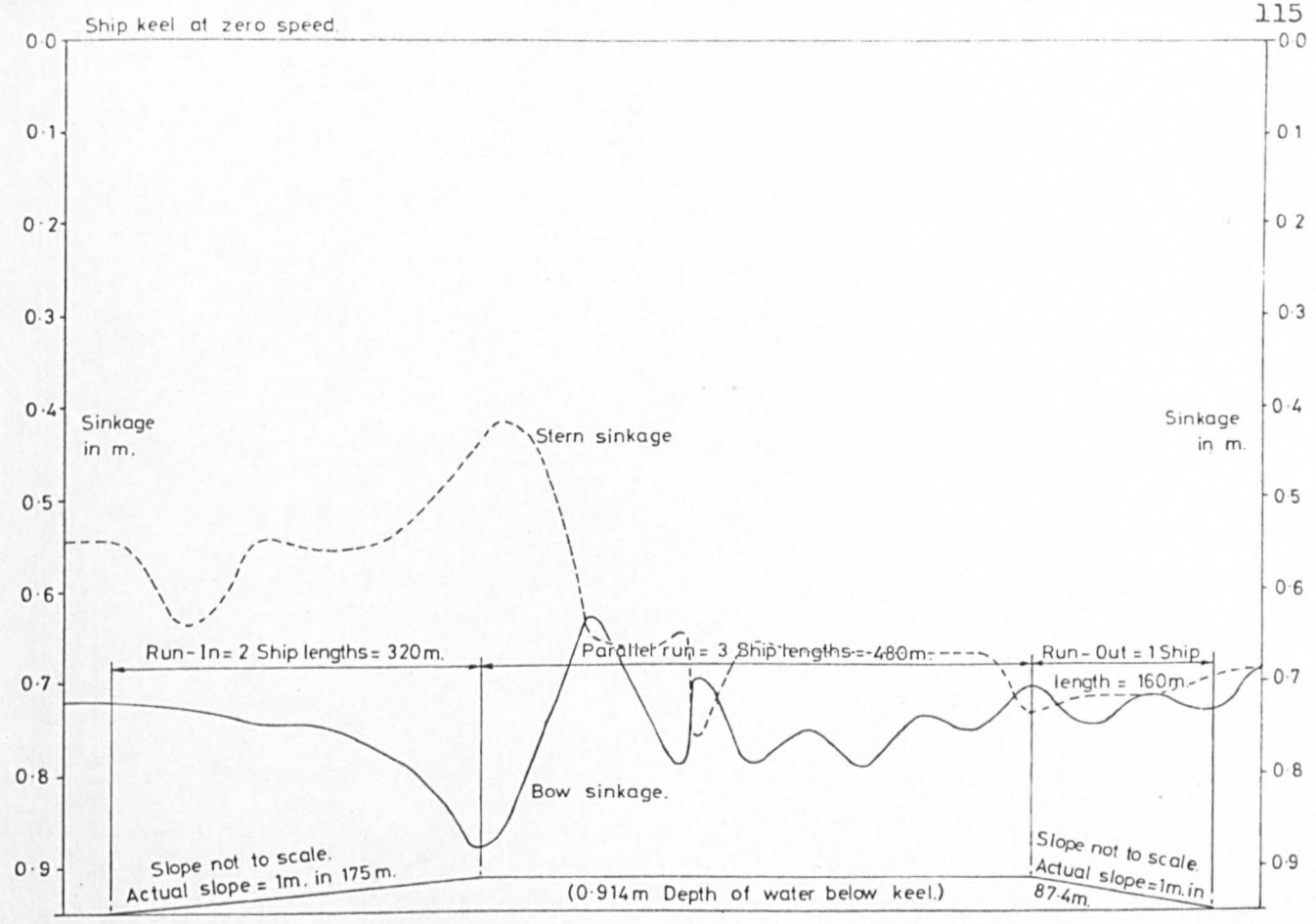

Fig.35 Bow and stern squat over sandbank in the incident condition at a depth-draught ratio of 1.1 over and 1.3 clear of sandbank at a speed of 9.5 knots

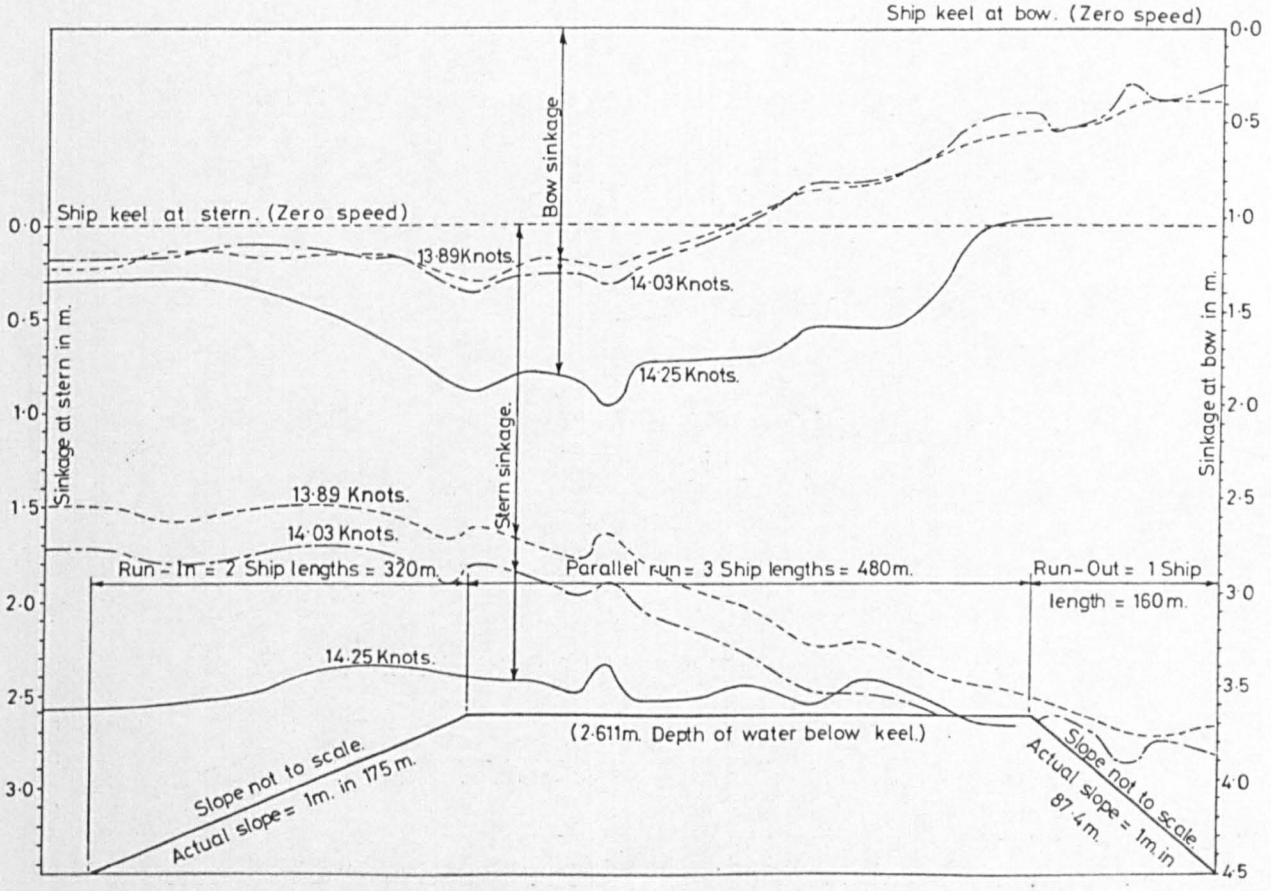

Fig.36 Bow and stern squat in the ballast condition at a depth-draught ratio of 1.37 over and 1.64 clear of sandbank

In the ballast, trim-by-stern condition, the results show that the ship's stern will encounter a potentially hazardous situation, frequently upon leaving the sandbank. Following an initial weak "sensing" dip, the ship's stern sinks progressively deeper while transitting the sandbank. This reaction is evident even when the hull bottom is well clear of the sandbank and at low speeds.

Clearly, the inherently unsteady ship trajectory cannot be obtained using the computer program. However, analysis of the results shows that the approximate grounding speed over an uneven bottom may be predicted conservatively provided the depth of water used is the estimated minimum.

The above results over the shoaling sandbank are proposed as guidelines for a safer operational procedure in the future. It must be remembered, however, that at present the results are useful only as a qualitative guide for any practical applications. This is because, in addition to the scaling problems discussed in section (4.5), the exact underkeel clearance, hull bottom and sandbank geometry, manner of propulsion, lateral restrictions etc. may be important in altering the transient squatting behaviour.

(4.4.b) Bow Shape Effect on Transient Behaviour

A number of the original test conditions were repeated with the modified Glasgow University bulb form described in (3.2.f) to examine the effect of the bulb-shape on the transient behaviour over the sandbank. A comparison of the experimental data indicates that a shape modification induces no measurable changes in the close-to-grounding behaviour and grounding speed in either the load or ballast draught conditions.

From a subjective point of view the bulbous-bow shape may have an influence once the bow touched bottom. No further experiments on this topic were carried out.

(4.5) Extrapolation to Full-Scale

Owing to the significant amount of model data, the model-scale squat component of underkeel clearance is one of a deterministic character. The prediction of the full-scale sinkage and trim is still fairly probabilistic, since the associated scaling problems present difficulties.

Model/full-scale correlation studies have been hampered by the understandable reluctance of shipboard personnel to hazard their vessels by conducting squat experiments under close-to-grounding conditions. Glasgow University has been involved in a number of encouraging model/full-scale correlation studies in laterally

unrestricted shallow-water, at depth-draught ratios greater than 1.4. The most recent indicate that, at a depth-draught ratio of 1.42, correlation in the load-draught level-keel condition is very reasonable at speeds less than about 12 knots. This is particularly so for trim although the mean sinkage tends to be greater for the ship than the model. A typical model/full-scale comparison for a C_B=0.82, 190,000 tonne tanker is presented in Fig.37, taken from Ferguson et al [22,29]. Similar qualitative deductions have been reported by Yamagouchi et al [87], for a 120,000 tonne (deadweight) tanker at depth-draught ratios of 1.3 and above. Field data in the restricted channel condition, also show an overall supportive agreement with model tests, see Tothill [72].

Bearing in mind the importance of viscous effects to the scaling procedure in shallow water, such agreement is unexpected. Frictional resistance constitutes the major proportion of full-form ship resistance at low speeds, and since the frictional coefficient is lower on the full scale, it is to be expected that model results for the trim component will overestimate the full-scale. For example, at a corresponding speed, the 3.05 m. representative mono-hull used has a frictional coefficient twice that of the 160 m. full-scale ship underway at 10 knots. It has been suggested that the good agreement is mainly because the predominant mean sinkage is almost entirely due to pressure changes over the hull, allowing direct scaling of this component without error of practical significance, see

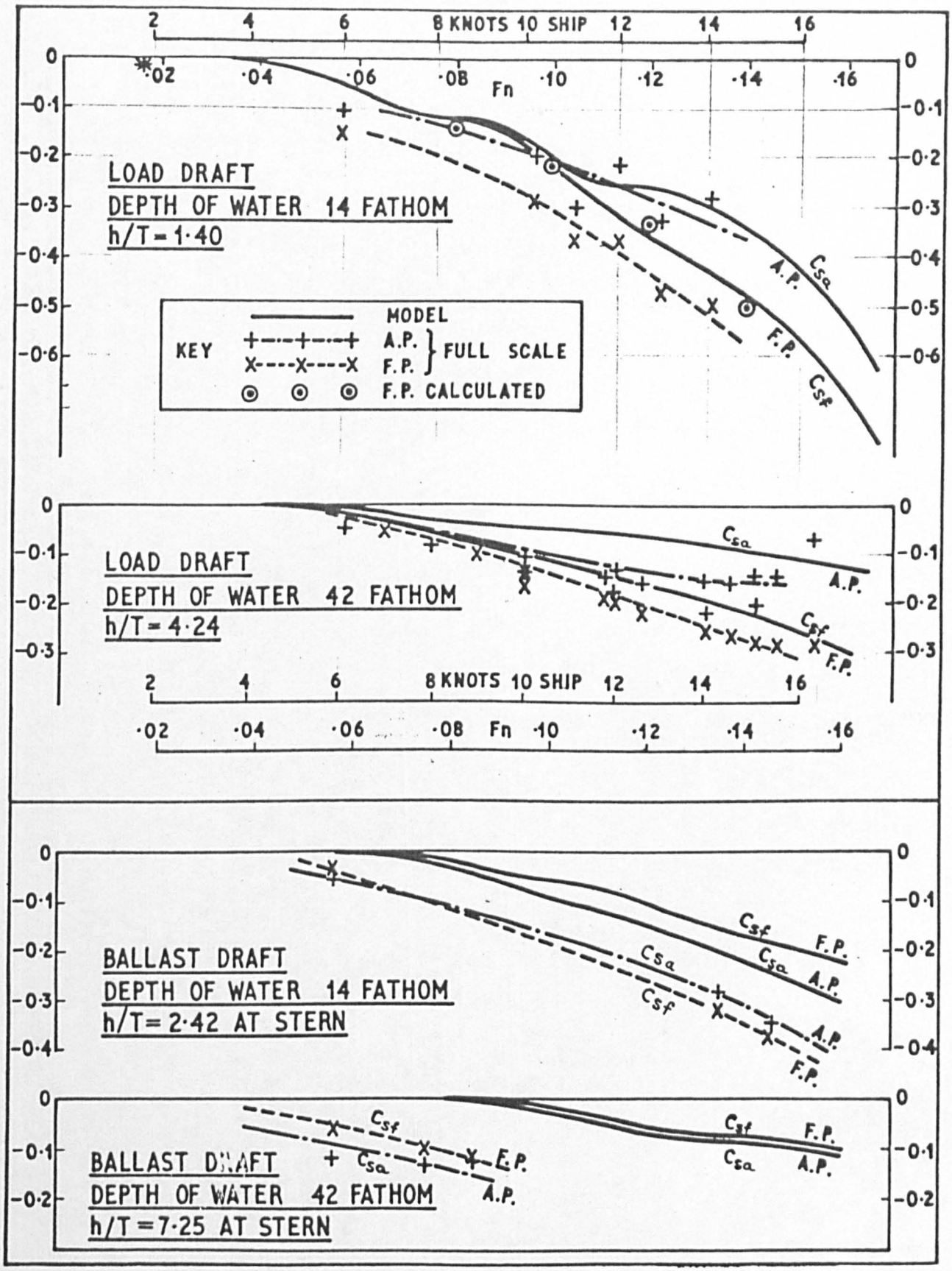

Fig 37 - Full Scale and Model Results C_B = 0.82, 190,000 tonne tanker [22]

Dand and Ferguson [23]. Although trim has an appreciable viscous component, the latter is probably counter-balanced by the pressure dominated self-propulsion effects. Any scaling difficulties in the self-propelled, load draught (level-keel) condition are, therefore, effectively obscured. However, it is suggested that since the model scale boundary layers are relatively thicker than full-scale, they will interact at a greater depth-draught ratio and introduce scaling difficulties in very shallow-water.

The model/full-scale comparisons in the self-propelled ballast (trim-by-stern) condition, indicate that the normal extrapolation procedure may be in error. The bulb proximity to the free-surface will modify the hull wave-system and the viscous flow and may induce vertical sinkage or lift forces, see Dand [21]. It is suggested that since the magnitude of the complex changes induced by the proximity to the free-surface is uncertain, extrapolation to full scale will be unreliable.

The above reasoning also suggests that in the absence of self-propulsion, prediction for the towed, naked-hull condition will be generally unreliable for the trim component.

The experimental set-up and procedures may also influence the results and merit discussion.

(4.5.a) Tank Blockage

The tank width was approximately 9 times the model breadth, resulting in conditions closely corresponding to laterally unrestricted shallow-water for the depths and speeds examined, see Sjostrom [67]. The finite-width effect is not expected to influence the trim component, see (3.2.c). Assuming the mean sinkage component depends mainly on pressure effects, blockage should not interfere with the scaling procedure. In any event, blockage induces a conservative error.

(4.5.b) The Propeller Size and Self-propulsion Point

There are no known rules as to the minimum propeller size necessary to avoid scale effect as compared with the full-scale. Laminar flow has been detected, for example, on model propellers in a relatively turbulent wake of a model, see Berry [7].

The model propeller used was not a geometrically similar propeller to that of the full-scale, but merely a means of ensuring a correct centre of thrust and flow characteristics at the stern.

The self-propulsion experiments were conducted at the model self-propulsion point. Following the usual practice, a small forward force is normally applied to account for the difference in the frictional resistance coefficient

between the model and full-scale, so that the full-scale propulsion point is reached. The magnitude of this extra force depends on the model to ship scale and will change with speed. Although in this way a more representative flow over the hull is obtained, past experiments indicate that the resulting effect on the measured sinkage and trim is negligible. This is because the extra force required is small in comparison to the large increase in resistance and the drop in efficiency to be overcome by the propeller in shallow water, see Dand and Ferguson [23].

(4.5.c) Turbulence Stimulation

The persistence of laminar flow around full-form ships depends to a great extent on the pressure gradient along the model bow, see PNA [11]. The precaution normally taken to ensure that the flow over the model is turbulent is the introduction of a turbulence stimulation device. However, the turbulence device, when attached to the model, increases the model resistance and, in addition to the change in the flow regime, will itself affect the measured sinkage and trim. The problem is compounded in shallow-water, since the relatively low speeds and delay in transition induced by the increased flow velocity, lead to a large wire diameter, see (5.3). Consequently, the stimulator has limited use unless it is possible to distinguish clearly between its detrimental effects and those arising from purely turbulent flow. Turbulence stimulation was not employed on the mono-hulls used

throughout the experiments. However, the writer is of the opinion that the flow over the concrete bottom ahead of the model was sufficient to create turbulence around the model and, therefore, the problem should not be as significant as in deep water.

(4.6) Range of Validity

The method's range of validity is determined primarily by the available experimental data, and as such applies with greatest accuracy to models of the following features,

(a) $0.8 \leq C_B \leq 0.9$

(b) $5.5 < L/B < 6.5$

(c) $3.0 < B/T < 4.0$

(d) $1.0 < h/T < 2.0$

(e) $0.1 \leq F_h \leq 0.6$

However, the writer is of the opinion that the approach is equally valid in the range $0.6 \leq C_B < 0.8$, throughout where the results will be of the correct order but, in the absence of model/full-scale correlation data, the accuracy cannot be guaranteed.

The approach is, therefore, broadly applicable to conventional displacement ship models, in either the level-keel or trimmed conditions, with trim not exceeding 1% of the ship length, underway at steady speed in calm water of uniform depth.

Full-scale extrapolation is provisionally limited to speeds less than 12 knots in the load draught, level-keel condition. Full-scale quantitative predictions are also possible in trimmed conditions, but should be treated with caution. In addition, it is to be noted that the exact nature of the sea-bed, current, sea-state, hull roughness etc. will create uncertainties relative to the predicted performance.

CHAPTER 5

Some Factors Influencing Multi-hull Analysis

The problems posed by model testing in towing tanks have been recognized for many years. The present chapter reports on several shallow and deep water investigations designed to shed light on some of the mechanisms and parameters affecting the asessment of multi-hull sinkage, trim and resistance. The results of these investigations have implications relative to the problems studied in the next chapters.

The problems examined are multi-hull blockage, turbulence stimulation, effects of towing point height and type of ballast. The models chosen consist of a SWATH configuration with streamlined vertical struts and cylindrical lower hulls, and a model of a bluff, twin-hulled semi-submersible crane vessel (SSCV) currently in operation in the North Sea. All the experiments were conducted with naked-hull models, towed through calm water in the transit draught condition. At the transit draught only the lower hulls are immersed, the remaining structure being clear of the water. Fuller particulars of the experimental procedures are detailed in Appendix C and the appropriate references in the text.

(5.1) Bluff-body Resistance Components

The force exerted by a fluid on a body in motion is the sum of the tangential and normal forces acting on its surface, resolved in the direction of motion. The resolved tangential force constitutes skin friction, for which the drag coefficient depends on the Reynolds number. The resolved normal forces constitute the total pressure drag, which can be sub-divided into;

(a) the wave-making resistance, which arises from the energy dissipated in generating a wave pattern and depends on the Froude number, and
(b) the form drag, which originates from the pressure gradient set-up along the body surface due to viscous effects and depends on the body shape. Its coefficient may depend on the Reynolds number.

The relative importance of the tangential and normal resistance components varies widely from a thin streamlined shape to a bluff body. On a streamlined body, such as the SWATH strut, boundary layer separation is prevented or retarded and its form drag is low, at the expense of increased skin friction. The wave-making resistance constitutes the dominant portion of the pressure resistance and together with the form drag is considered independent of the Reynold's number.

The main feature of flow past a bluff body is its

early separation from the body surface and the formation of a large wake. Observations as well as numerical experiments show that the wake of a bluff body is comprised of an alternating vortex street. The character of the vortices immediately behind the body, and the wake further downstream, depends on the body R_N and the turbulence present in the ambient flow, see ESDU [26]. The separation points may be mobile, as on a circular cylinder, or fixed at a discrete point, as on the edges of a rectangular barge form. When the separation point is fixed, the drag (and pressure) coefficients vary considerably less than those for the circular cylinder. Consequently, forms with fixed separation points generally experience a very high form drag which is considered insensitive to the R_N for all practical purposes.

Bluff forms experience a skin friction component, which depends on the Reynold's number, and is small in relation to the form drag. The contribution from the actual wave-making component is negligible throughout the normal full-scale working range of semi-submersible platforms, see Grekoussis and Miller [33].

(5.2) Blockage Effects

Bluff multi-hulled model tests are subject to considerable scaling difficulties in existing towing tanks. One of the normally unavoidable limiting factors is the need for an assessment of "blockage", the rather vague term

covering the interference of tank dimensions on model results, which limits the model size.

This section presents a short study of a theoretical formula for interpreting the constraints as an effective increase in the stream velocity. The theory is examined by means of an experimental method suggested by Horn [36], using 2 geosims of a bluff, twin-hulled semi-submersible crane vessel (SSCV), towed on the tank centre-line in the transit draught, level-keel condition. In the process, the effects of the Glasgow University tank blockage on the non-dimensional mean sinkage and trim coefficients in both deep and shallow-water are presented.

(5.2.a) Fundamental Causes

The fundamental causes of conventional ship blockage are reasonably well specified by past research. Blockage correctors, predominantly semi-empirical in character, are applied to conventional ship-form results with a reasonable degree of confidence. However, the established correction formulae remain, at present, untested for the offshore configurations of immediate interest.

For symmetric bodies it is possible to identify three different types of blockage effects,

(a) the conventional blockage effect, which arises as a result of the inability of the flow to expand laterally as

freely as it would in unconfined conditions. Mass continuity then implies an increase in the velocities past the model. When the drag is mainly frictional, as for a streamlined shape, this effect will dominate.

(b) the "wake blockage" effect, which arises as a result of the increase in flow velocity just outside the wake. This effect reduces the wake pressure below its value in the unconfined case and will react on the body to cause an additional increase in drag. In the case of bluff bodies with a large wake, this is the dominant factor. Actually, the wake developed is periodic in nature and past practice has been to consider an "effective" wake width.

(c) the effect resulting from the displacement thickness of the boundary layer on the side walls, which induces a longitudinally falling pressure gradient and tends to increase the measured resistance. This correction may be important in the case of streamlined bodies tested under severe constraints, but will be insignificant for bluff, high drag bodies tested in tanks of normal proportions.

In the case of bluff bodies, the tank boundaries can alter both the hydrodynamic resistance coefficients and the vortex shedding frequency of the model. It should be noted that effects (a) and (b) are particularly important in the case of well rounded bluff bodies, such as circular cylinders, for which small changes in the flow conditions may lead to drastic transitional changes in the flow regime. For example, the flow past past a smooth cylinder in the critical ($R_N \simeq 4 \times 10^5$) regime is characterised by a

laminar separation followed by a turbulent reattachment and eventual turbulent separation, upon which the drag coefficient decreases abruptly. The present study clearly excludes this case by considering a body with fixed separation points, whose R_N is independent of any constraints.

(5.2.b) A Theoretical Treatment of Multi-hull Blockage

The theoretical expression adopted as the basis for multi-hull blockage estimation on resistance is equation (2.4.7),

$$[\frac{U_1}{U}]^3 \frac{F_h^2}{2} - [1 - m + \frac{F_h^2}{2}][\frac{U_1}{U}] + 1 = 0 \qquad \ldots\ldots (5.2.1)$$

where $m = S_x/A$ and S_x, A are the complete midship and tank cross-sectional areas, respectively. Normally, the subsequent procedure requires the correction of the model speed or, alternatively, its resistance. Although this expression has no empirical element, it has been applied with reasonable success to mono-hulls at Glasgow within the normal range of speeds and full-forms. The theory is based on certain simplifying assumptions, which are discussed in detail in section (2.4).

(5.2.c) The Experimental Method of Analysis

The relationship between the blockage, as represented by the mean "back-flow" velocity, u, and the mean

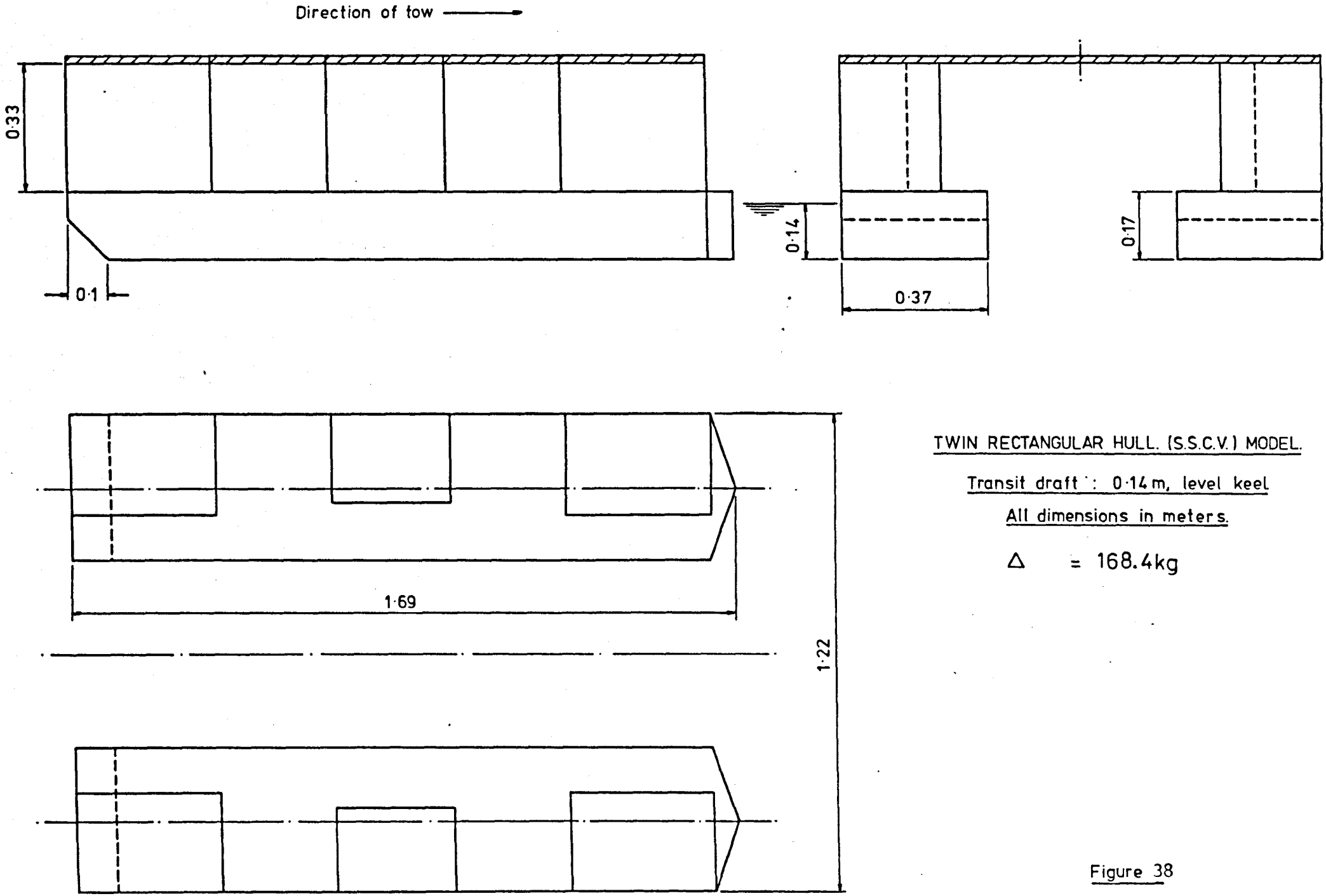

TWIN RECTANGULAR HULL. (S.S.C.V.) MODEL.

Transit draft : 0·14 m, level keel

All dimensions in meters.

Δ = 168.4kg

Figure 38

water-level depression, Δh, Fig.7, serves as the basis for the experimental method.

The point in question is the difference in the measured sinkages in unlimited water and in a laterally restricted channel. If mean sinkage measurements are taken on 2 (or more) geosims, the length of the shorter such that the blockage is insignificant and the speed of the larger such that the wave retardation effect is negligible, then at corresponding speeds the excess back-flow velocity of the larger model due to width and/or depth restrictions is given by,

$$\frac{u_2}{U_2} = \sqrt{1 + \frac{2g\Delta h_2}{U_2^2}} - \sqrt{1 + \frac{2g\Delta h_1}{U_1^2}} \qquad \ldots\ldots (5.2.2)$$

where $U_1^2 = r\, U_2^2$, $r = L_1/L_2$, g is the acceleration due to gravity, Δh the midship mean sinkage and the subscripts 1 and 2 refer to the small and large geosim, respectively.

(5.2.d) The Geosims

Two geometrically similar twin rectangular-hull models were constructed. The scales were 1/70th and 1/120th and model particulars are presented in Fig.38,72.

The size of the larger model was such as to allow, at most, a moderate blockage effect in shallow water. The scale of the smaller geosim was chosen so that at a

BLOCKAGE ESTIMATION ;
****

DATA USED ;

NOTE ; Y(1) IS CURVE-FIT FOR SMALL GEOSIM.
Y(2) IS CURVE-FIT FOR LARGE GEOSIM.

Y(1) = 0.00129 + -0.47885 X**1 + 9.43857 X**2 + 3.59010 X**3

Y(2) = -0.04533 + -0.01020 X**1 + 8.73977 X**2 + 4.91173 X**3

L.B.P. RATIO (LR) = 0.5839

NOTATION ;

V2 = SPEED OF LARGE GEOSIM
V1 = CORRESPONDING SMALL GEOSIM SPEED I.E. V2*(LR)
DV2 = LARGE GEOSIM BACK-FLOW
DV1 = SMALL GEOSIM BACK-FLOW
BC = BLOCKAGE CORRECTOR

V2 **** (M/S)	V1 **** (M/S)	DV2/V2 ******	DV1/V1 ******	DV2-DV1/V2 **********	BC ****
0.10	0.08	1.04	1.04	0.01	1.01
0.15	0.11	1.07	1.06	0.01	1.01
0.20	0.15	1.08	1.07	0.01	1.01
0.25	0.19	1.09	1.07	0.01	1.01
0.30	0.23	1.09	1.08	0.01	1.01
0.35	0.27	1.09	1.08	0.01	1.01
0.40	0.31	1.10	1.08	0.01	1.01
0.45	0.34	1.10	1.09	0.01	1.01
0.50	0.38	1.10	1.09	0.01	1.01
0.55	0.42	1.11	1.09	0.01	1.01
0.60	0.46	1.11	1.09	0.01	1.01
0.65	0.50	1.11	1.10	0.01	1.01
0.70	0.53	1.11	1.10	0.01	1.01
0.75	0.57	1.11	1.10	0.01	1.01
0.80	0.61	1.12	1.10	0.02	1.02
0.85	0.65	1.12	1.10	0.02	1.02
0.90	0.69	1.12	1.10	0.02	1.02
0.95	0.73	1.12	1.11	0.02	1.02
1.00	0.76	1.13	1.11	0.02	1.02

Table 11

CONBLOCOR EVALUATION

BLOCKAGE RATIO = 0.0100

CHANNEL (TANK) DEPTH = 2.3000

F_h	SPEED (M/S)	SPEED CORRECTOR
0.0500	0.2375	1.0101
0.0600	0.2850	1.0101
0.0700	0.3325	1.0102
0.0800	0.3800	1.0102
0.0900	0.4275	1.0102
0.1000	0.4750	1.0102
0.1100	0.5225	1.0102
0.1200	0.5700	1.0103
0.1300	0.6175	1.0103
0.1400	0.6650	1.0103
0.1500	0.7125	1.0103
0.1600	0.7600	1.0104
0.1700	0.8075	1.0104
0.1800	0.8550	1.0104
0.1900	0.9025	1.0105
0.2000	0.9500	1.0105

Table 12

depth-draught ratio of 1.1, based on the large geosim draught, the small geosim has a blockage factor of 0.05. In deep water this resulted in a blockage factor of 0.003 for the smaller geosim. Experiments were conducted in the towed, naked-hull condition in deep water and in shallow-water at a depth-draught ratio of 1.3 (referred to the large geosim draught).

(5.2.e) Deep-water Experiments

A computer program (HORN) was written to evaluate equation (5.2.2), using curve-fitted mean sinkage experimental data, Table 11. Equation (5.2.1) was programmed (CONBLOCOR) and the deep water blockage data, based on the total immersed model cross-sectional area, is shown Table 12. A comparison of theory and experiment, Tables 11 and 12 respectively, shows good agreement, suggesting that equation (5.2.1) is a reasonable first approximation to the blockage effect on model speed in deep water. The comparison also indicates that over the working speed range of offshore the sinkage is predominantly dependent on the velocity squared, i.e. the form effect.

Figs.39,40 present the non-dimensional C_S and C_T coefficients against F_L (based on hull waterline length) for the 2 geosims. The experimental data was curve-fitted using a least-squares-method computer routine (LSPLOT). Over the full-scale working speed range, i.e. $F_L < 0.15$, no scale effect on the C_T coefficient is apparent. This is in

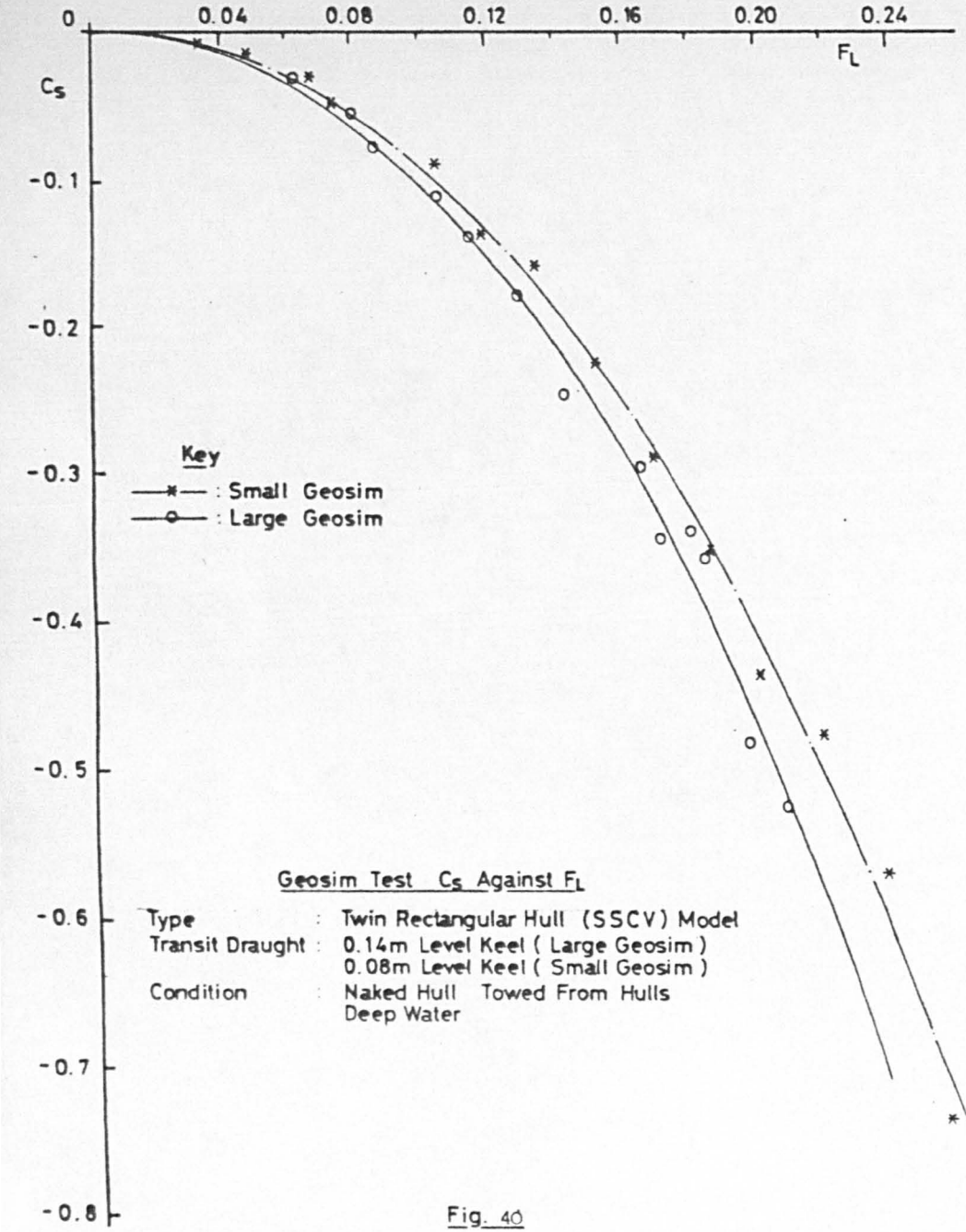
0
0.04
0.08
0.12
0.16
0.20
0.24
F_L
C_S
-0.1
-0.2
-0.3
-0.4
-0.5
-0.6
-0.7
-0.8
Key
: Small Geosim
: Large Geosim
Geosim Test C_S Against F_L
Type : Twin Rectangular Hull (SSCV) Model
Transit Draught : 0.14m Level Keel (Large Geosim)
0.08m Level Keel (Small Geosim)
Condition : Naked Hull Towed From Hulls
Deep Water

Fig. 40

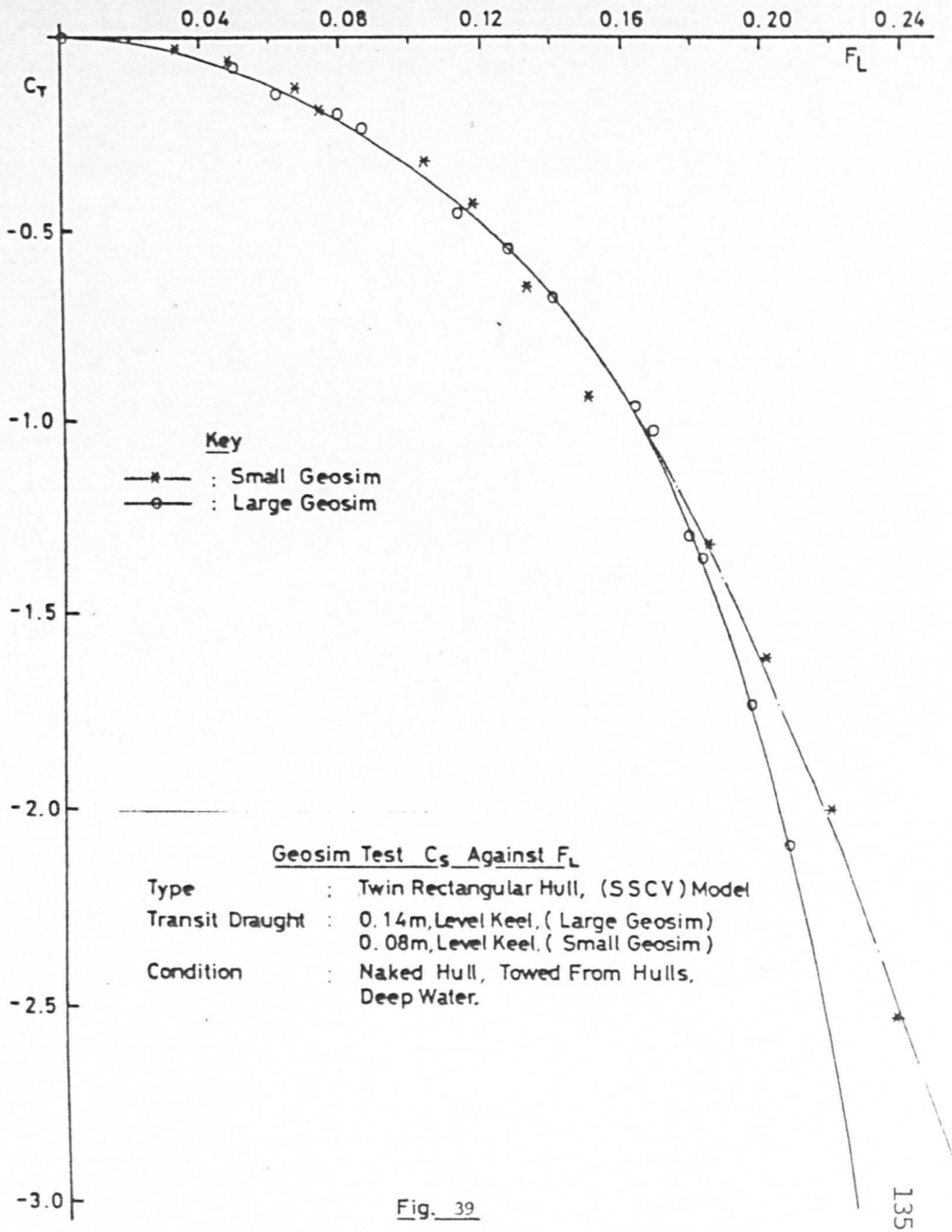
0.04
0.08
0.12
0.16
0.20
0.24
F_L
C_T
-0.5
-1.0
-1.5
-2.0
-2.5
-3.0
Key
: Small Geosim
: Large Geosim
Geosim Test C_S Against F_L
Type : Twin Rectangular Hull, (SSCV) Model
Transit Draught : 0.14m, Level Keel, (Large Geosim)
0.08m, Level Keel, (Small Geosim)
Condition : Naked Hull, Towed From Hulls,
Deep Water.

Fig. 39

agreement with the mono-hull experiments of section (3.2.c) which illustrated that, unless severe, lateral restrictions have a negligible influence on the trim underway. Moreover, assuming there exists a relationship between the viscous pressure resistance component and the hull trim, see Guilloton [34] and Dand [21], the results suggest that for the experimental set-up examined no changes in the viscous pressure component are to be expected. As $F_L > 0.15$, the larger geosim exhibited a greater and steadily increasing C_T in comparison to the smaller geosim. It appears, therefore, that for $F_L < 0.15$ the increase in mean sinkage due to blockage is responsible for the increase in resistance and, as the theory indicates, is almost entirely due to pressure changes.

(5.2.f) Shallow-water Experiments

The shallow-water depth examined was that appropriate to a depth-draught ratio of 1.3 based on the large geosim draught. This resulted in a depth-draught ratio of 2.2 for the small geosim. Analysis using the Horn method was attempted, but the results were erratic. This is because of the restrictions imposed on the speed range by the large geosim in shallow water. At very low speeds, the measurement of small differences between the sinkages of both geosims proved very difficult. Moreover, at times, the first term on the r.h.s. of the governing equation (5.2.2) yielded imaginary roots in a region where testing was possible (i.e. with no physical counterpart).

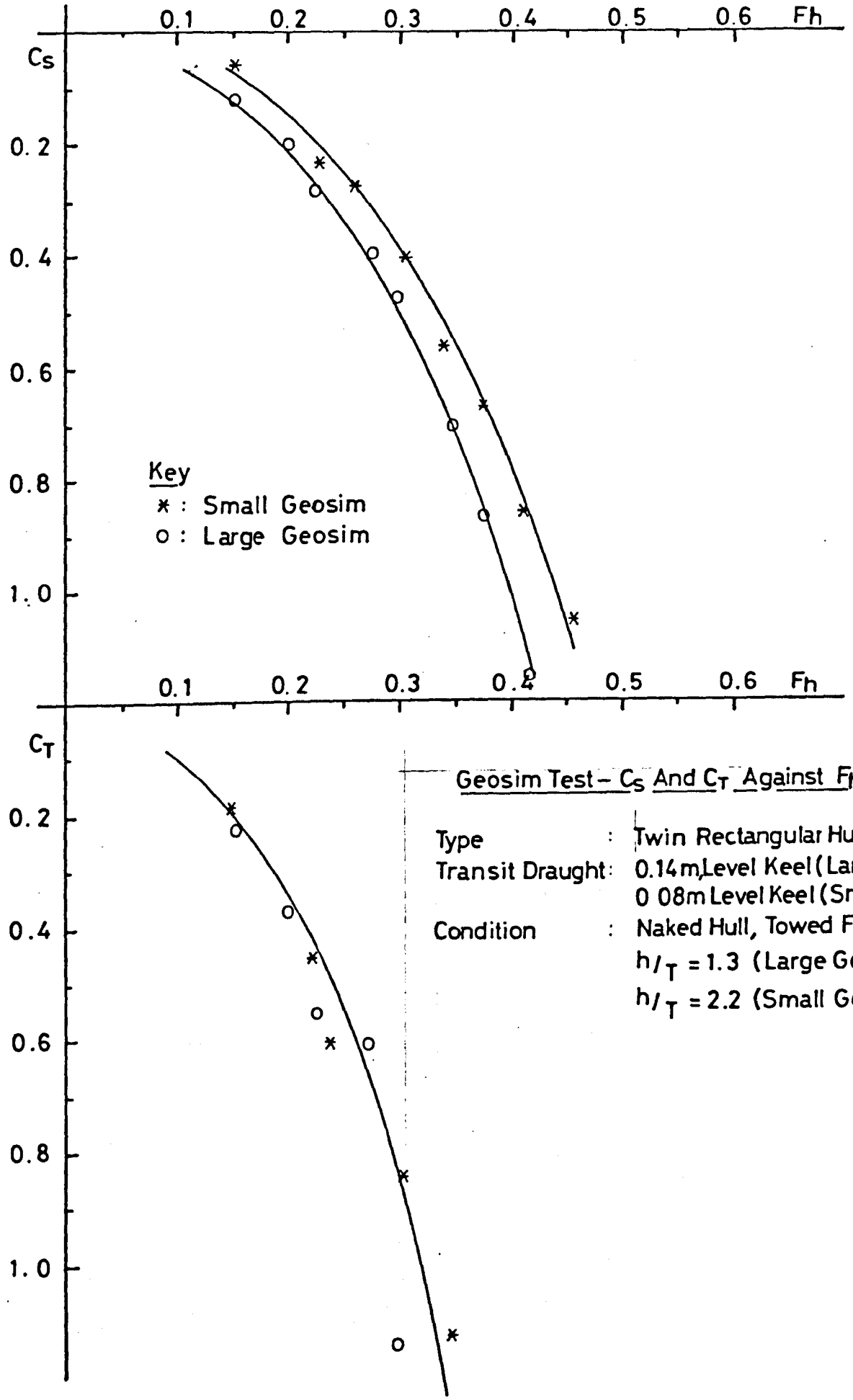

Geosim Test – C_S And C_T Against F_h

Type : Twin Rectangular Hull (SSCV) Model
Transit Draught : 0.14m Level Keel (Large Geosim)
0.08m Level Keel (Small Geosim)
Condition : Naked Hull, Towed From Hulls
$h/_T = 1.3$ (Large Geosim)
$h/_T = 2.2$ (Small Geosim)

Fig. 41

Fig.41 presents a comparison of the geosim C_S and C_T coefficients in shallow-water. In agreement with the deep-water results, no blockage effect on C_S is apparent. The larger geosim exhibits increased C_S coefficients at a given F_h, the trend being similar to that observed in deep water, except at very low underkeel clearances where bottom proximity and viscosity effects dominate.

(5.2.g) Conclusions

The experiments suggest that for a given Froude number within the full-scale multi-hull offshore platform speed range (i.e. $F_L < 0.15$), the effect of blockage on the non-dimensional trim coefficient, C_T, is negligible in both deep and shallow water. Over the same range, the mean sinkage coefficient, C_S, increases with the increase in blockage and is responsible for the changes in the measured total resistance. The (Conn) blockage formula, equation (5.2.1), provides a reasonable first approximation to the deep-water changes in back-flow speed induced by blockage.

The accuracy of the method is very difficult to determine in shallow water. However, it will be assumed that this approach also provides a practical means of blockage correction on resistance in shallow-water.

It should be noted that the present study is restricted to bluff models with an insignificant R_N dependence, to rule out any major transitional changes

in behaviour induced by blockage. Strictly, the conclusions are valid for the set-up examined. However, it is suggested that the findings are applicable to other similar, moderately constrained, bluff twin-hulls in transit, in tanks of similar proportions.

(5.3) The Effect of Turbulence Stimulation

In an attempt to reduce the discrepancy between the full-scale resistance and that determined from model tests, modelling techniques often involve the use of turbulence stimulators having known stimulation capabilities and known self-drag. The assumptions underlying the practice are well known. Since models are tested in towing tanks at R_N which are typically two to three orders of magnitude less than those occuring on full scale, laminar flow can be expected to persist over a significantly greater proportion of a smooth model than on the prototype hull. On bluff bodies with movable separation points, such as circular cylinders, this practice rules out changes in the position of separation and the resulting flow becomes practically independent of the R_N , sub-critical or post-critical, as the case may be. It has also been noted that comparative tests without turbulence stimulation may be misleading, as pressure gradients are altered and changes attributed to varying shape may be purely stimulation effects.

The ideal stimulator should incur negligible self-drag and should trip turbulence as "naturally" as possible. The question of which type of stimulator (sand-strip, studs and trip-wire are the most common) best satisfies the ideal, has never been resolved definitively because of their equal effectiveness based on the above main criteria, see McCarthy et al [47]. The final choice is made on other considerations, influenced by the unique experience of the

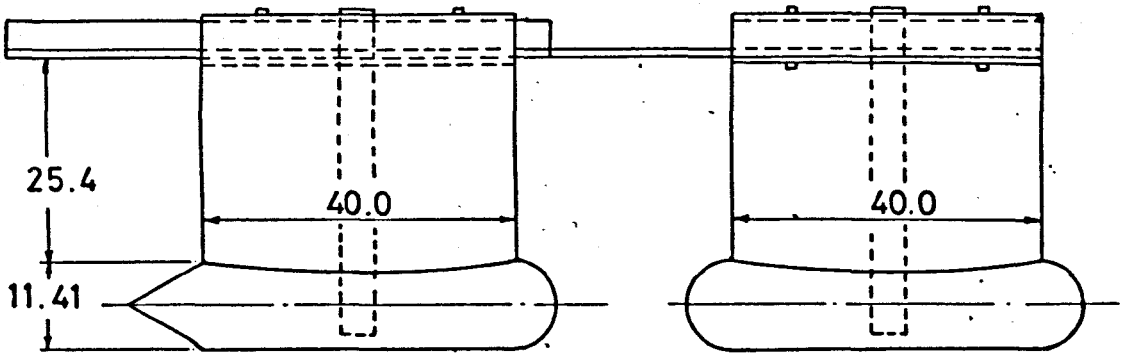

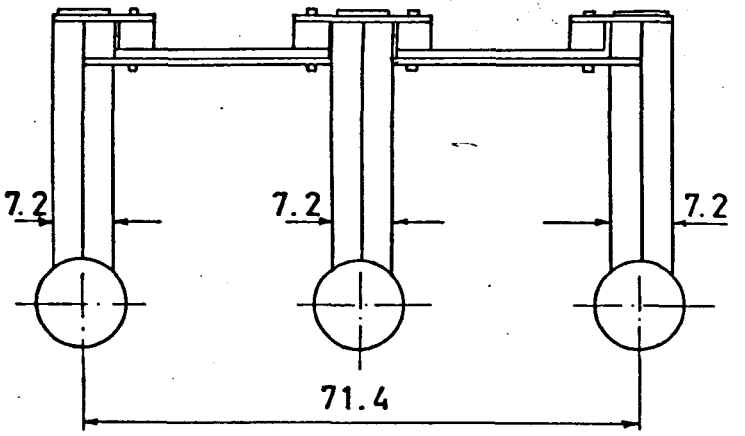

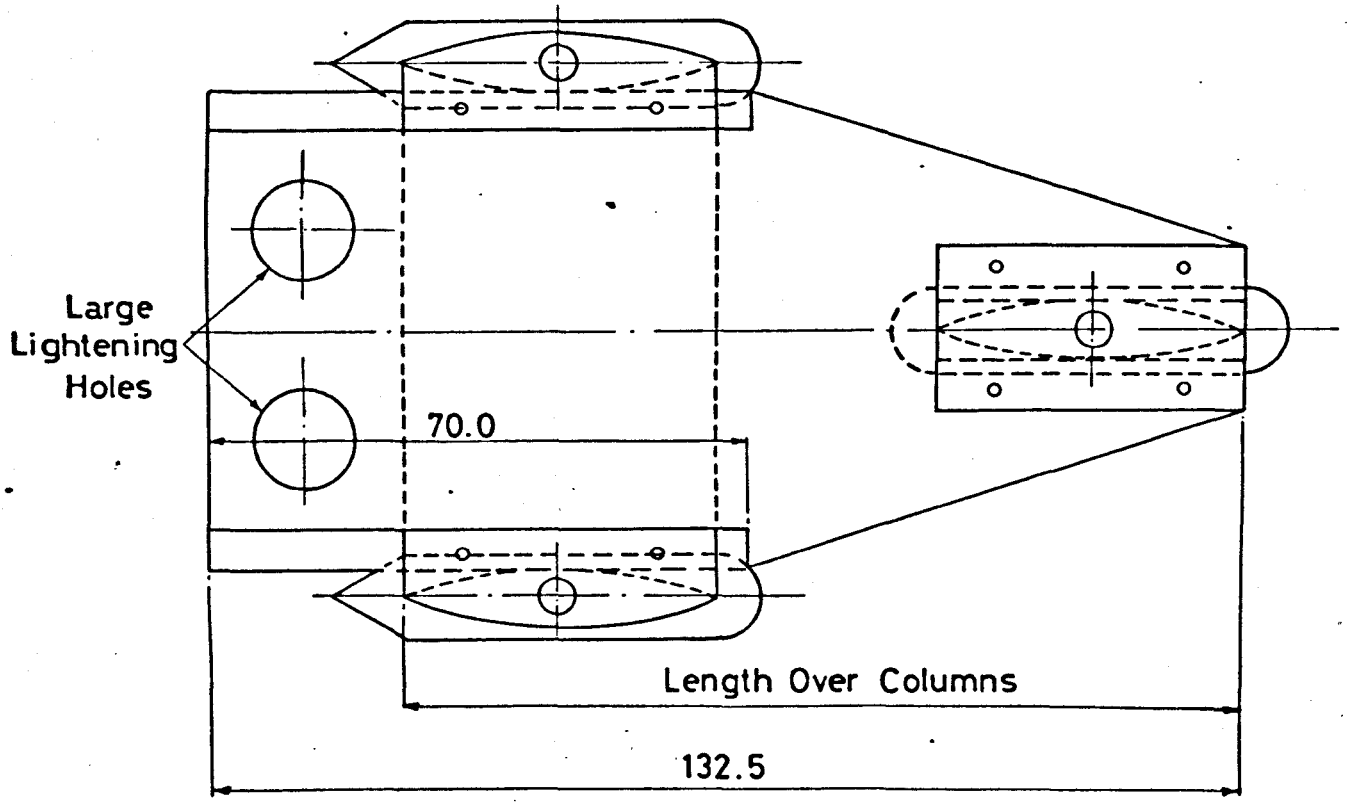

All Dimensions Are Model Sizes In cms
Drawing To Model Scale 1:10

Fig 42 Small Semi Submersible Model

laboratory in question.

In the absence of flow visualization experiments, the degree of success in obtaining turbulence is normally determined from the resistance curves. These tend to show if the model is conforming fully to a turbulent friction line or some transition line.

This section presents an attempt to assess the effects of adding a turbulence stimulating device in the form of a trip-wire on the shallow-water ($1.1 \leq h/T \leq 1.5$) and deep-water sinkage, trim and drag of 2 multi-hulls of widely varying form. The shallow-water experiments were conducted with a SWATH configuration, Fig.42, while the deep water evaluation was performed with a 1/120th scale bluff, twin-hulled semi-submersible (SSCV), Fig.72. A typical shallow water experimental set-up for the SWATH is presented in Fig.43. In order to evaluate the changes quantitatively, the experiments were performed with and without stimulators. For fuller details, see Seren et al [65].

(5.3.a) Trip-wire Diameter, Location and Self Drag

In accordance with the accepted practice at Glasgow University, trip wires were selected because they have precisely defined and fixed geometries, are easy to install and remove and because much more self-drag data are available for trip wires than for the other types of

T = Turbulent Flow Seperation

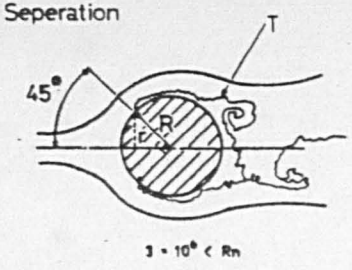

Radius Of Ring
= R sin 45°
$= \frac{11.41}{2} \cdot \frac{1}{\sqrt{2}}$
= 4.0cm/s

(a) Development Of Flow Around Long Circular Cylinder With Increasing Reynolds Number (Engineering Sciences Data Unit Ref (26)

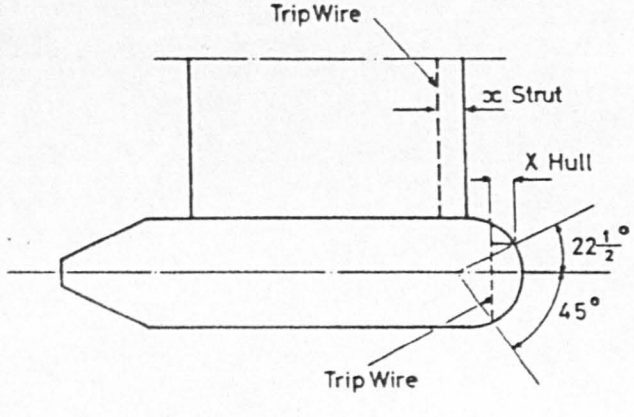

(b) Hull Strut Trip Wire Position, And Position Of Representative Arc Length 'x' Taken Along The Surface To The Boundary Of The Laminar Region (Up To The Trip Wire)

Figure. 44

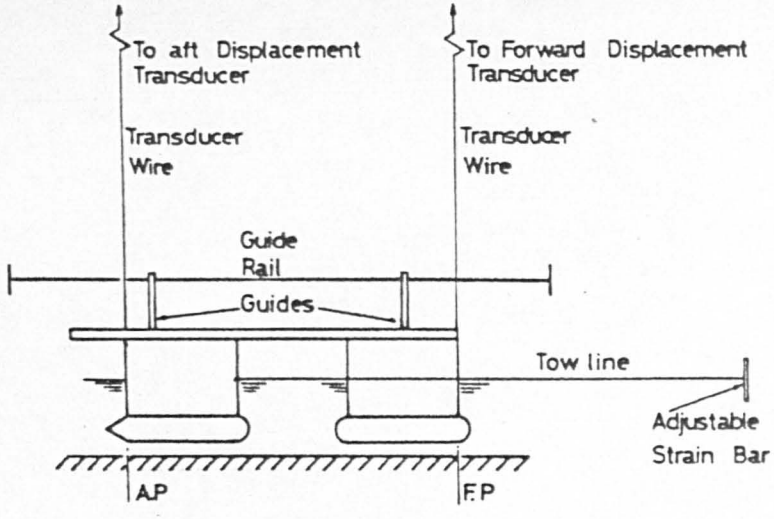

Table 1. Model Condition

Column ℄ Draft	=	9.8cm
Total Draft	=	21.2cm
Displacement	=	20.68 Kg
Length Over Columns	=	1.08m
Longitudinal GM	=	8.5cm
Height of Towpoint	=	0.5cm above W.L.

Figure 43:- Experimental Apparatus (N.T.S)

stimulators. From a practical viewpoint, only one size of trip wire could be installed over the models' entire speed range. Its' diameter was determined by its effectiveness at the lower model speeds of interest by a combination of Fage's criterion and flat-plate theory, see Appendix E. The method yielded a 1.5 mm. trip-wire for the SWATH and a 2.4 mm. trip-wire for the SSCV.

Normally, the trip wires were fitted 5% aft of the forward shoulder and around the hull perimeter, extending above the at-rest waterplane. For the hemispherical SWATH bow sections, x, the longitudinal distance from the leading edge, was taken to be the arc length along the surface (an "average line") to the boundary of the laminar region, Fig.44. In the absence of flow visualization, this was arbitrarily assumed to extend up to the trip wire and resulted in x = 0.022 m. for the hull. A linear extent of 5% of the SWATH strut length was adopted for the strut, i.e. x = 0.02 m. To simplify calculations, the value of 0.02 m. was used for both hull and strut.

The increment in total resistance, owing to wire self drag was estimated using a non-dimensional correction coefficient, based on empirical information, see Appendix E,

$$C_W = (\frac{V}{U})^2 (\frac{S_p}{S}) C_D \qquad \ldots\ldots (5.3.1)$$

Using the above equation the wire self drag is

presented as a ratio of the total measured SWATH resistance in Tables 13,14,15 for h/T = 1.1,1.3,1.5. Over the speed range examined, the trip wire self-drag estimations suggest that the self-drag is an appreciable percentage of the total measured resistance (8% - 17%) and shows no significant dependence on the depth-draught ratio. As speed is increased, the percentage increment due to wire self-drag reduces significantly.

(5.3.b) Resistance Decrement Upstream from Wire

When in position, the turbulence stimulators leave the laminar flow (assuming it exists) undisturbed over the initial part of the hull. Usual tank practice assumes that the diminution of the frictional resistance upstream of the stimulator balances the additional drag of the trip wire itself. In order for this assumption to be valid, transition on the tripped model must occur as far forward as on the untripped hull. Recent research has indicated that this requirement is not generally satisfied, see McCarthy et al [47].

An attempt was made to estimate the effect for a SWATH in shallow-water, using certain simplifying assumptions. In what follows it is assumed, see Schlichting [59], that behind the point of transition the boundary layer behaves as if it were turbulent from the leading edge. Hence from the drag of a wholly turbulent boundary layer it is necessary to subtract the turbulent drag of the length up

to the point of transition at the trip-wire location and add the laminar drag for the same length. The decrease is expressed as,

$$D_L = -\tfrac{1}{2}\rho U^2 S (C_{FT} - C_{FL}) \qquad \ldots\ldots (5.3.2)$$

where C_{FT}, C_{FL} denote the ITTC turbulent and Blasius laminar skin friction coefficients, respectively, and S the area covered by the laminar boundary layer.

Expressing the decrement as a ratio and noting that the x-Reynolds number (see section (5.3.a) for a definition of x) of both strut and hull is similar,

$$D_L = \frac{[S_{LS} + S_{LH}]\,[C_{FT}(\frac{Ux}{\nu}) - C_{FL}(\frac{Ux}{\nu})]}{S[C_{FT}(\frac{UL_H}{\nu}) + C_{FT}(\frac{UL_S}{\nu})]} \qquad \ldots\ldots (5.3.3)$$

where S_{LS}, S_{LH} are the strut and hull surface area assumed covered by laminar flow, respectively, and L_H , L_S the hull and strut lengths, respectively.

Using equation (5.3.3), the decrement in frictional resistance as a percentage of the total turbulent frictional resistance is obtained. Tables 16,17 indicate that the decrement in frictional resistance is reduced to a small and stable value (approx. 2%), which would be difficult to detect in practice.

U (ms^{-1})	ω	R_x	δ_T (m)	$(\frac{v}{U})$	C_ω	C_{TOT}	$100\ \frac{C_\omega}{C_{TOT}}$
0.1	1.037	1,821	2.57×10^{-3}	0.827	1.91×10^{-3}	15.6×10^{-3}	12.2
0.2	1.038	3,645	1.81×10^{-3}	0.97Ø	2.63×10^{-3}	17.9×10^{-3}	14.7
0.3	1.038	5,261	1.51×10^{-3}	1.Ø	2.79×10^{-3}	17.3×10^{-3}	16.1
0.4	1.039	7,305	1.28×10^{-3}	1.Ø	2.79×10^{-3}	17.6×10^{-3}	15.9
0.5	1.041	9,131	1.15×10^{-3}	1.Ø	2.79×10^{-3}	16×10^{-3}	17.4
0.6	1.042	10,975	1.05×10^{-3}	1.Ø	2.79×10^{-3}	17.2×10^{-3}	16.2
0.7	1.045	12,853	0.97×10^{-3}	1.Ø	2.79×10^{-3}	19.9×10^{-3}	14.Ø
0.8	1.048	14,715	0.90×10^{-3}	1.Ø	2.79×10^{-3}	24.4×10^{-3}	11.4
0.9	1.052	16,629	0.85×10^{-3}	1.Ø	2.79×10^{-3}	31.9×10^{-3}	8.7
1.Ø	1.055	18,525	0.80×10^{-3}	1.Ø	2.79×10^{-3}	37.2×10^{-3}	7.5

Table 15: Increment of Total Resistance due to Wire Self Drag as Percentage of Total Measured Resistance - H/T = 1.5

U (ms^{-1})	ω	R_x	δ_T (m)	$(\frac{v}{U})$	C_ω	C_{TOT}	$100\ \frac{C_\omega}{C_{TOT}}$ %
0.1	1.043	1,831	2.56×10^{-3}	0.829	1.92×10^{-3}	18×10^{-3}	10.7
0.2	1.044	3,666	1.81×10^{-3}	0.970	2.63×10^{-3}	23.8×10^{-3}	11.1
0.3	1.045	5,496	1.48×10^{-3}	1.Ø	2.79×10^{-3}	20×10^{-3}	14.Ø
0.4	1.046	7,340	1.28×10^{-3}	1.Ø	2.79×10^{-3}	18.4×10^{-3}	15.2
0.5	1.048	9,271	1.14×10^{-3}	1.Ø	2.79×10^{-3}	18.1×10^{-3}	15.4
0.6	1.051	11,080	1.04×10^{-3}	1.Ø	2.79×10^{-3}	19.7×10^{-3}	14.2
0.7	1.054	12,959	0.96×10^{-3}	1.Ø	2.79×10^{-3}	22.1×10^{-3}	12.6
0.8	1.058	14,855	0.90×10^{-3}	1.Ø	2.79×10^{-3}	28.8×10^{-3}	9.7

Table 13: Increment of Total Resistance due to Wire Self Drag as Percentage of Total Measured Resistance - H/T = 1.3

U (ms^{-1})	ω	R_x	δ_T (m)	$(\frac{v}{U})$	C_ω	C_{TOT}	$100\ \frac{C_\omega}{C_{TOT}}$ %
0.1	1.051	1,845	2.55×10^{-3}	0.83	1.92×10^{-3}	28.7×10^{-3}	6.7
0.2	1.052	3,694	1.80×10^{-3}	0.972	2.64×10^{-3}	$24.Ø \times 10^{-3}$	11.0
0.3	1.054	5,549	1.47×10^{-3}	1.Ø	2.79×10^{-3}	20.5×10^{-3}	13.6
0.4	1.056	7,410	1.27×10^{-3}	1.Ø	2.79×10^{-3}	22.8×10^{-3}	12.2

Table 14: Increment of Total Resistance due to Wire Self Drag as Percentage of Total Measured Resistance - H/T = 1.1

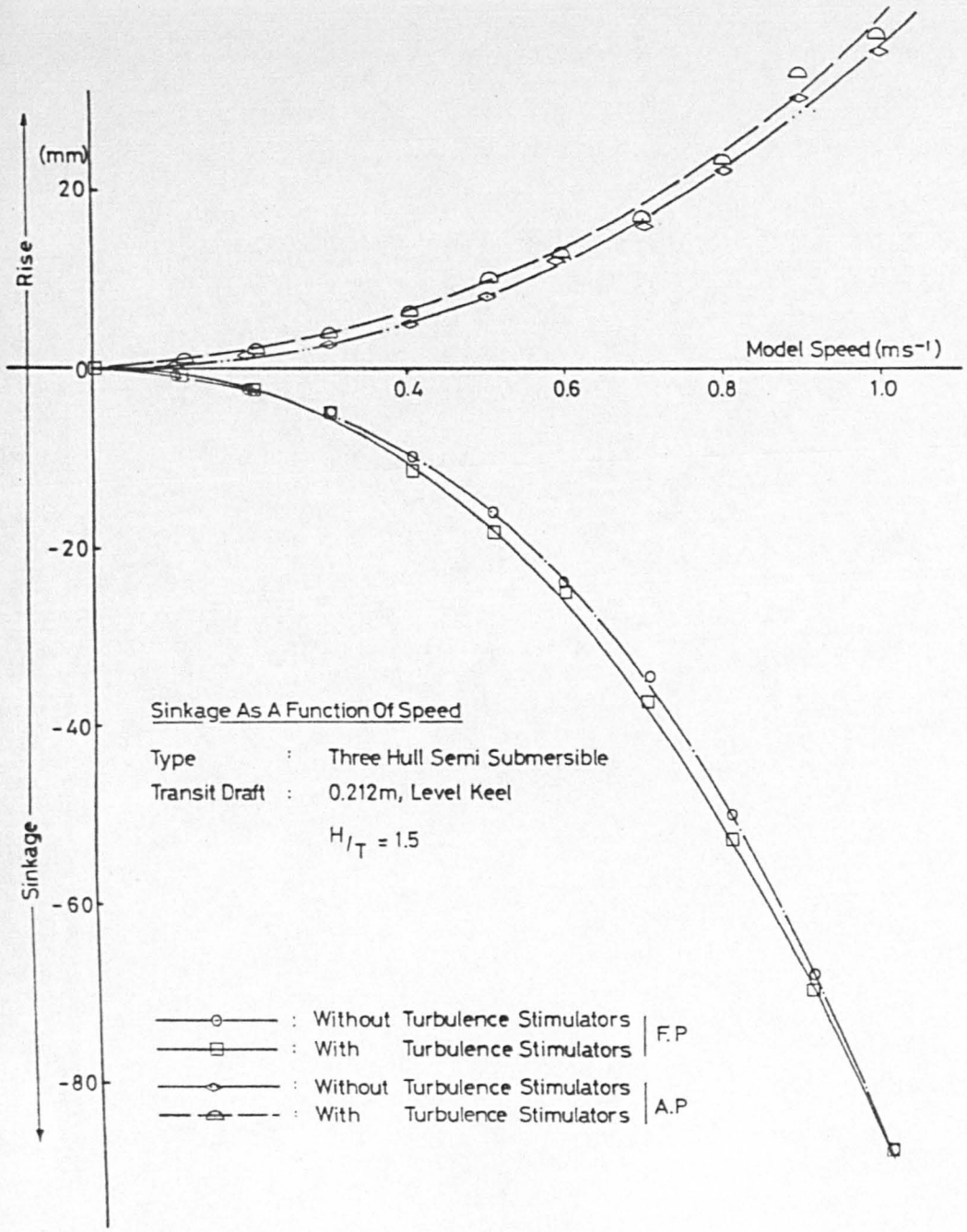

Figure 45

U (ms^{-1})	ω	U_1 ms^{-1}	R_x	C_{FT}(HULL) $(\frac{UL_H}{\nu})$	C_{FT}(STRUT) $(\frac{UL_S}{\nu})$	C_{FT} $(\frac{Ux}{\nu})$	C_{FL} $(\frac{Ux}{\nu})$	100% D_L %
0.3	1.038	0.311	5,261	0.0076	0.0081	0.0249	0.0183	1.8%
0.4	1.039	0.416	7,305	0.0070	0.0075	0.0216	0.0158	1.8%
0.5	1.041	0.520	9,131	0.0066	0.0071	0.0195	0.0139	1.7%
0.6	1.042	0.625	10,975	0.0063	0.0067	0.0180	0.0127	1.7%
0.7	1.045	0.732	12,853	0.0061	0.0064	0.0169	0.0117	1.7%
0.8	1.048	0.838	14,715	0.0059	0.0062	0.0160	0.0109	1.8%
0.9	1.052	0.947	16,629	0.0057	0.0060	0.0152	0.0103	1.8%

Table 16: Decrement in Frictional Resistance as Percent of Total Turbulent Frictional Resistance - H/T = 1.5

U (ms^{-1})	ω	U_1 (ms^{-1})	R_x	C_{FT}(HULL) $(\frac{UL_H}{\nu})$	C_{FT}(STRUT) $(\frac{UL_S}{\nu})$	C_{FT} $(\frac{Ux}{\nu})$	C_{FL} $(\frac{Ux}{\nu})$	100% D_L %
0.3	1.045	0.313	5,496	0.0076	0.0081	0.0247	0.0179	1.8%
0.4	1.046	0.418	7,340	0.0070	0.0075	0.0215	0.0155	1.7%
0.5	1.048	0.528	9,271	0.0066	0.0070	0.0194	0.0138	1.7%
0.6	1.051	0.631	11,080	0.0063	0.0067	0.0179	0.0126	1.7%
0.7	1.054	0.738	12,959	0.0061	0.0064	0.0168	0.0117	1.7%
0.8	1.058	0.846	14,855	0.0059	0.0062	0.0159	0.0109	1.7%

Table 17: Decrement in Frictional Resistance as Percent of Total Turbulent Frictional Resistance - H/T = 1.3

(5.3.c) Estimating the Effect of the Trip-wire on Trim

The effect of the trip-wire self drag on the SWATH trim was also estimated. Neglecting the vertical pressure force contribution to the trimming moment, the moment due to the horizontal (resistance) forces acting about the transverse axis may be estimated by,

$$M_H = R_T a \qquad \text{..... (5.3.4)}$$

where a is the distance between the centre of underwater resistance and the point of application of the towing force. If the additional drag due to the trip-wire, r_w, is assumed acting at the center of underwater resistance, the resulting additional trimming moment will be,

$$m_w = r_w a \qquad \text{..... (5.3.5.a)}$$

or

$$m_w = \frac{C_w}{C_{TOT}} M_H \qquad \text{..... (5.3.5.b)}$$

Equating this moment to the hydrostatic restoring moment and assuming small angles, the trim angle increase is obtained,

$$\frac{\Delta trim}{L} = \frac{1}{\rho g \nabla GM_L} \left(M_H \left(\frac{C_w}{C_{TOT}}\right)\right) \qquad \text{..... (5.3.6)}$$

or in terms of the non-dimensional trim coefficient, C_T,

$$\Delta C_T = \frac{M_H}{\rho g \nabla GM_L} \left(100 \left(\frac{C_w}{C_{TOT}}\right)\right) \qquad \text{..... (5.3.7)}$$

Values of $100\ (C_W / C_{TOT})$ are evaluated in Tables 13,14,15.

(5.3.d) Effect on SWATH in Shallow-water

In shallow-water the accentuation of the variations in speed and pressures around the hulls and columns may be expected to shift the points of transition from laminar to turbulent flow. The shallow-water experiments, conducted with a SWATH model, indicate that the addition of a trip-wire causes changes in the measured sinkages at the perpendiculars over the range $1.1 \leq h/T \leq 1.5$.

Fig.45 is typical of the data measured and shows that, in general, the change aft is more significant while forward the changes diminish with increasing speed. When plotted non-dimensionally, the trim appears to depend on the depth-draught ratio. Following the method outlined in section (5.3.c) the effect of the wire self-drag on the trim is plotted in Fig.46 together with the total measured trim change between the 2 conditions (i.e. with and without the trip-wire) for $h/T = 1.1$, 1.3 and 1.5. The changes were obtained by curve-fitting the $C_T - F_h$ experimental data, see Seren et al [65]. It is concluded from Fig.46 that the additional trim measured with the turbulence stimulators is predominantly due to the wire self-drag and not the vertical pressure redistribution owing to the transition to turbulent flow. The qualitative and quantitative (within 5%) agreement is perhaps as good

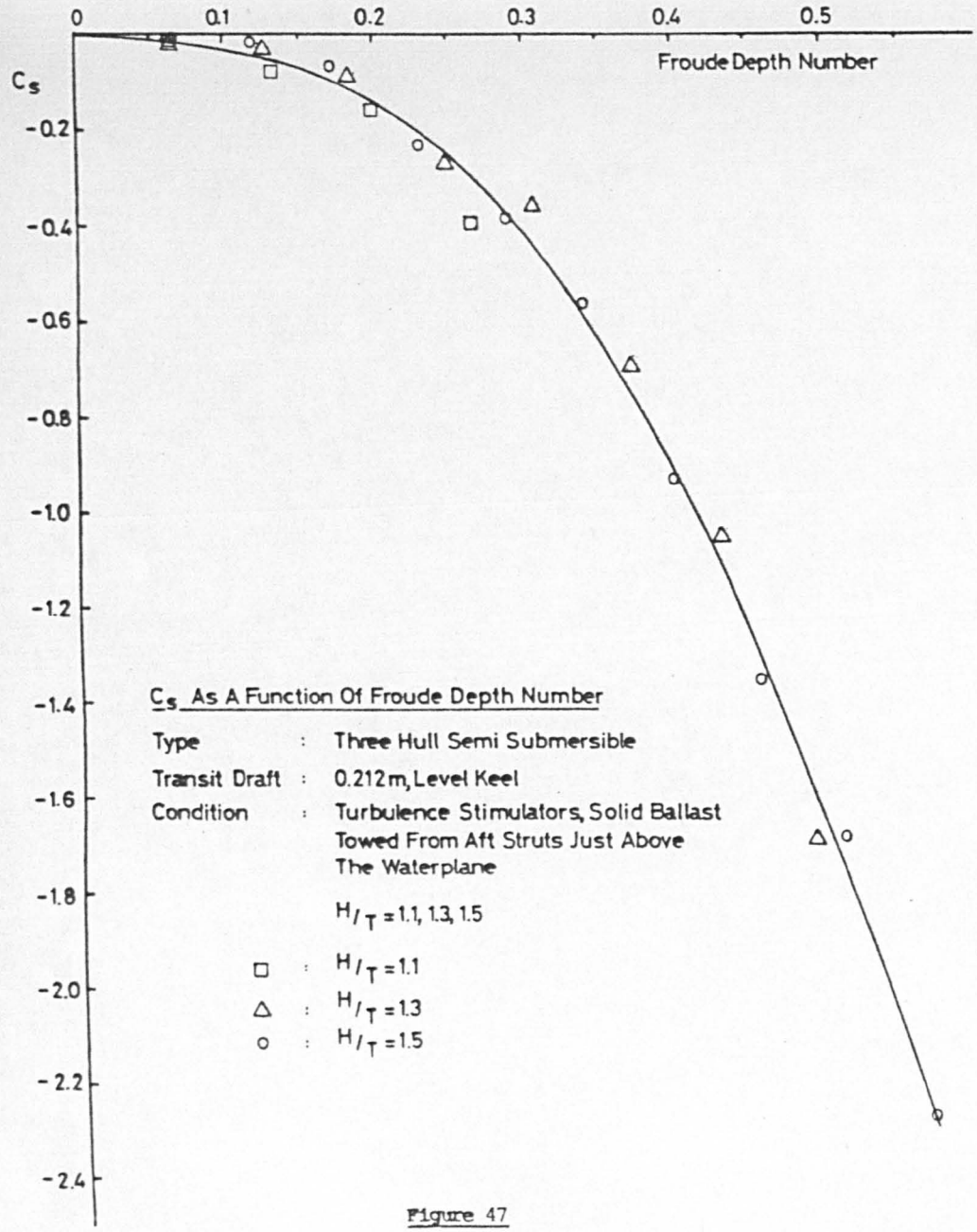

Figure 47

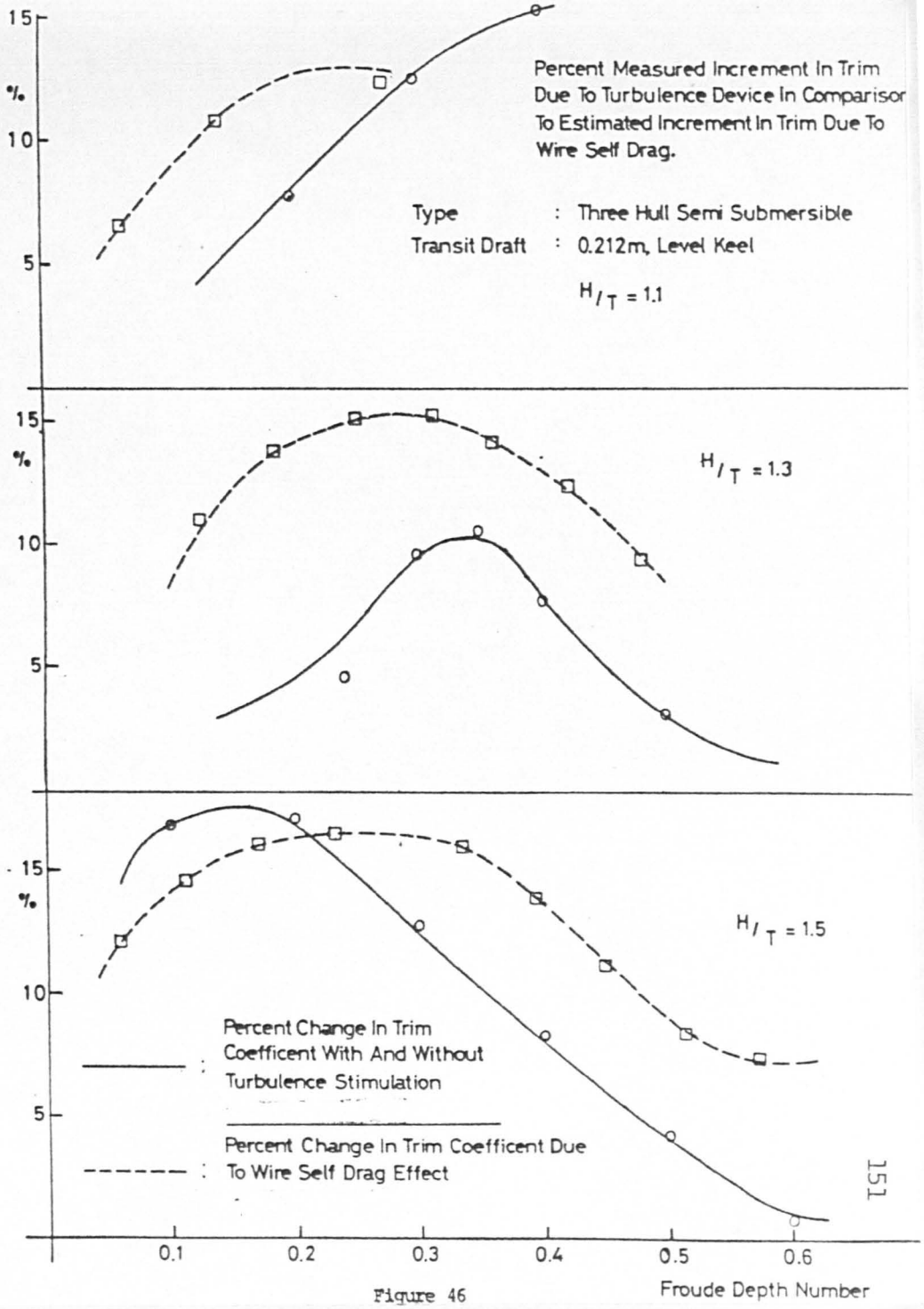

Figure 46

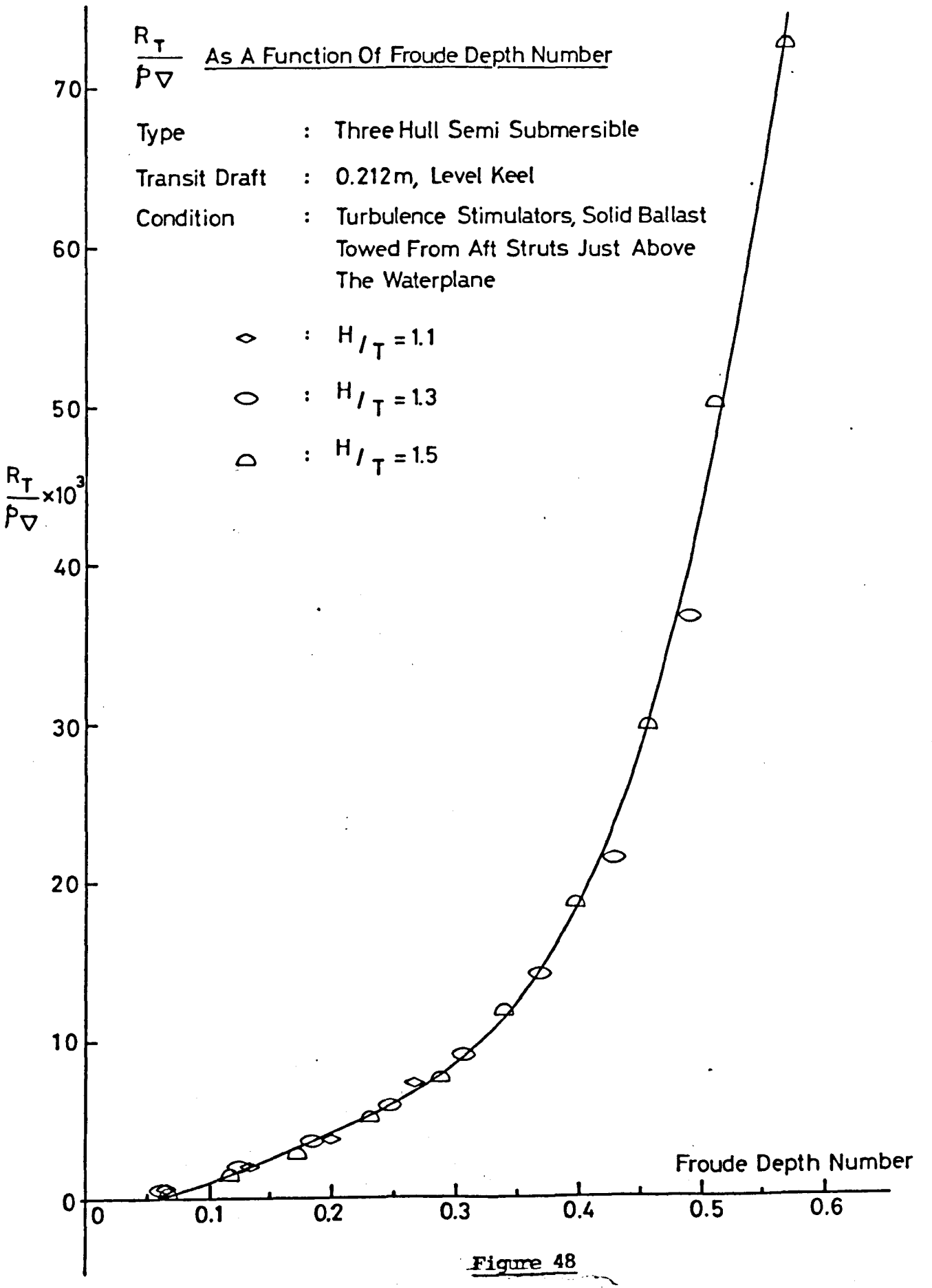
$\frac{R_T}{\rho\nabla}$ As A Function Of Froude Depth Number
Type : Three Hull Semi Submersible
Transit Draft : 0.212m, Level Keel
Condition : Turbulence Stimulators, Solid Ballast Towed From Aft Struts Just Above The Waterplane
: $H/T = 1.1$
: $H/T = 1.3$
: $H/T = 1.5$
$\frac{R_T}{\rho\nabla} \times 10^3$
70
60
50
40
30
20
10
0
0
0.1
0.2
0.3
0.4
0.5
0.6
Froude Depth Number

Figure 48

Effect Of Turbulence Stimulation

Reynolds Number - Drag Curve

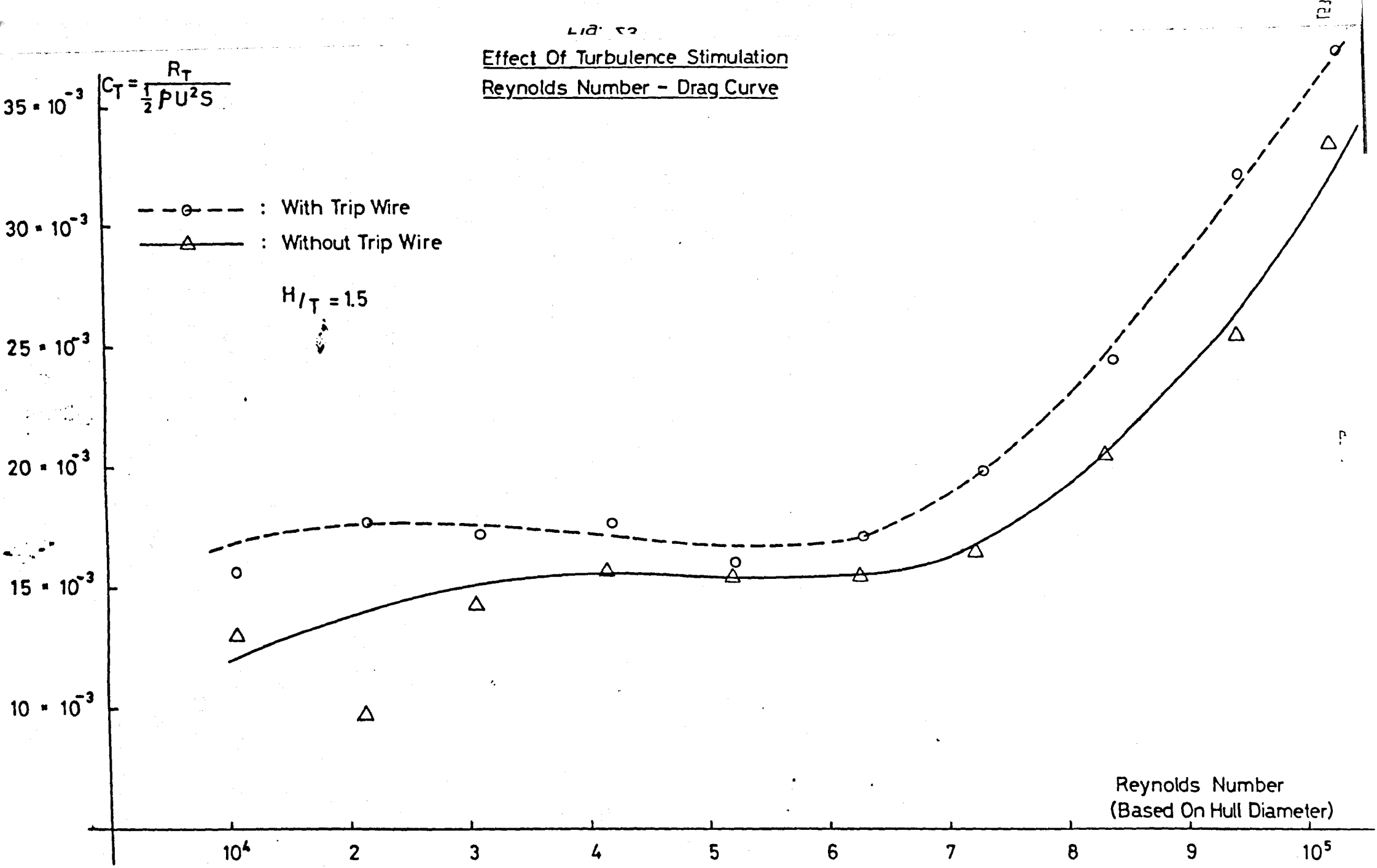

Fig. 49

as may be expected considering the approximations required in the process of obtaining the curves.

When plotted non-dimensionally both the mean sinkage, Fig.47, and the total measured resistance, Fig.48, are seen to be independent of the depth-draught ratio. This was the case both with and without turbulence stimulators.

Fig.49 presents a curve of drag versus Reynold's number, indicating that the model is not in a transition regime. Figs.50,51 present the changes in resistance due to the trip-wire in combination with the estimates of wire self-drag (section(5.3.a)) and decrement due to laminar flow over the initial part of the hull (section (5.3.b)). The comparison shows that most of the increment in the total measured resistance arises from the wire self-drag. Over the speed range examined, the trip-wire drag becomes a relatively large percentage of the total model resistance.

(5.3.e) Effect on SSCV in Deep-water

Experiments conducted with a bluff twin-hull model, Fig.38, in calm, deep water demonstrate that, a trip-wire diameter determined by its effectiveness at the lowest speed of interest, may lead to an "overstimulation" phenomenon which, contrary to intuition, may decrease the measured resistance, Fig.52, in a manner different to that observed on the more streamlined SWATH. Fig.53 indicates that the changes in the measured parameters are brought

Percent Increment Of Total Measured Resistance Due To Turbulence Device In Comparison To Increment Due To Wire Self Drag And Decrement Due To Laminar Flow Up To Trip Wire. As A Function Of Froude Depth Number

Type : Three Hull (Swath Type)

Transit Draft : 0.212m, Level Keel

$H/_T = 1.3$

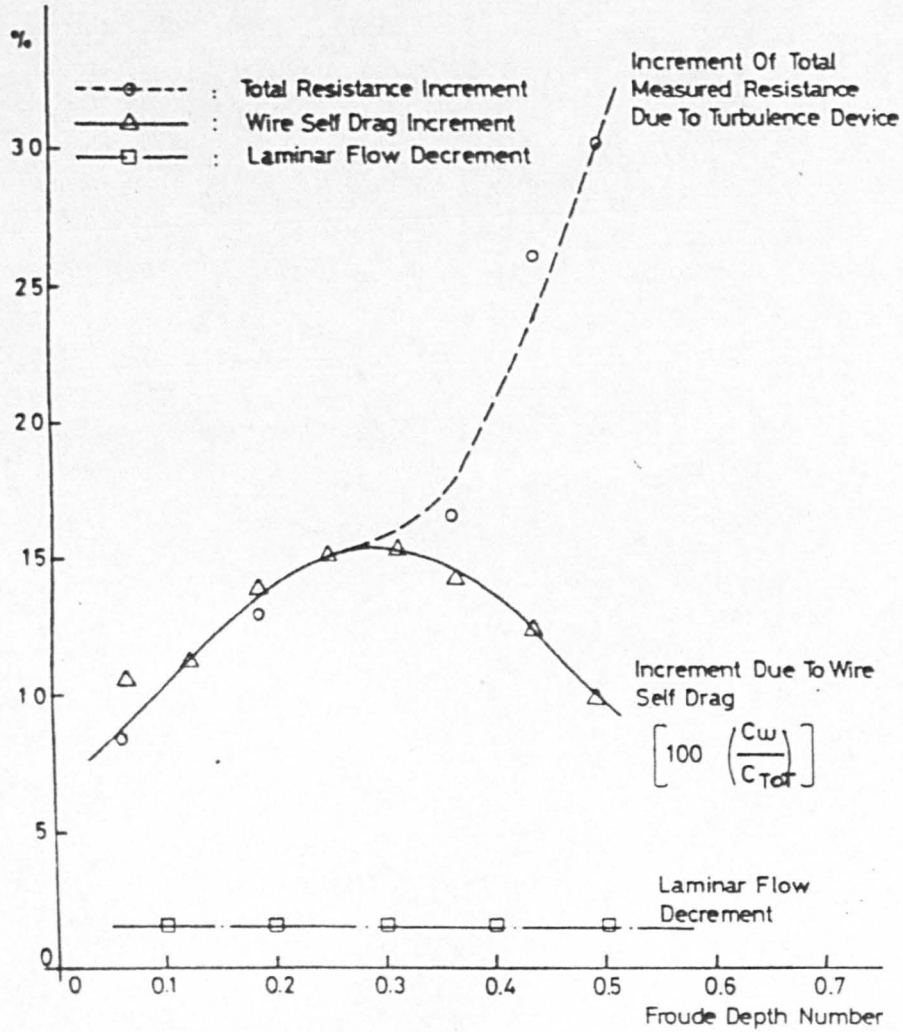

Fig. 51

Percent Increment Of Total Measured Resistance Due To Turbulence Device In Comparison To Increment Due To Wire Self Drag And Decrement Due To Laminar Flow Up To Trip Wire. As A Function Of The Froude Depth Number

Type : Three Hull (Swath Type)

Transit Draft : 0.212m, Level Keel

$H/_T = 1.5$

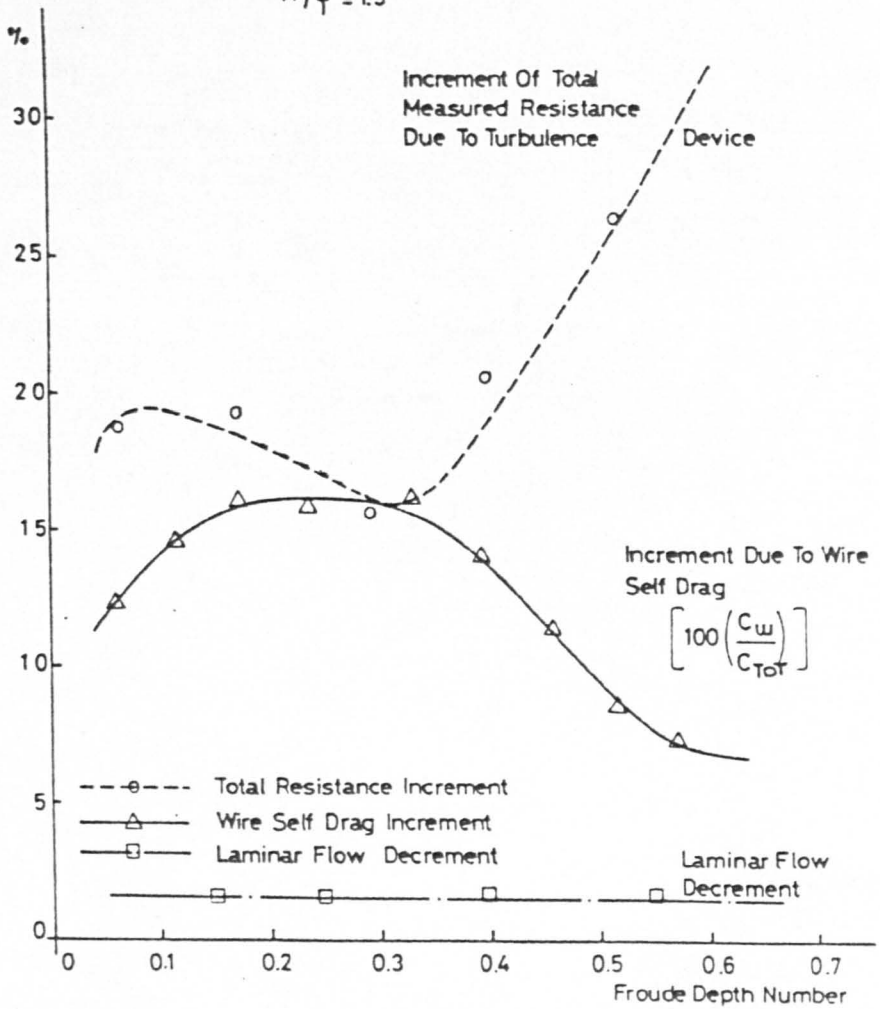

Fig 50

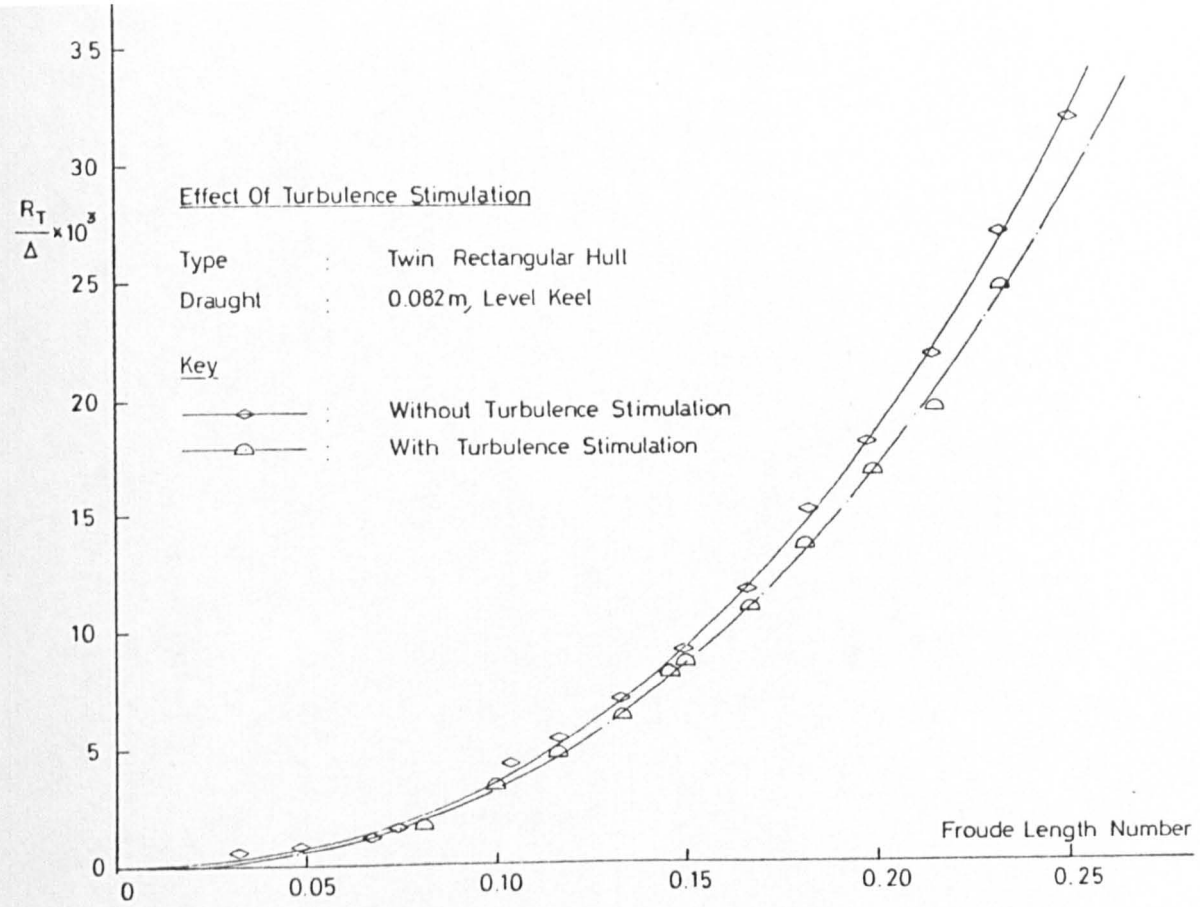

Figure 52

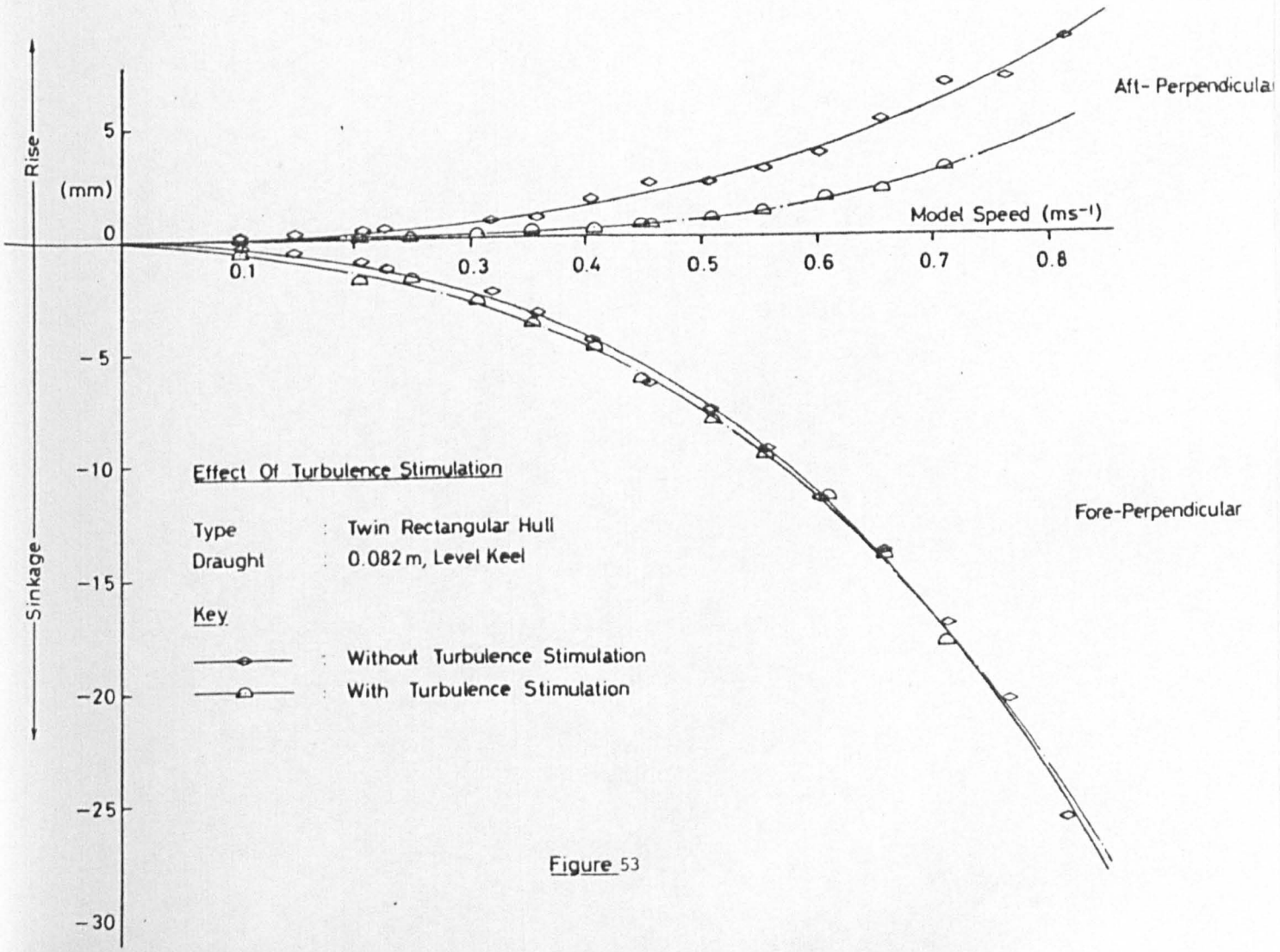

Figure 53

about by modified wake characteristics which affect the pressure recovery aft.

This stems from the fact that the major part of the resistance is form resistance. It appears reasonable to assume that accompanying the thickening of the boundary layer and wake, is a decrease in wake velocities and increase in suction pressures of sufficient magnitude to induce an increase in mean sinkage, Fig.54, and a decrease in trim-by-bow, Fig.55.

In contrast with theoretical considerations, the experiments suggest that the introduction of a disturbance into a separated and already turbulent flow may have advantageous applications. This requires confirmation.

(5.3.f) Conclusions

On the basis of the above evidence, it is concluded that multi-hull turbulence stimulation in shallow-water or over the working range of offshore platforms is of no real value at present. The use of a turbulence device under such conditions leads to two conflicting requirements. Trip wire size, determined by its effectiveness at the lowest speed of interest, results in a relatively large wire diameter. In the higher speed range, this lead to a significant trip wire self-drag. It is essential, but not normally possible, to carefully evaluate this self-drag, since it is extremely difficult to distinguish between it

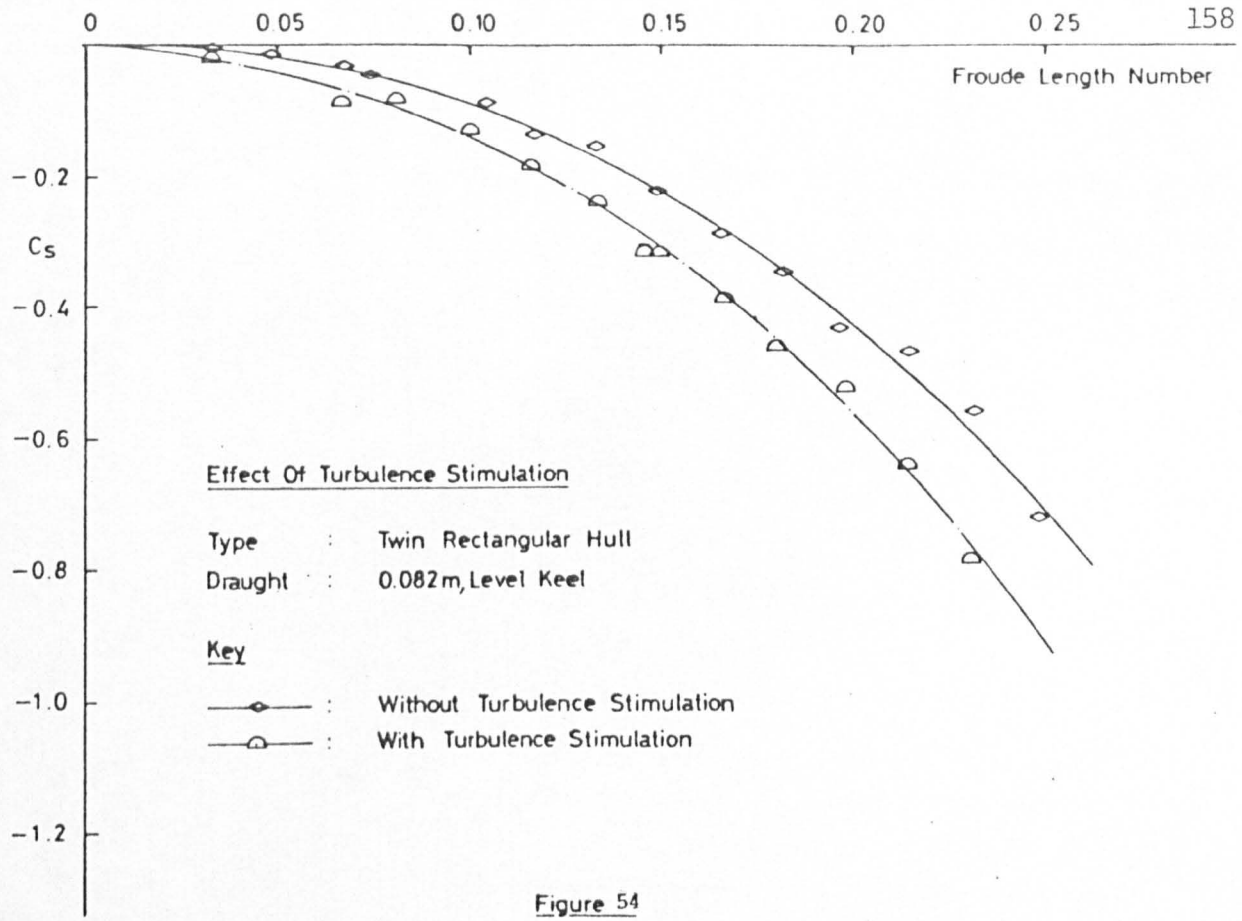

Figure 54

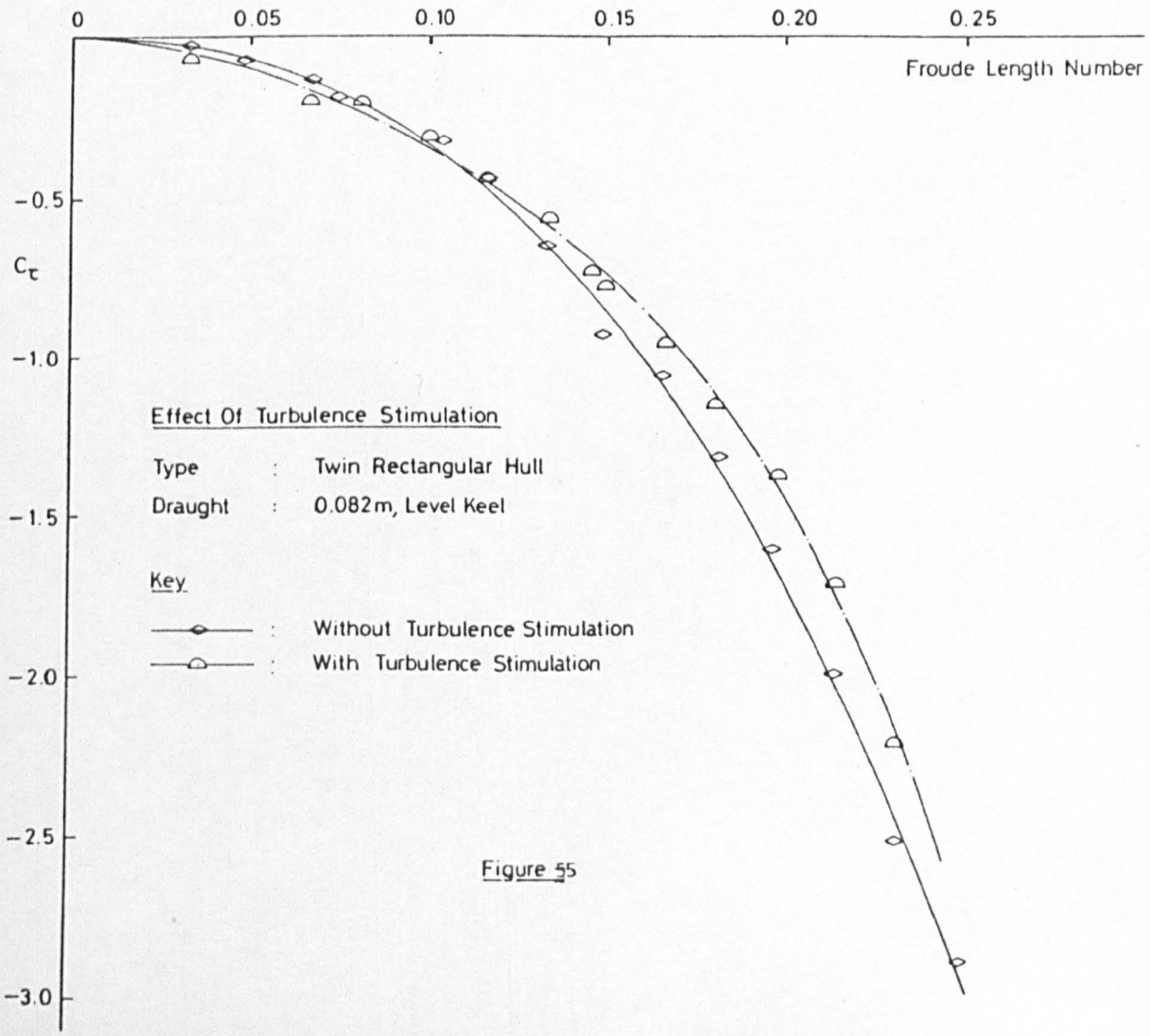

Figure 55

and any purely turbulent flow effects. An exception occurs in the case of comparative tests when, for instance, examining the effects of change in shape, which may itself induce transition, see section (6.3).

The effect of the trip-wire on the sinkage, trim and resistance of more streamlined shapes, such as the SWATH, is significant. Application of the normal trip-wire criteria to bluff twin-hulls yields "overstimulation" phenomena and will result in erroneous predictions on full-scale.

(5.4) The Effect of Towing Point Height

This section presents a study of the effect of the variation in towing point height on the shallow-water characteristics of the twin rectangular-hull semi-submersible (SSCV) and examines a theoretical corrector for its effect on trim. The method was empoyed in the previous section (5.3.c). For fuller details, see Seren et al [64].

When towing model or full-scale multi-hull platforms, it is not unusual to tow from the upper deck as distinct from the lower hulls. It is, therefore, of some practical value to model and full-scale to examine the changes induced by adopting a different towing arrangement.

(5.4.a) Experimental Study

If the line of action of the towing force is not aligned with the total resistance vector acting on the underwater part of the hull, a moment will be applied. Depending on whether the line of the applied force is below or above the horizontal resultant of resistance, the bow will rise or sink respectively.

The model particulars are presented in Fig.38. The two towing set-ups are shown in Fig.56, the tow-bar being aligned horizontally with the towing point when stationary. The effect of the variation of the point of application of

TOWING ARRANGEMENTS FOR TWIN
RECTANGULAR HULL. (S.S.C.V.) MODEL

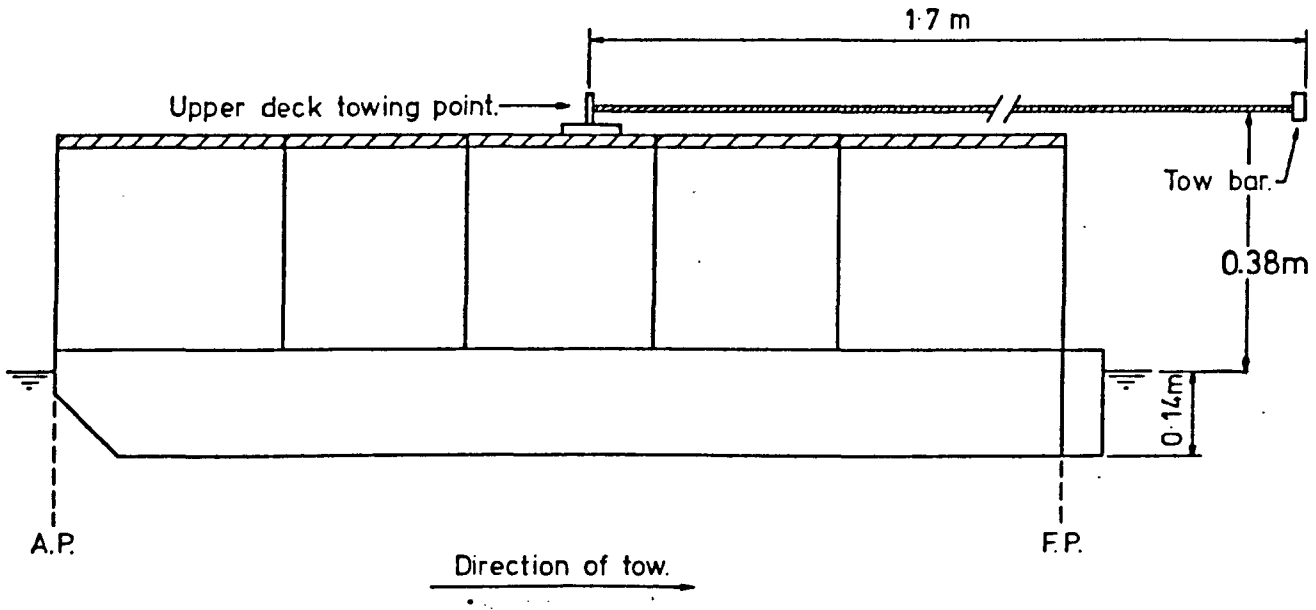

(a) UPPER DECK TOWING ARRANGEMENT.

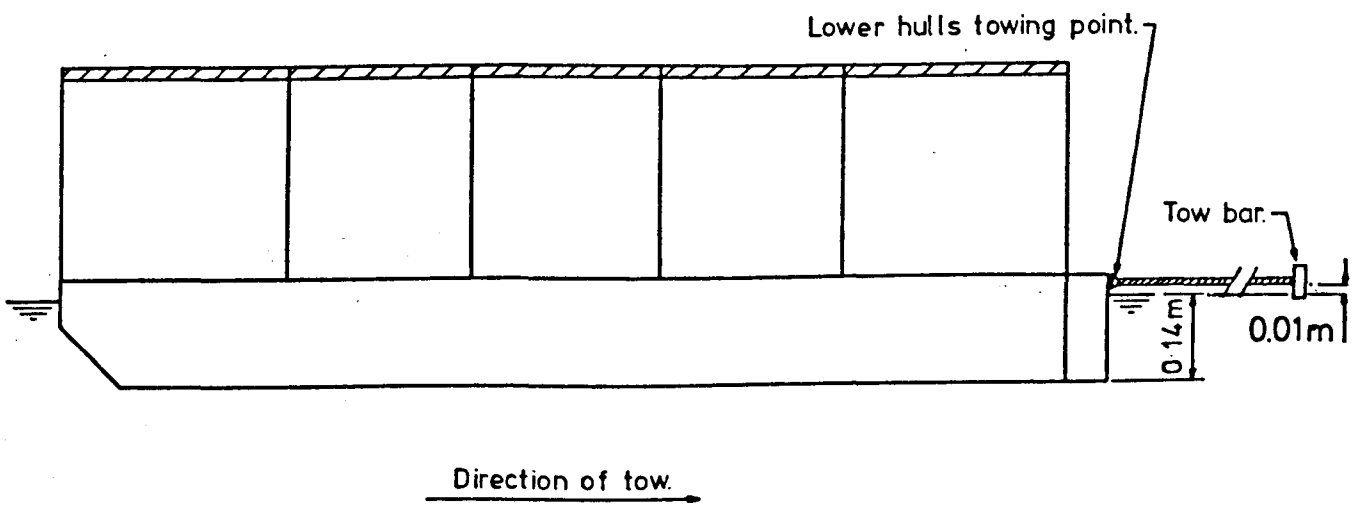

(b) LOWER HULLS TOWING ARRANGEMENT.

FIGURE 56

the towing force from the lower hulls to the upper deck on the measured sinkages is presented in Figs.57-60 for h/T = 1.1,1.3,1.5 and 2.0. The conclusions may be summed up as follows,

(a) The upper deck arrangement induces an increase in the sinkage measured forward and a decrease aft resulting in,
(b) a negligible increase in the mean sinkage throughout the depths and speeds tested (i.e. no change in displacement), Fig.61, and an increase in the trim-by-bow attitude, Fig.62.

The increasedd trim by bow attitude, and consequent lower underkeel clearances forward in the upper-deck towing arrangement affect the,

(c) general shallow-water behaviour owing to the greater proximity of the bow part of the hull to the bottom, which results in their respective boundary layers approaching one another, Figs.63,64, and increases the suctions aft.
(d) increased resistance at higher speeds, Figs.65,66 typically, which depends on the depth-draught ratio.

The results show that the measured shallow-water performance parameters can be significantly in error if either the correct towing arrangement or a correction for the effects of towing point height is not made.

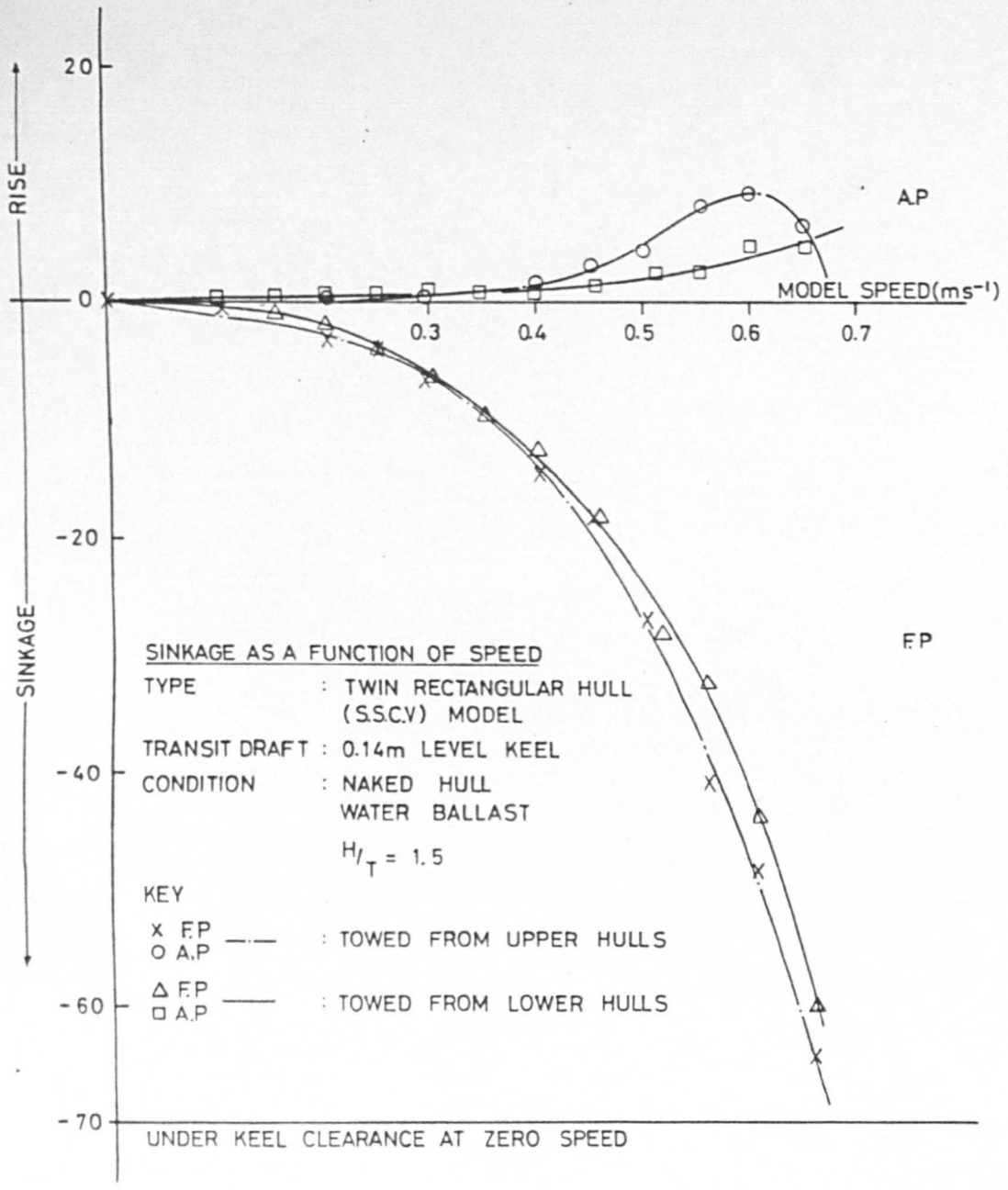

FIGURE 58

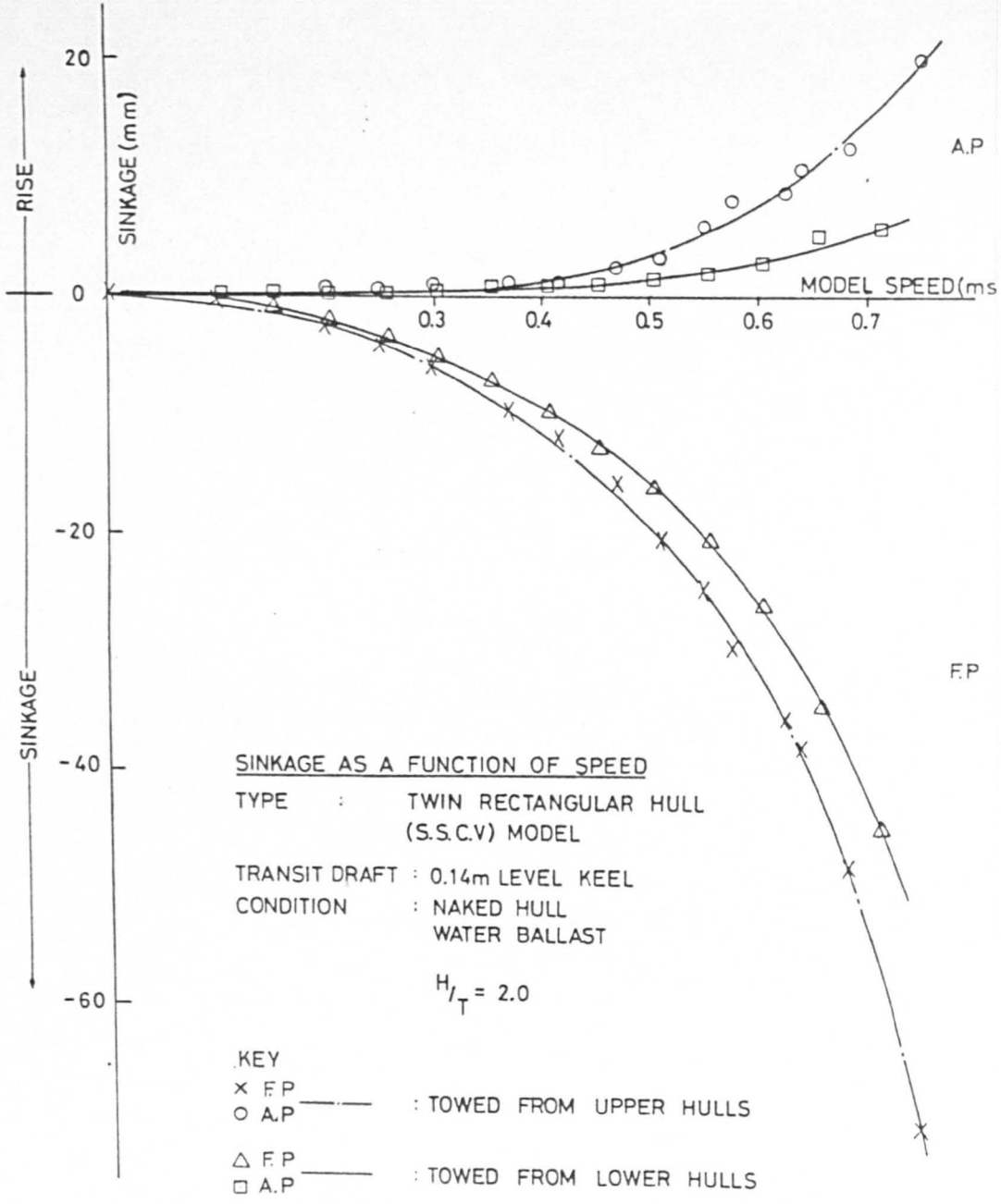

FIGURE 57

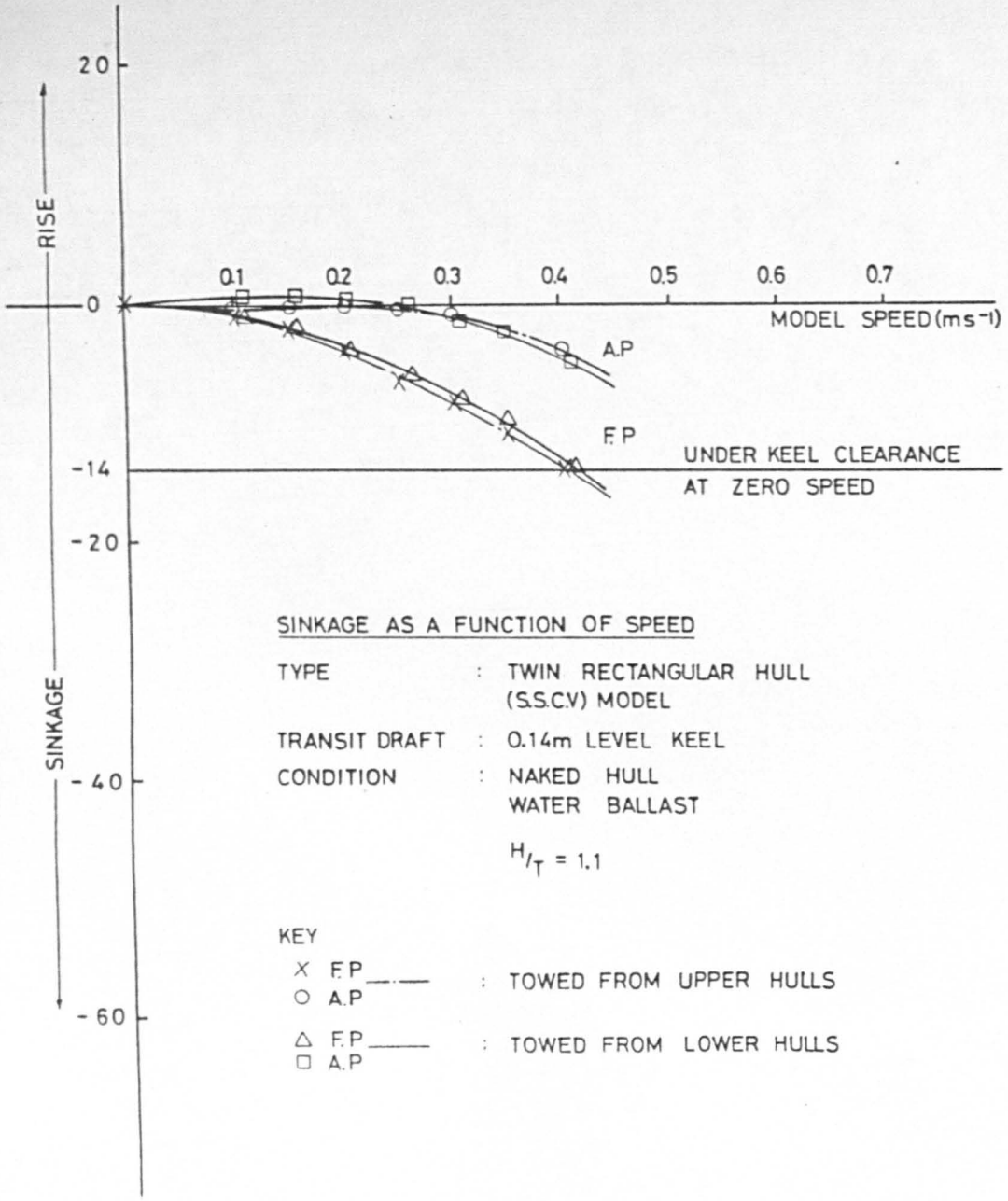

SINKAGE AS A FUNCTION OF SPEED

TYPE : TWIN RECTANGULAR HULL (S.S.C.V) MODEL

TRANSIT DRAFT : 0.14m LEVEL KEEL

CONDITION : NAKED HULL
WATER BALLAST

$H/_T = 1.1$

KEY

X F.P —·— : TOWED FROM UPPER HULLS
O A.P

△ F.P —— : TOWED FROM LOWER HULLS
□ A.P

FIGURE 60

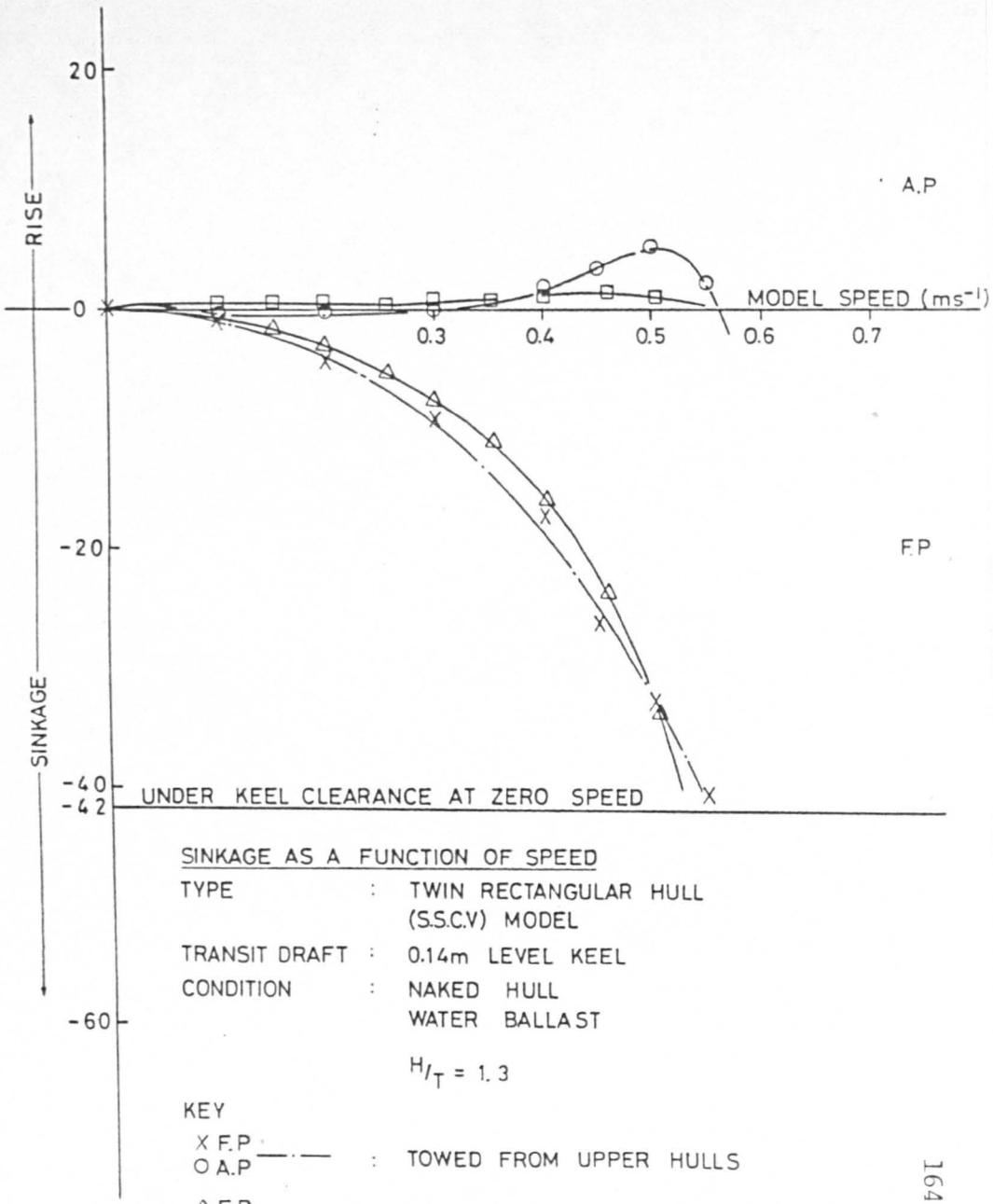

SINKAGE AS A FUNCTION OF SPEED

TYPE : TWIN RECTANGULAR HULL (S.S.C.V) MODEL

TRANSIT DRAFT : 0.14m LEVEL KEEL

CONDITION : NAKED HULL
WATER BALLAST

$H/_T = 1.3$

KEY

X F.P
O A.P —·— : TOWED FROM UPPER HULLS

△ F.P
□ A.P —— : TOWED FROM LOWER HULLS

FIGURE 59

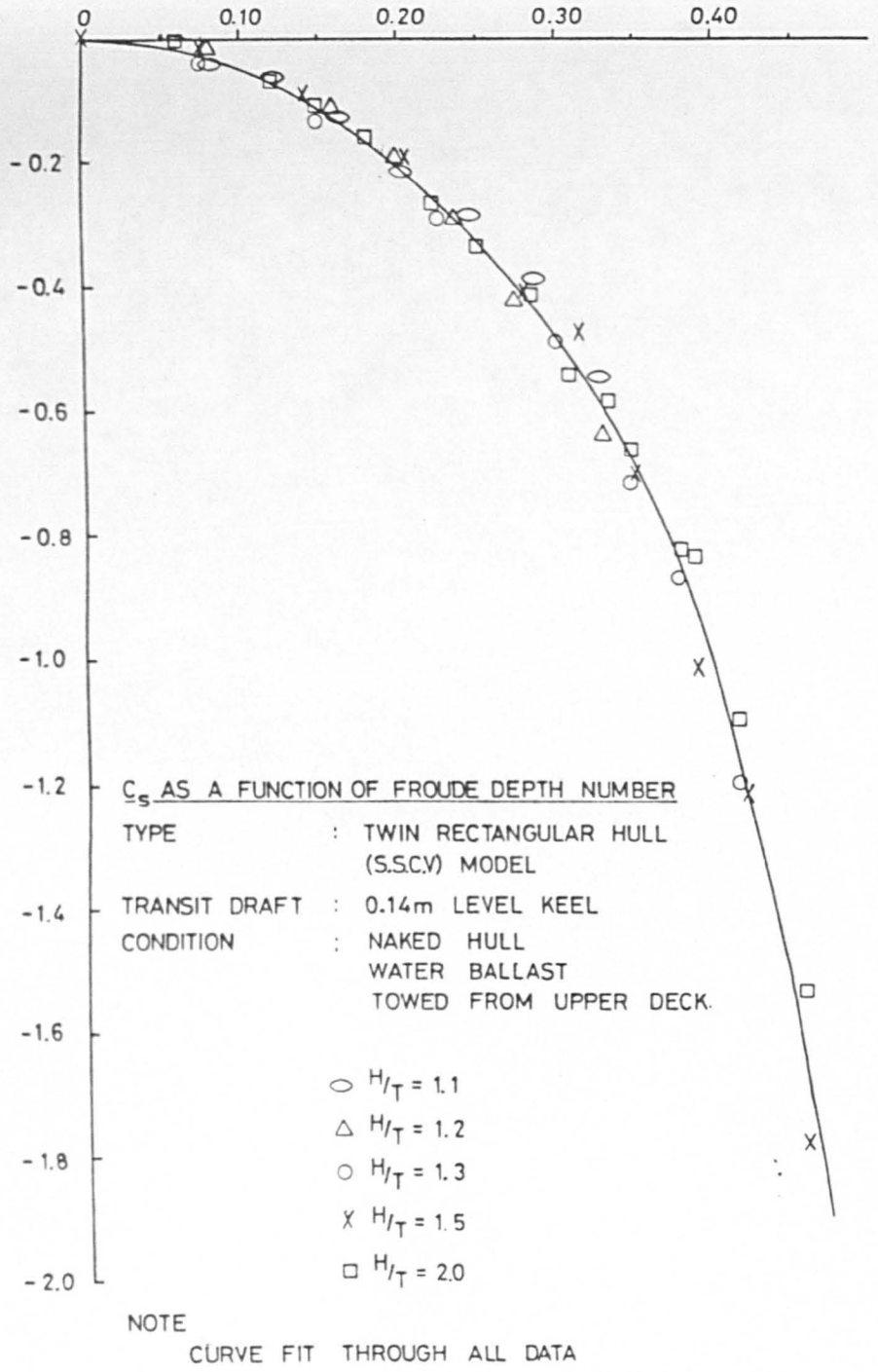

FIGURE 62

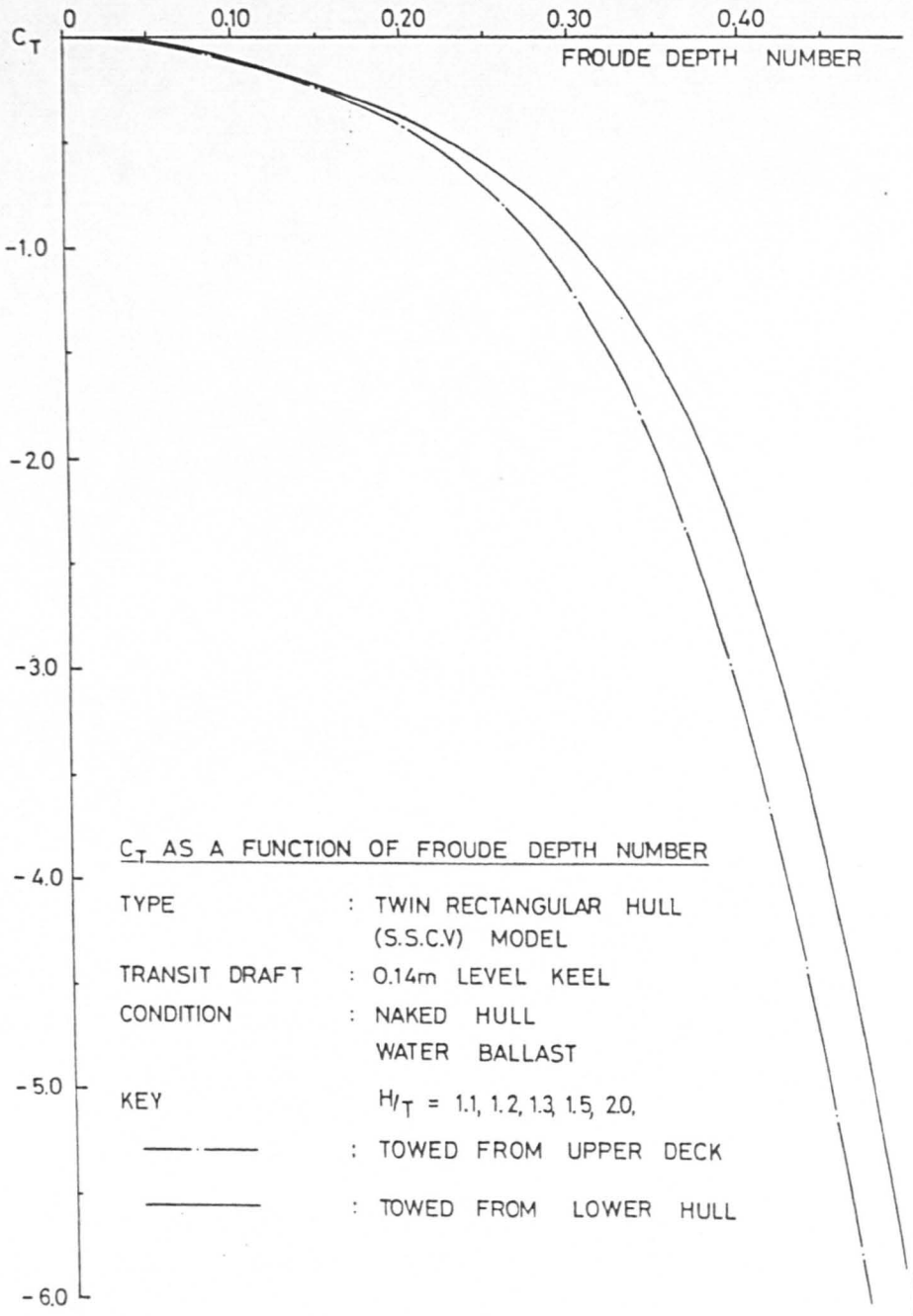

FIGURE 61

X(M)	R_X	δ^* HULL (mm)	$\delta^*/_{UKC}$	δ^* UKC (mm)
0·05	26,923	0·35	0·03	25·7
0·5	269,230	2·2	0·10	37·8
1·0	538,460	3·8	0·13	50·4
1·5	807,690	5·3	0·14	63·3

$H/_T = 1·5$

V = SPEED = 0·603 M/S

V_1 = CORR. SPEED = 0·70 M/S

$\nu = 1·306 \times 10^{-6}$ M²/S

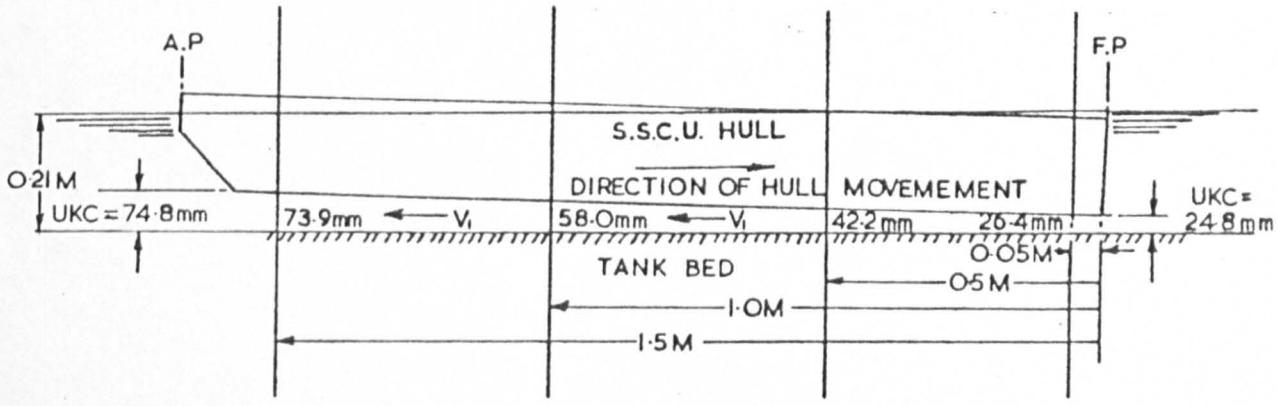

FIG. 63

NOTE:

$\delta^* = \delta^*$ HULL × 2

where

δ^* HULL = 0·14 δ

$\delta = 0·38 \times (R_x)^{-0·2}$

SHALLOW WATER SQUAT

X(M)	R_X	δ^* HULL (mm)	$\delta^*/_{UKC}$	δ^* UKC (mm)
0·05	16,000	0·4	0·06	14·5
0·5	160,000	2·4	0·250	14·5
1·0	320,000	4·2	0·35	15·3
1·5	480,000	5·8	0·42	16·4

$H/_T = 1·2$

V = SPEED = 0·354 M/S

V_1 = CORR. SPEED = 0·416 M/S

$\nu = 1·3 \times 10^{-6}$ M²/S

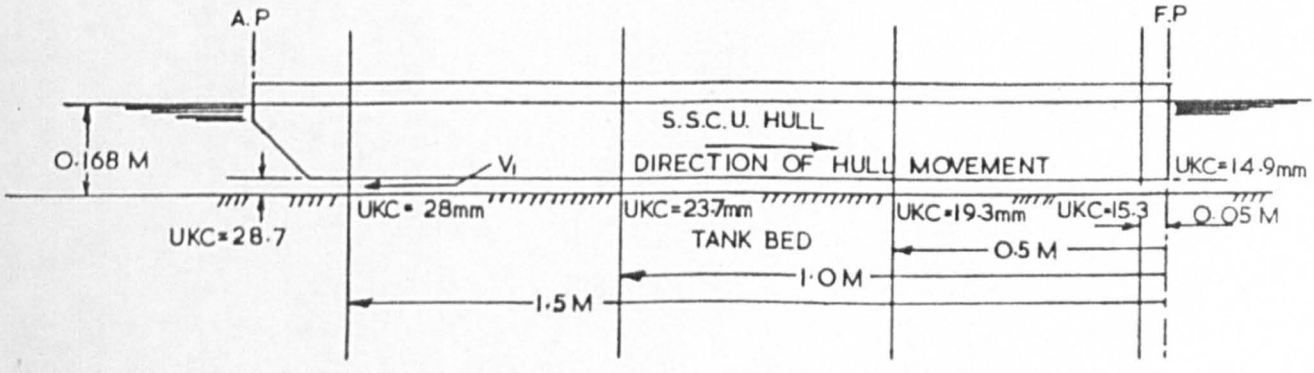

FIG. 64

NOTE:

$\delta^* = \delta^*$ HULL × 2

where

δ^* HULL = 0·14 × δ

δ 0·38 × $(R_x)^{-0·2}$

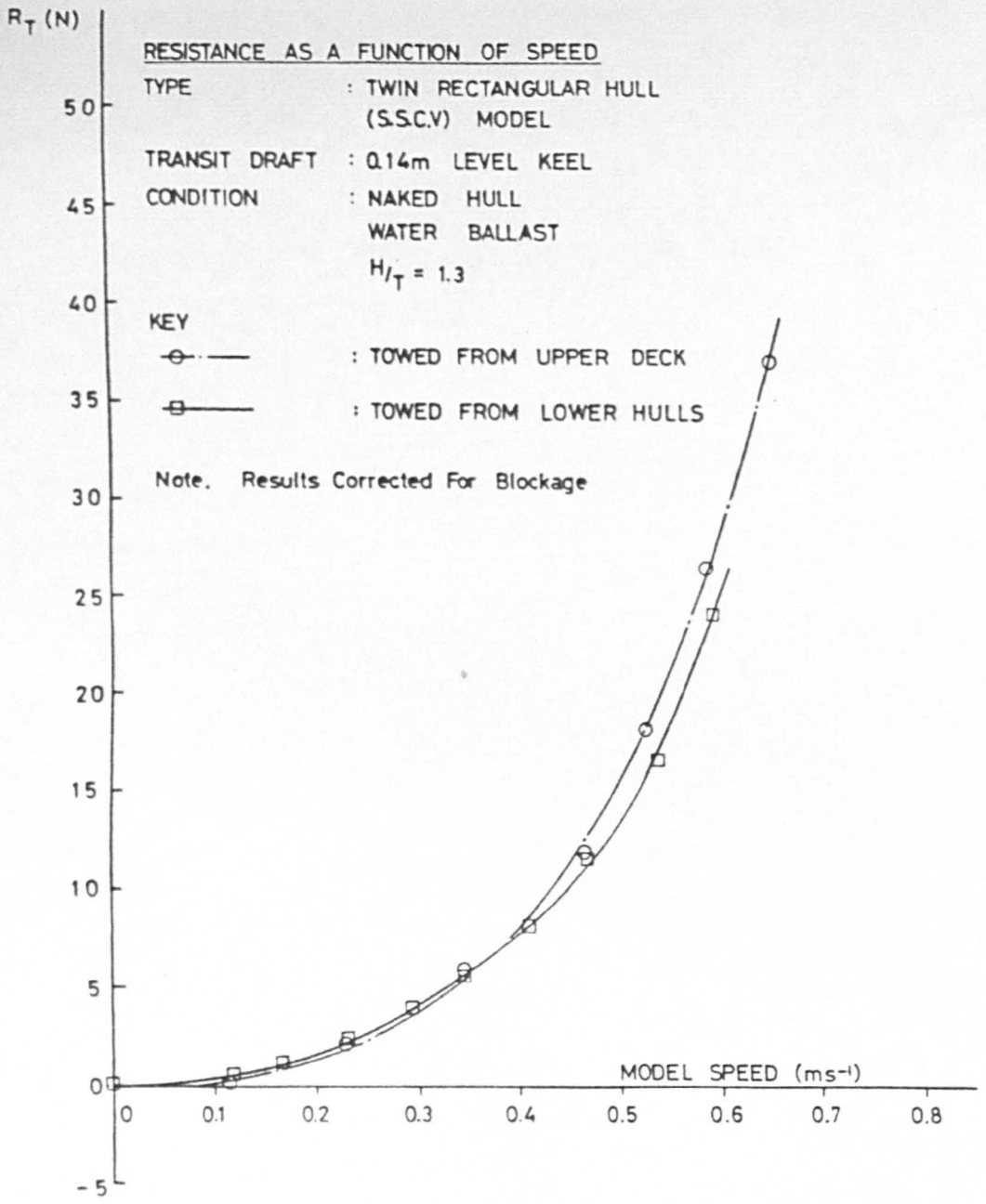
R_T (N)
RESISTANCE AS A FUNCTION OF SPEED
TYPE : TWIN RECTANGULAR HULL (S.S.C.V) MODEL
TRANSIT DRAFT : 0.14m LEVEL KEEL
CONDITION : NAKED HULL
WATER BALLAST
$H/_T$ = 1.3
KEY
: TOWED FROM UPPER DECK
: TOWED FROM LOWER HULLS
Note. Results Corrected For Blockage
MODEL SPEED (ms^{-1})
50
45
40
35
30
25
20
15
10
5
0
-5
0
0.1
0.2
0.3
0.4
0.5
0.6
0.7
0.8

Fig. 66

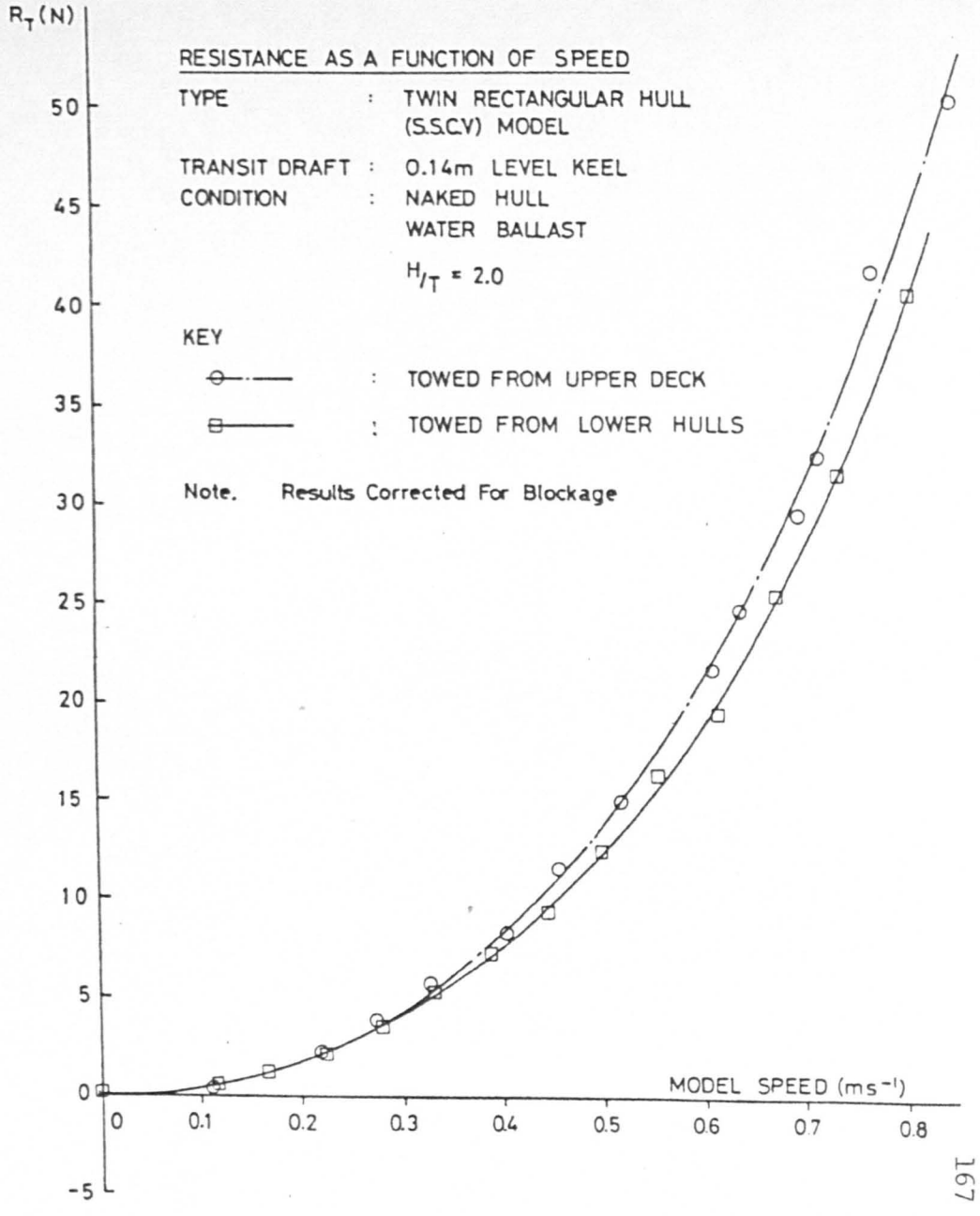
R_T (N)
RESISTANCE AS A FUNCTION OF SPEED
TYPE : TWIN RECTANGULAR HULL (S.S.C.V) MODEL
TRANSIT DRAFT : 0.14m LEVEL KEEL
CONDITION : NAKED HULL
WATER BALLAST
$H/_T$ = 2.0
KEY
: TOWED FROM UPPER DECK
: TOWED FROM LOWER HULLS
Note. Results Corrected For Blockage
MODEL SPEED (ms^{-1})
50
45
40
35
30
25
20
15
10
5
0
-5
0
0.1
0.2
0.3
0.4
0.5
0.6
0.7
0.8

Fig. 65

(5.4.b) Examination of a Theoretical Method

The "horizontal" trimming moment component will be proportional to,

$$a = d + z \qquad \ldots\ldots (5.4.1)$$

where d is the distance of the centre of underwater resistance below the waterline and z is the distance of the point of application of the towing force above the waterplane. Neglecting the influence of the C_B and speed, the centre of the underwater resistance will be assumed as acting at the centroid of the midship wetted surface. For rectangular cross-sections,

$$d = \frac{T(B/T + 1)}{(B/T + 2)} \qquad \ldots\ldots (5.4.2)$$

where T is the draught and B is (one) hull breadth.

By equating the horizontal trimming and restoring moments, the equivalent trim angle is obtained,

$$\tau = \frac{M_H}{g\Delta GM_L} (57.3) \qquad \ldots\ldots (5.4.3)$$

where Δ is the model displacement in kg. and GM_L is the longitudinal GM. The calculated trim owing to this moment is,

$$T_H = L_{\sin}\tau \qquad \ldots\ldots (5.4.4)$$

If,

$$T_T = T_V + T_H \quad \ldots\ldots (5.4.5)$$

where T is the total measured trim, T_H the calculated "horizontal" trim, and T_V the resulting trim due to the "vertical" forces. When measurements are taken at two towing points, one at height z_2 and the other at a (lower) height of z_1 , then

$$T_T(z_2) - T_H(z_2) = T_V = T_T(z_1) - T_H(z_1) \quad \ldots\ldots (5.4.6)$$

and a check on the accuracy of the method can be made.

The theoretical method was compared with experimental data for the upper deck towing arrangement. The results are presented Tables 18-21 for depth-draught ratios of 1.1,1.3,1.5 and 2.0, respectively. The value of d was first found to be 0.11m below the at-rest draught waterplane. Values of z_2 = 0.38m. and z_1 = 0.01m. were measured for the upper and lower towing arrangement, respectively, see Fig.56. For a similar analysis in the lower-hull towing arrangement, see Seren et al [64].

As observed from Tables 18-21, the method may be considered sufficiently accurate for correcting deep and shallow trim results for the effects of towing point height. The approach should, however, be used with extreme caution as the bottom is approached, Table 21. This is because at low underkeel clearances very significant

①	SPEED	(MS^{-1})	0.2	0.4	0.6
②	$R_T(Z_2)$	(N)	2.35	10.5	34.1
③	a_2	(CM)	49.0	49.0	49.0
④	M_H	(NxCM)	115.2	514.5	1670.9
⑤	τ_2		0.027	0.121	0.394
⑥	$T_H(Z_2)$	(CM)	0.077	0.346	1.123
⑦	$T(Z_2)$	(CM)	0.335	1.6Ø	5.8Ø
⑧	⑦-⑥ = $T_V(Z_2)$	(CM)	0.258	1.251	4.677
⑨	$R_T(Z_1)$	(N)	1.7	9.8	31.Ø
⑩	a_1	(CM)	12.Ø	12.Ø	12.Ø
⑪	M_H	(NxCM)	20.4	117.6	372.Ø
⑫	τ_1		0.005	0.028	0.088
⑬	$T_H(Z_1)$	(CM)	0.014	0.079	0.25
⑭	$T(Z_1)$	(CM)	0.230	1.25	4.84
⑮	⑭-⑬ = $T_V(Z_1)$	(CM)	0.216	1.171	4.59
⑯	⑮/⑧ x 100	%	83.7%	93.6%	98%

Table 19: Check on Theoretical Method for H/T = 1.5

①	SPEED	(MS^{-1})	Ø.2	Ø.4	Ø.6
②	$R_T(Z_2)$	(N)	2.3	11.4	27.5
③	a_2	(CM)	49.Ø	49.Ø	49.Ø
④	M_H	(N x CM)	112.7	558.6	1347.5
⑤	τ_2		0.026	0.132	0.318
⑥	$T_H(Z_2)$	(CM)	0.076	0.375	0.906
⑦	$T(Z_2)$	(CM)	0.315	1.5Ø	3.90
⑧	⑦-⑥ = $T_V(Z_2)$	(CM)	0.239	1.125	2.994
⑨	$R_T(Z_1)$	(N)	2.15	9.5	25.3
⑩	a_1	(CM)	12.Ø	12.Ø	12.Ø
⑪	M_H	(N x CM)	25.8	114.Ø	303.6
⑫	τ_1		0.006	0.027	0.072
⑬	$T_H(Z_1)$	(CM)	0.017	0.077	0.204
⑭	$T(Z_1)$	(CM)	0.225	1.06	2.87
⑮	⑭ - ⑬ = $T_V(Z_1)$	(CM)	0.208	0.983	2.666
⑯	⑮/⑧ x 100	(%)	87%	87.4%	89%

Table 18: Check on Theoretical Method for H/T = 2.0

①	SPEED	(MS^{-1})	0.2	0.25	0.3	0.35	0.4
②	$R_T(Z_2)$	(N)	2.6	4.1	7.2	13.9ø	23.ø
③	a_2	(CM)	49.ø	49.ø	49.ø	49.ø	49.ø
④	M_H	(NxCM)	127.4	200.9	352.8	681.1	1127.ø
⑤	τ_2		0.03		0.083		0.266
⑥	$T_H(Z_2)$	(CM)	0.086	0.135	0.237	0.458	0.757
⑦	$T(Z_2)$	(CM)	0.365	0.61	0.73	0.89	1.01
⑧	⑦-⑥ = $T_V(Z_2)$	(CM)	0.279	0.474	0.493	0.432	0.253
⑨	$R_T(Z_1)$	(N)	2.55	4.ø	7.ø	13.ø	20.5
⑩	a_1	(CM)	12.ø	12.ø	12.ø	12.ø	12.ø
⑪	M_H	(NxCM)	30.6	48.ø	84.ø	15.6	246.ø
⑫	τ_1		0.0072		0.02		0.058
⑬	$T_H(Z_1)$	(CM)	0.206	0.0323	0.056		0.165
⑭	$T(Z_1)$	(CM)	0.405	0.55	0.64	0.73	0.9
⑮	⑭-⑬ = $T_V(Z_1)$	(CM)	0.379	0.518	0.584	0.624	0.735
⑯	⑮/⑧ x 100	%	136%	109%	118%	145%	291%

Table 21: Check on Theoretical Method for H/T = 1.1

①	SPEED	(MS^{-1})	0.2	0.4	0.5
②	$R_T(Z_2)$	(N)	2.4	11.8	27.ø
③	a_2	(CM)	49.ø	49.ø	49.ø
④	M_H	(NxCM)	117.6	578.2	1323.ø
⑤	τ_2		0.0277	0.136	0.312
⑥	$T_H(Z_2)$	(CM)	0.079	0.389	0.889
⑦	$T(Z_2)$	(CM)	0.410	1.91	3.84
⑧	⑦-⑥ = $T_V(Z_2)$	(CM)	0.331	1.521	2.951
⑨	$R_T(Z_1)$	(N)	2.25	11.5	24.2
⑩	a_1	(CM)	12.ø	12.ø	12.ø
⑪	M_H	(NxCM)	27.ø	138.ø	290.4
⑫	τ_1		0.0064	0.0326	0.0685
⑬	$T_H(Z_1)$	(CM)	0.018	0.093	0.195
⑭	$T(Z_1)$	(CM)	0.355	1.72	3.50
⑮	⑭-⑬ = $T_V(Z_1)$	(CM)	0.337	1.627	3.305
⑯	⑮/⑧ x 100	%	102%	107%	112%

Table 20: Check on Theoretical Method for H/T = 1.3

changes occur with small changes in speed, rendering a comparison with any statically measured value questionable.

(5.4.c) Theoretical Method Applied to a SWATH

The SWATH type vessel has a rather large draught for its size and a low restoring moment in pitch, which render it particularly sensitive to towing point height. When applied to the SWATH, Fig.42, the theoretical approach demonstrates the significant effect of towing point height on the measured results in shallow-water, Table 22, see Seren [65].

SPEED(MS) ①	CALCULATED TRIM(CM) ②	H/T = 1.5 EXPERIMENTAL TRIM ③	$\frac{②}{③} \times 100$
0.2	0.264	0.39	68%
0.4	0.928	1.48	63%
0.6	1.998	3.6	55%
0.8	3.749	7.2	52%

Table 22: Effect of Towing Point Height, SWATH

(5.5) The Effect of Type of Ballast

The effect of the type of ballast on the measured parameters was also evaluated, see Seren et al [64].

The solid/liquid ballast distribution is shown in Figs.67,68. The two center transverse bulkheads reduce the momentum and allow a slow settling of the fluid in the three centre tanks. For symmetry, the two end tanks were completely full and the liquid in those tanks had no effect upon the trim other than that of a solid body of the same weight and centre of gravity. The solid ballast weights were inserted into the columns and the LCG and VCG values in both ballast conditions compared. The liquid ballast free-surface effects on the vessel GM were accounted for. Changes were examined over h/T = 1.1,1.3,1.5 and 2.0 in calm water and the transit draught condition.

Figs.69,70 and 71 show typical results of the comparison of the C_S , C_T and resistance data. These confirm that no trend or deviations of any practical significance occur as a result of varying the type of ballast from solid to liquid on the particular arrangement examined. It should be noted that in the above liquid ballast distribution, the free-surface effects were minimised. It is, however, reasonable to assume that the above conclusion will not be valid where the free-surface effect is large.

SOLID BALLAST DISTRIBUTION.

Type : S.S.C.V. Model.

Model GM_T : 1·10 m.

Transit draft : 0·14 m, level keel.

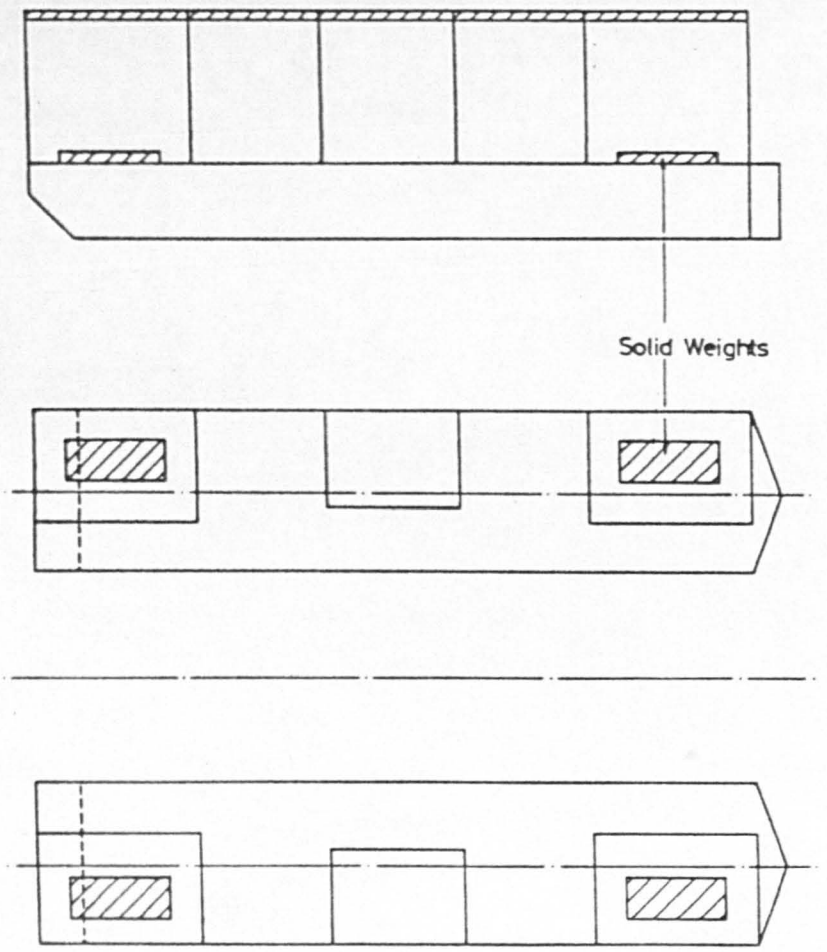

Figure. 68

Water Ballast Distribution

Type : S.S.C.V Model

Model GM_T : 1.151 m
; 1.11 m Corrected For Free Surface Effect

Transit Draft : 0.14 m Level Keel

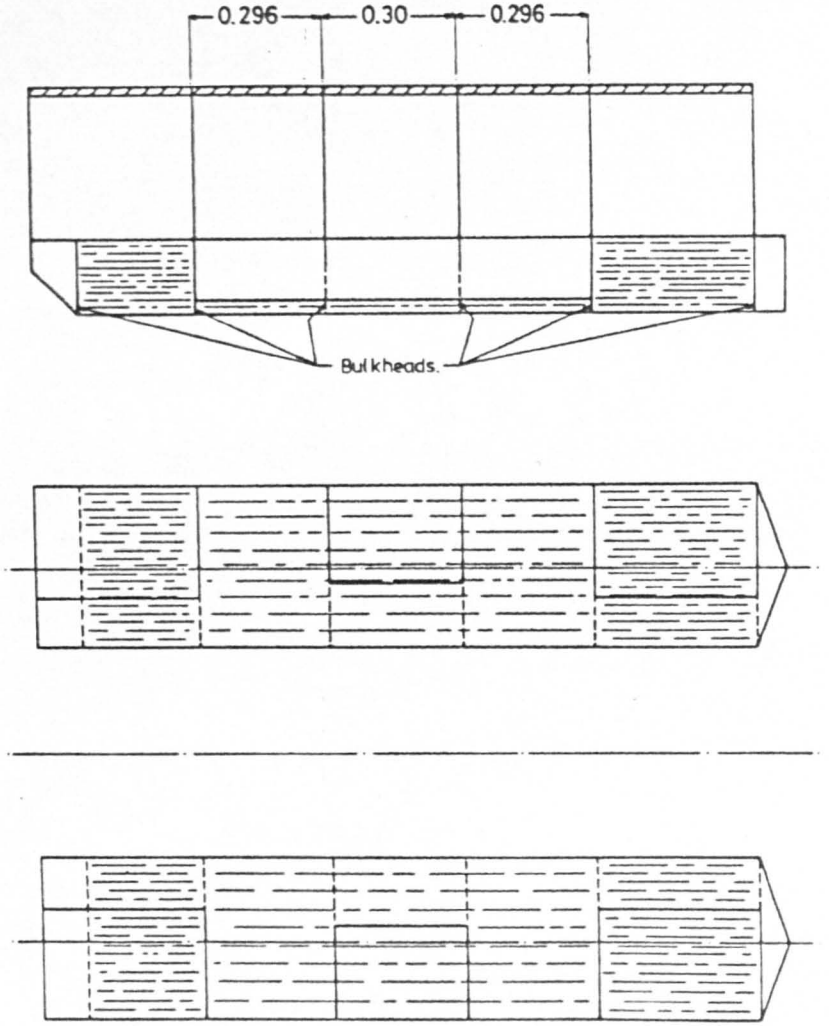

Figure 67

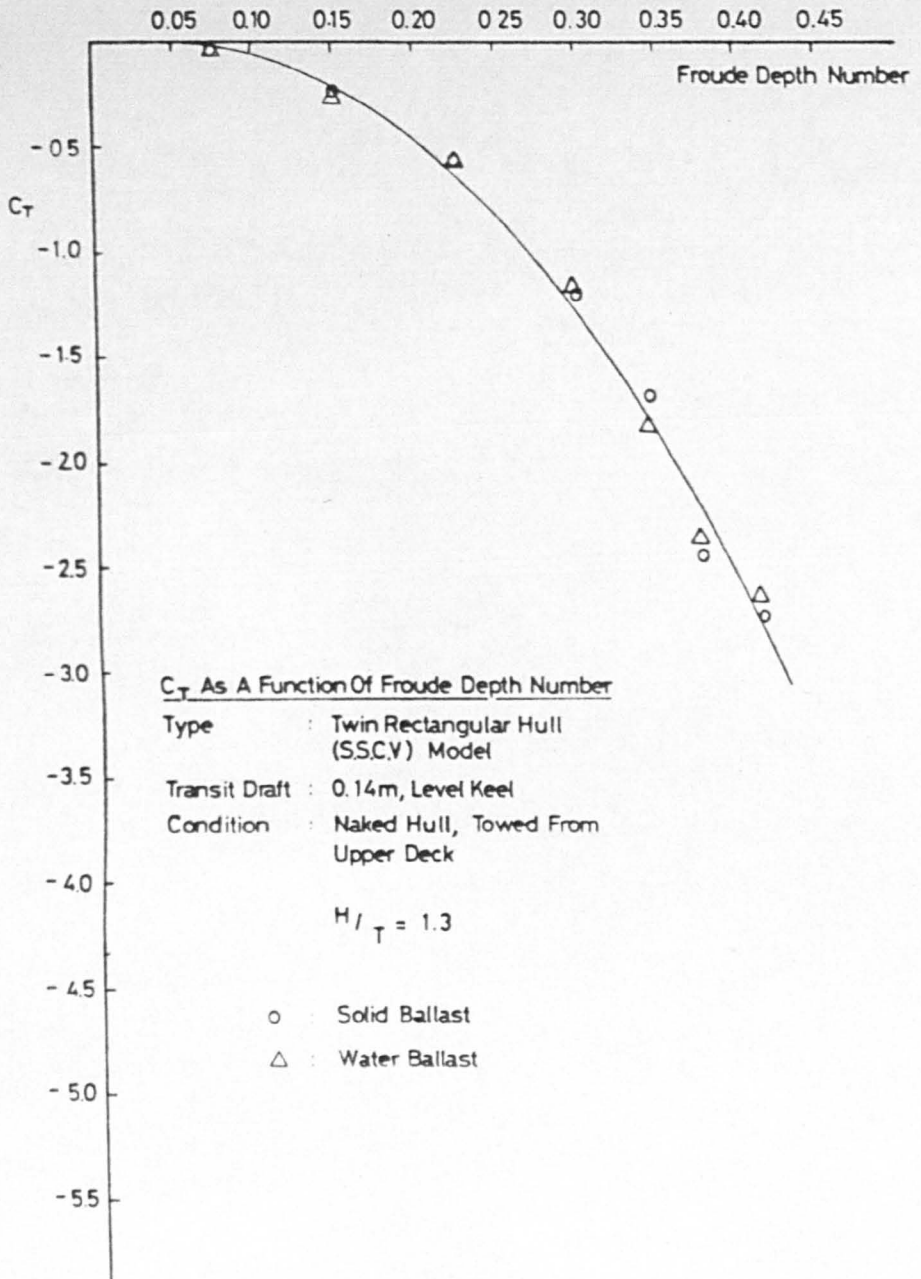

Figure 70

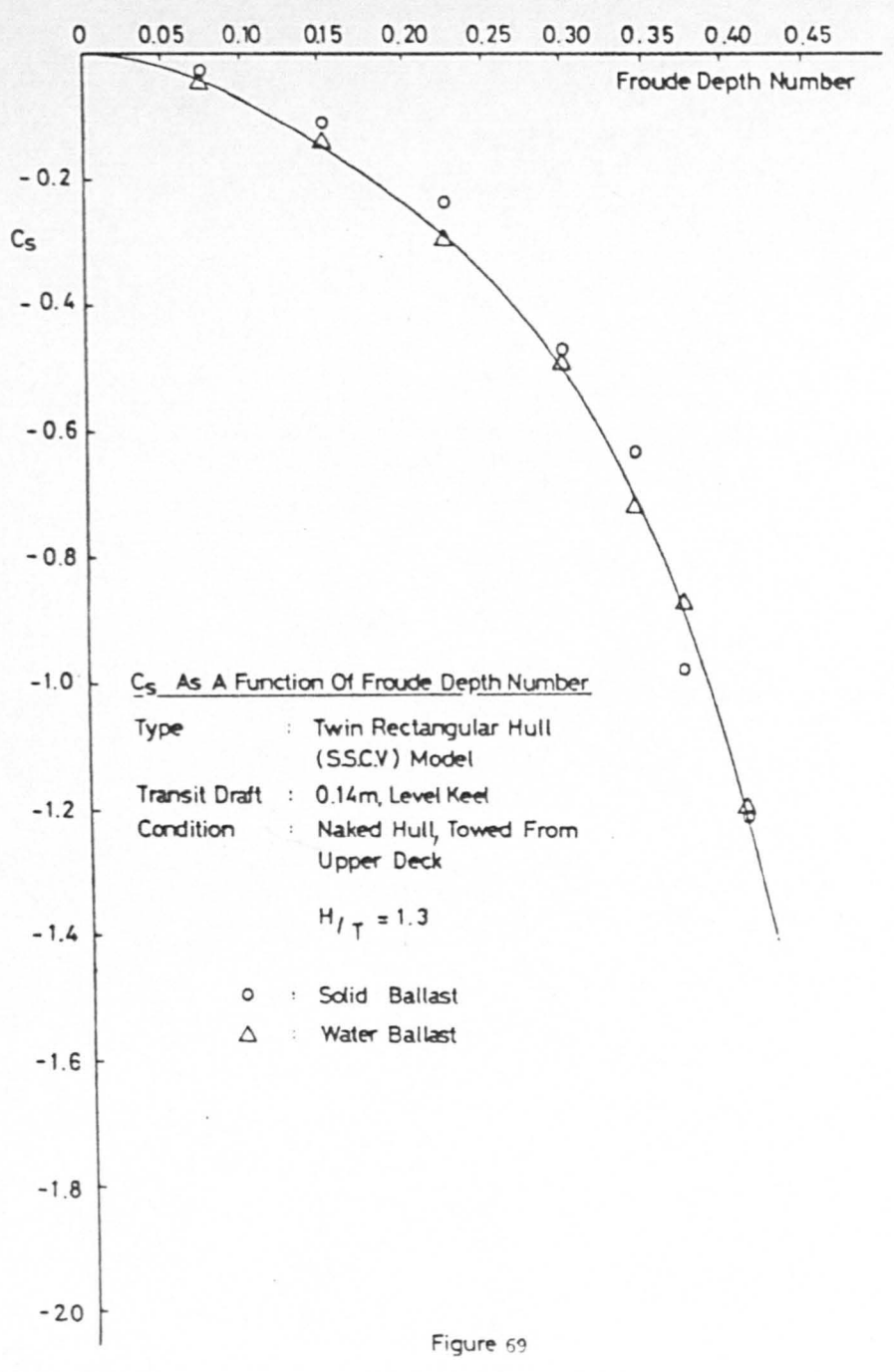

Figure 69

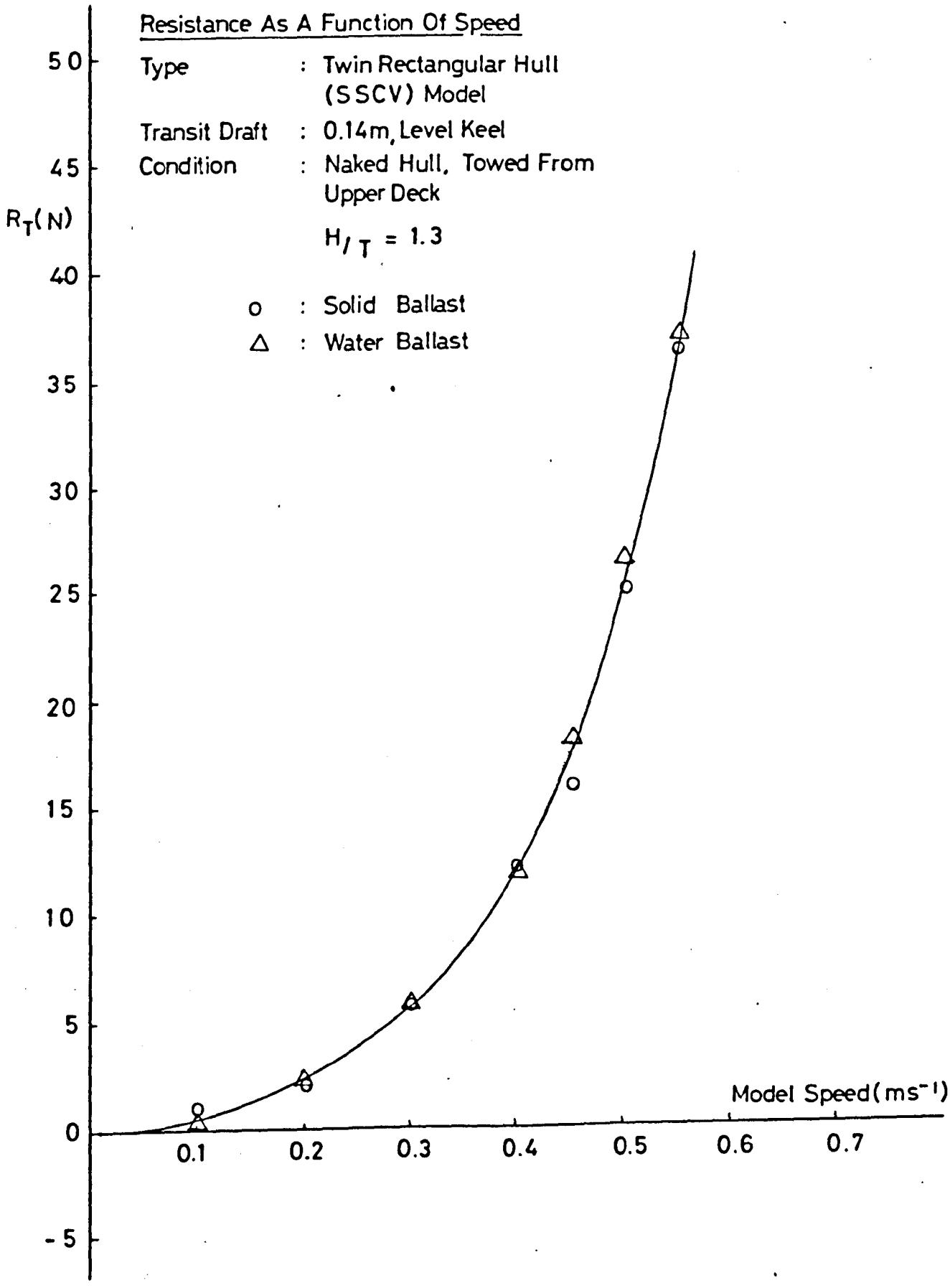
Resistance As A Function Of Speed
Type : Twin Rectangular Hull (SSCV) Model
Transit Draft : 0.14m, Level Keel
Condition : Naked Hull, Towed From Upper Deck
H/T = 1.3
o : Solid Ballast
△ : Water Ballast
RT(N)
50
45
40
35
30
25
20
15
10
5
0
-5
0.1
0.2
0.3
0.4
0.5
0.6
0.7
Model Speed(ms⁻¹)

Figure 71

CHAPTER 6

Multi-hull Aspects with Practical Implications

There is no practical method for obviating multi-hull full-scale sinkage and trim and the normal approach is to either accept it with a continous indication of its extent or attempt to minimise it. A number of possible options for minimising the squat and the resulting effect on the total measured resistance are examined in this chapter. These are the effect of hull spacing, shape of hull endings and the effect of a control surface to counter the trim underway.

(6.1) The Influence of Hull Separation

This section examines the effects of splitting a hull into a catamaran configuration and of varying the hull spacing on the deep water sinkage, trim and resistance of a bluff, twin-hulled model, Fig.72, in the transit draught condition, at steady speed.

(6.1.a) Catamaran Interference Effects

Catamaran hydrodynamics are complicated by interference effects between the demi-hulls. There are

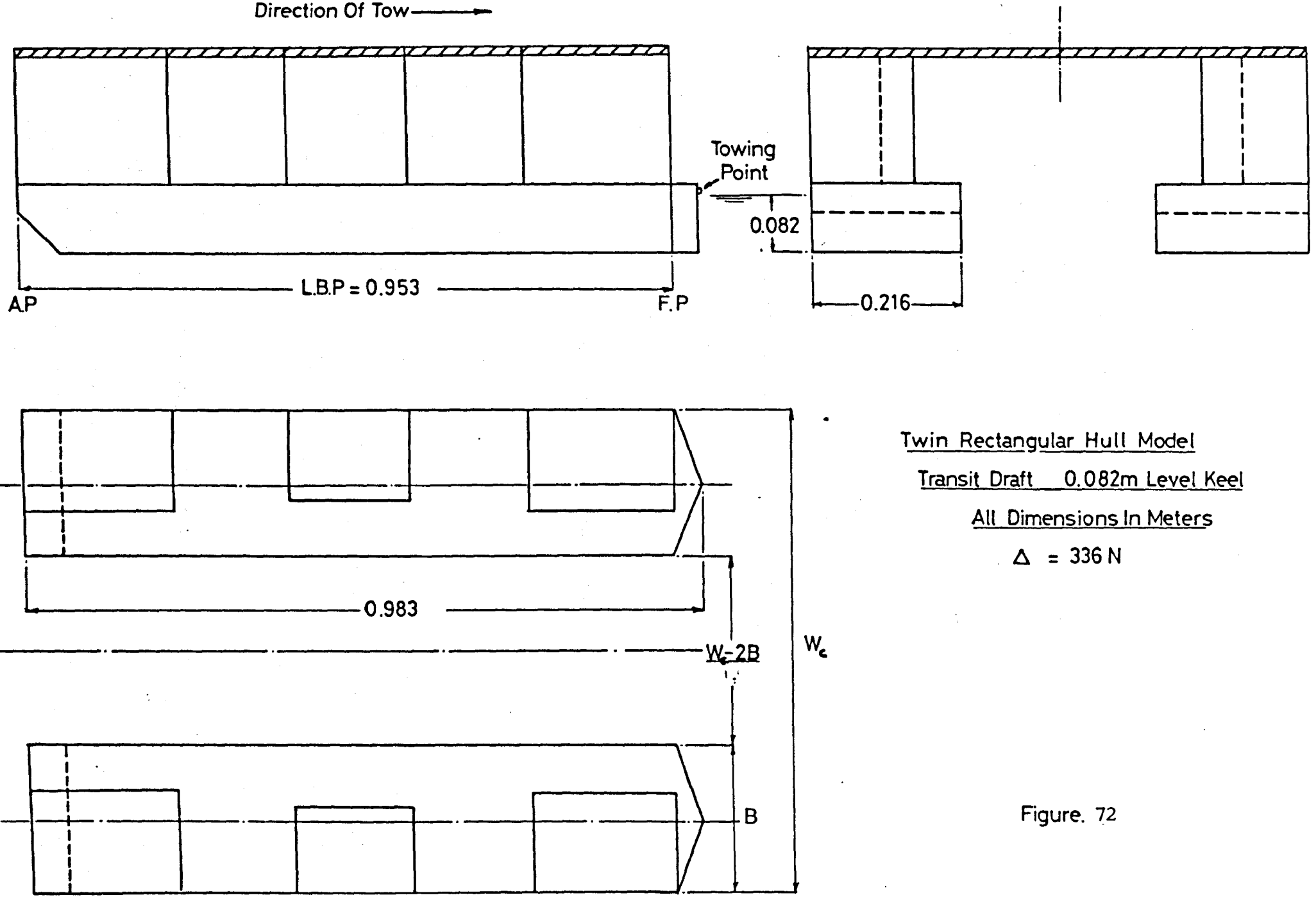

Twin Rectangular Hull Model

Transit Draft 0.082m Level Keel

All Dimensions In Meters

Δ = 336 N

Figure. 72

basically two types of interference, namely body (or displacement) interference and wave interference.

Wave interference arises due to the superposition of the two wave systems (one from each demi-hull) and these may reinforce or cancel each other partially. This will increase and reduce the wave resistance, respectively. Considering the theory, see Seren [66], it is found that the wave making resistance of the catamaran hull, R_w, is the sum of twice the resistance of a demi-hull, R_{wd}, and a resistance increase or decrease due to the interference between the wave systems of the demi-hulls, $2R_{wi}$, Namely,

$$R_w = 2R_{wd} + 2R_{wi}$$

where

$$R_{wd} = \frac{\pi\rho U^2}{4} \int_0^{\pi/2} [S(\theta)^2 + C(\theta)^2]\cos^3\theta d\theta$$

$$R_{wi} = \frac{\pi\rho U^2}{4} \int_0^{\pi/2} [S(\theta)^2 + C(\theta)^2]\cos(K_o\bar{y}\sin\theta\cos\theta)\cos^3\theta d\theta$$

and $S(\theta)$, $C(\theta)$ are amplitude factors of the sine and cosine wave components, respectively, which depend on the hull form and speed, $K_o = g/U^2$, and $\bar{y}$ is the transverse hull spacing.

It may be observed that the interference expression includes the hull spacing as a parameter and it is, therefore, of interest to consider it further. If $K_o y$ (in the argument of the cosine) tends to zero, that is the

speed is very high or the hull spacing very small, $\cos(K_o\bar{y}\ \sin\theta\ \cos\theta\ )$ tends to one and the wave resistance becomes 4 times that of a demi-hull. If, however, $K_o y$ tends to infinity, that is, ship speed is very low or the hull spacing very large, $\cos(K_o\bar{y}\ \sin\theta\ \cos\theta\ )$ tends to zero and the wave resistance becomes twice that of a demi-hull. In between the two extremes, the interference term may become negative, thus decreasing the wave resistance. Favourable wave interference is normally found to occur within a narrow range of speeds, and is influenced by the hull form and transverse spacing. The latter shift the F_L numbers at which beneficial interference occurs.

The applicability of the Michell-Havelock linearised wave resistance theory to the bluff demi-hull form was examined by comparing the theoretically derived wave resistance to the residual values obtained experimentally, by Seren [66]. The theory significantly overestimates the experiment, indicating that it cannot be considered reliable for the bluff form over the low speed range examined. This is due to a combination of theoretical limitations (for example, the inherent neglect of viscosity) and the difficulty in identifying the residual resistance with the actual wave resistance component owing to the high form drag.

At low speeds, for full forms it is apparent that body interference will be the dominating factor and account for any changes in the resistance, sinkage and trim. Body

interference is the result of the change in flow over one demi-hull due to the presence of the other. The subject of flow interference is complex and may be classified in many categories; separated and unseparated flows, steady and and time dependent flows, partial (i.e. affecting only one body) or mutual interference in all types of flows, etc. Careful reviews of bluff body interference, such as between two circular cylinders in various arrangements, have been presented by Zdravkovich [89] and ESDU [26], where extensive lists of references may be found. In the following, interference between two similar-sized bluff cylinders arranged side-by-side to the approaching flow is discussed. The flow is assumed steady, separated and subcritical in terms of the R_N .

Bluff body interference may be viewed as the result of the wake of one body influencing the force on another. Bodies spaced (where the spacing is measured between the centres of the two bodies) 5 diameters apart or more, have practically no interference. The interference drag increases gradually with the reduction in spacing but only down to a spacing of 2.2 diameters. Instead of rapidly increasing for spacings less than 2.2 diameters, the drag varies between a wide range of positive and negative values, i.e. the flow is bistable. This is the most striking feature of the side-by-side arrangement and is in spite of the fact that the geometrical arrangement is symmetrical with respect to the flow. For transverse spacings of 1.1 to 2.2 body diameters, the wakes of the two

cylinders are alternatingly entrained by each other. Consequently, wide and narrow wakes are formed behind the cylinders and give rise to changes in the base pressure of both cylinders from one steady value to another, fluctuating between the two extremes. The bistable nature of the flow was first observed by Biermann and Herrnstein [8], who noted that the flow may change from one type to another, even while the transverse spacing is held constant. This may give rise to severe vibrations and, therefore, such critical arrangements are normally avoided.

An interesting feature of the interference measured between two cylinders is that the sum of the bistable high and low drag is always less than twice the drag of a single cylinder. Moreover, the gap flow, biased to one side, produces a resultant (repulsive) force which is deflected relative to the free stream direction. As a result, there is a component of force acting perpendicular to the free stream direction (termed the "lift" force) which will be responsible for a side force and flow across the keel of each hull. This cross-flow appears to be negligible at low speeds and normal hull spacings, see Mizayawa [50]. At spacings less than 1.1 diameters the interference drag appears to increase very rapidly with decrease in spacing.

The results for the staggered arrangements show that the upstream and downstream cylinders may be subjected to significantly different "lift" and drag forces. Depending on their relative position or orientation to the flow, the

two cylinders may experience a negligible or strong "lift" force and reduced or enhanced drag force. It has been argued, see Zdravkovitch [89], that the bistable side-by-side arrangement represents a transition from the upstream to the downstream stagger.

At present, there appears to be little or no data on wake interaction, votex shedding frequencies and lift and drag forces on cylinders for R_N larger than about 2×10^5 . Very little is known about the existence of the biased flow and its bistable nature in the post-crtical flow regime. Since past research has concentrated largely on circular cylinders, there is little data on interference between side-by-side bodies with fixed separation points. It is to be expected that the wake behind a single cylinder will be narrower in supercritical flow compared with the subcritical regime. This will cause a contraction of the "interference boundary", which is defined as a line along which the "lift" force becomes zero. Further research is necessary to determine whether any other changes occur and affect the above discussed qualitative and quantitative behaviour at post-crtical R_N .

(6.1.b) The "Equivalent Mono-hull" Concept

In order to obtain some insight into the effect of splitting the mono-hull into demi-hulls, the catamaran was also tested with no gap between the hulls. The resulting "equivalent mono-hull" was then of the same length,

displacement and form aft but a slightly altered bow form.

It is common practice to introduce an "interference drag coefficient", defined as the difference between the drag coefficient measured on one of the bodies in the (side-by-side, tandem or staggered) arrangement and the drag coefficient of the single body at the same R_N, see Biermann and Herrnstein [8]. The combined interference drag is obtained by adding the interference drag coefficients of both bodies. The combined interference drag is then examined by comparison to twice that of a single body. A similar practice stems from the requirements of the linearised wave resistance theory, where the catamaran resistance is referred to twice that of its demi-hull (or the resistance of a catamaran with infinite hull spacing). This is a practical but not realistic procedure which is entirely arbitrary. Reservations must apply to this practice because the slenderness of the 2 demi-hulls may cause a reduction such that their combined effect is different from that of a double-beam "equivalent" mono-hull.

In the present study, the results were evaluated by comparison to the double beam mono-hull. This is also because the unstable demi-hull makes it impossible to measure its resistance, sinkage and trim in practice. However, the resulting form is somewhat unrealistic since in practice the twin-bow volume would need to be redistributed differently. It is expected that such a

modification will not affect the mean sinkage to any measurable extent since it is dominated by the parallel mid-body. Trim will not be affected significantly because for bluff forms it is predominantly determined by viscous effects, particularly the wake. These are largely determined by the blunt forward and aft "shoulders" of the SSCV and occur sufficiently far downstream not to be affected. Consequently, it is hypothesised that the overall effect will be such as not to affect the general conclusions which follow.

(6.1.c) Splitting the "Equivalent Mono-hull"

As the surface area of the catamaran is normally greater than that of the "equivalent mono-hull" it is to be expected that its resistance at low speeds will also be greater. This is difficult to detect experimentally, since for bluff forms it is obscured by the large form resistance. Fig.73 shows the "equivalent mono-hull" measured resistance superposed on the catamaran resistance at three hull spacings. At lower speeds, $F_L < 0.15$, where F_L is based on the hull length, no changes are detected by measurement. In the higher speed range, the mono-hull resistance is greater than the catamaran resistance. That is, the catamaran arrangement is advantageous in comparison to the "equivalent mono-hull" in this speed range.

When measured between the two hull centrelines, the spacings employed were, 3.63, 2.32 and 1.66 times the hull

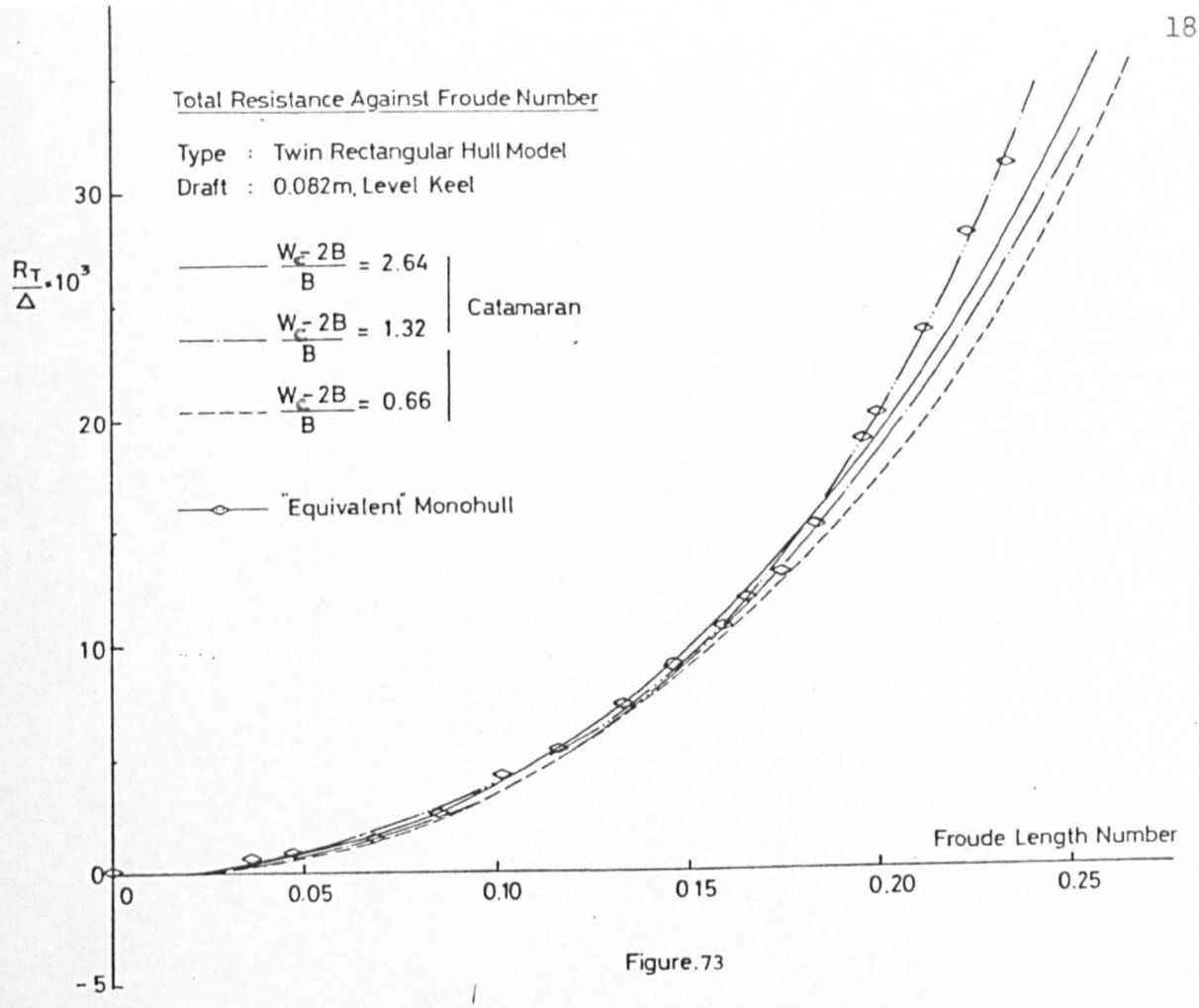

Figure.73

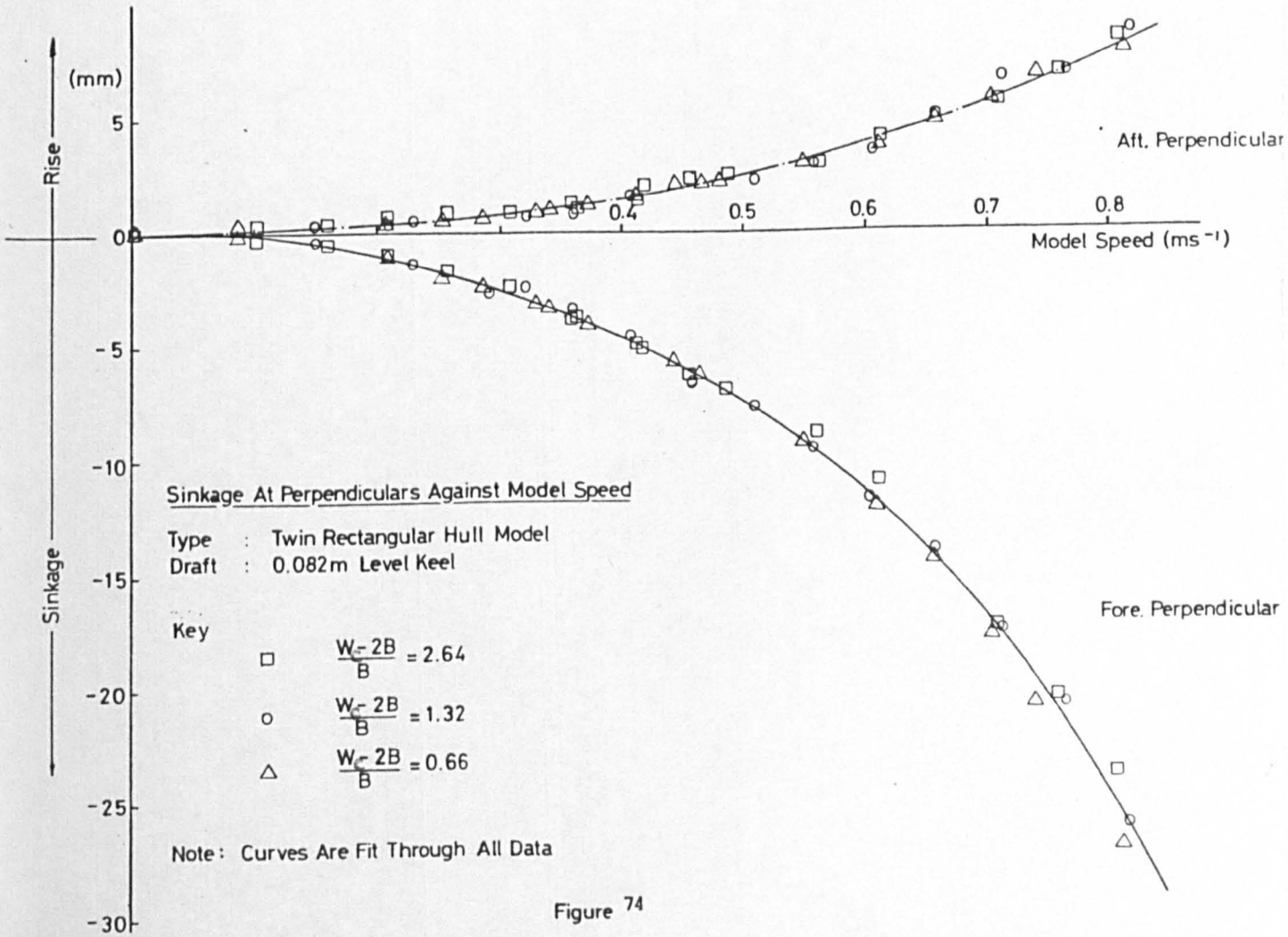

Figure 74

breadth. That is, outside, bordering on and inside the bistable region, as determined by experiments on bluff cylinders. However, no bistable type of behaviour was observed throughout the present experiments, with the highest R_N (based on the hull length) about 5×10^5. In fact, the exhibited behaviour is more common to that of streamlined struts than that of bluff cylinders. For the former, no bistable behaviour has been observed, see Biermann and Herrnstein [8]. The interference drag between two streamlined struts increases gradually with a decrease in spacing down to a spacing of about 2.5 diameters. For spacings less than 2.5 diameters, the interference increases rapidly with the decrease in spacing down to some spacing which is difficult to determine in wind tunnels owing to excessive vibration. The most reasonable explanation for this type of interference behaviour must be that the modifications induced by the separated flow on the bluff elongated demi-hull are such that the demi-hull and separated flow combine to form a more streamlined shape, which does not produce the oscillating pattern of vortices observed on cylinders.

Figs.74-76 show the effect on the measured sinkages at the perpendiculars and the non-dimensional sinkage and trim. The effect of splitting the hull into two demi-hulls causes a significant reduction in both, which implies a reduction in both frictional and form resistance. These results imply that there may be additional advantages in operating catamarans where water-depth is restricted. Any

penalties incurred by the resistance may then be minimised by aiming at a minimum B/T ratio, so that the surface area is minimised and by minimising interference effects.

(6.1.d) The Effect of Hull Separation

It may be observed from Figs.75,76 that varying the hull spacing has no significant effect on the mean sinkage or trim coefficient over the range of speeds tested. This implies that no measurable changes in form resistance occur at the spacings and speeds examined. Any increase in resistance is then probably due to interference effects.

It is pertinent to obtain some measure of the magnitude of the velocity increase due to body interference. This may be approximated by considering the flow around a pair of infinite circular cylinders and comparing the results to those of a single cylinder, see Mizayawa [50]. Although there will be differences between the actual catamaran hull form and and that of two cylinders in a side-by-side arrangement, it is suggested by Mizayawa that the approach will provide a good approximation to the mean velocity increment. Neglecting wave interference and introducing a parameter **e** where,

$$e = \frac{1}{\left(1 + \left(\frac{W_c - 2B}{B}\right)\right)} \quad \text{and } e < 1 \qquad \ldots\ldots (6.1.1)$$

where W_c is the total catamaran breadth and B the demi-hull breadth. The mean velocity increment on one cylinder

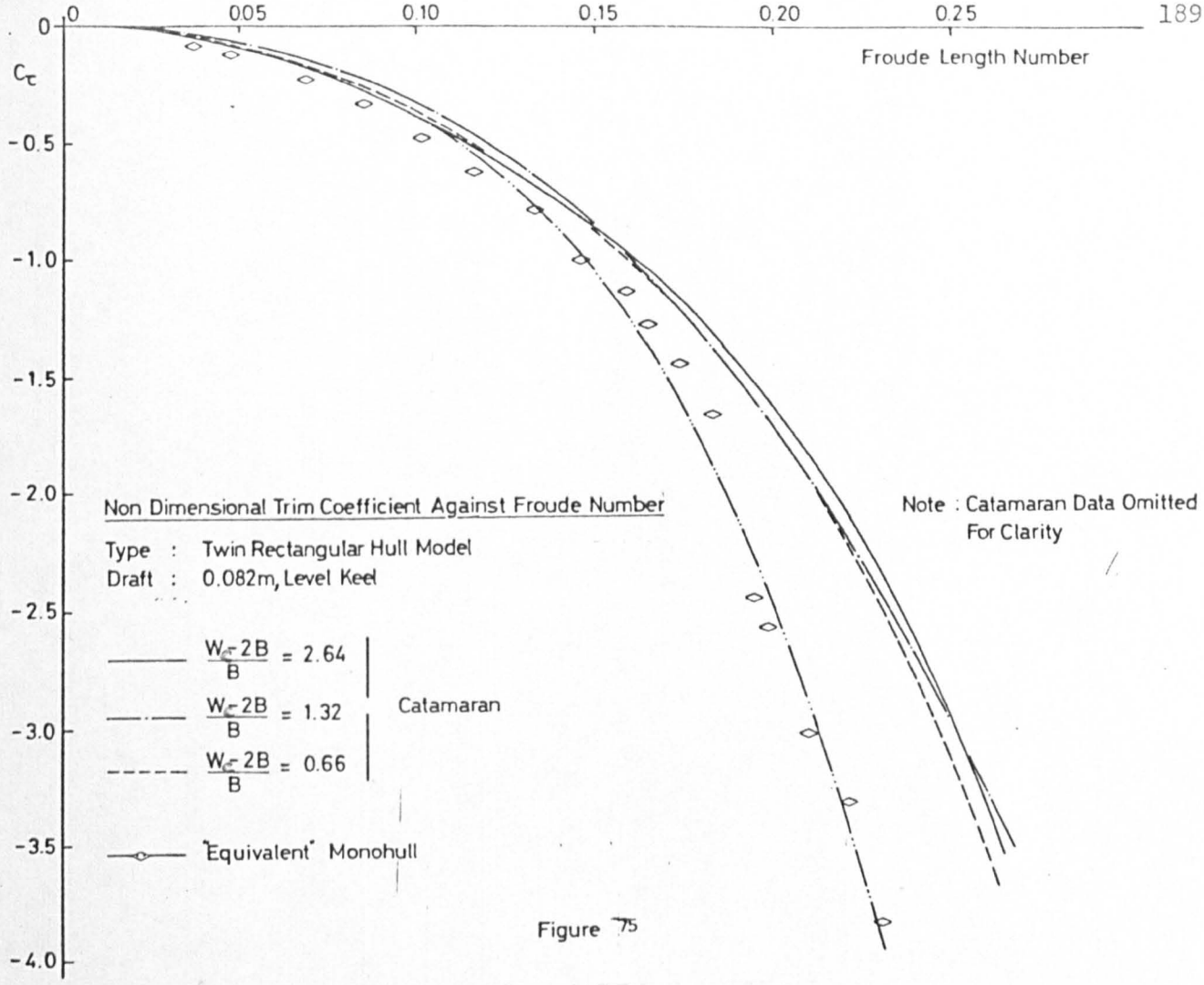

Figure 75

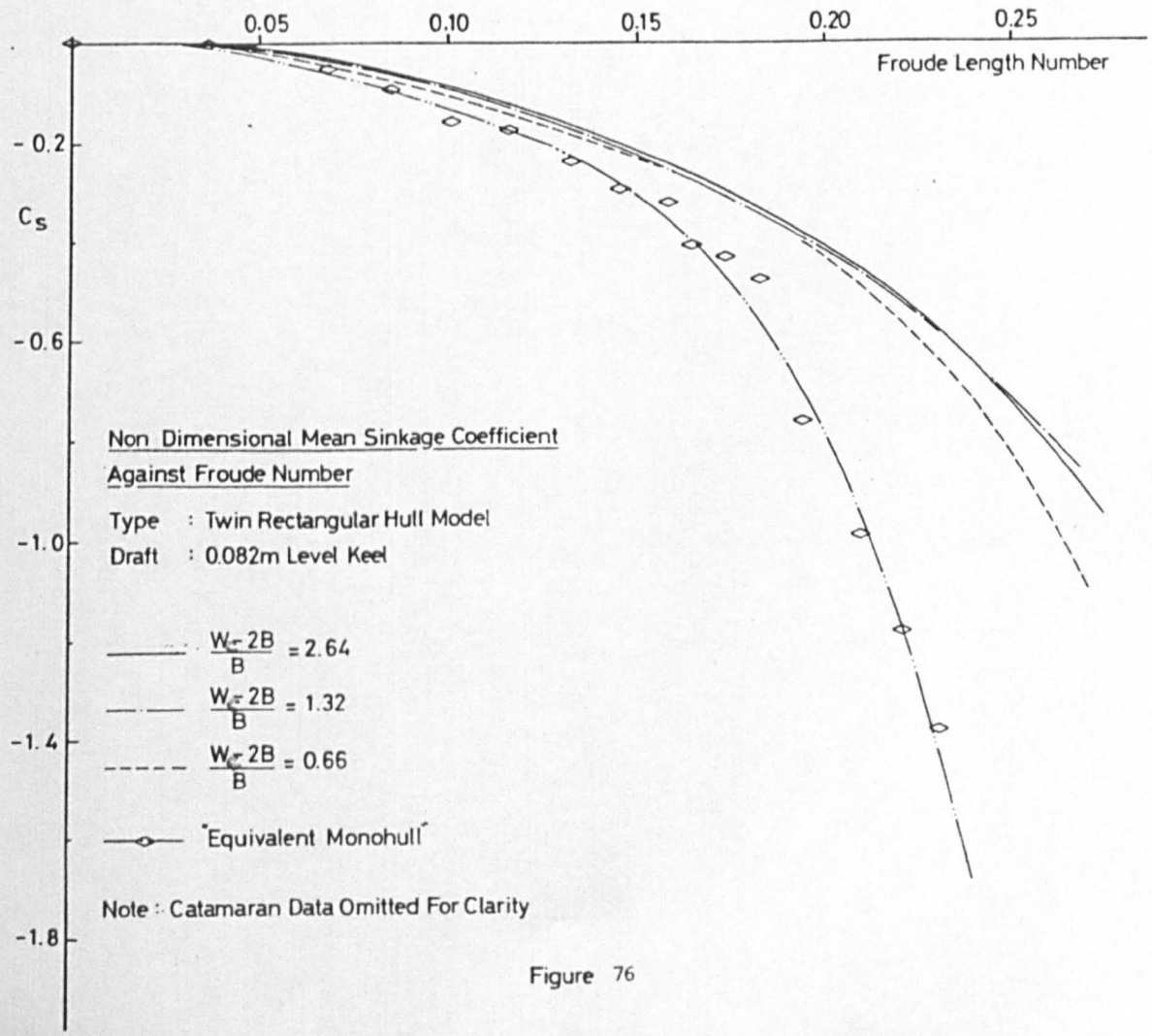

Figure 76

surface due to the presence of the other is $(e^2/4)U$, where U is the catamaran uniform speed. Assuming that the viscous resistance is proportional to the velocity squared then,

$$R_{vc} = (1 + \frac{e^2}{4})^2 2R_{vd} \quad \ldots\ldots (6.1.2.a)$$

$$= (1 + \frac{e^2}{2}) 2R_{vd} \quad \ldots\ldots (6.1.2.b)$$

where the subscripts "vc" and "vd" denote viscous catamaran and viscous demi-hull, respectively.

Expressions (6.1.2) themselves indicate that the resistance of the twin-hulled catamaran will be more than twice that of a demi-hull. This assumption has been confirmed at low speeds by wake surveys and wake pattern and velocity measurements between the demi-hulls by Mizayawa [50], who notes that the assymetrical property of the velocity field around each demi-hull has less influence on the resistance than the mean velocity augmentation. When applied to the 3 hull spacings examined, the procedure yields the values presented in Table 23 and confirms the experimental results of Fig.73. At higher speeds, $F_L > 0.15$, it is probable that the relatively large demi-hull breadth creates a wave resistance component.

Spacing Ratio	Velocity Increase	Resistance Increase	% Resistance Change Between Spacings
$(W_c-2B)/B$	$(1+\varepsilon^2/4)$	$(1+\varepsilon^2/2)$	/
0.66	1.09	1.18	---
			8.3
1.32	1.05	1.09	---
			4.8
2.64	1.02	1.04	---

Table 23: Mean velocity increment due to interference

(6.2) The Influence of the Hull-Endings Shape

One of the principal means of improving SWATH performance is by reducing the hydrodynamic drag. Such reductions may be effected by a number of advanced techniques, i.e. polymer additives, surface suction etc. or solely by proper shaping of the body.

Examination of model tests in the region $10^4 < R_N < 10^5$ suggest that the resistance of the SWATH design could be reduced by the adoption of ellipsoidal hull endings, see Smith [68]. This is supported by research into torpedo design and bodies of revolution, which has shown that elliptic sections are less susceptible to separation and cavitation abaft the head portion and almost as easy to fabricate. Any changes in drag are strongly linked with changes in the flow pattern and will affect the squatting behaviour.

This section presents an evaluation of the effect of changing the present hemispherical bow and conical stern sections, Fig.42, to ellipsoidal form. The shallow-water sinkage, trim and resistance of the SWATH are examined in order to determine whether the advantages outweigh the disadvantages inherent in the increase in wetted surface area and length, particularly at low speeds. In the process the pressure distribution over the hemispherical and ellipsoidal hull endings is calculated using Landweber's potential-flow method and the stimulation

problem discussed.

(6.2.a) The Ellipsoidal Hull-Endings

Fig.77 illustrates the ellipsoidal hull-endings used both forward and aft. The hull endings were constructed of perspex, similar to the SWATH model. The ellipse has an axis ratio of 1.67, the hemisphere a ratio of 1.0. The modification yielded cigar shaped hulls, symmetrical with respect to the (longitudinal and transverse) hull axis, rendering a more hydrodynamically efficient body.

The stimulation problems posed by this modification are of some importance. Comparative tests without stimulators may be misleading as the pressure gradients are altered and changes attributed to change in shape may be purely stimulation effects.

The pressure distribution is one of the most important factors governing the boundary-layer growth and development over the body. It is mainly determined by the potential-flow, with modifications arising from the boundary-layer particularly over the stern region. Near the tail, viscosity effects assume importance as the ratio of boundary-layer thickness to body radius becomes progressively larger and increasingly diverges from estimates based on ideal-fluid theories. The presence of adverse pressure gradients (or large R_N) tends to promote transition by increasing the instability of the laminar

boundary-layer and accelerating the amplification of the Tolmien-Schlichting disturbance waves, see Schlichting [59]. A negative pressure gradient is termed favourable and a positive pressure gradient adverse in connection with preventing separation.

(6.2.b) Bow Pressure Distribution by Landweber's Method

A number of potential-flow methods of varying complexity have been developed for calculating the pressure distribution on a body in uniform axial flow. That employed is due to Landweber [43] and was obtained by applying Green's theorem to the solution of the boundary value problem for the velocity potential, resulting in a Fredholm equation of the first kind for the unknown velocity distribution on the body surface. The mathematical formulation, derivation of the integral equations and the proposed closed-body iterative solution of the method used, are given by Landweber in the above reference and are not dwelt upon here.

Landweber's solution was subsequently extended to deal with the case of an infinite parallel sided body by Albone [3], who showed that there is no difficulty in obtaining solutions even with irregular body geometry (multi-stage rockets, for instance) and to deal equally well with sharp and blunt nosed bodies. Landweber's calculation method and the extension described by Albone, were used to construct computer programs which permit the prediction of the

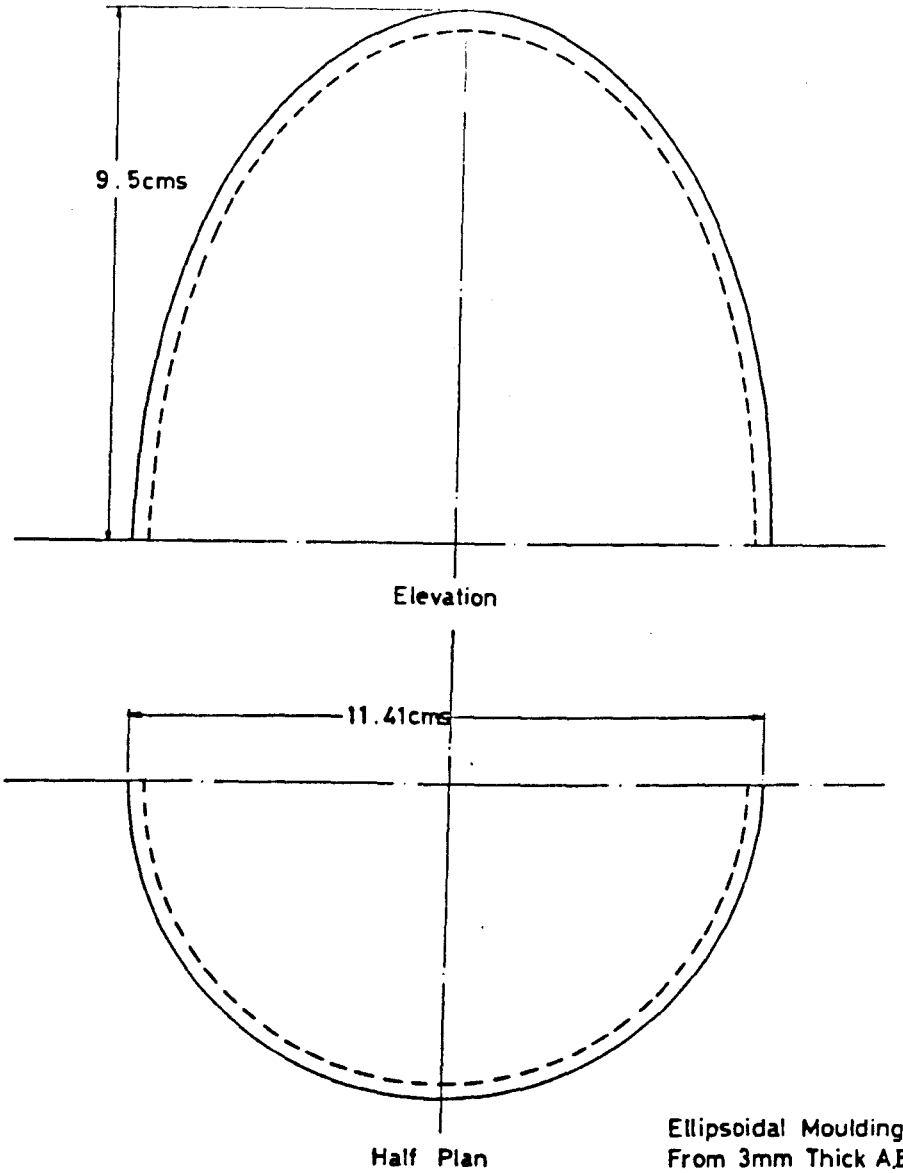

Ellipsoidal Mouldings
From 3mm Thick A,B,S
With Smooth Outer Surface

Fig 77

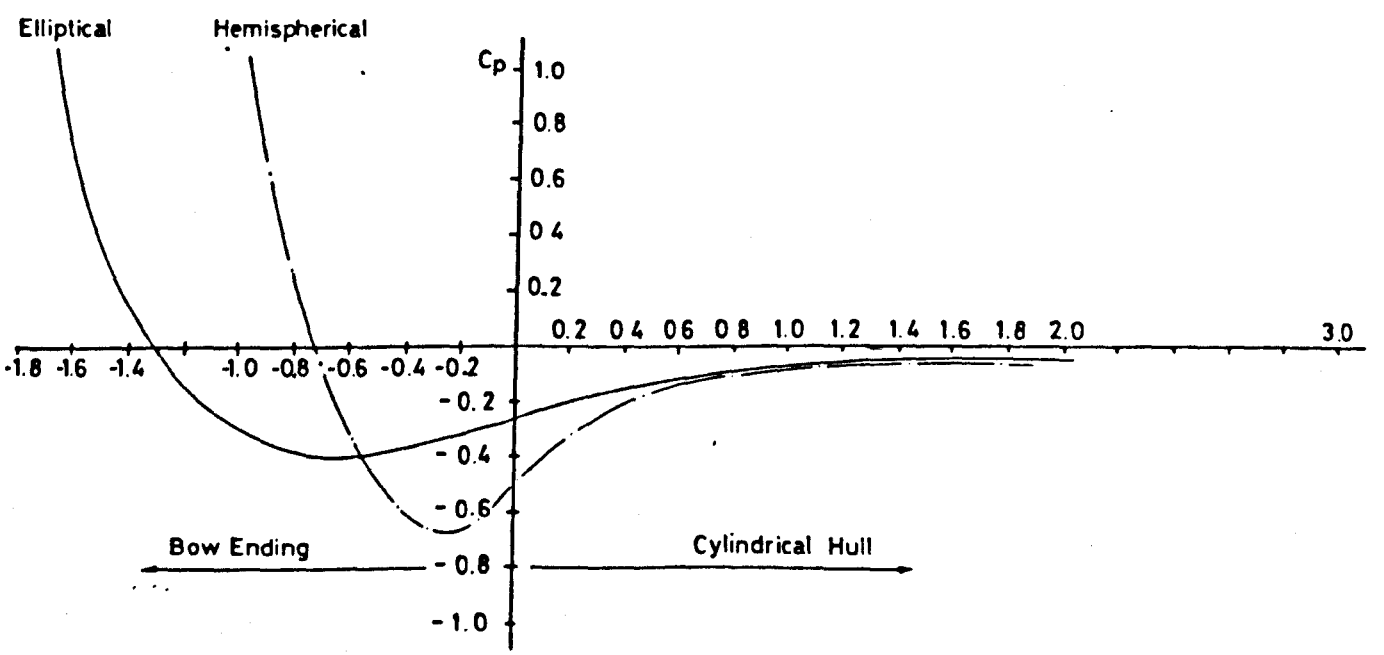

Pressure Distribution Along Hemispherical /Elliptical
Using Landwebers Method

Fig 78

NO. OF ITERATIONS = 16 MAX ERROR = 0.9984124E-03

X	Y	DY/DX	VELOCITY	PRESS. COEFF
-0.99845	0.055714	17.920813	0.0812	0.9934
-0.99183	0.127535	7.776976	0.1860	0.9654
-0.98001	0.198944	4.926074	0.2902	0.9158
-0.96310	0.269144	3.578385	0.3924	0.8460
-0.94128	0.337626	2.787937	0.4919	0.7580
-0.91478	0.403946	2.264617	0.5885	0.6537
-0.88389	0.467697	1.889874	0.6811	0.5360
-0.84893	0.528513	1.606252	0.7691	0.4084
-0.81026	0.586066	1.382545	0.8519	0.2743
-0.76831	0.640075	1.200346	0.9288	0.1373
-0.72352	0.690307	1.048109	0.9993	0.0014
-0.67635	0.736578	0.918236	1.0629	-0.1297
-0.62732	0.778763	0.805532	1.1190	-0.2523
-0.57693	0.816790	0.706344	1.1675	-0.3630
-0.52574	0.850648	0.618042	1.2080	-0.4592
-0.47426	0.880383	0.538702	1.2405	-0.5389
-0.42307	0.906099	0.466908	1.2653	-0.6010
-0.37268	0.927959	0.401614	1.2828	-0.6456
-0.32365	0.946178	0.342058	1.2936	-0.6734
-0.27648	0.961019	0.287698	1.2986	-0.6864
-0.23169	0.972790	0.238168	1.2988	-0.6868
-0.18974	0.981835	0.193247	1.2952	-0.6774
-0.15107	0.988522	0.152829	1.2888	-0.6611
-0.11611	0.993236	0.116902	1.2808	-0.6406
-0.08522	0.996362	0.085528	1.2721	-0.6183
-0.05872	0.998275	0.058821	1.2635	-0.5964
-0.03690	0.999319	0.036925	1.2556	-0.5766
-0.01999	0.999800	0.019993	1.2491	-0.5603
-0.00817	0.999967	0.008166	1.2443	-0.5484
-0.00155	0.999999	0.001553	1.2416	-0.5415
0.00156	1.000000	0.000000	1.2403	-0.5383
0.00823	1.000000	0.000000	1.2375	-0.5313
0.02040	1.000000	0.000000	1.2324	-0.5187
0.03831	1.000000	0.000000	1.2249	-0.5004
0.06238	1.000000	0.000000	1.2149	-0.4760
0.09316	1.000000	0.000000	1.2024	-0.4457
0.13136	1.000000	0.000000	1.1871	-0.4093
0.17796	1.000000	0.000000	1.1693	-0.3673
0.23417	1.000000	0.000000	1.1491	-0.3204
0.30155	1.000000	0.000000	1.1270	-0.2702
0.38214	1.000000	0.000000	1.1041	-0.2191
0.47852	1.000000	0.000000	1.0819	-0.1705
0.59409	1.000000	0.000000	1.0624	-0.1286
0.73330	1.000000	0.000000	1.0474	-0.0971
0.90210	1.000000	0.000000	1.0382	-0.0778
1.10853	1.000000	0.000000	1.0337	-0.0685
1.36370	1.000000	0.000000	1.0311	-0.0631
1.68326	1.000000	0.000000	1.0269	-0.0545
2.08978	1.000000	0.000000	1.0202	-0.0407
2.61686	1.000000	0.000000	1.0141	-0.0284
3.31615	1.000000	0.000000	1.0127	-0.0255
4.27046	1.000000	0.000000	1.0106	-0.0213
5.61924	1.000000	0.000000	1.0053	-0.0106
7.61243	1.000000	0.000000	1.0009	-0.0017

Table 24 - Hemispherical Ending

NO. OF ITERATIONS = 9 MAX ERROR = 0.9005232E-03

X	Y	DY/DX	VELOCITY	PRESS. COEFF
-1.66741	0.056035	10.669271	0.1164	0.9864
-1.65636	0.127675	4.651572	0.2620	0.9313
-1.63662	0.199034	2.948302	0.3997	0.8402
-1.60838	0.269211	2.142137	0.5256	0.7237
-1.57194	0.337679	1.669100	0.6386	0.5922
-1.52769	0.403990	1.355861	0.7375	0.4561
-1.47609	0.467736	1.131527	0.8226	0.3234
-1.41771	0.528547	0.961731	0.8949	0.1992
-1.35314	0.586097	0.827798	0.9559	0.0863
-1.28308	0.640103	0.718713	1.0069	-0.0138
-1.20827	0.690333	0.627564	1.0493	-0.1011
-1.12951	0.736603	0.549804	1.0843	-0.1756
-1.04762	0.778786	0.482323	1.1128	-0.2382
-0.96348	0.816812	0.422934	1.1355	-0.2894
-0.87798	0.850669	0.370062	1.1532	-0.3299
-0.79202	0.880403	0.322557	1.1663	-0.3603
-0.70652	0.906119	0.279570	1.1752	-0.3811
-0.62238	0.927979	0.240474	1.1803	-0.3932
-0.54049	0.946197	0.204814	1.1820	-0.3972
-0.46173	0.961037	0.172265	1.1809	-0.3945
-0.38692	0.972809	0.142608	1.1773	-0.3861
-0.31686	0.981853	0.115711	1.1720	-0.3737
-0.25229	0.988540	0.091509	1.1656	-0.3586
-0.19391	0.993254	0.069997	1.1586	-0.3424
-0.14231	0.996380	0.051212	1.1517	-0.3263
-0.09806	0.998293	0.035220	1.1452	-0.3114
-0.06162	0.999337	0.022110	1.1395	-0.2985
-0.03338	0.999818	0.011971	1.1350	-0.2882
-0.01364	0.999985	0.004890	1.1317	-0.2808
-0.00259	1.000017	0.000930	1.1299	-0.2766
0.00156	1.000000	0.000000	1.1292	-0.2750
0.00823	1.000000	0.000000	1.1281	-0.2725
0.02040	1.000000	0.000000	1.1260	-0.2679
0.03831	1.000000	0.000000	1.1230	-0.2612
0.06238	1.000000	0.000000	1.1190	-0.2522
0.09316	1.000000	0.000000	1.1139	-0.2408
0.13136	1.000000	0.000000	1.1077	-0.2270
0.17796	1.000000	0.000000	1.1003	-0.2107
0.23417	1.000000	0.000000	1.0918	-0.1921
0.30155	1.000000	0.000000	1.0822	-0.1712
0.38214	1.000000	0.000000	1.0718	-0.1488
0.47852	1.000000	0.000000	1.0610	-0.1258
0.59409	1.000000	0.000000	1.0504	-0.1034
0.73330	1.000000	0.000000	1.0408	-0.0834
0.90210	1.000000	0.000000	1.0330	-0.0670
1.10853	1.000000	0.000000	1.0272	-0.0551
1.36370	1.000000	0.000000	1.0231	-0.0468
1.68326	1.000000	0.000000	1.0198	-0.0400
2.08978	1.000000	0.000000	1.0161	-0.0324
2.61686	1.000000	0.000000	1.0124	-0.0250
3.31615	1.000000	0.000000	1.0112	-0.0226
4.27046	1.000000	0.000000	1.0095	-0.0192
5.61924	1.000000	0.000000	1.0048	-0.0096
7.61243	1.000000	0.000000	1.0007	-0.0015

Table 25 - Elliptical Ending

pressure distribution on both closed and semi-infinite bodies (programs CLOSED and INFINITE, respectively).

The distribution of the pressure coefficient along the surface of the ellipsoidal and hemispherical cylinders used in the experiment, is shown in Fig.78 and the appropriate computer output using INFINITE presented in Tables 24,25. As could be expected, the magnitude of the suction peaks and the subsequent adverse pressure gradients increase significantly with increasing fore-body fullness.

The above pressure distributions are in good agreement with those obtained using the Hess and Smith potential-flow method, illustrated by McCarthy [47]. By employing the corresponding distribution of laminar boundary layer pressure gradient parameter, denoted by γ , and the Curle-Skan-modified-Thwaites criterion [15] (i.e. $\gamma = -0.09$ at separation), the above reference predicts the onset of transition owing to laminar separation in the range of bow-entrance length/diameter ratios of Fig.79 and confirms its occurence experimentally over the range $10^6 < R_N < 10^7$. Fig.79 also demonstrates that the separation occurs at different distances from the bow and in order to move the transition position of both into line, turbulence stimulation is required, particularly in the lower range of R_N examined. 1.5mm. trip wires were used on the hulls and struts in accordance with section (5.3.a). The trip-wire ring used on both the elliptical and hemispherical fore-bodies was placed at a distance of 0.022m from the

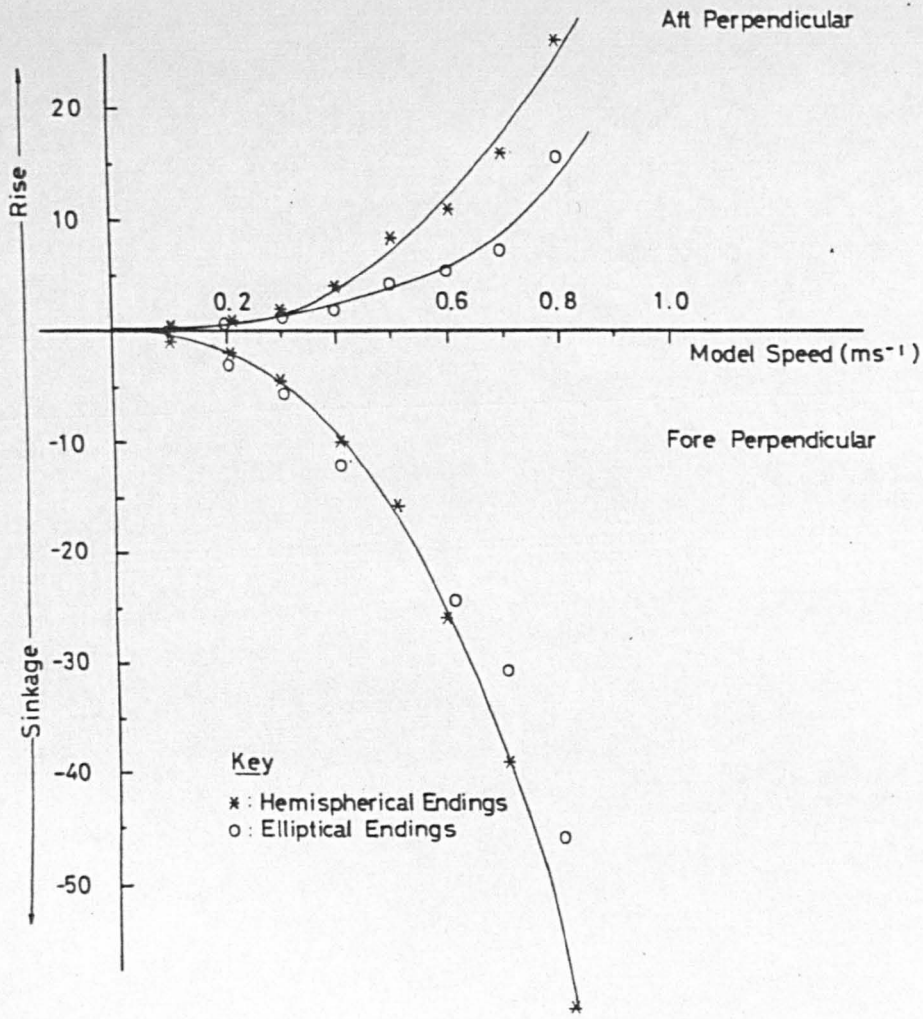

Hull Endings Comparison - Sinkage At F P/A P

Type	:	Three Hull, Semi-Submersible (SWATH) Model
Condition	:	No Foil, Turbulence Stimulators
Draught	:	0.212m Level Keel
		$h/T = 1.3$

Fig.80

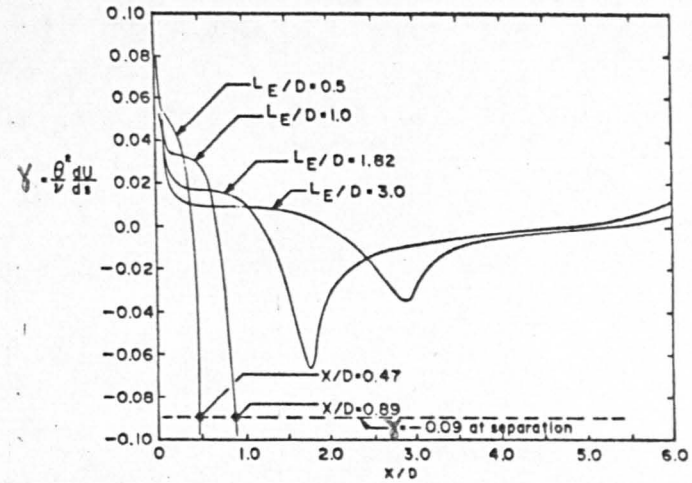

Fig.79; Computed distributions of pressure gradient parameter on the axisymmetric forebodies. [47]

bow.

(6.2.c) Results and Conclusions

Experiments were conducted at three depth-draught ratios with the hull towed and no appendages. Only results for a depth-draught ratio of 1.3 are presented, since the conclusions did not appear to be affected by changes in water depth.

A comparison of the sinkages measured at both perpendiculars is presented in Fig.80, where it may be noted that a noticeable increase in the aft sinkage occurs as a result of the modification. Resolved into mean sinkage and trim components, Fig.81, the results indicate that the elliptical hull endings increase the mean sinkage slightly but decrease the trim-by-bow. The overall effect is to decrease the measured total resistance , Fig.82. The results confirm the importance of the stern shape, which controls the boundary layer/near wake aft and affects the stern pressure distribution and consequent form drag.

In agreement with preliminary estimations, the elliptical hull endings reduce the total measured resistance in the higher speed range examined, but do not possess advantages of practical significance under shallow-water close-to-grounding situations.

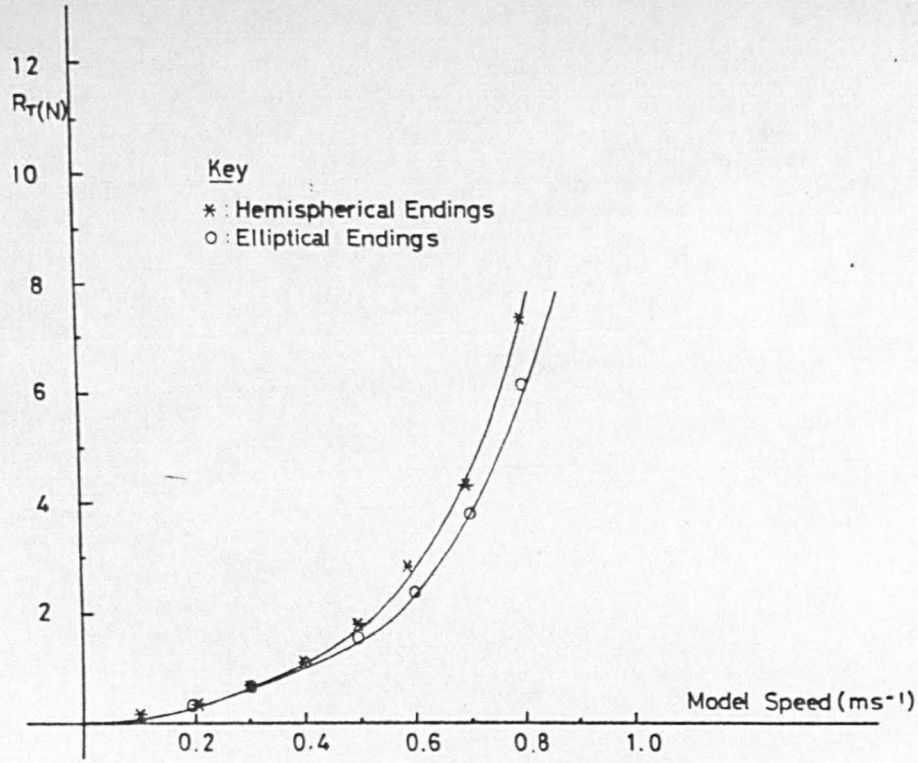

Hull Endings Comparison R_T Against Model Speed

Type : Three Hull, Semi-Submersible (SWATH) Model
Condition : No Foil, Turbulence Stimulators
Draught : 0.212m Level Keel
$h/_T = 1.3$

Fig. 82

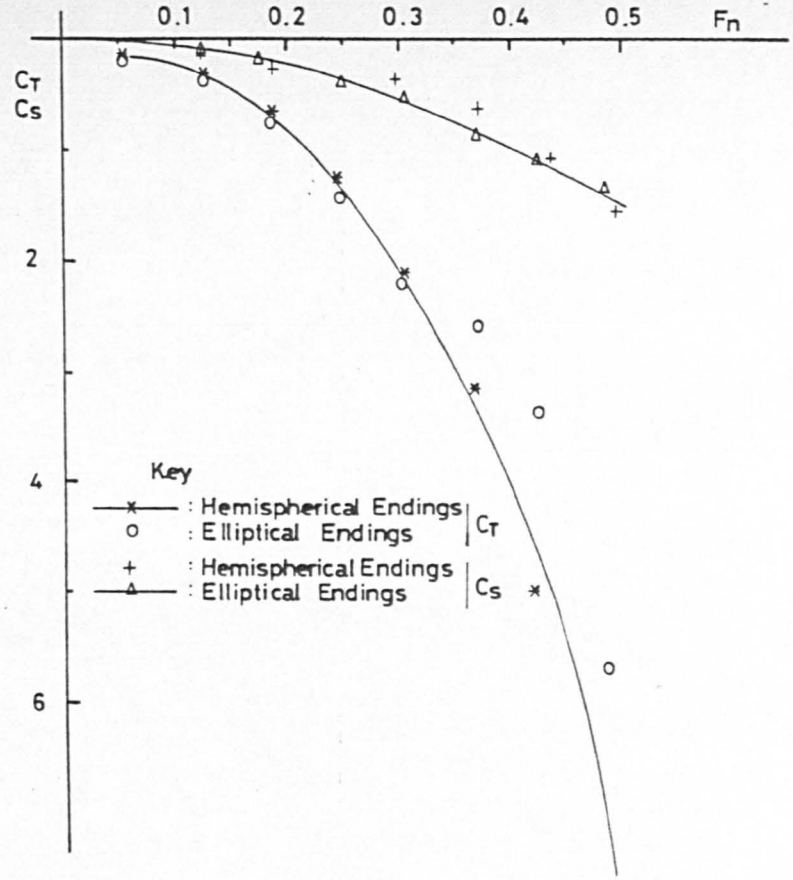

Hull Endings Comparison C_T/F_n, C_S/F_n

Type : Three Hull, Semi-Submersible (SWATH) Model
Condition : No Foil, Turbulence Stimulators
Draught : 0.212m Level Keel

Fig. 81

(6.3) The Effect of a Vertical-Plane Control Surface

Various investigations into the vertical plane stability of the SWATH concept, indicate that as speed increases beyond a certain limit the bare-hull model experiences an instability in pitch. The cause of this instability is the so-called Munk-moment generated by a body of revolution, which acts to increase the angle of attack to the flow. One of the most effective means of alleviating pitch instability and, simultaneously, increasing the degree of damping and trim control, is by means of a control-surface (or surfaces) placed between the hulls, see Smith [68].

The possibilty of adjusting the trim angle is advantageous in itself and an important aspect of SWATH design. In water restricted in depth and/or width, the squatting characteristics may set an upper limit to the speed at which the SWATH operates without touching bottom, even when reserve power exists to overcome the additional resistance induced by the restrictions. In addition to the obvious effect of altering trim, which alters the resistance, a hydrofoil trim-control device produces lift or sinkage, depending on the direction it is used. This, in turn, modifies the draught (or displacement) and is important because the SWATH concept requires a rather deep draught for its size.

(6.3.a) The Objectives

In what follows, the term "control-surface" applies to a trim control hydrofoil for modifying the running attitude in the vertical (zy) plane. The control-surface angle-of-attack is determined with reference to its chord, c, and the direction of motion, Fig.83, and is defined as negative with the leading edge downward from the neutral (0^{o}) angle parallel to the xy-plane. Fig.83 illustrates that the true foil angle-of-attack is a combination of the ship trim angle underway and the fixed foil angle-of-attack.

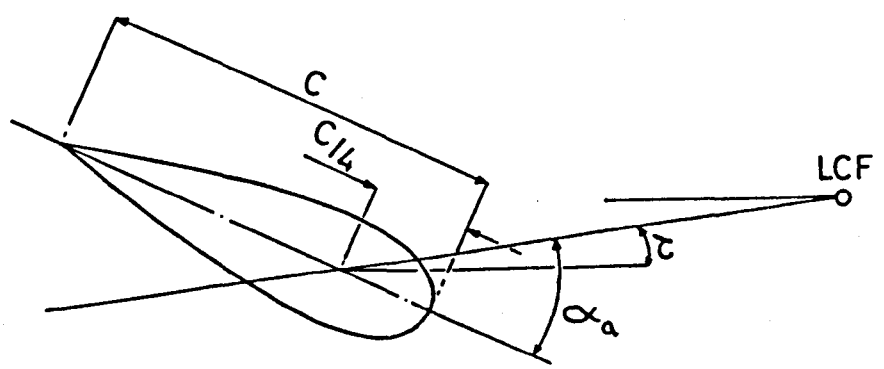

τ = Trim Angle
α_a = Foil Angle Of Attack

Fig. 83: Foil Angle-of-Attack

The experimental study attempted to determine the value of adding a trim control-surface at 2 fixed angles-of-attack on the subsequent sinkage, trim and resistance in shallow-water and to confirm whether this has

an effect on the the resistance other than that resulting from a change in the trim angle. This is done by comparing data obtained during systematic experiments at depth-draught ratios of 1.1, 1.3 and 1.5 as follows,

(a) SWATH without control surface
(b) SWATH with control surface @ 0°
(c) SWATH with control surface @ -5°

(6.3.b) Procedures Unique to SWATH Experiments

One of two techniques is usually applied to evaluate the effect of a movable control surface. One comprises the method of adopting a model with and without the control surface (or surfaces) fitted, unrestrained in sinkage and trim. The experiments are then carried out at constant speed to evaluate the influence of an angle-of-attack of the control-surface on the subsequent characteristics measured. The other technique consists of a model constrained in sinkage and trim, for which the longitudinal moment and vertical force are measured with the control surface fitted. In the case of the latter technique, the tests are normally required at various draughts and trim angles to be able to subsequently ascertain the interaction of the control surface on the resistance throughout the speed range tested.

The former method was employed in the following evaluation. However, it should be noted that the procedure

provides only a gross assessment of the control-surface characteristics, since the interaction effects between the foil and the hull are inherently included in the measurements.

(6.3.c) Possible Scale Effects

When conducting resistance, sinkage and trim tests, the model scale should be sufficiently large to avoid laminar flow on both the bare-hull and control-surface throughout the speed range examined. Although the use of a relatively large bare-hull model allows a reasonable estimation of the scale effect, appreciable scale effects may still occur in the control-surface lift and drag. This is because the Reynold's number of the control surface is normally too low to ensure that a turbulent flow exists on model scale and will result in incorrectly scaled lift and drag data. Owing to the different rate of change of the lift and drag coefficients with R_N for the different parts of the model, extrapolation is, at best, questionable.

In attempts to overcome this problem, it is not unusual to conduct deep-water experiments with the model constrained against sinkage and trim with no control-surface attached and subsequently correct for the effects of the control-surface by using full-scale drag and lift data. However, this procedure may lead to erroneous results since the influence of the control-surface on the sinkage and trim is not accounted for.

The doubtful effectiveness of turbulence stimulation during shallow-water resistance, sinkage and trim tests of the SWATH without a control-surface has been presented and discussed in section (5.3). It is suggested that due to the tank-bottom proximity, the flow ahead of the model was sufficiently turbulent and stimulation was not applied to the SWATH or control-surface under study in this section.

(6.3.d) The Position of the Control-Surface

Other things being equal, control-surfaces are best placed where the moments of the forces generated by them are greatest. This usually means placing a trim control-surface at the greatest practical distance from the vessel CG, either aft or forward. However, the control-surface also generates a drag force, whose moment about the vessel's centre of rotation normally acts to increase the trim-by-bow underway. Although the moment produced by the change in fin drag with angle-of-attack is small compared to that produced by the lift force, attention must also be given to the control-surface height. This is of particular importance at very low depth-draught ratios, when the lift-to-drag ratio is small.

As a matter of practical design and construction, the SWATH configuration examined had the control-surface fitted between the two aft struts, see Fig.84. In this position, the horizontal flow over the foil is accelerated by the channel effect of the struts, increasing its efficiency.

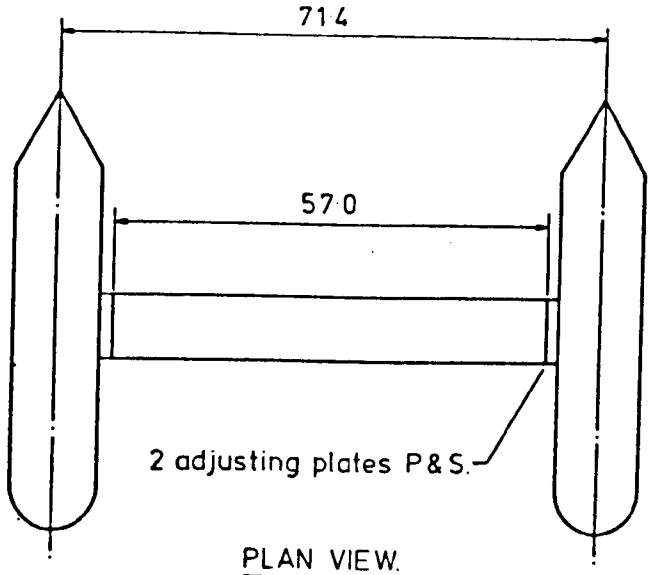

PLAN VIEW.

Drawing to model scale 1:10
(Dimensions are model sizes in cms.)

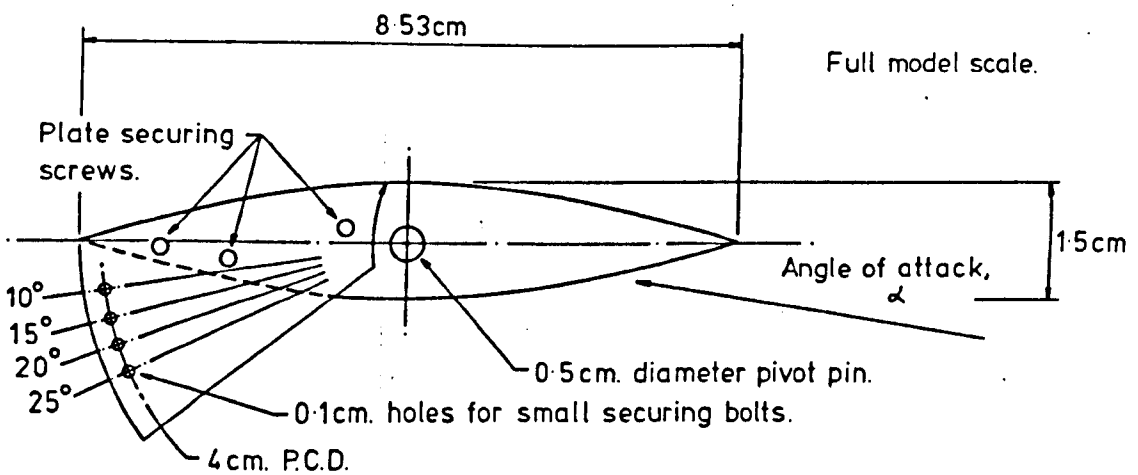

SECTION AT STARBOARD INBOARD ADJUSTING PLATE.

(Looking to port.)

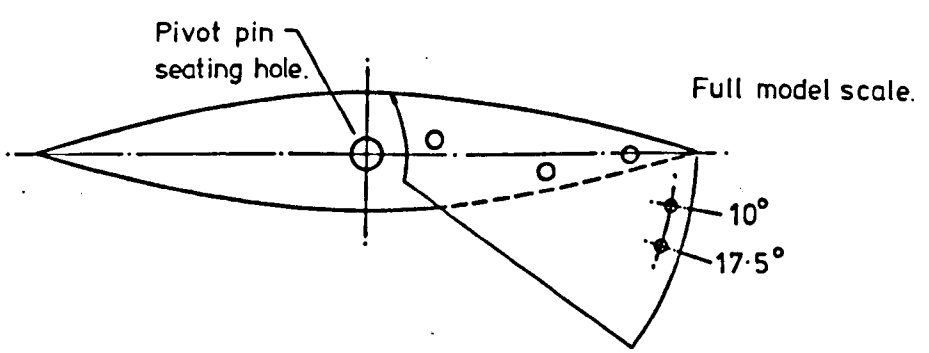

SECTION AT STARBOARD OUTBOARD ADJUSTING PLATE.

(Looking to starboard.)

Fig.84 THREE HULLED SEMI-SUBMERSIBLE SHIP, FIN & ADJUSTING MECHANISM

The arrangement also provides torsional rigidity and conveniently protects the control-surface. Other control-surface arrangements were not examined.

(6.3.e) Experimental Results and Conclusions

Figs.85,86 present the sinkage or rise experienced by the SWATH at the two angles-of-attack and 3 depth-draught ratios examined.

Figs.87-89 present C_T-F_h comparisons with and without the control-surface, which indicate that the 0° foil angle is inefficient up to $F_h = 0.35$ irrespective of water depth. Below this value the SWATH trim-by-bow is seen to increase at a given depth-draught ratio. Consequently, the control-surface is of no significance at the lowest depth-draught ratio of 1.1, where the trim is limited to small values. The trim behaviour is only slightly depth dependent, Fig.90. Because of the higher trim angles at speeds greater than $F_h = 0.35$, the lift-to-drag ratio, and hence the control-surface efficiency, increase. The SWATH trim angle reaches -2° before the trim-by-bow is reduced, although a level-keel condition is not attained over the speed range examined. The -5° angle-of-attack is immediately effective and beneficial at all depths and speeds examined. However, at a trim angle of -2° (or a true foil angle-of-attack of -7°), it starts reducing the trim-by-bow at a greater rate. A comparison with data for a NACA 0015 aerofoil, which the control-surface closely

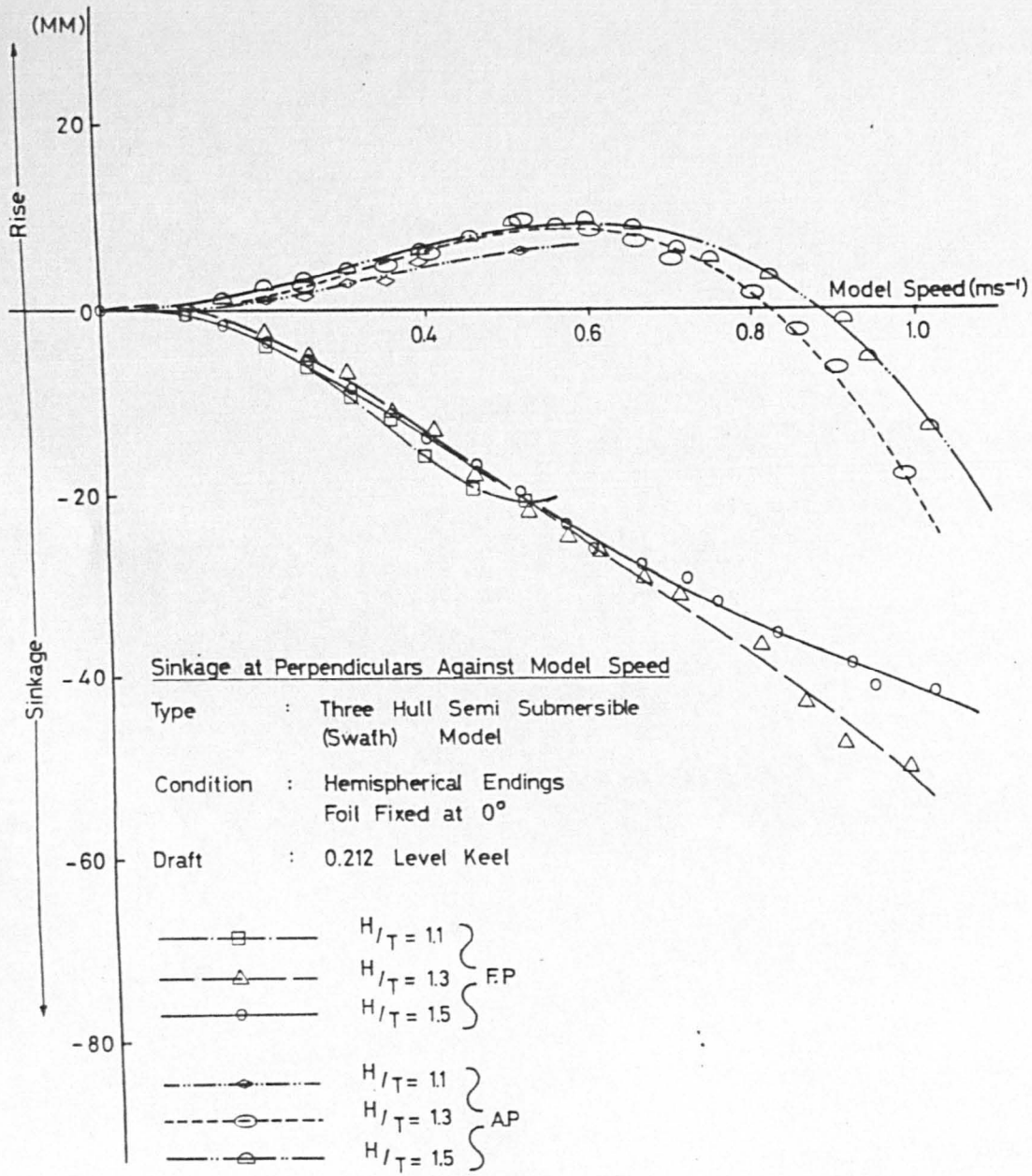
(MM)
20
0
-20
-40
-60
-80
Rise
Sinkage
0.4
0.6
0.8
1.0
Model Speed (ms⁻¹)
Sinkage at Perpendiculars Against Model Speed
Type : Three Hull Semi Submersible (Swath) Model
Condition : Hemispherical Endings Foil Fixed at 0°
Draft : 0.212 Level Keel
H/T = 1.1
H/T = 1.3
H/T = 1.5
F.P
H/T = 1.1
H/T = 1.3
H/T = 1.5
A.P

Fig. 36

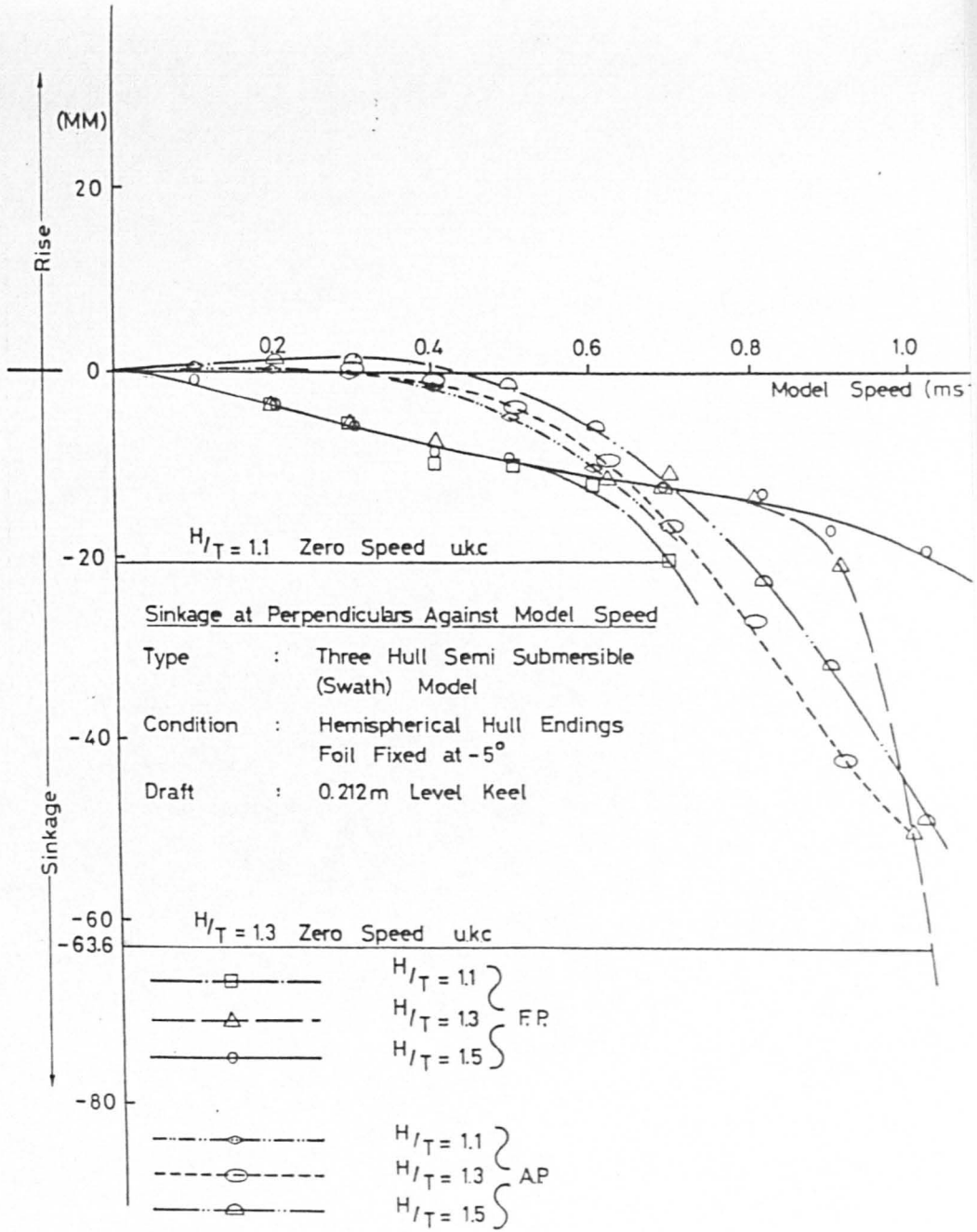
(MM)
20
0
-20
-40
-60
-63.6
-80
Rise
Sinkage
0.2
0.4
0.6
0.8
1.0
Model Speed (ms
H/T = 1.1 Zero Speed ukc
H/T = 1.3 Zero Speed ukc
Sinkage at Perpendiculars Against Model Speed
Type : Three Hull Semi Submersible (Swath) Model
Condition : Hemispherical Hull Endings Foil Fixed at -5°
Draft : 0.212m Level Keel
H/T = 1.1
H/T = 1.3
H/T = 1.5
F.P.
H/T = 1.1
H/T = 1.3
H/T = 1.5
A.P

Fig. 85

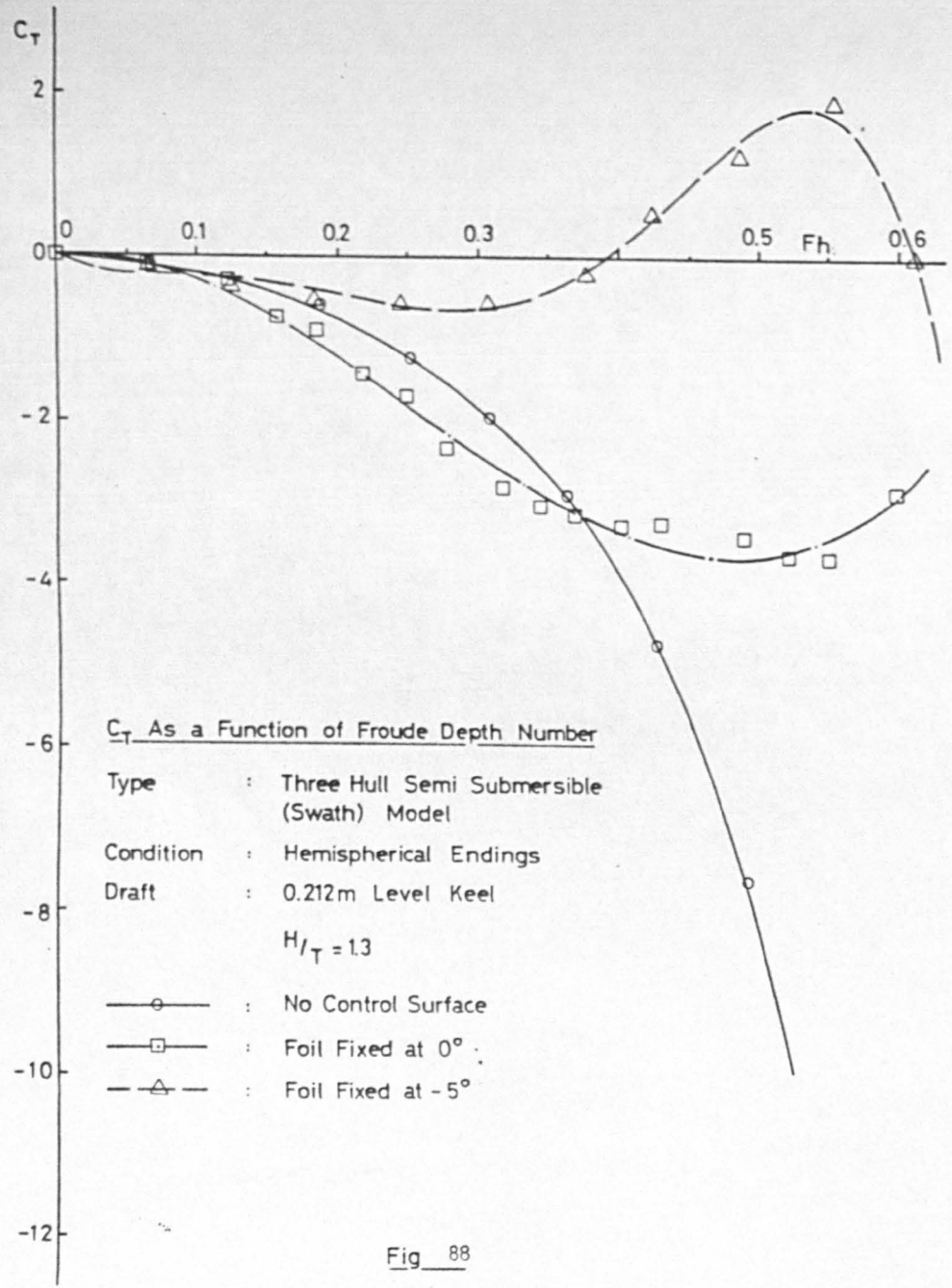
C_T
2
0
-2
-4
-6
-8
-10
-12
0
0.1
0.2
0.3
0.5
Fh
0.6
C_T As a Function of Froude Depth Number
Type : Three Hull Semi Submersible (Swath) Model
Condition : Hemispherical Endings
Draft : 0.212m Level Keel
$H/_T$ = 1.3
: No Control Surface
: Foil Fixed at 0°
: Foil Fixed at -5°

Fig 88

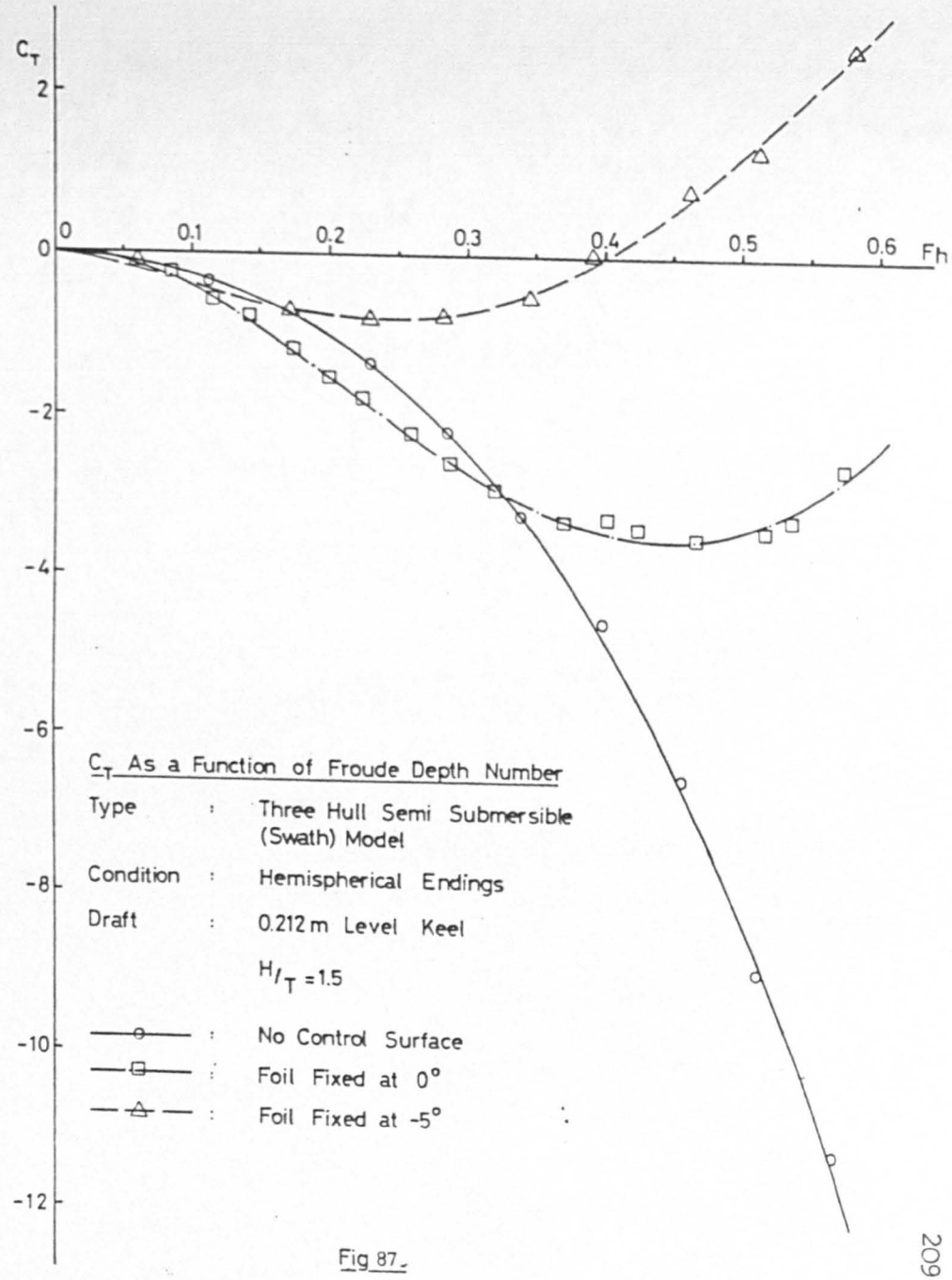
C_T
2
0
-2
-4
-6
-8
-10
-12
0
0.1
0.2
0.3
0.4
0.5
0.6
Fh
C_T As a Function of Froude Depth Number
Type : Three Hull Semi Submersible (Swath) Model
Condition : Hemispherical Endings
Draft : 0.212 m Level Keel
$H/_T$ = 1.5
: No Control Surface
: Foil Fixed at 0°
: Foil Fixed at -5°

Fig 87

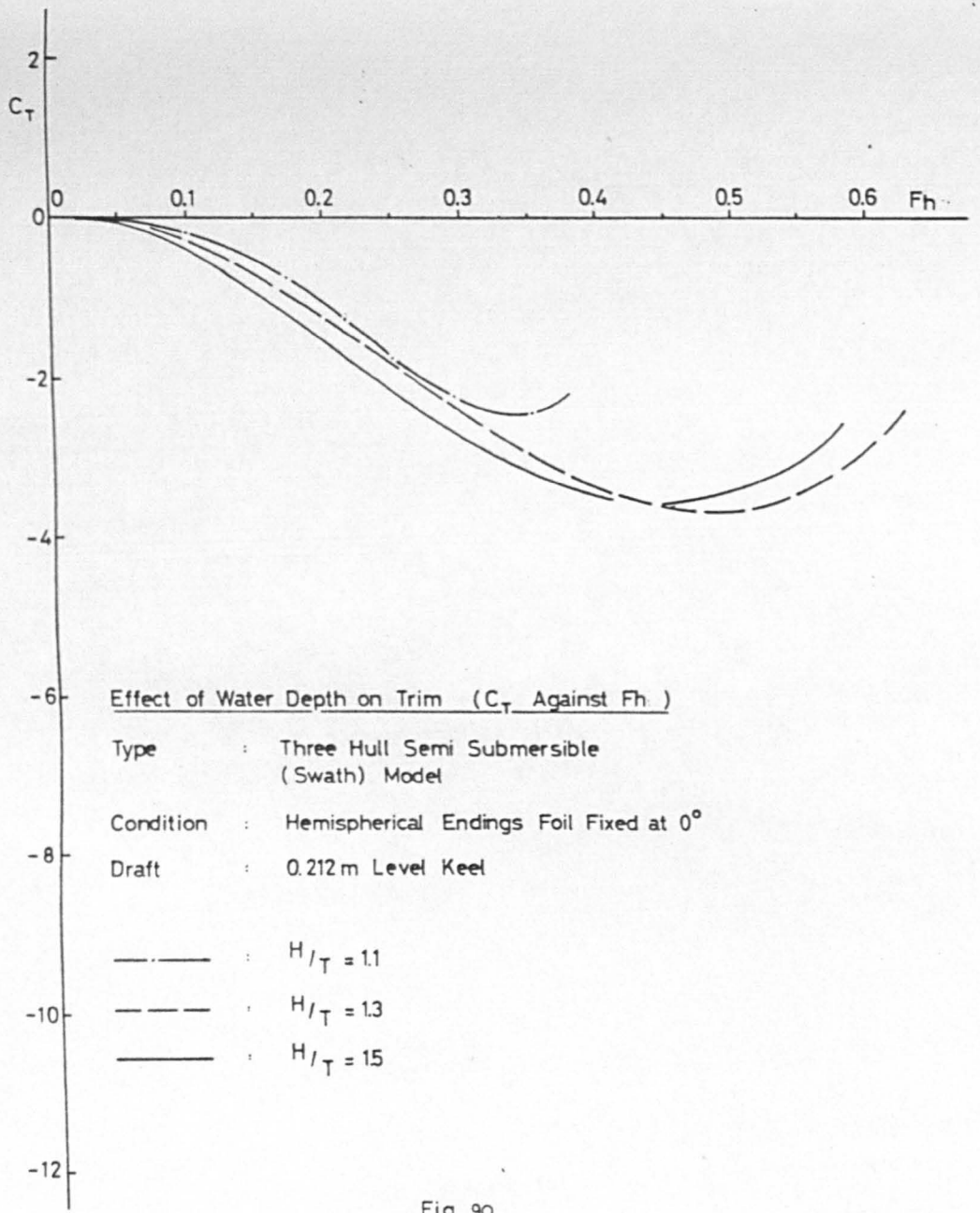

Effect of Water Depth on Trim (C_T Against Fh)

Type : Three Hull Semi Submersible (Swath) Model

Condition : Hemispherical Endings Foil Fixed at 0°

Draft : 0.212 m Level Keel

—·— : $H/T = 1.1$

— — — : $H/T = 1.3$

——— : $H/T = 1.5$

Fig 90

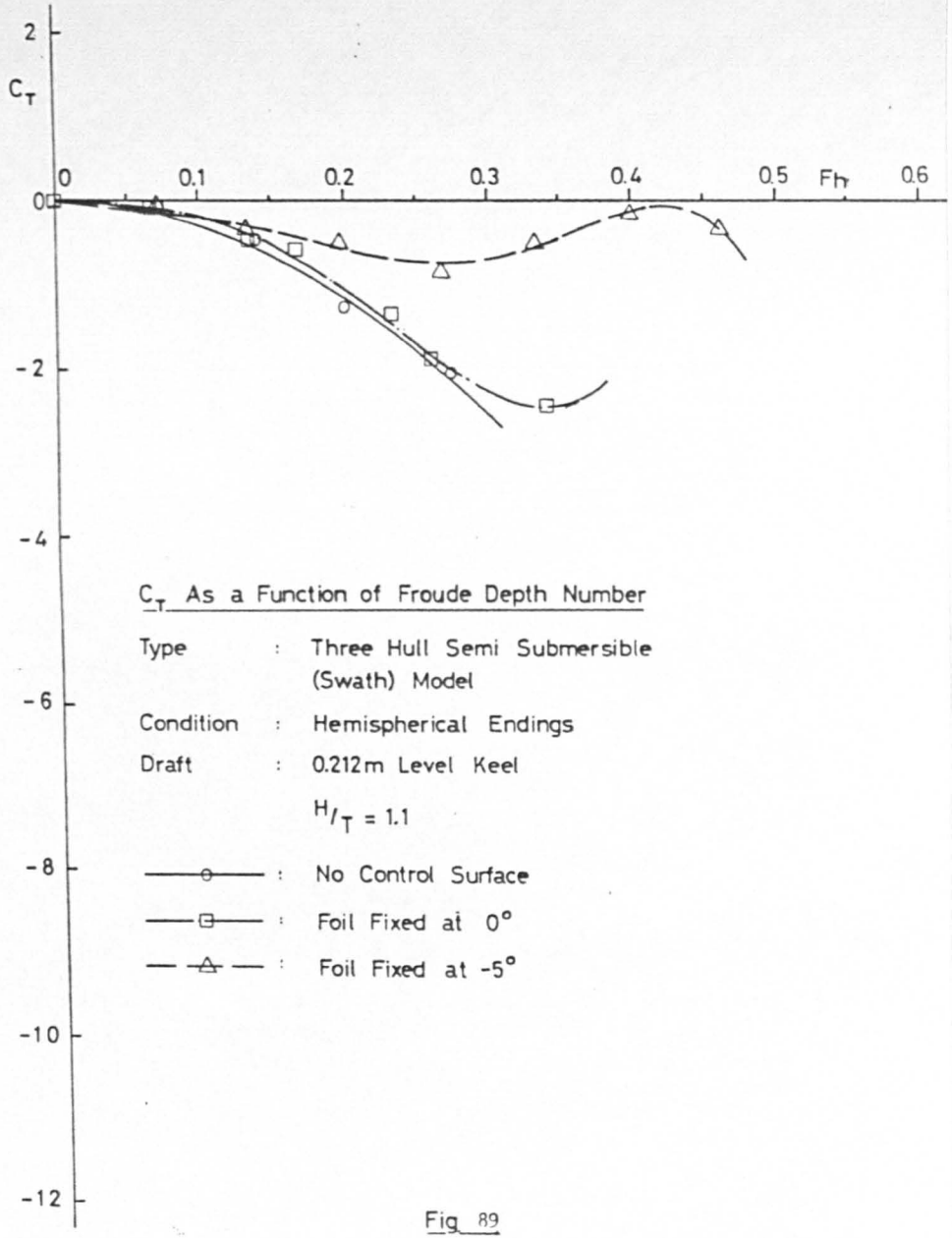

C_T As a Function of Froude Depth Number

Type : Three Hull Semi Submersible (Swath) Model

Condition : Hemispherical Endings

Draft : 0.212 m Level Keel

$H/T = 1.1$

—o— : No Control Surface

—□— : Foil Fixed at 0°

—△— : Foil Fixed at -5°

Fig 89

resembles, indicates that this true foil angle-of-attack is approximately that at which the maximum lift-to-drag ratio occurs. It was noted during the experiment that at this angle-of-attack the SWATH exhibited some instability in height at the fore-perpendicular, in comparison to the steady behaviour aft.

The C_S-F_h data appears to lie on unique curves, both with and without the control-surface and irrespective of the angle-of-attack. The comparison, Fig.91, illustrates that the control-surface not only alters the trim but also increases the mean sinkage. This increase is presented in Fig.92, relative to the mean sinkage without a control-surface. The increase between the angles-of-attack examined is approximately 15 -20%.

Fig.93 presents a typical resistance comparison with and without the control-surface. Figs.94,95 present the percentage increase in resistance for the 0^o and -5^osettings, respectively, relative to that without the foil for the range of shallow-water depths tested. The -5^osetting induces a higher resistance in comparison to the 0 setting. It is seen that for a given angle-of-attack the change in resistance owing to the addition of the control-surface, increases with an increase in water depth. It is suggested that this increase in the total measured resistance is responsible for the increase in bow trim, Figs.87-89.

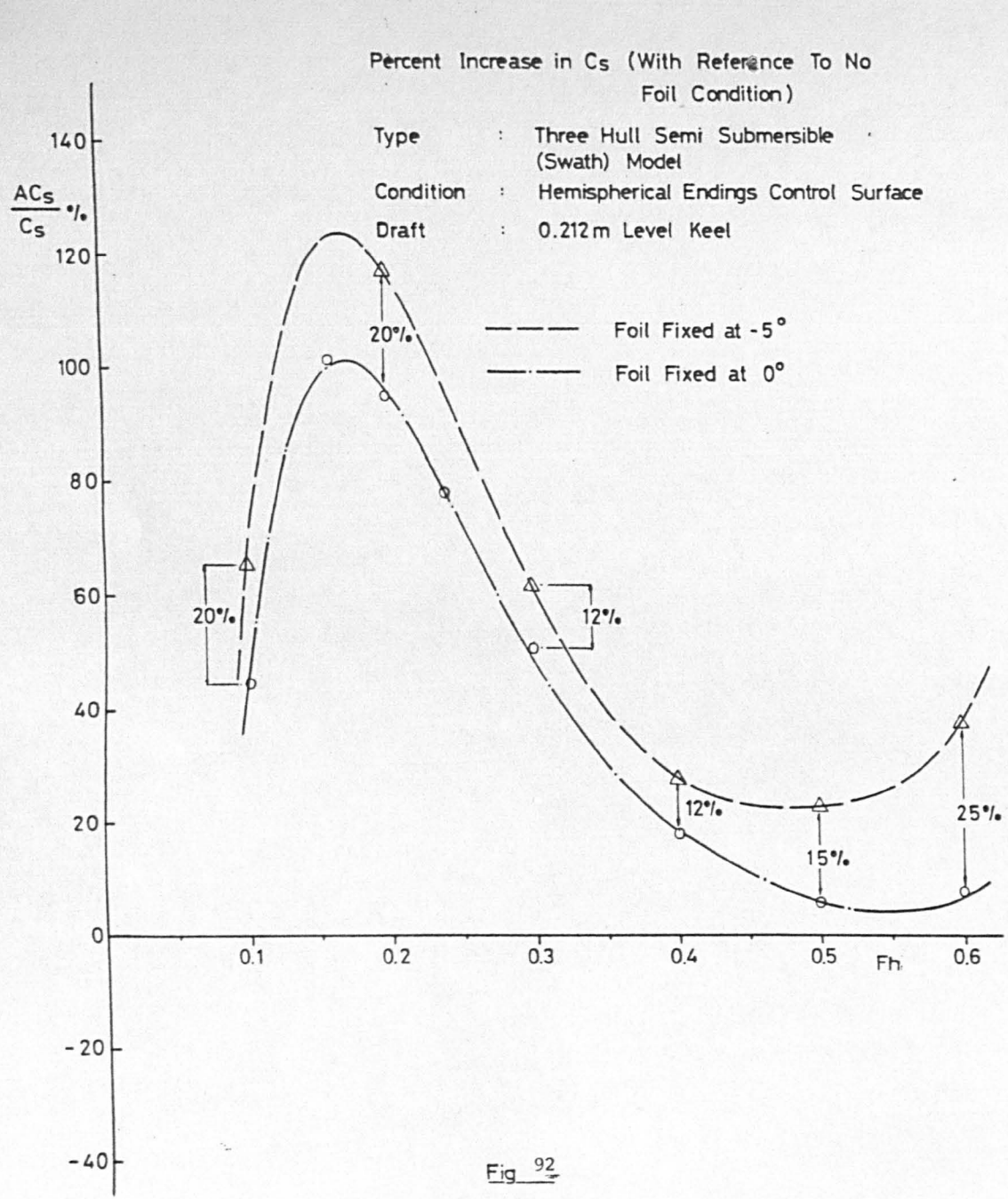
Percent Increase in Cs (With Reference To No Foil Condition)
Type : Three Hull Semi Submersible (Swath) Model
Condition : Hemispherical Endings Control Surface
Draft : 0.212m Level Keel
Foil Fixed at -5°
Foil Fixed at 0°
ΔCs/Cs %
140
120
100
80
60
40
20
0
-20
-40
20%
20%
12%
12%
15%
25%
0.1
0.2
0.3
0.4
0.5
Fh
0.6

Fig 92

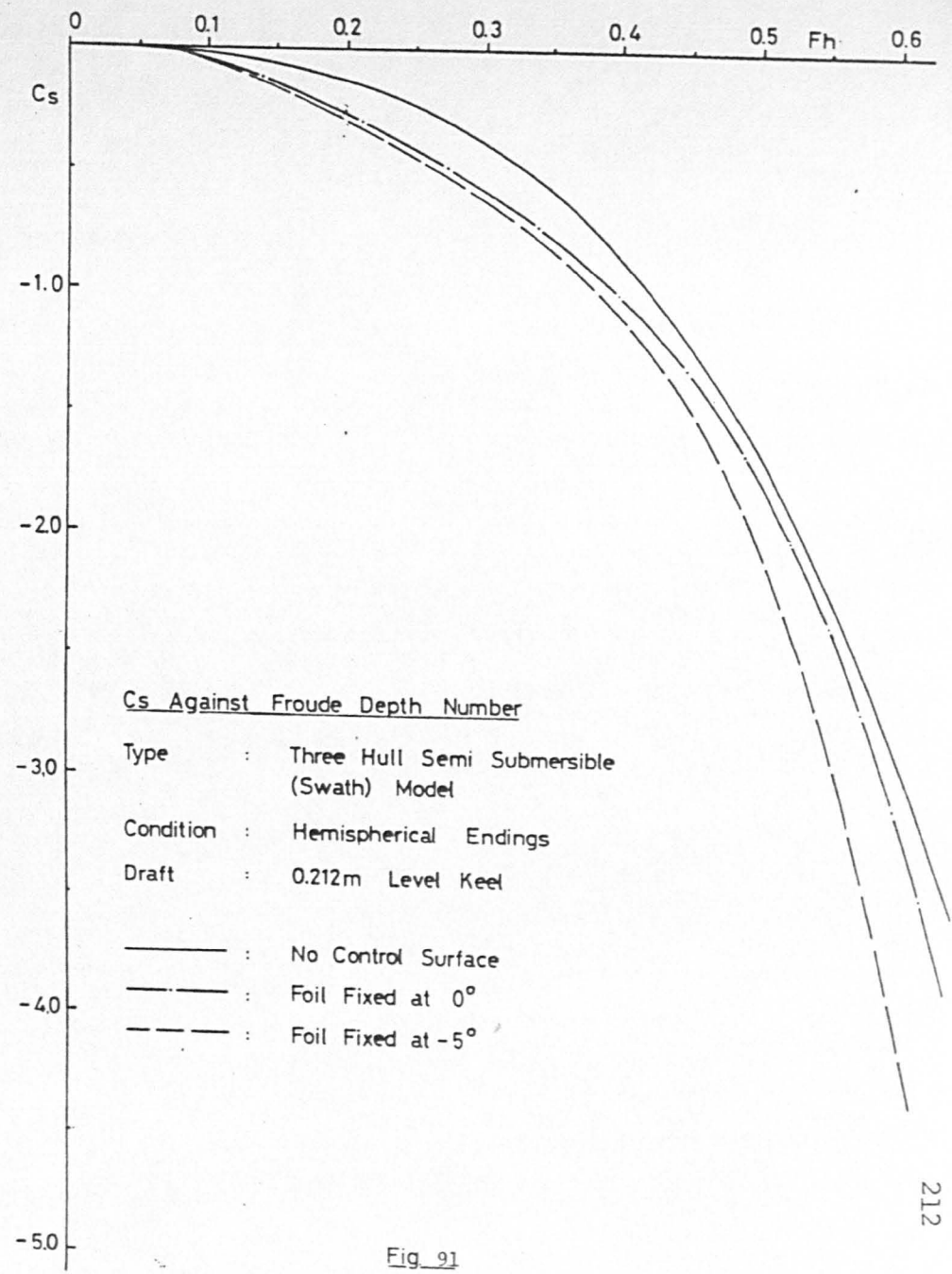
Cs
0
0.1
0.2
0.3
0.4
0.5
Fh
0.6
-1.0
-2.0
-3.0
-4.0
-5.0
Cs Against Froude Depth Number
Type : Three Hull Semi Submersible (Swath) Model
Condition : Hemispherical Endings
Draft : 0.212m Level Keel
: No Control Surface
: Foil Fixed at 0°
: Foil Fixed at -5°

Fig 91

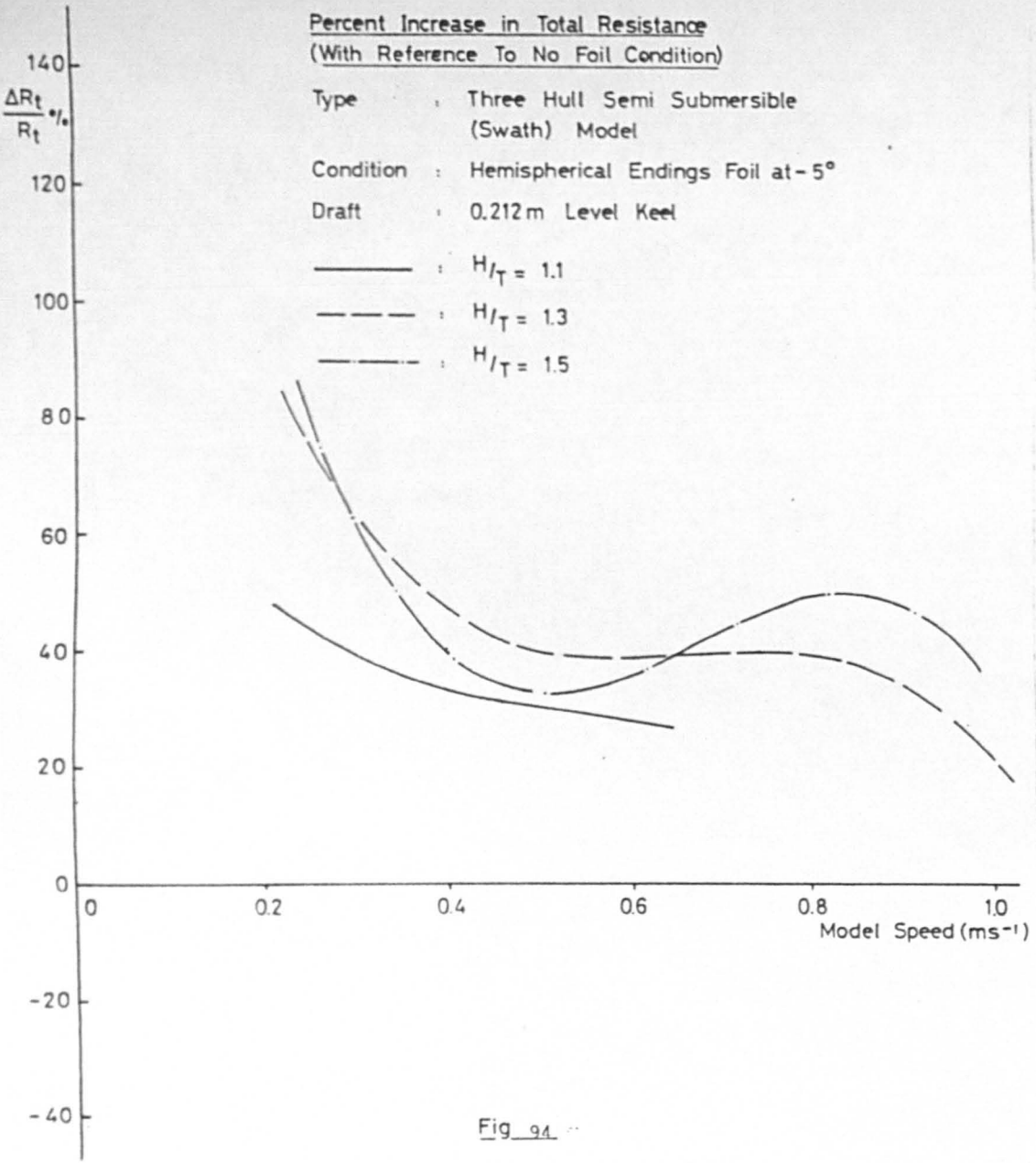
Percent Increase in Total Resistance
(With Reference To No Foil Condition)
Type : Three Hull Semi Submersible (Swath) Model
Condition : Hemispherical Endings Foil at -5°
Draft : 0.212m Level Keel
H/T = 1.1
H/T = 1.3
H/T = 1.5
ΔRt/Rt %
140
120
100
80
60
40
20
0
-20
-40
0
0.2
0.4
0.6
0.8
1.0
Model Speed (ms⁻¹)

Fig 94

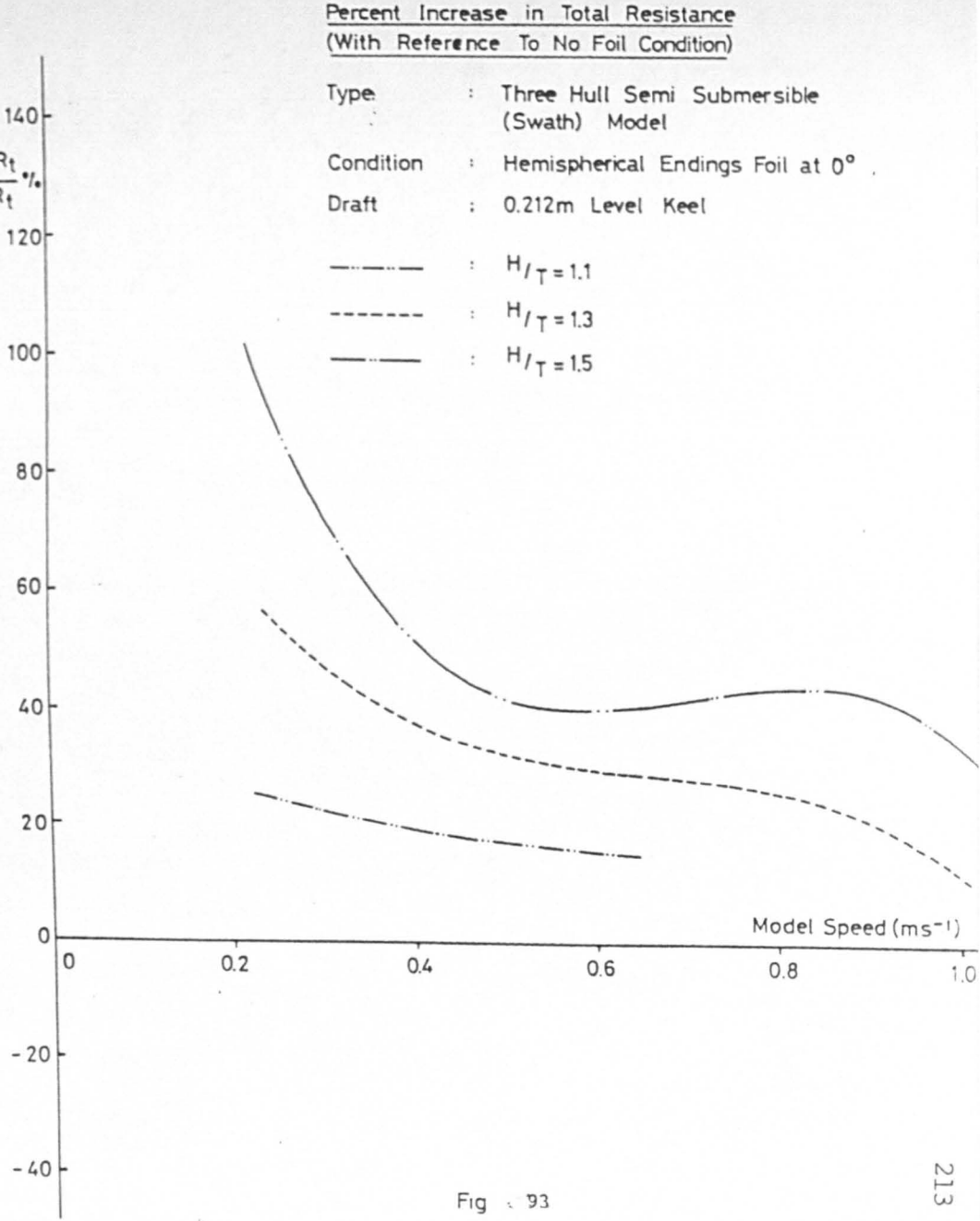
Percent Increase in Total Resistance
(With Reference To No Foil Condition)
Type : Three Hull Semi Submersible (Swath) Model
Condition : Hemispherical Endings Foil at 0°
Draft : 0.212m Level Keel
H/T = 1.1
H/T = 1.3
H/T = 1.5
ΔRt/Rt %
140
120
100
80
60
40
20
0
-20
-40
0
0.2
0.4
0.6
0.8
1.0
Model Speed (ms⁻¹)

Fig 93

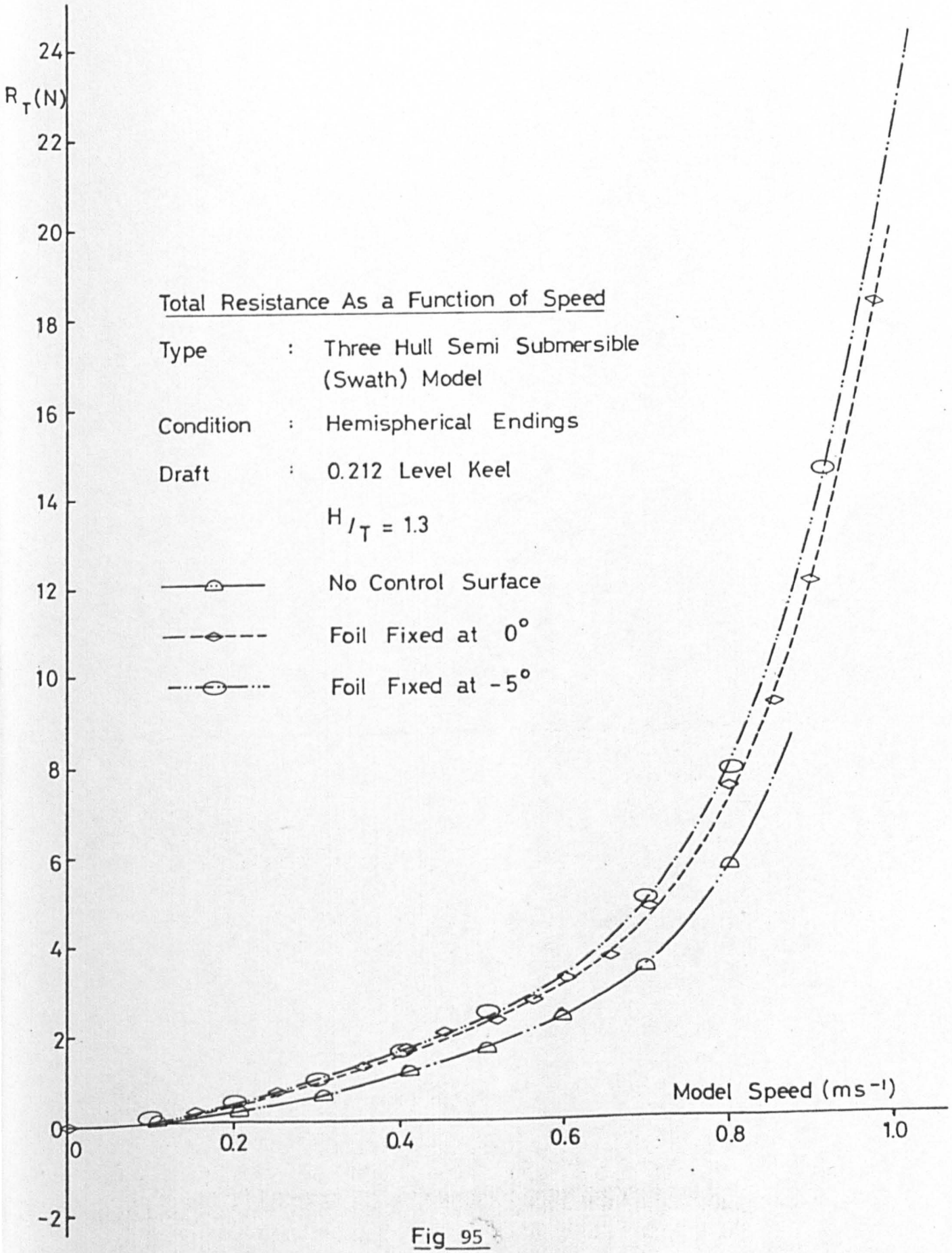
Total Resistance As a Function of Speed
Type : Three Hull Semi Submersible (Swath) Model
Condition : Hemispherical Endings
Draft : 0.212 Level Keel
H/T = 1.3
No Control Surface
Foil Fixed at 0°
Foil Fixed at -5°
R_T(N)
24
22
20
18
16
14
12
10
8
6
4
2
0
-2
0
0.2
0.4
0.6
0.8
1.0
Model Speed (ms⁻¹)

Fig 95

The development of a purely theoretical and quantitative procedure for estimating the effect of a given control-surface on a given bare-hull sinkage, trim and resistance (or any other behaviour characteristics) is complicated by the fact that the behaviour of the bare-hull plus fin depends on the lift and drag forces generated by the fin and, at the same time, the fin true angle-of-attack depends on the combined bare-hull plus fin behaviour.

The difficulties persist even when considering a particular design for which the variation in the trim angle and the true foil angle-of-attack are known. An attempt was made to correlate the above experimentally obtained change in trim with a theoretical procedure employing the lift and drag coefficients of the control-surface (using NACA 0015 aerofoil data). Assuming the lift and drag forces act at the foil centroid, their moments about the SWATH LCF were calculated but were found to significantly underestimate the measured trim change, the difference being of the order of approximately 75%. A similar result was obtained upon comparing the foil lift force to the measured change in sinkage or the foil drag force to the measured change in resistance. That is, the test procedure employed during the experiments does not yield detailed data for the control-surface itself nor does it yield the interaction effects between it and the bare-hull. The reasons for the disagreement are many and, in addition to the difficulties inherent in the testing procedure, also result from the simplifying assumptions made in deriving

the theoretical approach. The first simplifying assumption made when estimating the change in resistance, for example, is that the total resistance is equal to the sum of the separate hull and control-surface resistances, and that ventilation, cavitation or transverse cross-flow do not occur. Morover, the lift and drag data for aerofoils is normally obtained in wind tunnels, at high R_N in terms of the fin chord. Hence the available viscous drag formulations are applicable to turbulent flow conditions. Velocity augmentation due to the "tunnel" effect of the twin-hull is not accounted for, nor is any dependence on Froude number effects. As speed increases the hull wave resistance component will play an increasingly important role and will be affected by the change in trim induced by the control surface.

It is illustrated that by paying a penalty in resistance, a SWATH can attain improved shallow-water characteristics. The final choice of the location of the control-surface is normally determined by other aspects of SWATH behaviour. The disadvantage of the control-surface in its present position is that in order to counteract the inherent trim-by-bow attitude, the foil must generate a negative lift (or sinkage) which increases the SWATH displacement. This lowers the overall underwater centre of resistance and acts to increase the trim-by-bow. The effect would be similar on any other design. Owing to the increased mean sinkage and resistance of the present configuration, the author is of the opinion that a split

system would be more beneficial, particularly if the design is expected to operate in and out of shallow-water.

(6.3.f) Wing-in-Ground Effects

It may be observed that for a given F_h both the trim-by-bow, Fig.90 and the resistance, Fig.94, decrease as water depth is reduced. It is suggested that the increased effectiveness of the control-surface is due to wing-in-ground (WIG) effects in the proximity of the bottom.

Experimentally, as ground is approached there is a rapid increase in negative pressures over the lower plane of the control-surface, near the leading edge, whereas the upper surface pressures remain essentially the same. Shallow-water flow restrictions result in a reduced downwash which reduces the induced drag of the control surface. The combined effect is to increase the lift-drag ratio as bottom is approached. However, since the resistance increase owing to the increased mean sinkage is greater, the total resistance measured increases in comparison to that without the control-surface.

CHAPTER 7

Twin-Hull Resistance and Squat in Shallow-water

The towing of offshore structures in shallow-water involves large forces on which there is little published information. The normal design optimization and operational philosophy of offshore platforms yields configurations dominated by the special attention paid to (deep-water) operational-draught motion characteristics. The aim of this section is to examine the effect of the resulting variations in hull geometry on the resistance and squat of offshore platforms in the transit draught condition, when normally only the lower hulls (or caissons) are immersed. This is performed by examining the experimental data of a number of basic twin-hulled geometries towed in calm, shallow-water. A comparison with the three-hulled SWATH data suggests that the range of validity of the conclusions may be extended.

(7.1) Types of Offshore Platform Models Examined

The gradual increase in the size of offshore platforms and the extension of offshore construction into deeper and more hostile waters, have led designers to a wide range of geometrical arrangements.

The existing offshore platforms can be divided into two main types, (a) Fixed Platforms, normally used for production and storage purposes and (b) Mobile Platforms, used for exploration, pipe-laying and various support purposes. An immense program would be required to examine all current operational designs. Consequently, emphasis is placed on mobile twin-hulled semi-submersible platforms, which are required to operate at any depth and may do considerable travelling, either self-propelled or under tow, to increase their work capability. Owing to the wide range of dimensions and geometrical features, the full-scale transit draught is chosen as the common criterion to assist in obtaining more meaningful comparisons.

The platforms examined are the twin rectangular-hulled SSCV, Fig.38, the twin circular-hulled semi-submersible, Fig.96 and a twin rectangular-hulled model with triangular endings ("Aker" type), Fig.97. The principal particulars of the SWATH appear in Fig.42. Experiments were conducted over the range $1.1 \leq h/T \leq 1.5$ with naked-hull models. The relevant experimental set-up and procedures are detailed in Appendix C and the appropriate sections of this chapter.

(7.2) Shallow-water Resistance - Model Results

In shallow-water, the flow is restricted resulting in higher velocities near the hull, increasing both the tangential and pressure resistance components.

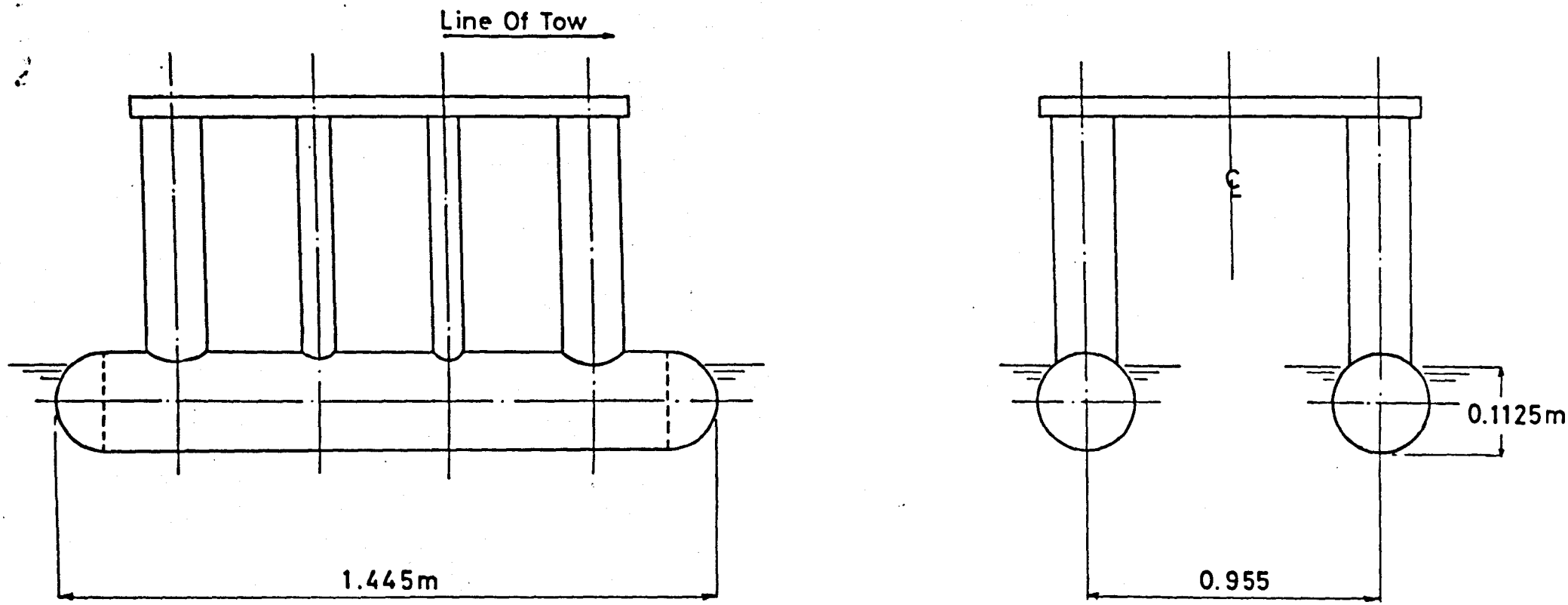

Twin Circular Hull Semi Submersible Model

Model Platform

Principle Characteristics

$\Delta = 645.5$ N

Fig 96

Model Dimensions

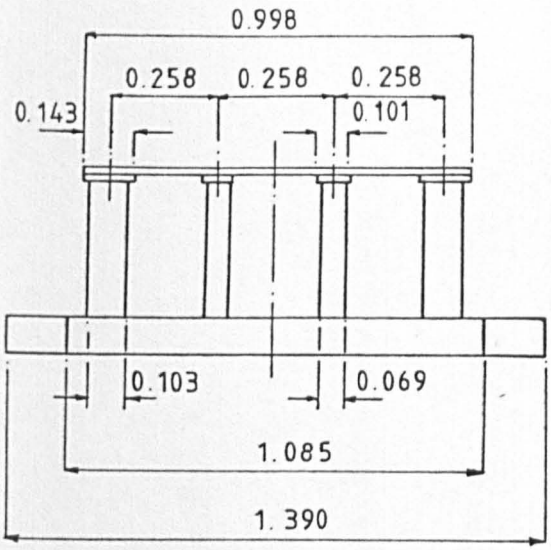

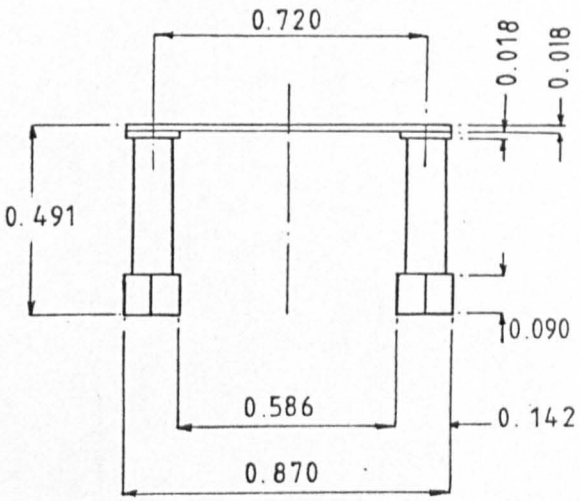

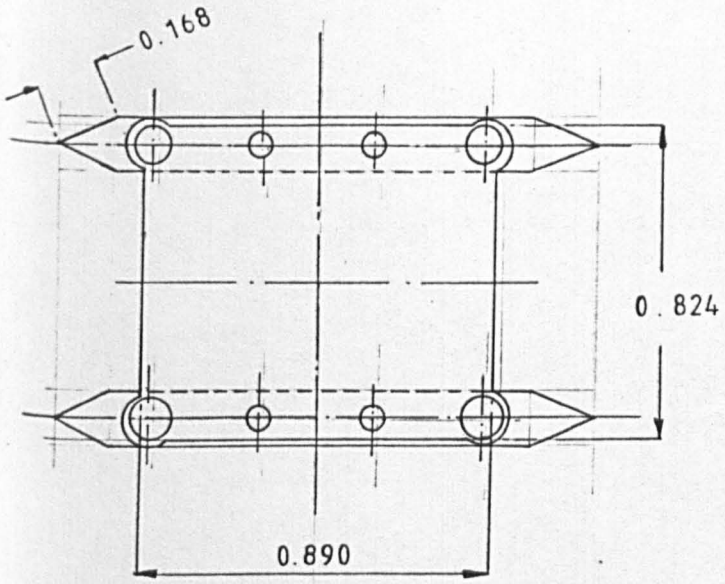

$\Delta = 282.7$ N

Transit Draught 0.08 m

All Dimensions In Metres

Scale 1:78

Fig 97

At a given speed, total resistance increases with decreasing water depth for all the models examined. Various methods of plotting the resistance data were considered. It was observed that, after accounting for blockage effects, a plot of R_T/Δ against F_h yields a unique curve over the range $1.1 \leq h/T \leq 1.5$. That is, when the resistance is non-dimensionalised by the displacement, it is independent of the depth-draught ratio at a given F_h. Fig.98 presents the SSCV results. Similar characteristics were obtained with the twin circular-hulled semi-submersible. Upon correcting for the effects of blockage on model speed, the calculation procedure using model viscous form and frictional resistance coefficients yielded good agreement with the shallow-water experiment for the twin cyllindrical-hulled model. A plot of the three-hulled SWATH data, Fig.48, also yields a unique curve although the SWATH has a considerably deeper transit draught at which its vertical struts are partially immersed. This suggests that the conclusion may be applicable to a wider range of configurations than examined. However, additional experiments are required to verify this, particularly since bluff-strut interference effects may affect behaviour at deeper draughts.

Fig.99 presents a comparative plot of the twin-hulled models tested and has useful applications in shallow-water resistance estimation for the towed, level-keel, transit draught condition within the range of hull spacings normally determined by stability and motion requirements.

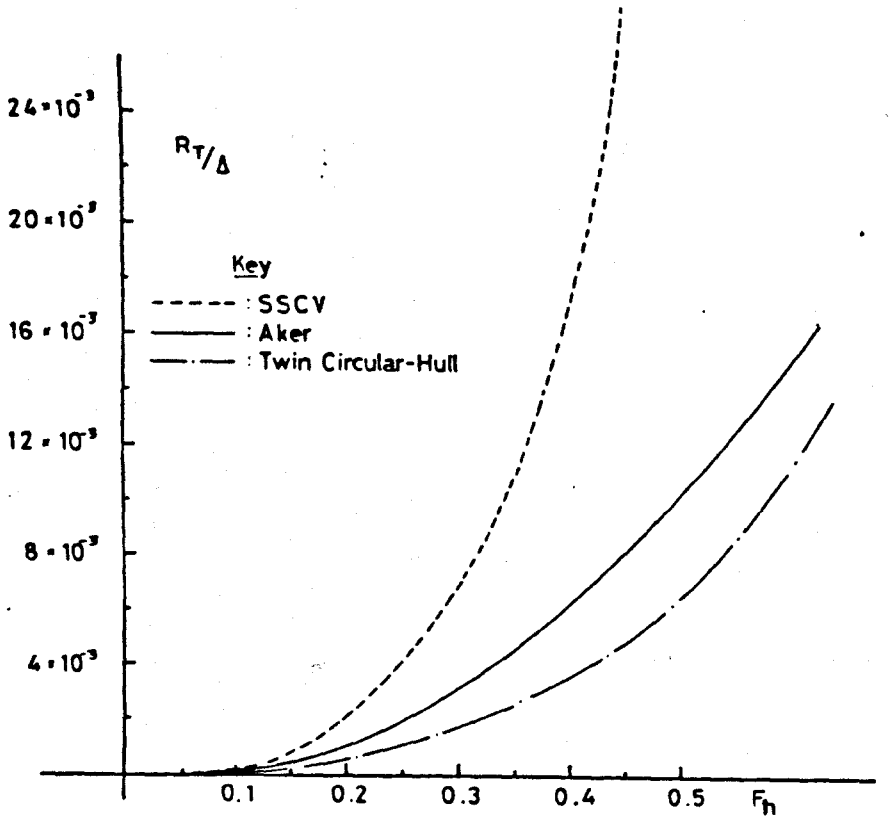

Twin Hull R_T/Δ - F_n Plot

Draught : Transit Draught Level Keel
Condition : Naked Hull Towed From L.H
$1.1 \leq h/T \leq 1.5$

Fig. 99

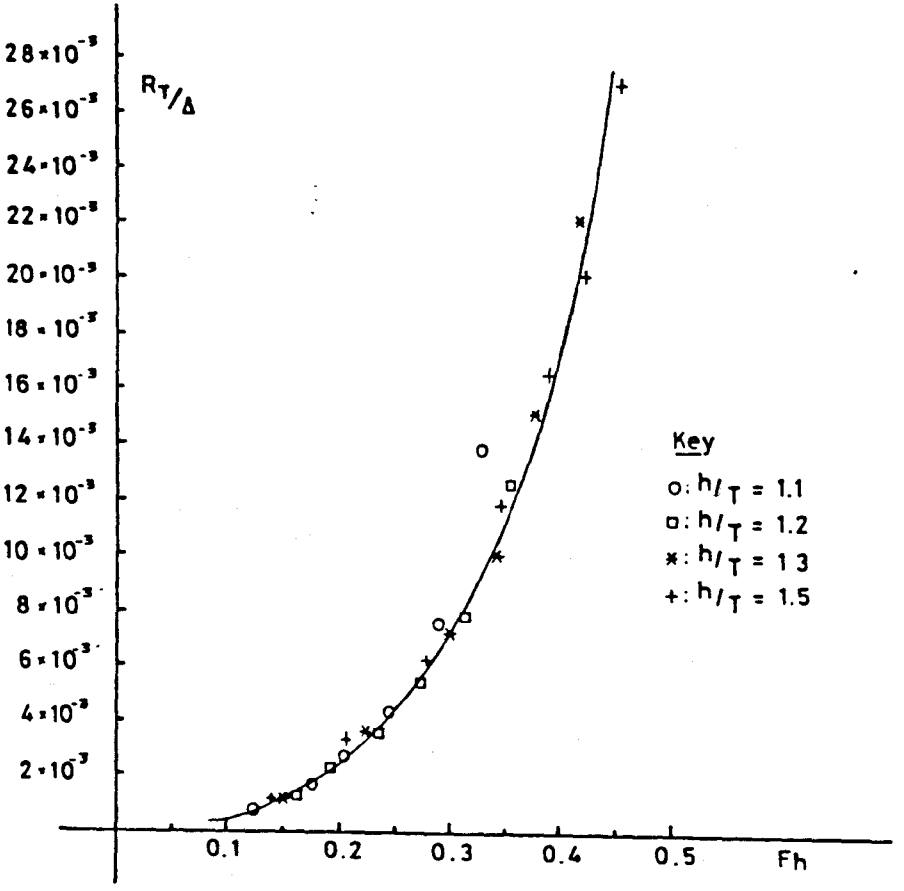

R_T/Δ Against F_n

Type : TwinRectangular Hull, Semi-Submersible
Transit Draught : 0.14m Level Keel
Condition : Solid Ballast, Towed From U.D
$1.1 \leq h/T \leq 1.5$

Fig. 98

(7.3) Sinkage and Trim - Model Results

In parallel, measurements of the shallow-water sinkage and trim behaviour of each platform were carried out with the objective of examining the behaviour and the possibilty of prediction by the existing SQUAT computer program, see (4).

In all the cases examined, a plot of C_S against F_h resulted in a unique curve, independent of the depth-draught ratio in the range $1.1 \leq h/T \leq 2.0$. Figs.62,100,101 present the plot of the mean sinkage coefficient for the twin-hulls examined. Fig.47 demonstrates that this is also the case for the SWATH.

A plot of the trim coefficient of the SSCV, Fig.107, indicates that twin rectangular-hulled platform behaviour is divided into two types, depending on the depth-draught ratio,

(a) behaviour at $h/T < 1.3$
(b) behaviour at $h/T \geq 1.3$

The change in behaviour at $h/T=1.3$ is induced by the proximity of a solid bed under the hull which distorts the normal shallow-water flow appreciably. As $h/T < 1.3$, there is a limit to the downward flow which can take place under the bows, creating a "blocking" effect, which results in a greater body of fluid passing around than underneath the

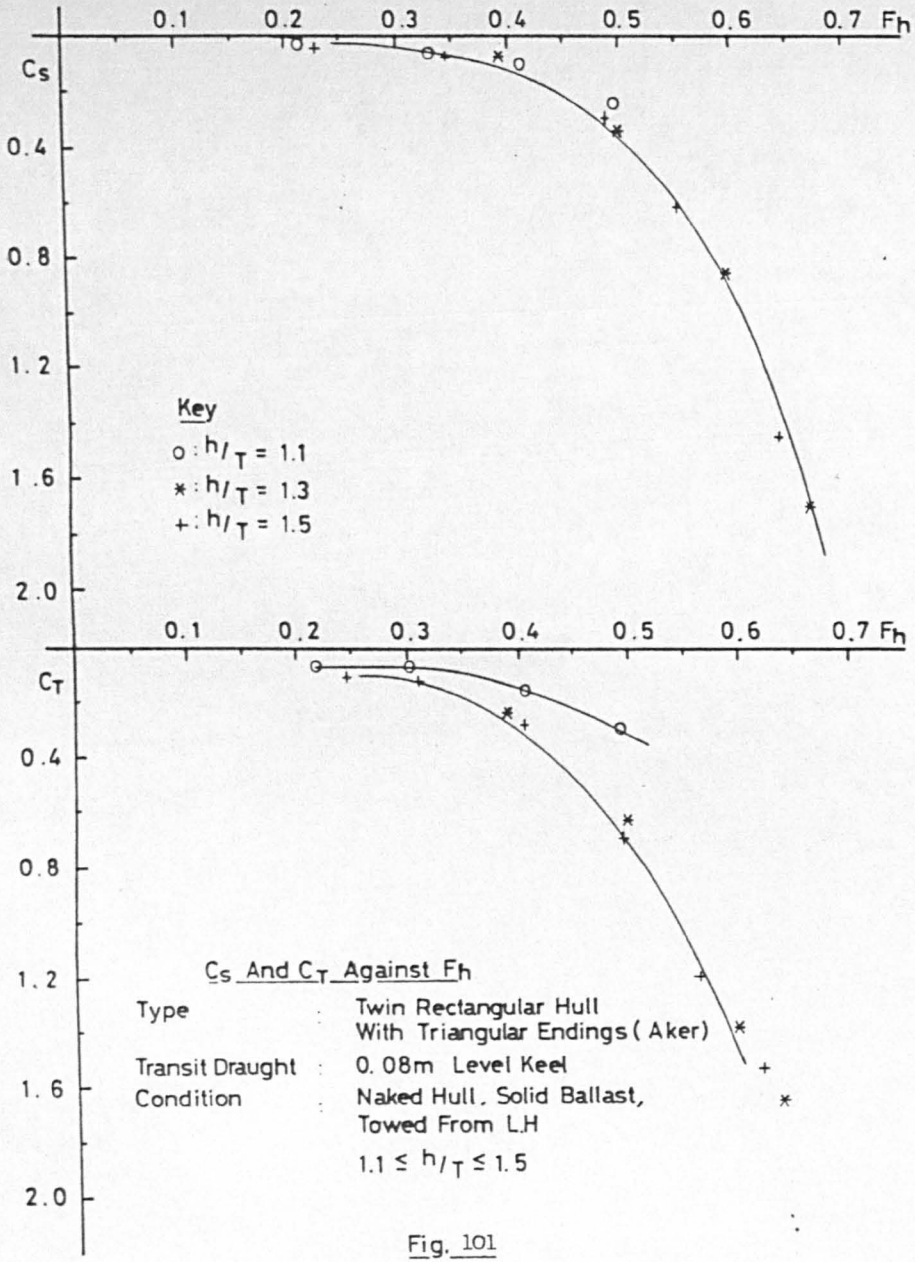

Fig. 101

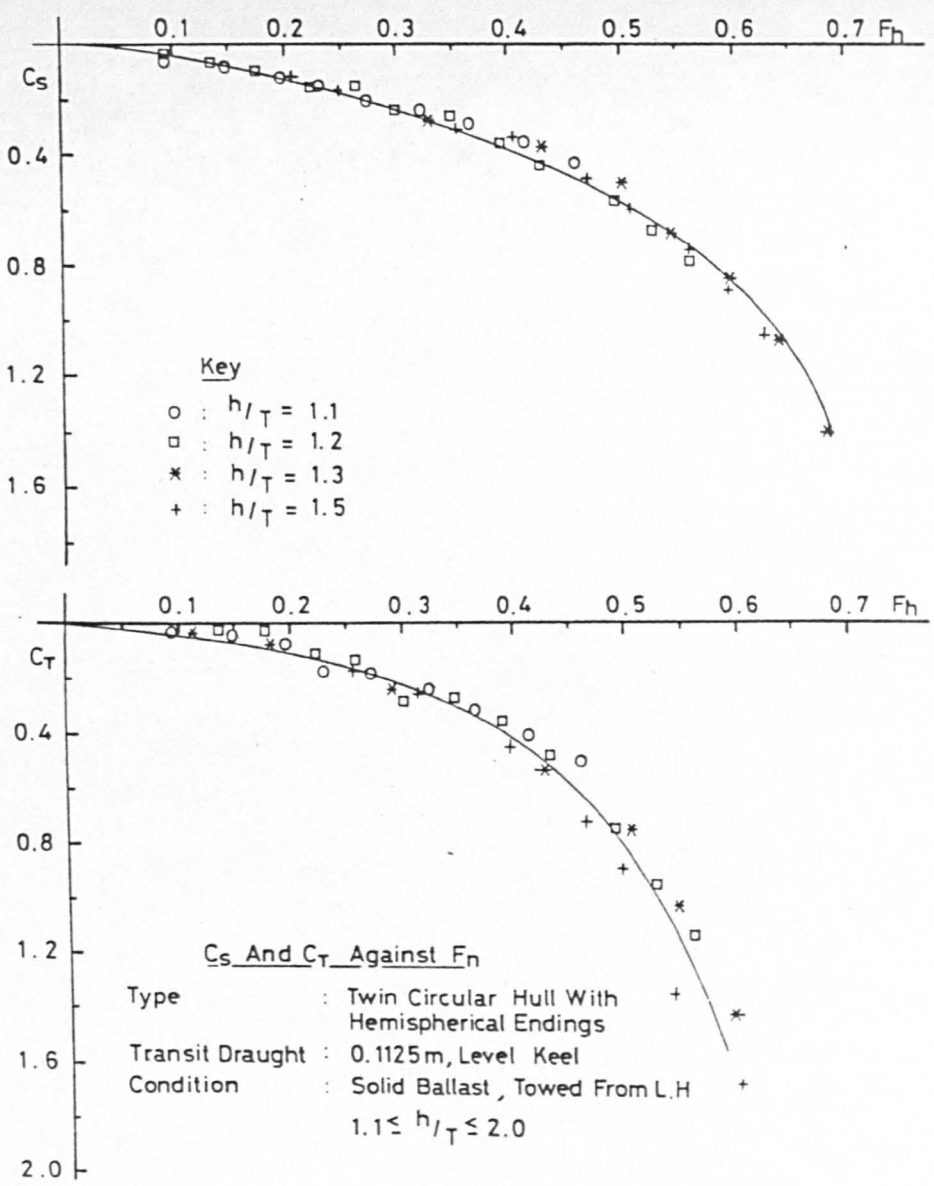

Fig 100

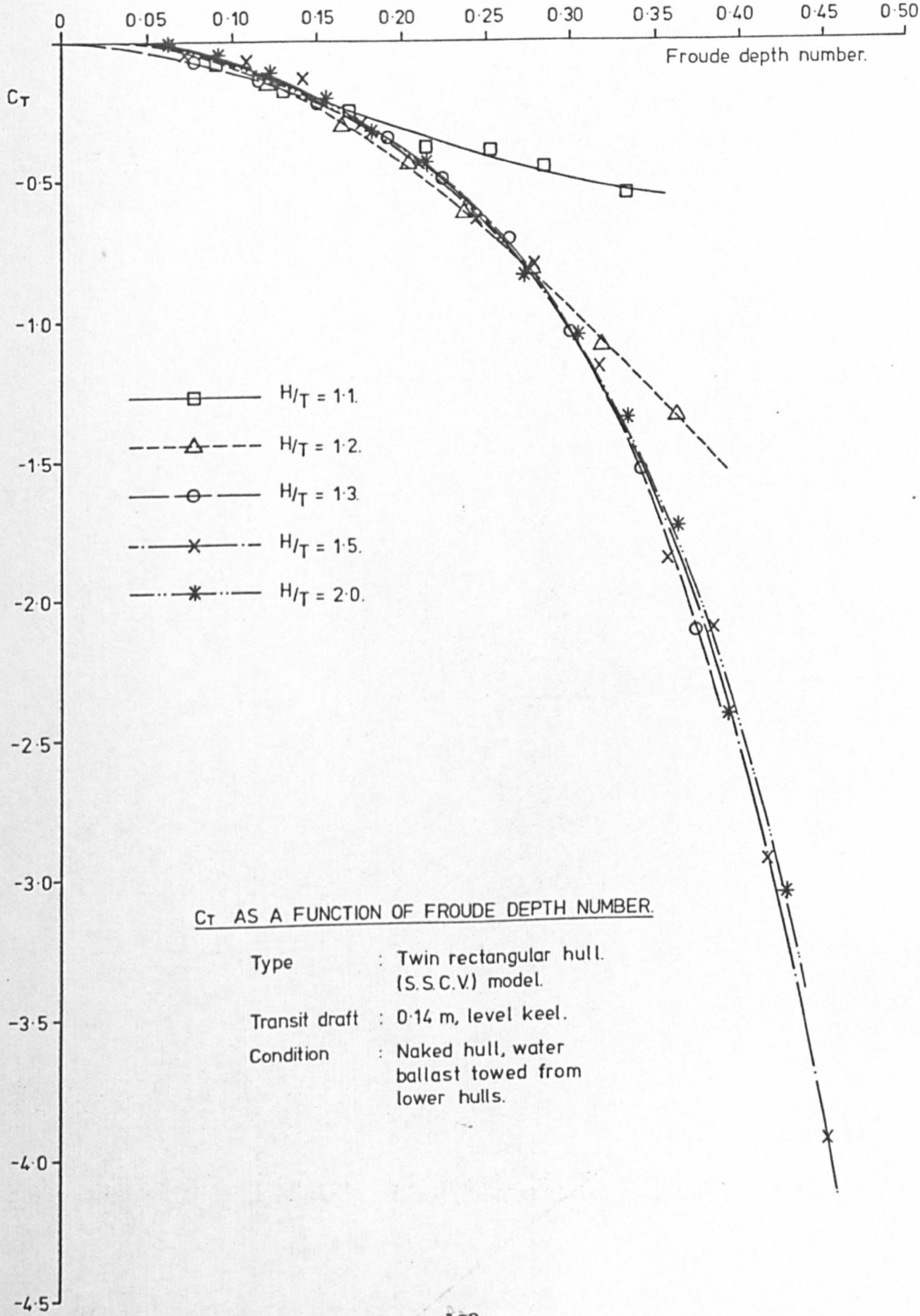

C_T AS A FUNCTION OF FROUDE DEPTH NUMBER.

Type : Twin rectangular hull. (S.S.C.V.) model.

Transit draft : 0·14 m, level keel.

Condition : Naked hull, water ballast towed from lower hulls.

Figure 102

hulls. This creates regions of retarded flow, affecting the pressure distribution around the hulls. Simultaneously, boundary layer growth creates regions of of increased suctions over the stern. The combined effect of these phenomena is to induce a reduced trim-by-bow attitude with decrease in water depth as $h/T < 1.3$.

In physical terms, the results indicate that for a given F_h the total vertical force is not affected by depth-draught ratio. Only its distribution about the hulls is affected. Similar behaviour was observed for the "Aker" type platform, Fig.101, and for a square-shaped Gravity type model, see Seren et al [62]. This clear change in trimming behaviour was not observed with the twin circular-hulled model, Fig.105, which exhibited a qualitative, but not quantitative, behaviour common to full-form mono-hulls, see section (3.2). That is, only a slight dependence of the trim coefficient on the h/T ratio at a given F_h, which may be neglected to a first approximation.

It is to be noted that, in contrast with mono-hulls, twin-hull trim and sinkage effects assume equal magnitude throughout the F_h range examined. In common with mono-hulls, the relative importance of trim may exceed that of the mean sinkage at very-low underkeel clearances. It is particularly significant that trim changes are not reflected in the R/Δ curves. This suggests that for a given h/T the additional horizontal pressure forces induced

by the increase in the trim-by-bow, are balanced by a redistribution of vertical pressure forces over the bottom and stern region.

(7.3.a) Theoretical Difficulties

A short study was made of the applicability of the presently available theoretical approaches to the prediction of twin-hull squat. The theoretical approaches detailed in (2) are of limited value where the flow fields are significantly affected by viscous flow phenomena. The problems resulting from the inherent neglect of viscosity and non-linearities are discussed in detail in (3.3.a). The early separation and boundary-layer formation experienced by the bluff forms examined, results in a different "effective" body being presented to the flow. The immersed cross-sectional area is increased by the depth and width of the separation zones along its length, affecting the pressure distribution and, consequently, both mean sinkage and trim underway. The semi-empirical factors derived for full-form mono-hulls, see (3.2.b), were found to be unsuitable. Although the growth of the boundary-layer along the hull/sea-bed may be accounted for by calculating the boundary layer displacement thickness along the length of both hulls, the resulting simulation did not agree with experiment as the bottom was approached. The approach predicts grounding by-the-stern, while the naked-hull experiments show that grounding occurs by-the-bow.

Moreover, owing to the symmetry of the demi-hulls, the theories detailed in (2) predict a constant pressure value along the hull length. This is in contrast with the above experimentally derived data, which shows that for bluff-forms the trim component is of great importance. In fact, to a first approximation, a doubling of the mean sinkage component appears to yield a good approximation to the overall squat experienced by the twin-hulls examined. Although the qualitative behaviour of twin-hulls is similar to that of mono-hulls, there is a significant quantitative difference which is influenced by the exact geometry of the demi-hulls. Owing to the wide range of contributing factors beyond the capability of presently available mathematical models, it follows that theoretical results must be supplemented and modified through reference to systematic experimental data. Only in this manner can the complicated effects of viscosity, self-propulsion, hull wave-system etc. be approximately accounted for. This is not possible at present, since considerably more systematic model tests are required to determine and incorporate reasonable empirical factors and confirm the behaviour characterists for the hull geometries in service.

(7.4) Model/Full-Scale Extrapolation

Separation is the key phenomenon affecting the behaviour of the twin-hulled forms dealt with in this chapter. The phenomenon itself remains enigmatic and is, at present, best understood in terms of its consequences.

The latter are discussed in section (5.1) from which it is evident that there is a fundamental interaction between the body and its separated flow, particularly in the near-wake region, which is influenced (amongst others) by the location of the point of separation. It is also clear that when the flow over the forebody becomes turbulent, significant changes in the forces acting on the body occur. There is at present, however, a large gap between the highest R_N attained by experiments and the R_N encountered full-scale. The problem is somewhat complicated by the fact that the majority of the experimental observations at higher R_N do not consider the physical movement of the body, i.e. its sinkage and trim. The movement of a body will alter its boundary-layer characteristics, thus influencing the position of the points of separation and transition (on bodies with movable separation points). In shallow-water, the accelerating flow will tend to shift the points of transition and separation to higher R_N. In the absence of full-scale data, deductive reasoning is applied to estimate the qualitative effects of scale on the resistance, sinkage and trim of towed, twin-hulled platforms in the transit draught condition.

Skin-friction is but a small component of the total measured resistance of a bluff-body, see section (5.1). The full-scale skin-friction component is only slightly reduced from that of the model and any correction, including the allowance for the increased back-flow velocities in shallow-water, should be very small and

within the expected accuracy of the experiment. This applies to demi-hulls with either fixed or movable separation points.

A reasonable conjecture is that dramatic changes are not likely to occur in the boundary layers of twin-hulls with fixed separation points at R_N much higher than those examined in this thesis. It may then be assumed that for such bodies the full-scale flow conditions are reasonably reproduced on model scale and, to a first order, the total resistance may be calculated using the viscous form and frictional resistance components determined on model scale but corrected for the "back-flow" effect and side-by-side interference. Sinkage and trim may then also be scaled directly from model to ship without appreciable error. The sinkage and trim components in the transit draught condition are not influenced by the side-by-side interference effects within the normal range of hull spacings employed full-scale.

This need not be the case for the cylindrical hulls with hemispherical endings (or other bodies without sharp edges) where the form resistance, depending on the surface roughness and free-stream turbulence, may be sensitive to R_N. In this case, model resistance will overestimate the full scale, since the latter normally have a lower form and frictional drag coefficients. Unlike their horizontal (resistance) counterpart, for which R_N dependent drag coefficients exist, no analogous sinkage and trim data

exists to assist full-scale estimation. This is of particular importance for bodies with movable separation points. For example, lift force data are far less plentiful and less consistent than drag force data. Indications are that the lift force also undergoes a dramatic change in the range of the critical R_N, yielding generally lower values at post-critical R_N. This suggests lower sinkage values full-scale. Hence, linear scaling of the sinkage results will tend to err conservatively. The lower frictional and form drag coefficients also suggest lower trim values full-scale for forms with movable separation points. The results obtained during the blockage experiments of section (5.2), indicate that, outwith the critical R_N range, the small changes experienced by the trim component due to change in scale, will be difficult to detect experimentally. It is evident, however, that full-scale data is necessary to verify the above and establish correlation with more confidence.

CHAPTER 8

Summary of Conclusions

It was shown that although the available hydrodynamic and hydraulic models provide a valuable insight into the problem of ship-to-bottom interaction in shallow water, a universally applicable theory, which allows a routine solution with arbitrary Froude depth number and lateral restrictions, does not exist at present. The experimental work demonstrated limitations and illustrated features not apparent from the theoretical studies by examining relevant aspects of mono-hull and multi-hull behaviour in laterally restricted and unrestricted shallow water.

The appropriate theoretical basis was found to be a combination of the hydraulic and hydrodynamic approaches. Owing to the wide range of contributing factors and because the available theoretical concepts are based on inherent simplifications, empirical correction factors were shown to play an important role in connecting theory and experiment. A computer program was written based on a semi-empirical approach and its utility in predicting mono-hull squat in restricted water demonstrated by comparison with experiment. The method is broadly applicable to conventional full-form mono-hull models, towed or

self-propelled at steady speed in shallow water of uniform depth and any width. Extrapolation to full-scale is generally uncertain and, at present, is provisionally limited to speeds less than 12 knots in the load draught, level-keel condition.

Experiments conducted on hulls with fixed and movable separation points indicated that, in principle, the prediction of multi-hull squat in the transit draught condition, may be accomplished by the same approach. However, the wide range of additional contributing factors, combined with the limited empirical data available, do not permit an extension of the mono-hull semi-empirical procedure at present.

The work provided a useful compedium of information on a wide range of aspects of mono-hull and multi-hull behaviour in restricted water with broader experimental and practical applications. The detailed conclusions resulting from the study follow.

(8.1) Mono-hulls

In the towed condition, the mono-hull laterally unrestricted C_S and C_T coefficients were found to be independent of the depth-draught ratio at a given F_h. Under close-to-grounding conditions, the importance of the trim component of squat was shown to equal that of the mean sinkage. The hydrodynamic approach was found to provide a

rough quantitative prediction, underestimating the experimental results. Based on the actual tank width, the hydraulic model considerably underestimated both sinkage and trim in laterally unrestricted shallow-water. Employing a fictitious channel width of one ship length, good agreement with the experimental mean sinkage was obtained. The trim remained, however, considerably underestimated. When self-propelled, the same model exhibited a clear dependence of the C_S and C_T on the depth-draught ratio at a set F_h. Self-propulsion was found to increase the mean sinkage by a steady 15%, independent of h/T or F_h. The effect of self-propulsion on trim was more complicated and a function of both h/T and F_h. In general, self-propulsion induced a decrease in trim-by-bow in comparison with that when towed. Good agreement was found with the semi-empirical procedures suggested by Dand and Ferguson [23], which allowed the correction of the sinkage and trim obtained using the hydraulic model to the "3-D" towed and self-propelled modes.

The channel experiments indicated a slight dependence of C_S and C_T on the h/T for a set F_h for the towed model. The finite-width hydrodynamic theory was found to provide poor agreement with experiment and was unable to account for the effects of limiting speed. Both approaches failed to predict the sudden reversal in trim upon grounding. The effects of self-propulsion did not appear to be affected by the presence of side-walls.

The introduction of side walls was shown to induce a significant increase in sinkage but a very small increase in trim underway. The experiments confirmed the theoretical deductions of Tuck [75] in both tendency and magnitude, indicating that the ratios of the infinite to finite-width mean sinkage and trim lie on universal curves. This agreement was shown not be affected by the depth-draught ratio or self-propulsion effects.

Initial (at-rest) trim and draught are an important factor in the subsequent sinkage and trim experienced and must be accounted for. Maintaining a given displacement (or mean sinkage) affected the subsequent trim underway only. Changes in both the initial trim and initial draught, altered both components underway. Particular care should be taken in the ballast draught (trim-by-stern) condition as the model experiments indicated that the subsequent behaviour may be contrary to intuition. The experiments showed that in the ballast draught, trim-by-stern condition in shallow water, the inherent tendency to trim-by-bow is neutralized. Consequently, the ship experienced a change in the mean sinkage only, which induced a grounding at the stern.

Upon approaching trenches or ridges across the fairway, where the vessel moved relatively suddenly from deeper to shallower water, the transient behaviour induced a maximum instantaneous draught which was greater than the steady-state draught underway. The results indicated that,

in the load draught, level-keel condition, the bow had a dangerous tendency to move towards the sandbank. It appeared to "sense" the incipience of a shallower region. The stern exhibited a similar attraction force as the bow left the sandbank. In the ballast, trim-by-stern condition, the results showed that the vessel's stern will encounter a potentially dangerous situation, frequently upon leaving the sandbank. Analysis of the results shows that the approximate grounding speed over the shallow region may be obtained using steady-state data, provided the depth of water used is the estimated minimum.

The theory/experiment comparisons suggest that the theoretical models must be supplemented and modified by reference to systematic experimental data to cater efficiently for hull form, viscosity, non-linearities, hull-wave system and self-propulsion, particularly for a reasonable prediction of trim. Bulbous-bows appeared to modify only the trim underway, but had negligible effects on the close-to-grounding behaviour.

(8.2) Multi-hulls

The results suggest that the Conn theoretical blockage formula provides a reasonable first approximation to the deep-water increase in back-flow velocity induced by blockage on a model with fixed separation points. The effect of blockage on the trim coefficient, C_T, was negligible in both deep and shallow water. The mean

sinkage coefficient increased with an increase in blockage and was responsible for any changes in the measured model resistance. This may not be the case for bodies with movable separation points, for which small changes in flow conditions may induce significant transitional changes in the flow regime.

Turbulence stimulation on bodies with movable separation points, is of no practical value over the working range of full-scale platforms in shallow water, since the requirement of trip-wire effectiveness at low speeds leads to large wire diameters. The increase in trim and resistance was predominantly due to the wire self-drag which is normally impossible to separate from purely turbulent effects. Application of the normal trip-wire criteria to bodies with fixed separation points may yield "overstimulation" phenomenon and resulted in erroneous sinkage and trim measurments. The results suggested that the introduction of a disturbance into a separated (and already turbulent) flow, may have advantageous applications.

Varying the towing point height from the lower to the upper deck increased the subsequent trim-by-bow and resistance without affecting the mean sinkage. A theoretical method to correct for the effect of towing point height on trim was examined and argued to be sufficiently accurate except for extremely shallow water.

Changing the type of ballast from liquid to solid had no measurable influence on the measured resistance and squat of the particular arrangement examined. It was suggested that this conclusion will not be valid when the free-surface effects are considerable.

Comparisons with an "equivalent" mono-hull, (ie. the catamaran with no hull spacing) showed that the catamaran configuration had advantages where water depth was restricted. Upon splitting the "equivalent" mono-hull both the mean sinkage and trim-by-bow underway were reduced. The advantages in resistance became evident only in the higher speed range. Varying the hull spacing had no effect on the subsequent squat, but resistance was steadily increased as hull spacing was reduced. The bistable behaviour normally observed during experiments with bluff-bodies in a side-by-side arrangement was not detected. The exhibited behaviour was found to be common with that of streamlined struts arranged side-by-side. A plausible explanation is that that the bluff demi-hull and separated flow combined to form a more streamlined body.

Changing the SWATH hull-ending shape from hemispherical to elliptical, increased the mean sinkage somewhat but decreased the trim-by-bow. The overall effect was to decrease the measured total resistance. The influence under close-to-grounding conditions was of no practical significance.

Experiments conducted with a SWATH fitted with a control-surface spanning the hulls aft, indicate that in addition to the obvious effect of counteracting the inherent tendency to trim-by-bow, the control-surface increases both mean sinkage and resistance underway. Increasing the angle-of-attack increases the total resistance penalty. The change in total resistance in comparison with that without the foil, however, decreases as water depth was reduced. It was suggested that this increased foil effectiveness at lower underkeel clearances was due to wing-in-ground effects from the proximity of the bottom. The experimental procedure provided only a gross assessment of the control-surface characteristics, since the interaction effects between it and the bare-hull were inherently included in the measurements.

Analysis of a number of twin-hulled offshore platforms in the transit draught, level-keel condition and a SWATH vessel, indicated that a plot of R_T/Δ and C_S against F_h yields unique curves, independent of the depth-draught ratio, over the range $1.1 \leq h/T \leq 1.5$. The trim behaviour is complex and sensistive to the immersed geometry. The trim coefficient of the rectangular-hulled platforms was clearly influenced by bottom proximity. The more streamlined SWATH or twin circular-hulled model, exhibited only a minor dependence on the depth-draught ratio. In contrast with mono-hulls, mean sinkage and trim assumed approximately equal magnitude throughout the speed range. It was suggested that the extrapolation of the sinkage,

trim and resistance measured on models with fixed separation points, is possible without appreciable error. In the case of models with movable separation points, outwith the critical R_N regime, extrapolation will err conservatively.

(8.3) Recommendations for Future Work

During this work it has become evident that much more research into the wider range of individual factors affecting the vessel underkeel clearance is required. With a view to extending the framework of the existing monohull computer program, it is recommended that future research be divided between theory and experiment and concentrate on,

(a) the influence of the vertical motions caused by waves and swell, bearing in mind the type of seas likely in restricted water and the problems that may arise due to squat occuring simultaneously.

(b) the effects of current, tide and wind, the longitudinal component of which will affect squat, particularly at low speeds. The influence of wind will assume particular importance in the ballast conditions.

(c) the effect of scale in shallow water, particularly in the trimmed conditions. There is insufficient quantified model/full scale correlation data at very low depth-draught ratios.

(d) a systematic programme embracing a variety of irregular-shaped channels,

(e) the effect of a steady angle of heel, induced by rudder action, waterway bends, cargo shift, wind, or by other means.

The above recommendations should be carried out with the same monohull model used throughout this thesis and, ideally, on the equivalent full-scale ship. Additional research should also be carried out into,

(g) the effect of bottom topography, to verify the observed transient squat phenomena in restricted water and
(h) the influence on squat of those parameters which are chosen at the vessel's design stage and, therefore, "fixed". The most relevant monohull variables appear to be, the block coefficient, the L/B and B/T ratios, the longitudinal radius of gyration and position of the LCB. This study should initially be carried out in the naked hull condition, with represenatative models of modern vessels.

The above recommendations apply equally well to multi-hulls in transit. However, at the present state-of-the-art of multi-hull squat, it is recommended to initially concentrate on,

(i) the collection of experimental data on the sinkage and trim of various multi-hulls. Considerably more systematic model data are required to determine and incorporate reasonable empirical factors and confirm behaviour

characteristics. This task should be assisted by adopting the practice of conducting sinkage and trim measurements in conjuction with resistance tests.

(j) the effect of self-propulsion on squat in restricted water, in the transit draught condition,

(k) the effect of increasing draught from the transit to the operational (i.e. that at which the columns are also submerged) in restricted water, with particular emphasis on the influence of intereference effects on squat.

References

1. Abramowitz, M. and Stegun, I.A., "Handbook of Mathematical Functions", National Bureau of Standards, U.S. Department of Commerce, June 1964.

2. Acevedo, M.L., "On the Use of Trip Wires as Turbulence Stimulators", Schiffstechnik, Heft 21, 1957.

3. Albone, C.M., "Fortran Programmes for Axisymmetric Potential Flow Around Closed and Semi-Infinite Bodies", ARC, CP No. 1216, 1972.

4. Bazilevsky, Y.S., Poostoshniy, A.F. and Stumpf, V.M., "Modern Means to Control Flow Separation on Full-Form Models", Proc. 12th ITTC, Rome, 1969, pp.249-252.

5. Beck, R.F., "Forces and Moments on a Ship Moving in a Shallow Channel", Journal of Ship Research, Vol.21, No.2, 1977.

6. Beck, R.F., Newman, J.N., and Tuck, E.O., "Hydrodynamic Forces on Ships in Dredged Channels", Journal of Ship Research, No.19, pp.66-171.

7. Berry, L.W., "Propeller Boundary Layer Flow and Scale Effect", Ship Division Report No.12, NPL, 1959

8. Biermann, D. and Herrnstein, W.H., "The Interference between Struts in Various Combinations", NACA Report 468, 1933.

9. Bradley, C., Ferguson, A.M. and McGregor, R.C., "Hydrodynamic Laboratory Bed Analysis (Part 1)", UOG Report NAOE-HL-79-11C, 1979.

10. Burke, R.J., "The Consequences of Extreme Loadings on Ship Structures", Proc. Extreme Loads Symp., Arlington, 1981, pp.5-18.

11. Comstock, J.P.(Editor) "Principles of Naval Architecture", SNAME New York, 1967.

12. Conn, J.F.C. and Ferguson, A.M., "Results Obtained with a Series of Geometrically Similar Models", TRINA, Vol.110, 1968, p.255.

13. Constantine, T. "The Behaviour of Ships Moving in Restricted Waterways", Proceedings of the Institution of Civil Engineers, Vol.19, 1961, p.549.

14. Crane, C.L., "Maneuvring Trials of a 278,000 DWT Tanker in Shallow and Deep Waters", TSNAME, Vol.87, pp.251-283.

15. Curle, N. and Skan S.W., "Approximate Methods for Predicting Separation Properties of Laminar Boundary Layers", The Aeronautical Quarterly, August 1957.

16. Dand, I.W., "Some Measurements of Squat in Shallow Water", NPL Ship Division, TM No.294, November 1970.

17. Dand, I.W., "Squat Measurements: Bulbous Bow Ships in Shallow Water", NPL Ship Division, TM No.305, March 1971.

18. Dand, I.W., "Shallow Water Work at Ship Division NPL", NPL TM No.325, January 1972.

19. Dand, I.W., "Full Form Ships in Shallow Water; Some Methods for the Prediction of Squat in Subcritical Flows", NPL Ship Division, Report 160, January 1972.

20. Dand, I.W., "Some Calculations Illustrating the Effect of Initial Trim on the Squat of Full Ships in Shallow Water", NPL Ship Division, TM No.334, April 1972.

21. Dand I.W., "The Wavemaking Resistance of Ships; Vertical Force and Form Resistance of a Hull at Uniform Velocity", Ph.D Thesis, The Univeristy of Glasgow, 1967.

22. Dand, I.W. and Ferguson, A.M., "Squat", Proc. Conf. on Ship Behaviour in Confined Waters, 1974.

23. Dand I.W. and Ferguson, A.M. "The Squat of Full Ships in Shallow Water", TRINA, Vol.115, 1973.

24. Dickson,A.F., "Underkeel Clearance", Journal of Inst. of Navigation, Vol.20, No.4, 1967, pp.363-387.

25. Eng, K.S. and Breslin, P., "Theoretical-Experimental Study of the Effect of Viscosity on Wave Resistance", Davidson Laboratory Report 1236, Oct.1967.

26. Engineering Sciences Data Unit, "Fluid Mechanics, External Flow-Mean Loads on Structures", Wind Engineering Sub-Series,
Vol.2a, "Mean Loads on Structures", March 1980.
Vol.3, "Fluctuating Loads and Response of Structures", July 1981.

27. Ferguson, A.M., "Factors Affecting the Components of Ship Resistance", Ph.D Thesis, University of Glasgow, 1976.

28. Ferguson, A.M., Seren, D.B., McGregor, R.C., "Experimental Investigation of Grounding on a Shoaling Sandbank", The Naval Architect, Journal of RINA, Sept.1982.

29. Ferguson, A.M., "Full Scale Measurements of Sinkage and Trim Due to Forward Speed and Underkeel Clearance for 250,000 ton Oil Tanker", Report for Chamber of Shipping, University of Glasgow, January 1972.

30. Friedrichs, K.O., "On the Derivation of the Shallow-water Theory", Appendix to J.J. Stoker, Comm. on Pure and Applied Maths, Vol.1,1948, pp.81-85

31. Gadd, G.E., "A Method of Calculating the Flows over Hulls", TRINA, Vol.112, 1970, p.335.

32. Graff, W., Kracht, A., and Weinblum, G. "Some Extensions of D.W. Taylors Standard Series", TSNAME 1964, pp. 374-403.

33. Grekoussis, C., and Miller, N.S., "The Resistance of Semi-Submersibles", Joint RINA-IESS Conf., Paper No.1413, Feb.1978.

34. Guilloton, R., "A Note on the Experimental Determination of Wave Resistance", TRINA, Vol.96, 1954.

35. Hogner, E., "Eine Interpolationsformel fur den Wellenwiderstand Von Schiffen", J.S.T.G., Bd.33, 1932.

36. Horn, F., "Einfluss der Form auf dem Reibungswiderstand", Verandlungen der Tagung der leiter der Schleppversuchsanstalten, Berlin 1937.

37. Hooft, J.P., "On the Critical Speed Range of Ships in Restricted Waterways", International Shipbuilding Progress, May 1969, p.145.

38. Hooft, J.P., "The Behaviour of a Ship at Head Waves at Restricted Water Depths", NSS/TNO Report No.188S, 1974.

39. Joukowski, N.E., "On the Wave of Translation", Complete Works 4, ONTI, 1937.

40. Kaa, E.J. van de, "Power and Speed of Push Tows in Canals", Symp. on Aspects of Navigability, Vol.3, Delft, 1978.

41. Kinoshita, M., "On the Restricted Water Effect on Ship Resistance", Society of Naval Architects of Japan, Spring Meeting 1946, JSNA, Vol.76, 1954.

42. Kreitner, J., "Uber dem Schiffwiderstand auf Beschrenkten Wasser", W.R.H., Vol.15, 1934.

43. Landweber, L., "Potential Flow About Bodies of Revolution and Symmetric Two-Dimesional Forms", Iowa Inst. of Hydraulic Research, Dec. 1959.

44. Lea , G.K. and Feldman, J.P., "Transcrtical Flow Past Slender Ships", Proc. 10th Symp. on Naval Hydrodynamics, 1974, pp.1527-1542.

45. Maruo, H., "Calculation of the Wave Resistance of Ships, the Draught of which is as Small as the Beam", Journal of the Zosen Kiokai, Vol.112, 1962.

46. Maruo, H. and Tachibana, T., "An Invstigation into the Sinkage of a Ship at Transcritical Speed in Shallow Water", Society of the Naval Arch. of Japan, Vol.19, 1981, pp.29-35.

47. McCarthy, J.H., Power, J.L. and Huang, T.T., "The Roles of Transition, Laminar Separation, and Turbulence Stimulation in the Analysis of Axisymmetric Body Drag", 11th Symposium on Naval Hydrodynamics, London, 1976.

48. McNown, J.S.,"Sinkage and Resistance of Ships in Channels", Jour. of Waterways, Harbours and Coastal Div., ASCE, 1975.

49. Mei, C.C., "Flow Around a Thin Body Moving in Shallow Water", Jour. of Fluid Mechanics, Vol.77, 1976, pp.737-752.

50. Mizayawa, M., "A Study of the Flow Around a Catamaran", J.S.N.A. Japan, Vol.145, 1979.

51. Michell, J.H., "The Wave Resistance of a Ship", Phil. Mag., 1898, p.106.

52. Moody, C.G., "The Handling of Ships through a Widened and Asymmetrically Deepened Section of Gaillard Cut in the Panama Canal", DTMB Report 1705, August 1964.

53. National Ports Council, "Port Approach Design- A Survey of Ship Behaviour Studies", (2 Vols), London, 1975.

54. National Ports Council, "Ship Behaviour in Ports and Their Approaches-"
Part 1- "Bow and Stern Sinkage Caused by Interaction Between Passing Ships", ISBN-0-86073-0360, Jan.1980.

Part 2- "Additional Sinkage caused by Sailing in the Proximity of a Channel Bank", ISBN-0-86073-048-4, August 1980.

55. Newman, J.N. and Tuck E.O., "Current Progress in the Slender Body Theory for Ship Motions", Proc. 5th Symp. on Naval Hydrodynamics, 1964, pp.129-166.

56. Peters, A.S. and Stoker, J.J., "The Motion of a Ship as a Floating Rigid Body in a Seaway", Inst. of Math. Sciences, Report No.IMM-203, NY Univ., 1954.

57. Roshko, A., "On the Wake and Drag of Bluff Bodies", Journal of the Aeronautical Sciences, Feb.1955, pp.124-132.

58. Saunders, H.E., "Hydrodynamics in Ship Design Vol. 1,2,3", SNAME, New York, 1957.

59. Schlichting, H., "Boundary-Layer Theory", Sixth Ed., McGraw-Hill Book Company, New York, N.Y. ,1968.

60. Schuster, S. "Untersuchungen uber Stromungs - und Widerstandsuerhatrisse bei der Fahrt von Schiffen in Beschrantem Wasser", J.S.T.G., 1952.

61. Seren, D.B., Ferguson, A.M. and McGregor R.C., "Squat-An Examination of Two Practical Prediction Methods", The Naval Architect, Jour. of RINA, Sept. 1981.

62. Seren D.B., Ferguson A.M. and McGregor R.C., "Model Tests on a Circular Hull and a Gravity Platform in Shallow Water", UOG/NAOE Report NAOE-HL-79-09, 1979.

63. Seren, D.B., Ferguson A.M. and McGregor R.C., "Computer Analysis of Sinkage and Trim of Large Ships in Shallow Water", UOG/NAOE Report NAOE-79-12 (Rev 1), 1981.

64. Seren, D.B., Ferguson, A.M. and McGregor R.C., "An Investigation into the Shallow Water Drag and Squatting Behaviour of a Twin Rectangular-Hull Semi-Submersible in Steady Motion at Sub-Critical Speeds. Part 1", UOG/NAOE Report NAOE-HL-79-27, 1979.
Part 2 - "The Effect of Variation in Type of Ballast", UOG/NAOE Report NAOE-HL-80-01, 1980.
Part 3 - "The Effect of Changing the Point of Application of the Towing Force", UOG/NAOE Report NAOE-HL-80-02, 1980.

65. Seren, D.B., Smith, S.N., Ferguson, A.M. and McGregor R.C., "The Shallow Water Performance of a Three-Hulled Semi-Submersible in Steady Motion - Part 1", UOG/NAOE Report NAOE-HL-80-09, 1980.
Part 3 - "The Effect of Turbulence Stimulators on the Sinkage, Trim and Total Resistance", UOG/NAOE Report NAOE-HL-80-24, 1980.

66. Seren, D.B., "The Effect of Hull Spacing on the Resistance and Squat of a Full-Form Twin-Hull Vessel with Reference to the Linearised Wave Resistance Theory", UOG/NAOE Report NAOE-HL-80-27, 1980.

67. Sjostrom, C.H., "Effect of Shallow Water on Speed and Trim", Naval Engineers Journal , Vol.79, April 1967, p.271.

68. Smith, S.N., "Design and Hydrodynamic Assessment of a Small Semi-Submersible (SWATH) Research Vessel, Ph.D Thesis, University of Glasgow, 1982.

69. Sneddon, I.N., "Fourier Transforms", McGraw-Hill Book Company, New-York, 1951.

70. Sorensen, R.M., "Waves Generated by Model Ship Hull", Journal of the Waterways and Harbour Div., Proc. ASCE, Vol.95., No.WW4, 1969.

71. Stoker J.J, "Water Waves", Interscience Publishers Inc., New-York, 1957.

72. Tothill, J.T. "Ships in Restricted Channels, a Correlation of Model Tests, Field Measurements and Theory." Marine Technology, April 1967, p.111.

73. Tuck, E.O., "The Steady Motion of a Slender Ship", Ph.D. Thesis, Cambridge, 1963.

74. Tuck, E.O., "Shallow-Water Flows Past Slender Bodies", Journal of Fluid Mechanics, Vol. 26, 1966, pp.81-95.

75. Tuck, E.O., "Sinkage and Trim in Shallow Water of Finite Width", Schiffstechnik, Band 14, Heft 73, 1967, pp.92-94.

76. Tuck, E.O. and Taylor, P.J., "Shallow Water Problems in Ship Hydrodynamics", Proc. 8th Symposium on Naval Hydrodynamics, Pasadena, August 1970.

77. Tuck, E.O., "Ship Motions in Shallow Water", Journal of Ship Research, Decmber 1970, p.317.

78. Tuck, E.O., "Some Classical Water-wave Problems in Varying Depth", I.U.T.A.M. Symp. Waves on Water of Varying Depth, Aust. Acad. Sci., Canberra, 1976, pp.9-20.

79. Van Dyke, M.D., "Perturbation Methods in Fluid Mechanics", New York, Academic Press, 1964.

80. Vermeer, H., "The Behaviour of Ships in Restricted Water", Intnl. Shipbldg. Progress, 1977, pp.323-336.

81. Vossers, G., "Some Applications of Slender Body Theory in Hydrodynamics", Doctoral Dissertation, Delft, 1962.

82. Wehausen, J.V., "An Approach to Thin Ship Theory", Int. Seminar on Theoretical Wave Resistance, Ann Arbor, 1963, p.821.

83. Weinblum, G., "Wellenwiderstand auf Bechranktem Wasser", J.S.T.G., 1938.

84. Wigley, W.C.S., "The Collected Papers of Sir Thomas Havelock", ONR/ACR-103, 1963.

85. Wilson, R.A, Savitsky, M. and Stevens, M.J., "Status of Hydrodynamic Technology as Related to Model Tests of High Speed Marine Vehicles", DTNSRDC Report 81/026, 1981.

86. Yamagouchi, A., Honda, K., Matsuki, S. and Hara, K. "Model Test on Sinkage of Vessel Underway in Restricted Channel." Journal of the Nautical Society of Japan, January 1967.

87. Yamagouchi, A., Honda, K., Matsuki, S., Mirota, M. and Hara, K. "Full Scale Test on Sinkage of Super Tanker through Shallow Water." Journal of the Nautical Society of Japan, January 1968, p.15.

88. Yeung, R.W., "Sinkage and Trim in First-Order Thin-Ship Theory", Journal of Ship Research, Vol.16, 1972, pp.47-59.

89. Zdravkovich, M.M., "Review of Flow Interference Between Two Circular Cylinders in Various Arrangements", Jour. of Fluids Eng., Trans. ASME, Vol.99, No.4, 1977, pp.618-633.

APPENDIX A

Finite-Width "Outer" Boundary-Value Problem Solution

The problem is formulated and outlined in section (2.3). The "outer" boundary-value problem solution is derived by applying a Fourier transform in x,

$$\psi(r,y) = \int_{-\infty}^{\infty} \exp(irx)\,\phi(x,y)\,dx \qquad \ldots\ldots \text{(A.1)}$$

to the relations (2.2.12), (2.2.17) and (2.3.1). Once the transform ψ has been found by solving the latter problem, the inverse formula,

$$\phi(x,y) = \frac{1}{2\pi} \int_{-\infty}^{\infty} \exp(-irx)\,\psi(r,y)\,dr \qquad \ldots\ldots \text{(A.2)}$$

yields the solution for ϕ .

Transforming (2.2.17) using (A.1) results in an ordinary differential equation,

$$\psi_{yy}(r,y) - \delta^2 r^2 \psi_y(r,y) = 0 \qquad \ldots\ldots \text{(A.3)}$$

The transform is similarly applied to the body boundary condition (2.2.12). Expressing the Fourier transform of the derivative of the ship cross-sectional area, S'(x), in

terms of the Fourier transform of S(x),

$$\psi_y(r,0_{\pm}) = \frac{\dot{\imath}rUS^*(r)}{2h} \qquad \ldots\ldots \text{(A.4)}$$

where,

$$S^*(r) = \int_{-L/2}^{L/2} \exp(irx)S(x)dx$$

is the Fourier transform of S(x).

Transforming (2.3.1),

$$\psi_y(r,\pm\tfrac{1}{2}W) = 0 \qquad \ldots\ldots \text{(A.5.a)}$$

and similarly, (2.3.2),

$$-\dot{\imath}r\,\psi(r,y) = 0 \longleftrightarrow \psi(r,y) = 0 \qquad \ldots\ldots \text{(A.5.b)}$$

$$\psi_y(r,y) = 0 \qquad \ldots\ldots \text{(A.5.c)}$$

as $x \longrightarrow \pm\,\infty$, $|y| < 1/2W$.

Expressing the ordinary differential equation in terms of an operator D,

$$(D^2 - \delta^2 r^2)\psi = 0$$

the auxillary equation is,

$$\lambda^2 - \delta^2 r^2 = 0$$

and its solution is,

$$\lambda = \pm r\delta \qquad \ldots\ldots \text{(A.6)}$$

Therefore, the solution of (A.3) is,

$$\psi(r,y) = A\exp(\lambda y) + B\exp(-\lambda y) \qquad \ldots\ldots \text{(A.7)}$$

and

$$\psi_y(r,y) = A\lambda\exp(\lambda y) - B\lambda\exp(-\lambda y) \qquad \ldots\ldots \text{(A.8)}$$

Applying boundary conditions (A.4) and (A.5) simulataneously to (A.8), the solution procedure may be expressed by determinants as follows,

$$\begin{bmatrix} 1 & -1 \\ \exp(\lambda\tfrac{1}{2}W) & -\exp(-\lambda\tfrac{1}{2}W) \end{bmatrix} \begin{bmatrix} A\lambda \\ B\lambda \end{bmatrix} = \begin{bmatrix} \frac{irUS^*(r)}{2h} \\ 0 \end{bmatrix} \qquad \ldots\ldots \text{(A.9)}$$

so that,

$$D = \begin{bmatrix} 1 & -1 \\ \exp(\lambda\tfrac{1}{2}W) & -\exp(-\lambda\tfrac{1}{2}W) \end{bmatrix} = \exp(\lambda\tfrac{1}{2}W) - \exp(-\lambda\tfrac{1}{2}W)$$

$$d1 = \begin{bmatrix} \frac{irUS^*(r)}{2h} & -1 \\ 0 & -\exp(-\lambda\tfrac{1}{2}W) \end{bmatrix} = \frac{-irUS^*(r)}{2h}\exp(-\lambda\tfrac{1}{2}W)$$

$$d2 = \begin{bmatrix} 1 & \frac{irUS^*(r)}{2h} \\ \exp(\lambda\tfrac{1}{2}W) & 0 \end{bmatrix} = \frac{-irUS^*(r)}{2h}\exp(\lambda\tfrac{1}{2}W)$$

Thus,

$$A\lambda = \frac{d1}{D} = \frac{\frac{irUS^*(r)}{2h}\exp(-\lambda\tfrac{1}{2}W)}{\exp(\lambda\tfrac{1}{2}W) - \exp(-\lambda\tfrac{1}{2}W)} \qquad \ldots\ldots \text{(A.10.a)}$$

$$B\lambda = \frac{d2}{D} = \frac{\frac{-irUS^*(r)}{2h}\exp(\lambda\tfrac{1}{2}W)}{\exp(\lambda\tfrac{1}{2}W) - \exp(-\lambda\tfrac{1}{2}W)} \qquad \ldots\ldots \text{(A.10.b)}$$

and inserting these values into (A.7) and (A.8), the following expressions for ψ (r,y) is obtained,

$$\psi(r,y) = \frac{iU}{2h\delta} S^*(r)\cosh[r\delta[|y| - \tfrac{1}{2}W]]\operatorname{cosech}(\tfrac{1}{2}Wr\delta)$$

$$\ldots\ldots \text{(A.11)}$$

where the modulus of y results from asymptotic behaviour considerations.

Inverting this result by means of (A.2) yields the velocity potential ϕ (x,y)

$$\phi(x,y) = \frac{iU}{4\pi h\delta}\int_{-\infty}^{\infty} \exp(-irx) S^*(r)\cosh[r\delta[|y| - \tfrac{1}{2}W]]\operatorname{cosech}(\tfrac{1}{2}Wr\delta)dr$$

$$\ldots\ldots \text{(A.12)}$$

APPENDIX B

An Approximate Solution - "Hydraulic Analogy" Approach

From continuity, (for symbols see Fig.3, section 2.4),

$$AU = (A-S(x) -W\Delta h)(U + u(x))$$

$$= AU-(S(x) + W\Delta h)U + Au(x)-(S(x) + W\Delta h)u(x) \quad \ldots\ldots \text{(B.1)}$$

Neglecting the $\Delta h u(x)$ term, as being of 2nd order,

$$\frac{u(x)}{U} = \frac{S(x) + W\Delta h}{A-S(x)-W\Delta h} \quad \ldots\ldots \text{(B.2)}$$

Neglecting the W Δh term in the denominator,

$$\frac{u(x)}{U} = \frac{S(x) + W\Delta h}{A-S(x)} \quad \ldots\ldots \text{(B.3)}$$

By Bernoulli's theorem,

$$\Delta h = \frac{Uu(x)}{2g} - \frac{(U(x))^2}{2g} \quad \ldots\ldots \text{(B.4)}$$

neglecting the $(u(x))^2/2g$ term, from (B.3),

$$[A-S(x)]u(x) = S(x)U + \frac{WU^2u(x)}{g} \quad \ldots\ldots \text{(B.5)}$$

Therefore, from equation (B.3),

$$u(x) = \frac{Um(x)}{1-m(x)-F_h^2} \qquad \ldots\ldots \text{(B.6)}$$

where $m(x)=S(x)/A$ is the local blockage.

APPENDIX C

Experimental Details, Set-up and Procedures

To furnish background information necessary for a proper evaluation of the test results, the experimental details are summarised.

(1) General

All the experiments were performed in the Hydrodynamics Laboratory Tank of the Dept. of Naval Architecture and Ocean Engineering at the University of Glasgow. Before commencing the experimental programme, a very detailed survey of the tank bottom was carried out and measures taken to provide a level smooth surface to permit experiments at very low water depths, see Bradley et al [9]. Shallow-water depths were obtained by lowering the tank water level as required. The tank dimensions are 76.2 m. x 4.6 m. x 2.3 m., for other details see Conn and Ferguson [12].

All the experiments were conducted with the model towed or self-propelled on the tank centerline, free in pitch, heave and surge but constrained otherwise. During the mono-hull towing tests, the towing point was kept at

the at-rest waterplane, exerting a negligible trimming moment. Unless stated to the contrary, no turbulence stimulators were attached. Total resistance and sinkages at both perpendiculars were measured in calm water conditions over a speed range up to the grounding speed at the particular depth examined. Resistance was monitored by a strain gauged cantilever of such a design as to allow for variations in water depth or towing point height. Sinkages at both perpendiculars were measured using linear displacement transducers which, in common with the strain gauged cantilever, were coupled to a multi-channel pen recorder. Sinkage measurements were measured from the tank carriage which served as an ideal reference and observation platform. Ground speed was measured by a radial grating device with both a visual and a digital print-out display. Tests at which the model grounded were repeated and observations made. Care was taken when calibrating, the strain bar being calibrated each day while the sinkage transducers were of necessity calibrated before starting experiments at a new depth. Water depth was measured at three places along the tank length by a special plumb with the particular depth marked off. The draught and trim condition of the model were rechecked before starting at each new depth and an appropriate waiting time between runs was observed. Temperature measurments were taken at 3 points along the tank length. At each point measurements were taken at the water surface and at a depth of 10 cm. The value of density and kinematic viscosity used were those appropriate to the temperature existing during the

particular experiment.

Values of the sinkage and resistance were taken from mean lines of the pen recorder traces. These traces always show some fluctuation about a mean value even when at steady speed. Readings were taken only when no significant fluctuations could be detected.

(2) Mono-hull Experiments

The representative full-form model used throughout the mono-hull experiments was a 1/52 scale model of the M.V. WELLPARK, constructed of glass reinforced plastic from lines supplied by the ship's builder, MHI of Japan. At the time of the experimental programme (1979-1982), the ship was a recently built (1977), ocean going bulk-carrier with principal dimensions as follows,

LBP = 160.0 m

B = 27.2 m.

T = 10.19 m.

C_B = 0.8

Δ = 37,000 tonnes

See Fig.R1 for full-scale photograph. No rudder or other appendages, except the propeller, were fitted to the model.

Fig. R1

M.V. Wellpark Experiments

Distribution of Model Ballast

(a) LOAD DRAUGHT CONDITION

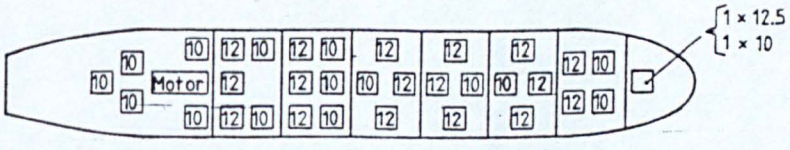

APPROX. WEIGHT OF BALLAST

(18 × 12.5) lbs. + (16 × 10) lbs. = 385.0 lbs.

(d) BALLAST CONDITION

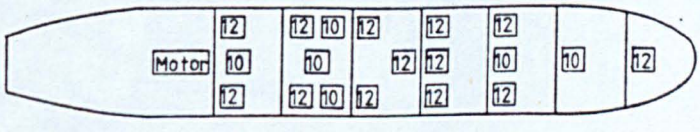

APPROX. WEIGHT OF BALLAST

(13 × 12.5) lbs. + (6 × 10) lbs. = 222.5 lbs.

CONDITIONS

(a) Load Draught; 0.174 M, Level Keel

(d) Ballast Draught; 0.113 M Fwd.

0.133 M Aft

Figure R2

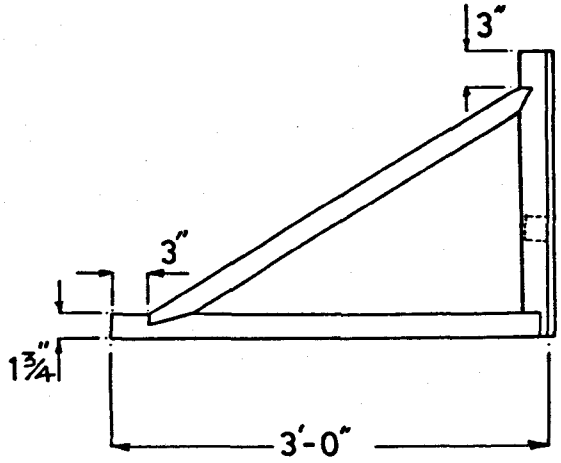

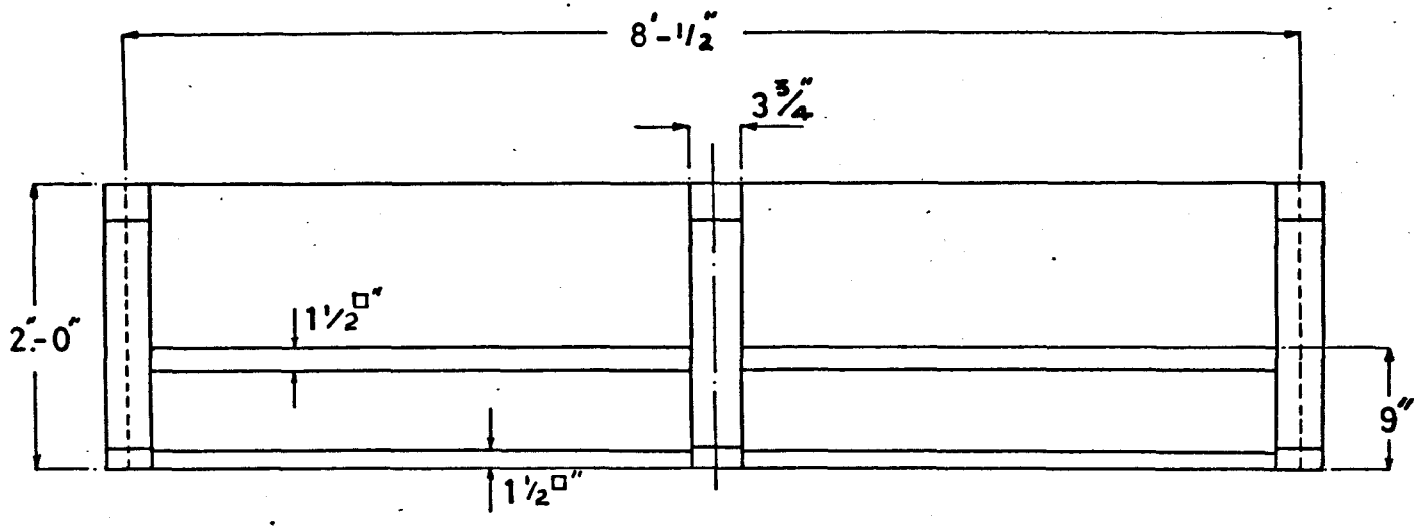

Sheet Mat^{l} – ½" Marine Ply
Supports – W.P.D

Restricted Channel Particulars

Channel Length 50m
Channel Breadth 2m

Fig R4

(2.a) Self-propulsion

Model self-propusion was by means of a DC electric motor driving a stock 4-blade propeller. Thrust and torque were not recorded. RPM were measured using a 100 pulse/rev counter and digital display. The model self-propulsion point was used.

When self-propelled, the procedure involved accelerating the model to the desired test speed with the aid of the carriage and then adjusting propeller rpm to bring the model under self-propulsion up to the carriage speed.

(2.b) Test Conditions

Tests were conducted at 3 load draughts and 1 ballast draught condition, as follows;

(a) Load draught; 0.174 m., level-keel
(equivalent to 9.14 m. full-scale)
(b) Load draught; 0.194 m. fwd., 0.154 m. aft)
(equivalent to 10.19 m. fwd., 8.1 m. aft, full-scale)
(c) Load draught; 0.154 m. fwd., 0.194 m. aft)
(equivalent to 8.1 m. fwd., 10.19 m. aft, full-scale)
(d) Ballast draught, 0.113 m. fwd., 0.133 m. aft)
(equivalent to 5.95 m. fwd, 6.99 m. aft, full-scale)

The distribution of the model ballast for the two main

conditions, (a) and (d), is shown in Fig.R2.

(2.c) Test Programme

The test programme consisted of,

(1) Deep water tests.

These were conducted in test conditions (a) and (d), towed and self-propelled, with the original bulbous-bow only.

(2) Laterally Unrestricted Shallow-water.

Experiments were conducted over a level-bed and over a shoaling sandbank, in test conditions (a) and (d), towed and self-propelled and the Glasgow University and original bulbous bows, see Table R3.

Draught	Load		Ballast	
Bulb	Original	Glasgow	Original	Glasgow
h/T				
1.05	✓ x(1.25)	✓	✓	
1.1	✓ x(1.3)	✓ x(1.3)	✓	
1.2	✓	✓		
1.37			✓ x(1.64)	✓
1.44			✓ x(1.70)	✓ x(1.70)
1.57			✓	✓
2.00	✓			
2.67			✓	

Table R3: Test Conditions Examined in Unrestricted Shallow Water

where ✓ indicates experiments over the level-bed and x( ) indicate experiments over the sandbank with the h/T clear of sandbank in the parenthesis.

(3) Laterally Restricted Shallow-water.

A channel was set up in the tank, using one of the fixed tank walls as a channel wall. The sections of the other

channel wall, consisted of a number of marine plywood units assembled to the desired channel length, see Fig.R4 for scheme. Total channel length, 50 m. and breadth 2 m. The plywood units were mounted and butted end-to-end on wooden frames which were bolted to the basin floor. The joint between the wooden frames and basin floor was sealed from leakage and the consequent variance of pressure inside the channel. The angle between the channel walls and the basin floor was set at 90°. Experiments in all test conditions were carried out as shown in Table R5. See (2.b) above for test draughts.

Test Draught	(a)		(b)		(c)		(d)	
Test Condition	Towed	S.P.	Towed	S.P.	Towed	S.P.	Towed	S.P.
1.1	*	*					*	*
1.16			*	*				
1.3	*	*						
1.35			*	*	*	*		
1.44							*	*
1.5	*	*						
1.70							*	*
1.79				*	*	*		
1.96							*	*
2.0	*	*						
2.62							*	*

Table R5: Test Conditions Examined in Channel

(3) Multi-hull Experiments

All multi-hull experiments were carried out in the naked-hull condition. The particulars of the models appear in Figs.38,42,101,102. A typical shallow-water set-up is shown in Fig.43. Relevant information as to particular experiments appear in the appropriate sections of the text.

APPENDIX D

Evaluation of the Limiting (Lower Critical) Speed

In this Appendix, the limiting (or lower critical) speed expression used in the SQUAT computer program of Chapter 4 is derived.

The fundamental cubic equation (2.4.7) of the restricted channel problem may be written in the form,

$$F_1^3 - F_1\{2(1 - m(x)) + F^2\} + 2F = 0 \qquad \text{..... (D.1)}$$

where

$$F_1 = \frac{U_1^2}{gh_1} \quad , \quad F = \frac{U^2}{gh}$$

This is of the standard form,

$$F_1^3 + 3pF_1 + 2q = 0 \qquad \text{..... (D.2)}$$

where

$$p = -\frac{1}{3}\{2(1 - m(x)) + F^2\}$$

and

$$q = F$$

The two real solutions which are admissible are,

$$F_1 = 2r\cos\left(\frac{180^\circ + \zeta}{3}\right) \qquad \text{..... (D.3.a)}$$

$$F_1 = 2r\cos\left(\frac{180^\circ - \zeta}{3}\right) \qquad \ldots\ldots \text{(D.3.b)}$$

where $r = \sqrt{|p|}$ and $\cos\zeta = q/r^3$

Writing expression (D.1) as,

$$F = F_1 - m(x)F_1 - \tfrac{1}{2}F_1^3 + \tfrac{1}{2}F_1F^2$$

then $$\frac{dF}{dF_1} = 1 - m(x) - \frac{3}{2}F_1^2 + \tfrac{1}{2}F^2 + F_1F\frac{dF}{dF_1}$$

Equating to zero for maximum value and eliminating F_1,

$$F^2 = \frac{8}{27}\left(1 - m(x) - \tfrac{1}{2}F_1^2\right)^3 \qquad \ldots\ldots \text{(D.4)}$$

The 2 real roots which are applicable are,

$$F_h^L = \left\{6\cos\left(\frac{\theta + 180^\circ}{3}\right) - 2(1 - m(x))\right\}^{\frac{1}{2}} \qquad \ldots\ldots \text{(D.5.a)}$$

$$F_h^U = \left\{6\cos\left(\frac{\theta - 180^\circ}{3}\right) - 2(1 - m(x))\right\}^{\frac{1}{2}} \qquad \ldots\ldots \text{(D.5.b)}$$

where $\theta = 1 - m(x)$

and F_h^L , F_h^U are termed the lower-critical and upper-critical (limiting) Froude depth numbers, respectively.

APPENDIX E

Trip Wire Diameter and Self-Drag

(1) Trip-wire Diameter

The trip-wire diameter was determined by a combination of Fage's criterion, see Acevedo [2], and flat-plate theory. Fage's criterion states,

$$\frac{vq}{\nu} \geq 400 \qquad \ldots\ldots \text{(E.1)}$$

where v is the velocity in the boundary layer at the wire location (without the wire) at a distance of the wire diameter q from the hull and ν is the kinematic viscosity of the fluid.

The criterion adopts the form of a Reynolds Number, showing that, depending on the wire diameter, a minimum inflow velocity v is required in order that the wire be effective. Usually v is assumed to be equivalent to U, the free stream velocity, for most purposes. Since a more accurate estimation of v was required, flat-plate theory was employed, as follows.

Following Pohlhausen's approximate method, see

Schlichting [59], the Blasius laminar velocity profile may be approximated by assuming a suitable expression for the velocity distribution v(y) in the boundary layer, taking care that it satisfies the appropriate boundary conditions, that is:

$$\frac{v}{U} = f\left(\frac{y}{\delta_T(x)}\right) = f(i) \qquad \ldots\ldots \text{(E.2)}$$

where $i = y/\delta_T(x)$ is the dimensionless distance from the wall referred to the boundary layer thickness $\delta_T(x)$. The function f(i) must vanish at the wall (i = 0) and tend to the value 1 for large i. The velocity distribution may then be closely represented by a parabola:

$$\frac{v}{U} = 2i - i^2 \qquad \ldots\ldots \text{(E.3)}$$

or

$$\frac{v}{U} = 2\left(\frac{y}{\delta_T}\right) - \left(\frac{y}{\delta_T}\right)^2 \qquad \ldots\ldots \text{(E.4)}$$

where y is the distance along the normal to the surface and δ_T the boundary layer thickness defined as that for which v = 0.99U.

This approximate approach yields the general formula for δ_T as,

$$\delta_T = \sqrt{\frac{2B}{\alpha}}\,\frac{x}{\sqrt{R_x}} \qquad \ldots\ldots \text{(E.5)}$$

where the numerical values for the parabolic velocity distribution α , β are given by:

$$\alpha = \int_0^1 f(i)(1-f(i))di = 0.133$$

$$\beta = f'(o) = 2$$

Thus for this distribution:

$$\delta_T = x\sqrt{\frac{30}{R_x}} \qquad \ldots\ldots (E.6)$$

where x is the longitudinal distance from the leading edge and R_x is the x-Reynolds Number = xU/ν

To compute the boundary layer velocity v at a height of the wire diameter q, we let y = q in equation (E.4). Then

$$\frac{v}{U} = \frac{2q}{\delta_T} - \left(\frac{q}{\delta_T}\right)^2 \qquad \ldots\ldots (E.7)$$

NOTE: The Blasius curve yields for comparison α = 0.135 and β = 1.63. The principle difference between the two solutions being the milder slope of the latter profile in the proximity of the hull.

Using a value of 0.3 ms. in equation (E.6) yielded v/U = 1.0 by (E.7) and, therefore, U was employed to estimate the wire diameter by (E.1).

(2) Trip-wire Self Drag

Tests with and without turbulence stimulators yield changes in total resistance, R , which may be written as:

$$\Delta R_T = \Delta R_F + \Delta R_R + r_w \quad \ldots\ldots \text{(E.8)}$$

where the Δ's indicate the actual changes in the component resistances and

R_R is the model residuary resistance

R_F is the model frictional resistance

and r_w is the increment in drag due to the turbulence device.

Under the assertion that R_R is not critical, it is usually assumed that the total increase in measured model resistance due to turbulence stimulation is frictional only, that is,

$$\Delta R_R = 0$$

and

$$\Delta R_T = \Delta R_F + r_w \quad \ldots\ldots \text{(E.9)}$$

(A point to be made here is that although it is assumed frictional on model scale, the excess resistance is actually treated as residuary resistance for scaling purposes).

Experiments conducted on protrusions, see Schlichting [59], have shown that the increment of drag induced by a small protrusion in the boundary layer, may be approximated

by:

$$r_w = \tfrac{1}{2}\rho v^2 S_p C_D \qquad \ldots\ldots \text{(E.10)}$$

where v is the speed in the boundary layer at a distance of a wire diameter q, S_p is the protrusion projected area and C_D is the drag coefficient appropriate to the stimulator itself in free steam velocity (v = U) based on its projected area and correct Reynolds Number.

Assuming the flow ahead of the stimulator is laminar, the correction to model resistance owing to trip wire self drag, r_w , was approximated as follows:

C_w = the non dimensional correction coefficient

$$= C_{TOT}\left(\frac{r_w}{R_T}\right) \qquad \ldots\ldots \text{(E.11)}$$

where $$C_{TOT} = \frac{R_T}{\tfrac{1}{2}\rho U^2 S w^2}$$

S is the model wetted surface area, U is the model speed and $w = U_1/U$ the correction for back-flow effect on shallow-water speed, obtained by equation (2.4.3).

The correction coefficient may be also written as:

$$C_w = \left(\frac{v}{U}\right)^2 \left(\frac{S_p}{S}\right) C_D \qquad \ldots\ldots \text{(E.12)}$$

where v/U may be derived by use of equation (E.4) and (E.5).

C_D is taken to be 1.0. Owing to the experimental difficulties encountered in making trip wire drag measurements, some differences in the results have been reported by various researchers, see McCarthy [47]. In the range $1.5 \times 10^2 < \frac{wUq}{\nu} < 1.5 \times 10^3$, $C_D = 0.8$ appears to represent a reasonable mean value. However, this value is on the low side when compared to data on infinite cylinders which yield $C_D = 1.2$, see Schlichting [59], and consequently an average value was used in the present calculations.

GLASGOW UNIVERSITY